THE MOON AS VIEWED BY LUNAR ORBITER

NATIONAL AERONAUTICS AND SPACE ADMINISTRATION

NASA SP-200

THE MOON AS VIEWED BY LUNAR ORBITER

By L. J. KOSOFSKY and FAROUK EL-BAZ

Scientific and Technical Information Division
OFFICE OF TECHNOLOGY UTILIZATION 1970
NATIONAL AERONAUTICS AND SPACE ADMINISTRATION
Washington, D.C.

FOR SALE BY THE SUPERINTENDENT OF DOCUMENTS, U.S. GOVERNMENT PRINTING OFFICE
WASHINGTON, D.C. 20402 - PRICE $7.75 - LIBRARY OF CONGRESS CATALOG CARD NUMBER 75-601482

FOREWORD

Throughout history men have wondered and dreamed about the landscape of the distant Moon. The initial step in detailed knowledge of our nearest neighbor occurred with the invention of the telescope. A larger step came with the advent of the space age. Automated spacecraft have provided us photography of virtually the entire lunar surface supplemented with other types of data from a few discrete points. These spacecraft have paved the way men are now following.

A dedicated Government-industry team placed five successful Lunar Orbiters into close orbits about the Moon in as many attempts. Thousands of photographs were returned giving reality to the dreams of centuries. Some show areas smooth enough for initial manned landings; others reveal a fascinating variety of features for future exploration missions. Some answer ancient scientific questions; others raise new questions.

This book contains a selected compilation of Lunar Orbiter photographs that clearly illustrates the heterogeneous nature of the lunar surface. Many features shown are similar to those found on Earth; others have no terrestrial counterpart. By comparing the similarities and contrasting the differences, we can hope to understand better our own planet and to recognize possible implications for the origin of the solar system. Increased understanding may profoundly affect our philosophic view of ourselves and our place in nature. There may also be benefits directly affecting our well-being.

The largest step of all in our search for answers is manned exploration directly on the lunar surface. Included in this book are the photographic guideposts that have been and are being used to plan the most ambitious travels man has yet undertaken.

L. R. Scherer
Director,
Apollo Lunar Exploration,
National Aeronautics and
Space Administration

C. H. Nelson
Assistant Director,
Langley Research Center,
National Aeronautics and
Space Administration

PREFACE

If one were to purchase a complete set of Lunar Orbiter photographs from the National Space Science Data Center, he would have about 3100 20- by 24-inch prints. To examine this material for any useful purpose, he would have to make some selection. This book includes selected parts of Lunar Orbiter photographs that illustrate some of the salient features of the lunar surface. Complete coverage of the lunar surface is provided in NASA's forthcoming publication: *The Lunar Orbiter Photographic Atlas of the Moon* (NASA SP–206).

Included in the Introduction are brief descriptions of the Orbiter project, the spacecraft and camera systems, and the lunar surface coverage of the five Orbiter missions flown during the 12-month period from August 1966 to August 1967. Chapters 2 and 3 present the distant and close-up Lunar Orbiter photographs selected. These two chapters are complementary: chapter 2 gives substantially full, small-scale coverage of the lunar surface, and chapter 3 gives salient lunar surface features in greater detail. In several instances a medium-resolution photograph of the complete feature is followed by several photographs, at a larger scale and showing greater detail, of selected parts of the feature.

In the appendix are four stereoscopic views of selected features as well as index charts of footprints of all Lunar Orbiter frames. Technical data (Photo Reference Table) pertaining to the photographs in this book also are in the appendix.

The Lunar Orbiter project was carried out under the direction of the NASA Langley Research Center. The Boeing Co. was the prime contractor for the operation of all five missions. We wish to pay particular tribute to the leadership of the late Robert J. Helberg, who was manager of the Lunar Orbiter program for The Boeing Co.

The authors are indebted to several agencies, especially the U. S. Army Topographic Command, for their continued help and support in pursuing this project. In preparing the picture captions, we received considerable help from D. E. Wilhelms, J. F. McCauley, H. J. Moore, M. H. Carr, and N. J. Trask of the U. S. Geological Survey, Branch of Astrogeology. Help was also provided by personnel of the Apollo Lunar Exploration Office of NASA's Office of Manned Space Flight. We are especially grateful to R. P. Bryson for his assistance and counsel in every phase of the preparation of this book.

L. J. Kosofsky
Apollo Lunar Exploration
Office, National Aeronautics and
Space Administration

Farouk El-Baz
Supervisor,
Lunar Science Planning
Bellcomm, Inc.

CONTENTS

CHAPTER 1

INTRODUCTION

THE PROGRAM

The Lunar Orbiter program was conceived, together with the Ranger and Surveyor programs, with the primary objective of providing information essential for a successful manned Apollo lunar landing. The Lunar Orbiter program comprised five missions, all of which were successful. As the primary objectives for the Apollo program were essentially accomplished on completion of the third mission, the fourth and fifth missions were devoted largely to broader, scientific objectives—photography of the entire lunar nearside during Mission IV and photography of 36 areas of particular scientific interest on the nearside during Mission V. Photography of the farside during the five missions resulted in an accumulated coverage of more than 99 percent of that hemisphere. The detail visible in the farside coverage generally exceeds that previously attained by Earth-based photographs of the nearside; in some areas objects as small as 30 meters are detectable.

Initiated in early 1964, the Lunar Orbiter program included the design, development, and utilization of a complex automated spacecraft technology to support the acquisition of detailed photographs of the lunar surface from circumlunar orbit. The five spacecraft were launched at 3-month intervals between August 10, 1966, and August 1, 1967.

In addition to its photographic accomplishments, the program provided information on the size and shape of the Moon and the major irregularities of its gravitational field. This selenodetic information was derived from the tracking data. Micrometeoroid and radiation detectors, mounted on the spacecraft for operational purposes, monitored those aspects of the lunar environment.

PHOTOGRAPHIC ACCOMPLISHMENTS

Photographs for Apollo (Missions I, II, and III)

The primary objective of the Lunar Orbiter program was to locate smooth, level areas on the Moon's nearside and to confirm their suitability as manned landing sites for the Apollo program. To accomplish this, photographic coverage at a ground resolution of 1 meter was required of areas within 5° of the equator between longitudes 45° E and 45° W—the zone of primary interest to the Apollo program.

Twenty potential landing sites, selected on the basis of Earth observations, were photographed during the site search missions of Lunar Orbiters I and II. Lunar Orbiter III rephotographed 12 of the most promising of these areas during its site-confirmation mission. Following analysis of these photographs, consideration was further reduced to the eight most promising areas. However, to make the final selection of the candidate Apollo landing sites, additional photographs of various types were required at all but three of these areas. These photographs, obtained during Mission V, provided sufficient data to permit the final site selection and mapping.

Approximately three-fourths of the film supply of the first three missions was used to photograph areas of interest to the Apollo program primarily. The remainder could not be used for such areas because of operational film-handling requirements; i.e., the film could not remain stationary in the camera for long periods of time lest it deteriorate. Photographs taken when the areas of primary interest were not in view, referred to as film-set frames, were expended in a variety of ways and for several reasons. In the Mission I flight plan, such sites were selected, in real time, for diagnostic tests of certain spacecraft malfunctions, for reconnaissance of potential photo sites for subsequent missions, and for photography of the Moon's farside. To minimize operational demands on Mission I, nearly all of the film-set exposures were made using conventional maneuvers of the spacecraft. This resulted in near-vertical photographs for all but two areas covered during Mission I. Two oblique photographs of the Moon's farside, with the Earth in the background, were taken while the spacecraft was passing behind the Moon's eastern limb. The scene provided in these oblique views and the flawless execution by the spacecraft of every single maneuver command during Mission I prompted more rigorous performance demands for the following missions.

Specific plans to use the film-set frames were included in the preflight design of Missions II and III. Several outstanding

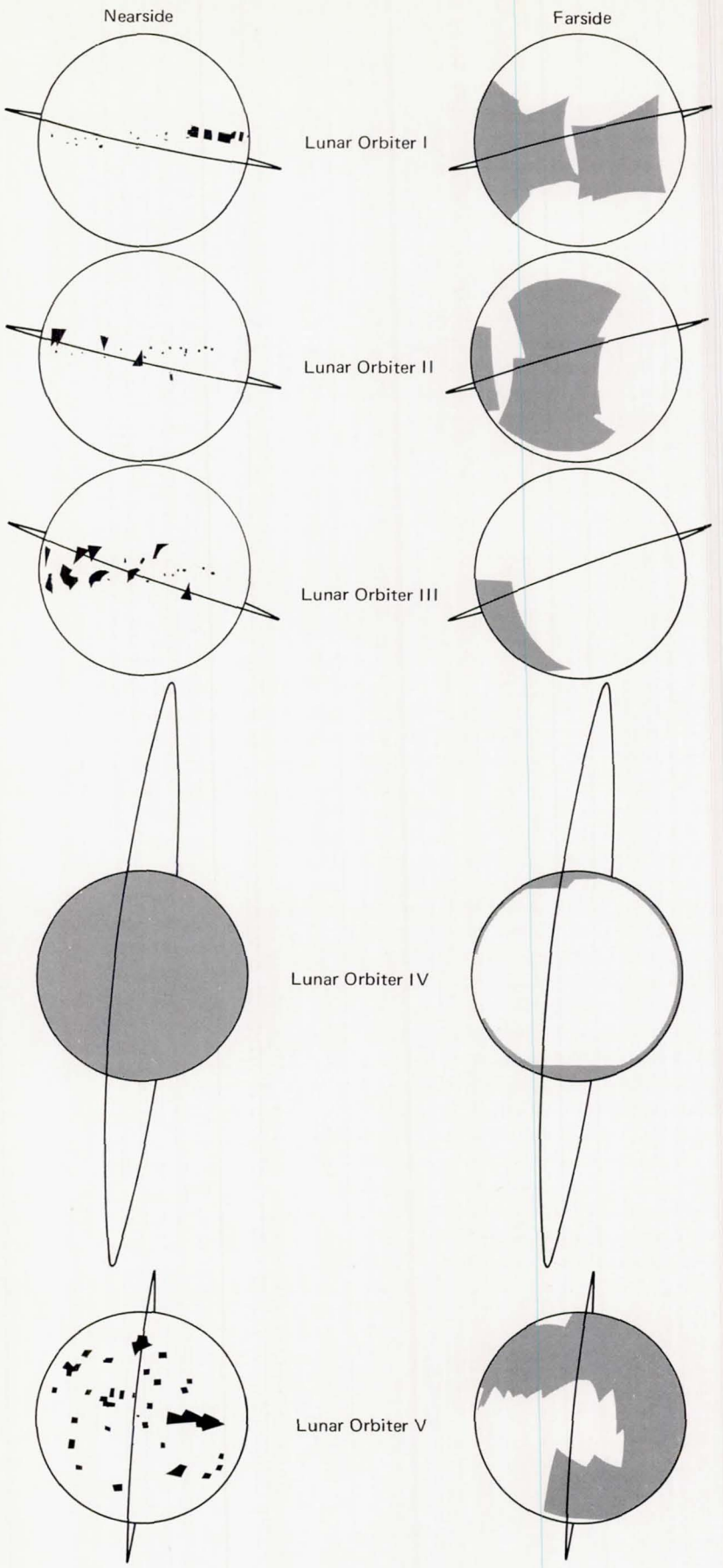

Figure 1. Photographic Coverage [REPRINTED BY PERMISSION FROM "THE LUNAR ORBITER MISSIONS TO THE MOON" BY LEVIN, VIELE, AND ELDRENKAMP. COPYRIGHT MAY 1968 BY SCIENTIFIC AMERICAN, INC. ALL RIGHTS RESERVED.]

oblique photographs were obtained on both the nearside and the farside. The Mission II oblique view of the crater Copernicus is a notable example.

Because the area of Apollo interest was near the equator and 1-meter resolution was required, photographs taken during Missions I, II, and III were made from low inclination, close-in orbits. This restricted the north and south latitude range for photography and also the total area coverage obtained. These restrictions were relaxed for the final two missions.

Photographs of General Scientific Interest (Missions IV and V)

The flight plans for Missions IV and V incorporated near-polar circumlunar orbits from which virtually any part of the Moon could be photographed. Mission IV photography, conducted from high-altitude orbit, was a broad, systematic survey of the entire nearside. Most of this photography contains detail down to 60 meters ground resolution, and the remainder is no coarser than 150 meters. The east and west limbs and both polar regions were covered in near-vertical views.

The primary objective of Mission V was to obtain closeup photographs of geologically interesting features in 36 selected areas of the Moon's nearside. In addition, some photographs were taken to complete the Apollo requirements and to complete the coverage of the lunar farside. All of these objectives were attained with the faultless execution of Mission V, completing the Lunar Orbiter program.

Figure 1 summarizes the five missions, showing the orbit of each one and the area that each covered photographically.

TYPICAL MISSION PROFILE

Each mission started with the launch from Cape Kennedy by an Atlas-Agena D launch vehicle. Following separation from the Atlas, the Agena engine put the spacecraft into Earth orbit. After a coasting period, a second burn of the Agena engine, before separating from it, placed the spacecraft on a translunar course. A small correction in the trajectory was accomplished by a short burn of the spacecraft's velocity-control engine some 20 to 30 hours after leaving Earth orbit. Upon arriving at the lunar encounter point, after some 90 hours, the spacecraft velocity was reduced by a retrofiring of its engine, leaving it in an elliptical posigrade lunar orbit. Injection into orbit was scheduled in all cases within a few days of new Moon, and an orbit was established with perilune (point of closest approach) near the equator on the Moon's eastern limb.

After being tracked in this orbit for several days, the spacecraft was slowed again, lowering the orbital perilune to the desired photographic altitude. The perilune altitude was about 46 kilometers on the first three missions, 1000 kilometers on Mission IV, and 100 kilometers on Mission V.

The placement of the orbital plane had to be such that, when the Moon's rotation brought the selected sites beneath the perilune, the site would be properly illuminated for photography (i.e., have the Sun 10° to 30° above the local horizon). In general, the sites on the Moon's nearside were photographed with sunrise illumination and the farside areas with sunset illumination.

The picture-taking phase was completed about the time of the full Moon, and the entire photographic mission ended with the readout and transmission of the last of the photographic data in about 30 days. The spacecraft remained in orbit and was tracked for extended periods to provide additional lunar gravitational and other environmental data. The longest lifetime in orbit was 335 days, for Lunar Orbiter II. All the spacecraft except Lunar Orbit IV were deliberately crashed onto the Moon, by a final burn of the velocity-control engine, to ensure that they would not interfere with communication between the Earth and later spacecraft. Communication with Lunar Orbiter IV was lost after 70 days in orbit, about 3 months before it is believed to have crashed.

Lunar Orbiter Spacecraft

Figure 2 shows the Lunar Orbiter spacecraft in its flight configuration. It weighed approximately 390 kilograms (850 pounds) at launch. At launch, the spacecraft rode within an aerodynamic nose fairing atop the Atlas/Agena D launch vehicle, its solar panels folded under the spacecraft base and antennas held against its sides. In this launch configuration the spacecraft was approximately 1.5 meters (5 feet) in diameter and 2 meters high. After injection into the cislunar trajectory, with the solar

panels and antennas deployed, the maximum span became 5.2 meters along the antenna booms and 3.8 meters across the solar panels.

Three-axis stabilization was provided using the Sun and the star Canopus as primary references and a three-axis inertial system for periods when the spacecraft was required to operate off celestial references during maneuvers or when the Sun and Canopus were occulted by the Moon. After assuming the commanded attitude for a picture-taking sequence, the spacecraft would maintain that attitude through the sequence. Attitude control was maintained by cold-gas thrusters. A flight programmer with a 128-word memory provided the capability for up to 16 hours of automatic spacecraft and camera operation or for action on real-time commands.

Photographic System

The complete Lunar Orbiter photographic system included the spacecraft's photographic subsystem; the ground reconstruction electronics (GRE); and the communications system.

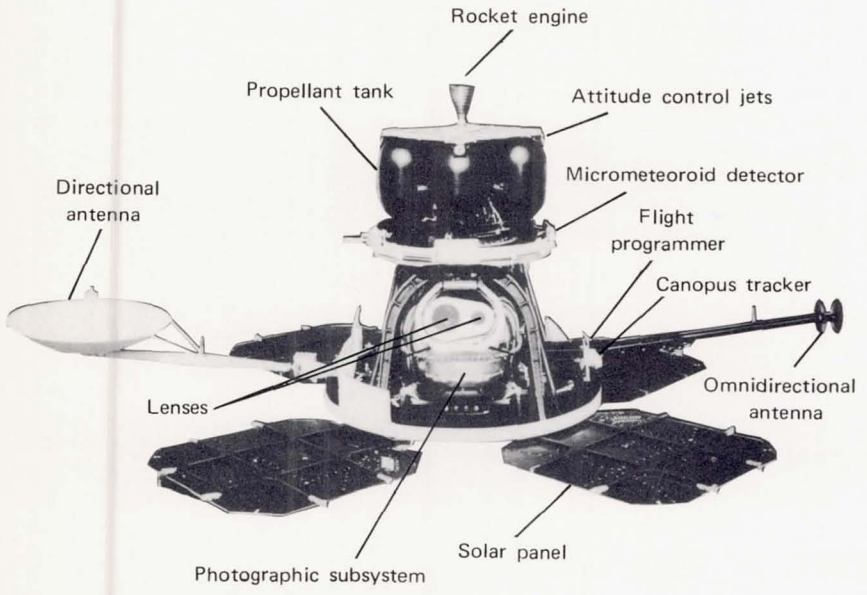

Figure 2. Lunar Orbiter Spacecraft

The photographic subsystem recorded a negative image of lunar scenes on film that was developed and scanned to provide electrical signals for transmission to the deep space stations (DSS). The video signals from the communications system were fed to the GRE which reconverted these signals into photographic images at a scale 7.18 times the spacecraft scale. The transmitted signals were also recorded on magnetic tape. A brief description of the Lunar Orbiter photographic system follows. For a more detailed description, the reader is directed to the group of five papers in the *Journal of Society of Motion Picture and Television Engineers,* August 1967, pages 733–773.

The Photographic Subsystem

The spacecraft's photographic subsystem, shown schematically in figure 3, comprised a dual camera, a film processing unit, a readout scanner, and film-handling apparatus. The two cameras operated simultaneously, placing two discrete frame exposures on a common roll of 70-mm film. Each camera operated at a fixed f/5.6 lens aperture, at shutter speeds of either 1/25, 1/50, or 1/100 second. The high-resolution (H) frame was exposed through a 610-mm narrow-angle lens and a focal plane shutter. The medium-resolution (M) frame was exposed through an 80-mm wide-angle lens and a between-the-lens shutter.

The film supply consisted of 79 meters of unperforated 70-mm Kodak special high definition aerial film, type SO–243. This fine-grain film has a recording capability (450 lines/mm) well above the photographic subsystem requirements (approximately 76 lines/mm) and a low enough speed (aerial index of approximately 3.0) to make it relatively insensitive to space environment radiation.

The selection of a slow-speed film to meet the Apollo requirements for 1- and 8-meter resolution photographs necessitated that image-motion compensation (IMC) be provided to minimize smear. An electric-optical sensor viewed the lunar surface through a portion of the 610-mm lens and determined the ratio of the spacecraft's velocity to its altitude—referred to as the velocity-to-height (V/H) ratio. The V/H sensor output, in the form of a mechanical camshaft rotation, was used for direct drive of the camera platens (and film) at the proper rate to ensure IMC during exposure. The V/H sensor also controlled the spacing of exposures during multiple exposure sequences.

The two camera axes were coincident, so that the coverage of the H-frame was centered within the M-frame coverage as shown in the upper left portion of figure 4. Because of the physical arrangement of the two-lens system, adjacent exposures were recorded on the film in the interlaced manner shown in the lower portion of the figure. Exposure times were recorded in digital form on the film alongside the M-frames. The least reading of time was 0.1 second.

The upper right part of the figure shows an enlarged portion of the edge data preexposed on the film. The pattern included a gray scale and resolution bars to permit later calibration and evaluation of the photographs, various markings for the control of the readout operation, and framelet numbers to facilitate the reassembly of the frames on the ground.

The film-processing method was the Kodak Bimat diffusion transfer technique. The film, on entering the processor, was laminated with the processing web, as indicated in figure 3. A gelatin layer on the processing web was slightly damp, having been soaked in the monobath processing solution before being loaded into the spacecraft. The monobath solution developed the exposed portions of the SO–243 film to a negative image and transferred the undeveloped silver ions to the processing web, where they were reduced to form a positive image. (This is essentially the technique used with Polaroid Land black-and-white film.) As the process went to completion within 3½ minutes of contact time, image quality was not affected by prolonged contact. Coming off the processing drum, the two films were separated. The negative film went through the drying section, and the processing web was wound on a takeup spool. (No use was made of the positive images on the web.)

After being dried, the negative film went through the readout scanner to its takeup spool. During readout, the film moved backward through the scanner. The readout looper shown between the processor and the scanner made it possible to read out selected portions of the film before photography was completed.

Upon completion of photography, the processing web was cut and pulled free of the processor. The negative film could then be read out completely (from the last exposure to the first) and be pulled through the processor and camera onto the supply spool.

The readout scanner (fig. 5) converted the photographic images into electrical signals by scanning the negative film with a microscopic spot of high-intensity light. The source of the light was the linescan tube shown at the upper left. This was a special cathode-ray tube whose phosphor layer was coated on a rotating cylindrical metal anode. Its output was a bright spot of light that repetitively traced a line across the phosphor drum.

The scanner lens focused a 0.005-mm spot of light on the film. The electrical scan of the spot traced a line 2.68-mm long on the film in the direction parallel to the film edge.

The mechanical scan of the line across the width of the film was accomplished by the slow back-and-forth movement of the scanner lens. One traverse of the scanner lens required 22 seconds, during which time the electrical scan was repeated over 17,000 times. Before the scanner lens started across the film in the reverse direction, the film was moved 2.54-mm in the readout gate. The resulting sections of spacecraft film scanned

in this manner, referred to as framelets, are the basic units eventually used for the ground reassembly. The scanning of a complete dual exposure took 43 minutes.

The intensity of light reaching the photomultiplier tube was modulated by the density of the image on the film. An electrical signal proportional to the intensity of the transmitted light was generated, amplified, and fed to the spacecraft communications subsystem.

TRANSMISSION AND RECONSTRUCTION OF PHOTOGRAPHS

The video data coming from the photographic subsystem occupied a frequency spectrum from 0 to 230 kilohertz. This signal was modulated on a 310-kHz subcarrier (single sideband, suppressed carrier). The video signal, telemetry signals, and a 38.75-kHz pilot tone were summed, and the resulting composite signal phase-modulated the S-band (2295-MHz) carrier.

A 10-watt traveling-wave tube amplifier and a 92-cm parabolic antenna transmitted the signal to Earth, where it was received at one of the three deep space stations (DSS). The 10-MHz intermediate frequency of the DSS receiver, containing the composite signal, was recorded on magnetic tape for permanent storage. At the same time, it was passed to the ground communications equipment which recovered the telemetry and video.

The video signal was fed to the ground reconstruction electronics (GRE) where it was converted into an intensity modulated line on the face of a cathode-ray tube. In a continuous motion camera, 35-mm film was pulled past the image of this line, recording each readout framelet at 7.18 times the

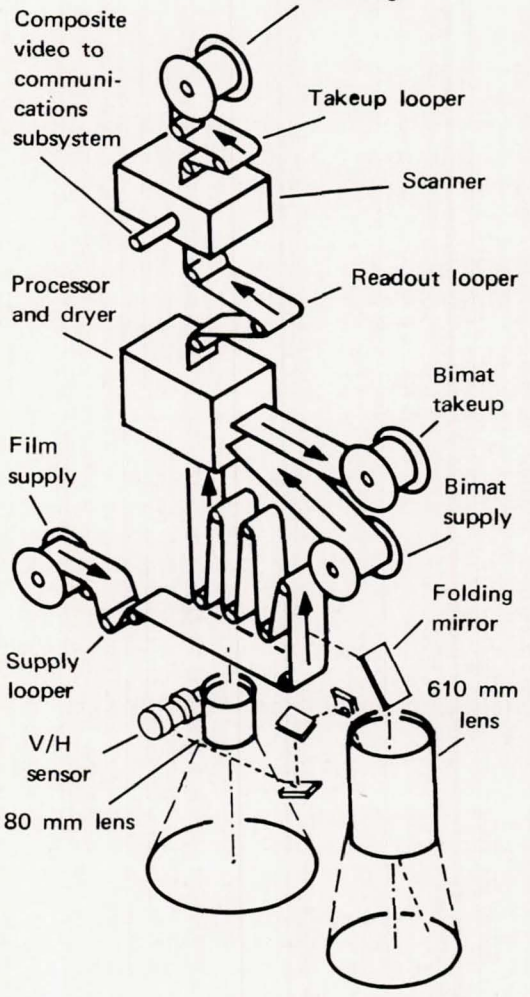

Figure 3. Photographic Subsystem

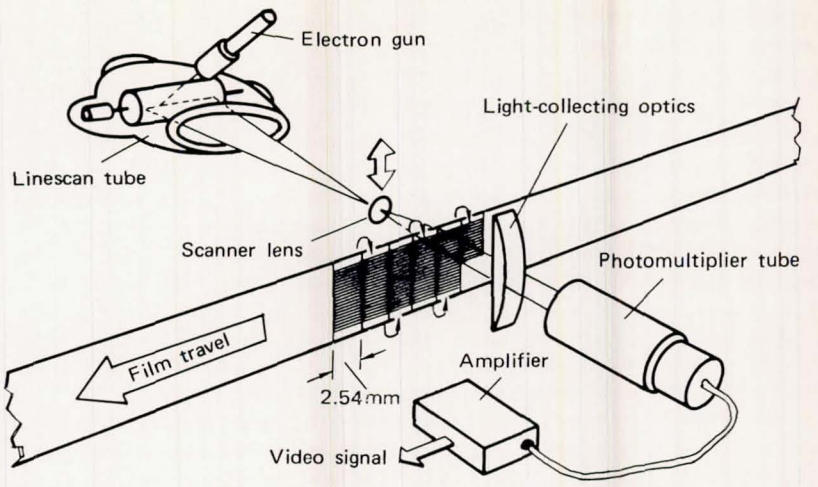

Figure 5. Readout Scanner

spacecraft's image size. The recording film was cut up into framelets, which were then reassembled into enlarged replicas of the original spacecraft frames. The M-frames were reassembled in complete form, while the H-frames, which would be about 1.5 meters long if fully reassembled, were reassembled into three component sections.

PATTERNS OF PHOTOGRAPHIC COVERAGE

A single exposure of the dual-frame camera produced the nested ground coverage shown in the upper left portion of figure 6. (The ground dimensions are shown for a vertical camera attitude and a flight altitude of 46 kilometers.) The ground coverage could be expanded in the direction of flight by sequential exposures, and in the perpendicular direction by photographing from successive orbits.

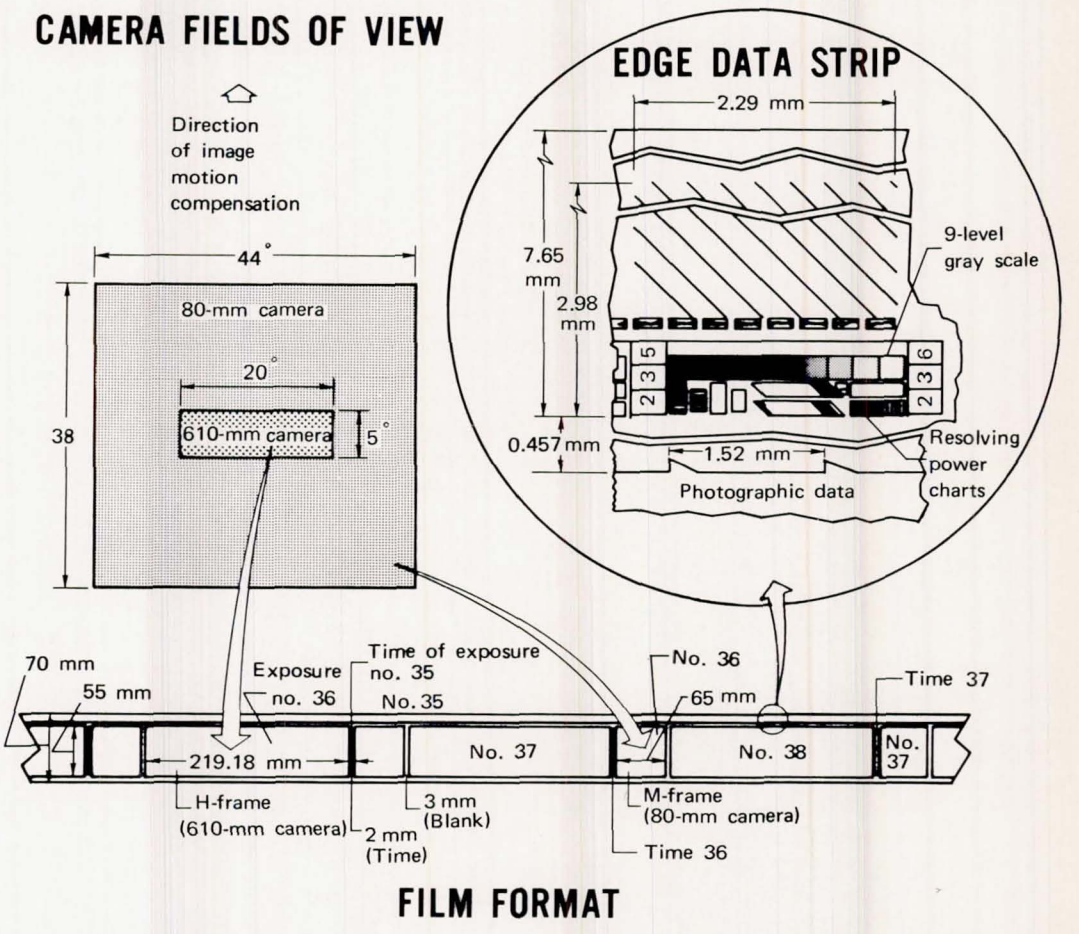

Figure 4. Film Format

Exposure sequences consisted of 1, 4, 8, and 16 exposures. A slow or a fast repetition rate could be selected. At either rate, the timing of successive exposures was automatically determined by the V/H sensor.

A sequence of eight exposures at the slow rate produced the coverage pattern shown at the upper right of figure 6. The M-frames overlapped by 52 percent, providing continuous stereoscopic coverage over nearly the full length of the strip. The areas covered by the eight H-frames were evenly spaced along the strip, separated by gaps.

Selection of the fast repetition rate produced 5 percent overlap of the H-frames thus providing high-resolution coverage of a shorter strip without gaps. The overlaps of the M-frames at the fast rate was 88 percent.

The lower left portion of figure 6 shows the coverage pattern produced by two eight-exposure sequences at the fast rate, exposed on successive orbits. A small overlap between the adjacent strips of H-frames provided contiguous high-resolution coverage of a considerable area.

The pattern at the lower right was also produced by two eight-exposure sequences at the fast rate. Here the camera was tilted in the cross-track direction during one of the sequences, so that the two strips of H-frames completely overlapped. The advantage of the duplicated high-resolution coverage was that (because of the angle of convergence between the two orbital tracks) it permitted stereoscopic study of the H-frames.

The patterns shown in figure 6 were typical of the first three missions, on which the frontside exposures were made from low-inclination orbits near their perilune. The orbits of Missions IV and V had high inclinations, and the frontside exposures were made while the spacecraft was going from south to north. The coverage patterns are shown in figure 7.

The left half of figure 7 shows the typical ground coverage of the H-frames on two successive orbits during Mission IV. This pattern was repeated during 29 orbits to obtain complete coverage of the Moon's nearside. Note that for Mission IV only, the long dimension of the H-frame is oriented approximately in the direction of flight. Each M-frame covered nearly all of the lunar surface visible to the spacecraft.

At the right are shown typical coverage patterns produced by fast and slow sequences of four exposures each during Mission V. The anaglyphs at the end of this book were all printed from the stereoscopic M-frame coverage of such sequences. A convergent stereo coverage pattern (not shown) was also employed on this mission to permit stereoscopic examination of the H-frames.

ABOUT THE PICTURES

The pictures reproduced in this book are portions of the original frames that have been cropped and enlarged or reduced to illustrate selected lunar features at scales appropriate to the material. The Photo Reference Table in the Appendix supplies the mission and frame number for each picture, as well as the designation M (for the medium resolution, or 80-mm focal length, camera) or H (for the high resolution, or 610-mm focal length, camera).

A set of thin parallel lines, that can be seen in each picture, represents the borders of the framelets introduced by the readout process (as explained in the Photographic Subsystem section). Although these framelet lines are a pictorial distraction, they do supply several kinds of helpful information concerning the pictures. They provide the most convenient reference for defining the scale, which is indicated in each caption as the number of meters on the Moon covered by one framelet's width. They also help in visualizing the size relationship between the picture and the original frame, because each M-frame comprises 26, and each H-frame 86, framelets.

Lastly, the framelet lines provide a reference for the azimuth orientation of each picture when used in conjunction with the Photo Reference Table.

Most of the pictures are oriented with North approximately at the top and East at the right, following the convention adopted by the International Astronomical Union at Berkeley in 1961. Oblique photographs may be oriented in other directions as they can only be viewed naturally when the horizon is at the top. Others were rotated from the normal orientation in order to fit selected features within the rectangular format of the book at the most favorable scale for viewing. These can easily be identified, as the framelet lines are not parallel to the picture edges. These pictures include a small arrow showing the North direction.

The pictures whose framelet lines are parallel to the picture edges do not have the North direction precisely at the top. The cameras actually were oriented parallel to the ground track of the spacecraft on Missions I, II, III, and V, in order to achieve image-motion compensation, and the framelet lines also are parallel to the ground track. (On Mission IV, where the orbital altitude made image-motion compensation unnecessary, the

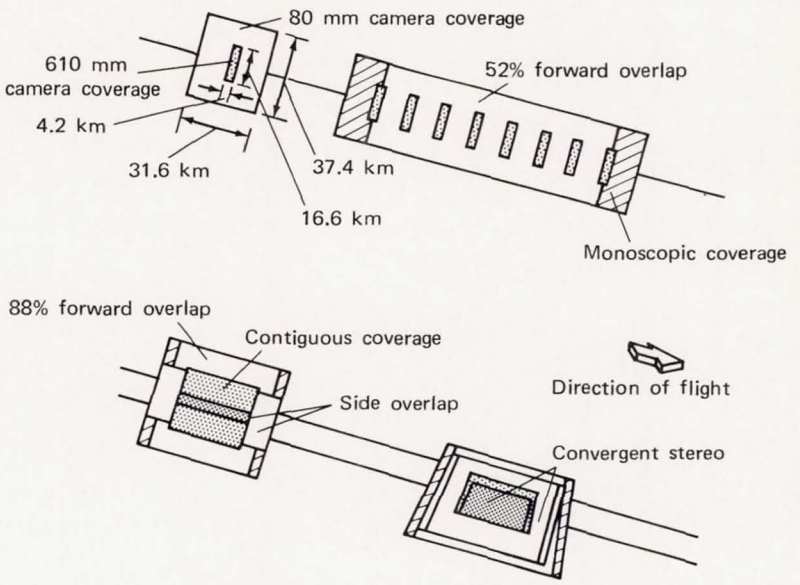

Figure 6. Coverage Patterns—Missions I, II, and III

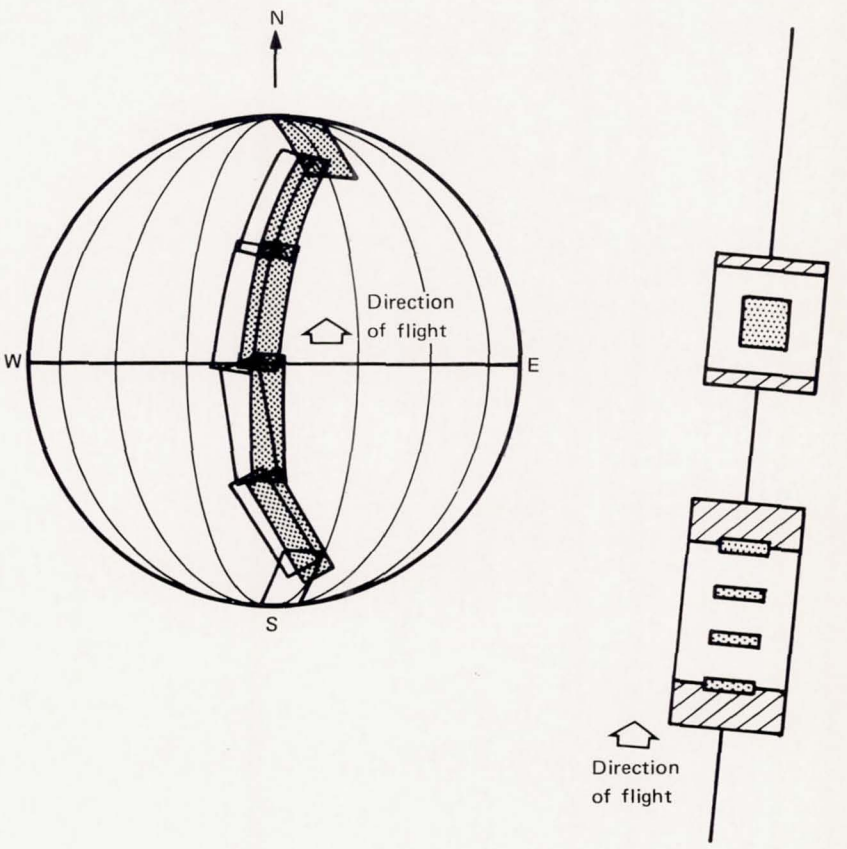

Figure 7. Coverage Patterns—Missions IV and V

camera orientation was determined by lighting considerations.) The framelet lines of these pictures are always within 22° of the Moon's cardinal directions, and the captions do not have a North arrow. In order to know their orientation more precisely, the reader should refer to the Photo Reference Table, which gives the lunar bearing of the framelet lines.

The pictures of the lunar frontside in this book were all taken near the sunrise terminator, so that the Sun was low in the east. The solar elevation at the center of each frame is also given in the Photo Reference Table. In viewing these pictures for the first time, many people have difficulty in distinguishing between protuberances and indentations. This can be cleared up by remembering that the direction of illumination was from the right (east). Some viewers find it helpful to hold the book so that a window of the room is at the right side.

The farside pictures were taken near the sunset terminator, so that the Sun was in the west and the direction of illumination was from the left. (For the purpose of this discussion, the series of pictures of the Mare Orientale region, at the Moon's western limb, are considered frontside pictures.)

Some of the pictures show white lines or bars that are perpendicular to the framelet lines. They are not likely to be confused with actual lunar features. The short ones that only extend across indiviual framelets are caused by momentary signal dropouts during the readout and transmission of the photographs. The long, very thin ones are caused by scratches in the spacecraft film.

The careful viewer may see a pattern of tiny white crosses (in the shape of plus signs) across most of the pictures. They appear most distinctly in shadow areas. These are "reseau marks," which were preexposed on the film to aid in the photogrammetric recovery of the original exposures' geometrical relationships. They were used on all missions except the first.

The pairs of sharp-edged white triangles on a few of the pictures are artifacts produced by the film-processing equipment.

There are several types of irregular white marks which are caused by processing blemishes on the spacecraft film. Some are roughly circular, and some resemble asterisks. Attention is called to them in the captions wherever it seems likely that they could be confused with lunar features. The captions also point out areas of processing "freckles."

Nearly all of the pictures in this book are portions of single photographs. In a few cases, mosaics of two photographs were required to show some feature completely. The junctions between photographs on these mosaics were made straight, so that they will not be mistaken for natural lunar features. The framelet lines are, of course, offset at these junction lines.

CHAPTER 2

A DISTANT VIEW

Most of the pictures in this book are closeup photographs that show lunar features at levels of detail from 10 to 1000 times finer than can ever be photographed through an Earth-based telescope. Before examining these pictures in detail, it is instructive to see the Moon as a whole; to understand the regional background within which each feature is set.

The set of pictures that make up this chapter covers nearly the entire lunar surface, with a substantial overlap between individual pictures. The general plan of organization is to follow the Sun around, starting at the eastern limb (as seen from the Earth), proceeding westward across the more familiar visible side to the western limb, and continuing westward across the farside to complete the journey where it started. In the course of this sweep, attention shifts between the northern and southern hemispheres, and between polar and equatorial zones.

Each picture covers a broad enough region to exhibit the effect of the gross curvature of the lunar sphere. Each frontside frame is vertical at the center, with the surface progressively foreshortened away from the center. Many of the farside frames are obliques in which the camera, flying on the night side of the Moon, was faced westward to photograph the illuminated region beyond the sunset terminator.

Wherever two or three pictures have been placed on one page, it appears more natural to place the westernmost picture on the left side. Therefore, if the reader wishes to proceed steadily in the westward direction, he should see the right-hand picture and its caption first.

Wherever the captions name features that will be seen in greater detail later, the names are printed in italics. The captions for this chapter do not directly indicate scale because of the great variation in scale across the pictures. Instead, wherever practicable, the dimensions of some feature visible in the picture are given in the caption. Frontside crater dimensions were taken from the *System of Lunar Craters,* a catalog prepared by the Lunar and Planetary Laboratory of the University of Arizona.

The dimensions and locations of farside features were scaled from the Provisional Edition of the *Lunar Farside Chart* (LFC-1) produced by the Aeronautical Chart and Information Center, U. S. Air Force. They should all be regarded as approximate at this time.

With regard to farside regional designations, it should be noted that the 180° meridian marks the middle of the farside. The region that extends eastward from there to longitude 90° W is called the "eastern farside." Similarly, the "western farside" extends from the 180° meridian westward to longitude 90° E.

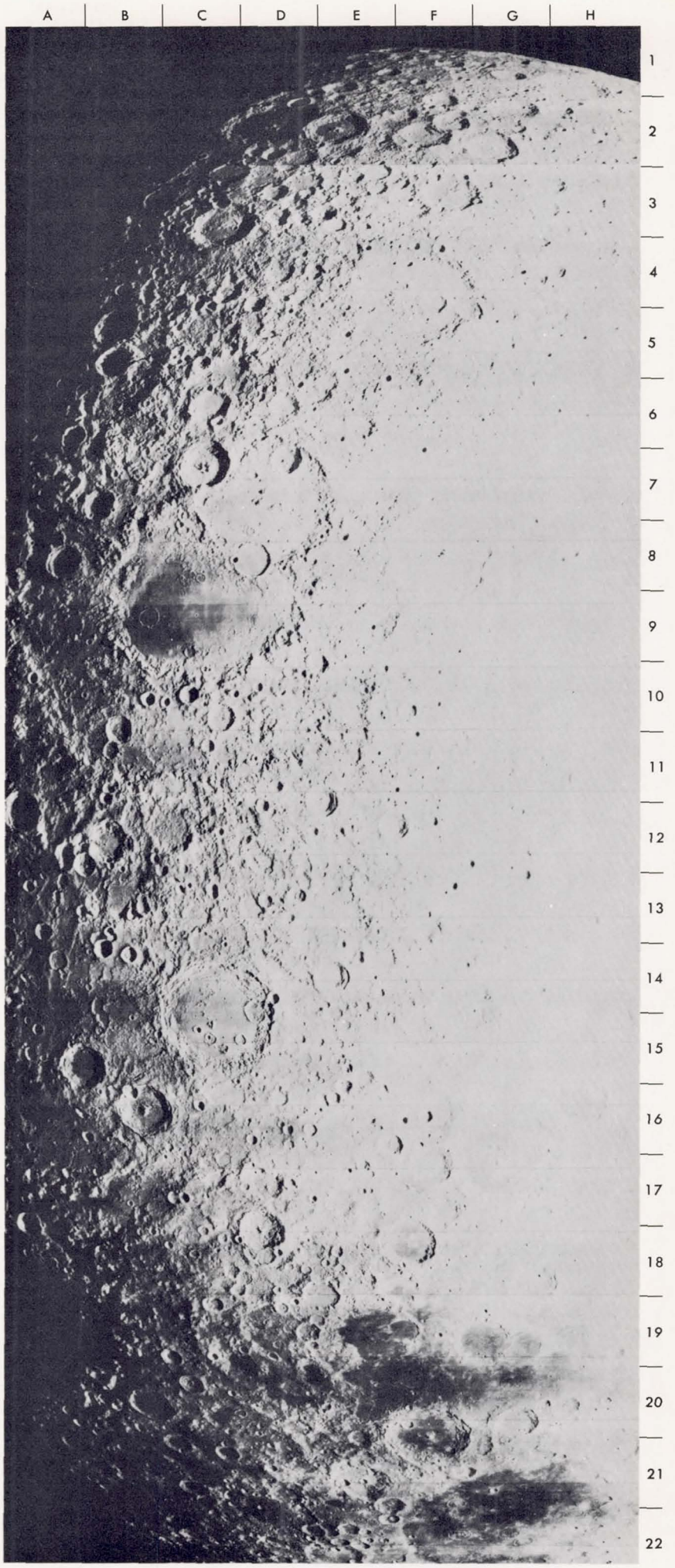

The eastern limb area in the northern hemisphere. Mare Smythii (G22) straddles the equator at longitude 90° E. North of it is Mare Marginis (F20), and west of that, at the terminator, is the circular Mare Crisium (A19). Mare Humboldtianum (C9) is about latitude 55° N. The north pole is at C2.

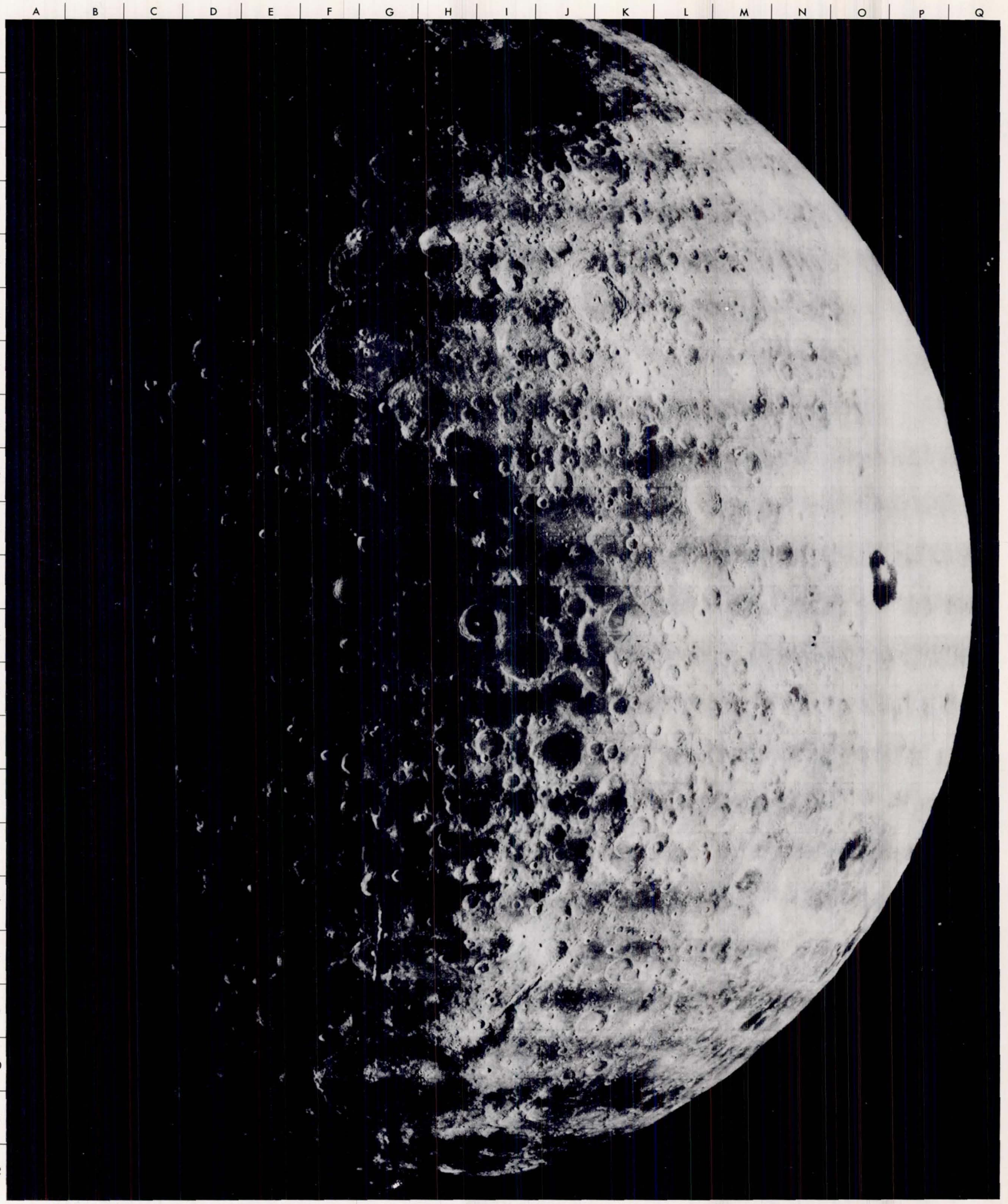

The eastern limb area in the southern hemisphere. The dark patch at I2 is Mare Smythii. The crater *Humboldt* (G7) is 200 kilometers in diameter. The large irregularly-shaped, dark area south of Humboldt is Mare Australe. The unnamed, double-walled basin at G20, with its spectacular radiating clefts, is located about 70° S, 130° E. The very prominent crater *Tsiolkovsky* (O11) is due north of it, about 20° S, 130° E. Both will be seen in detail in the next chapter.

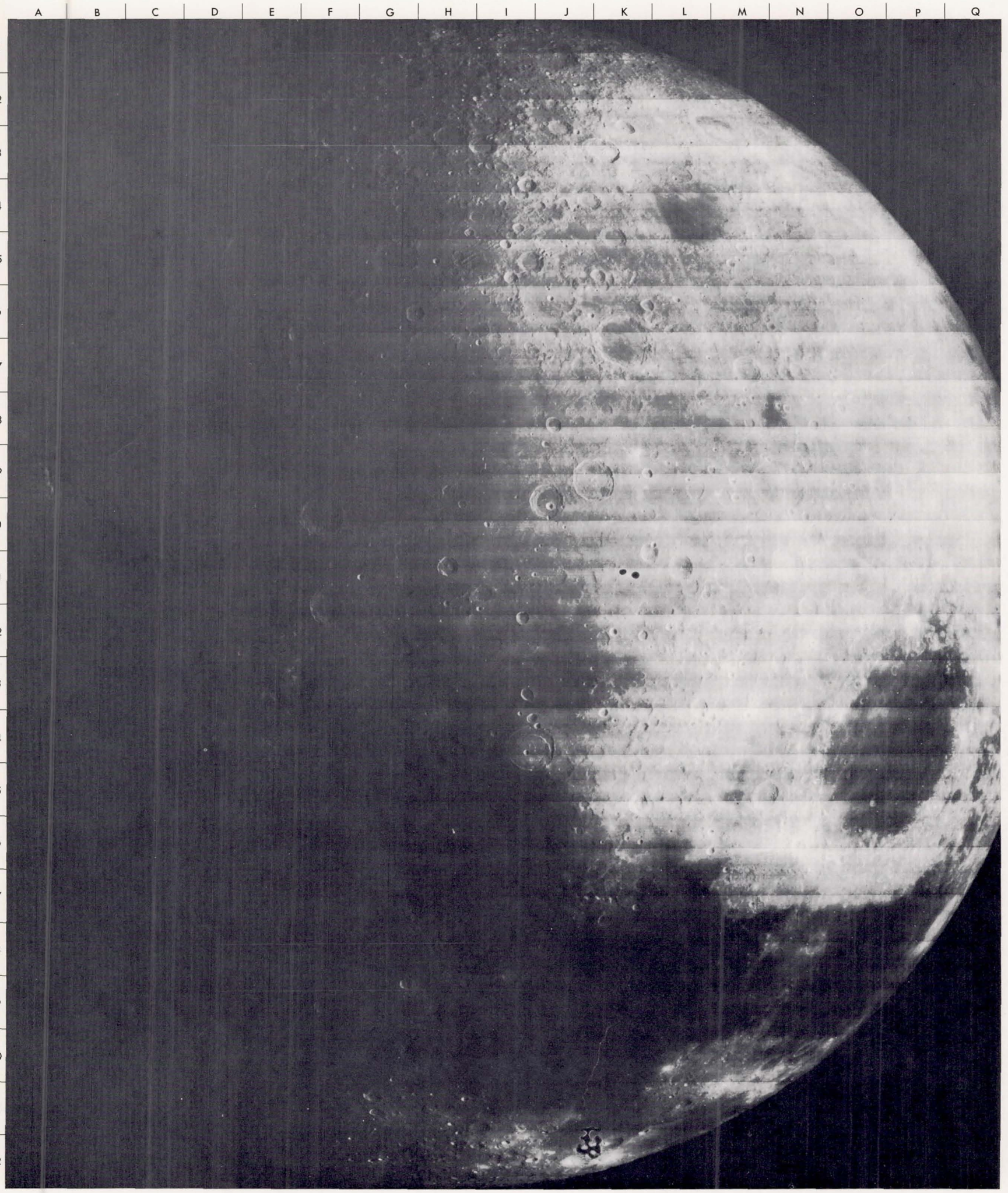

The eastern regions of the northern hemisphere. Mare Crisium is at P14, and Mare Humboldtianum at L4. The crater Endymion (K7) is 125 kilometers in diameter. Northwest of the crater Hercules (J10) is Mare Frigoris. The dark patch at N8 is Mare Struve. The crater *Posidonius* (I14) lies between Lacus Somniorum to the north and Mare Serenitatis to the south and west. The craters Atlas (K9), Macrobius (M15), and *Taruntius* (N18) mark approximately the 45° East meridian.

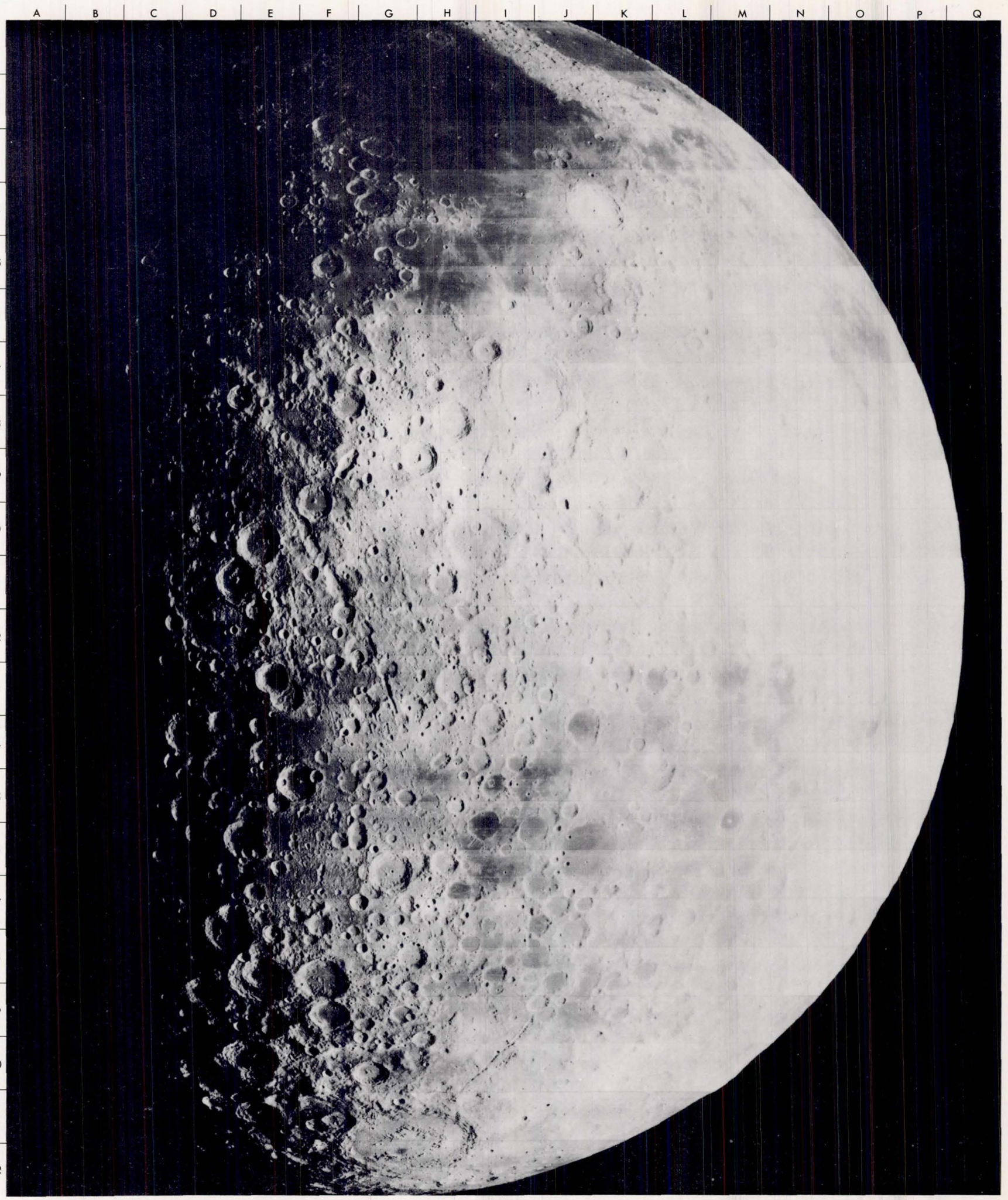

The eastern regions of the southern hemisphere. The 60° East meridian may be traced by the craters Langrenus (K4), Petavius (J7, 177 kilometers in diameter), Furnerius (I10), Boussingault (E18), and Demonax (E20). The great gash running southeastward from Mare Nectaris (whose center is at D4) is the Rheita valley. It is shown here in relation to its counterpart, the previously unknown valley that runs northward (H21 to I19) from the double-rimmed depression at the bottom of the photograph.

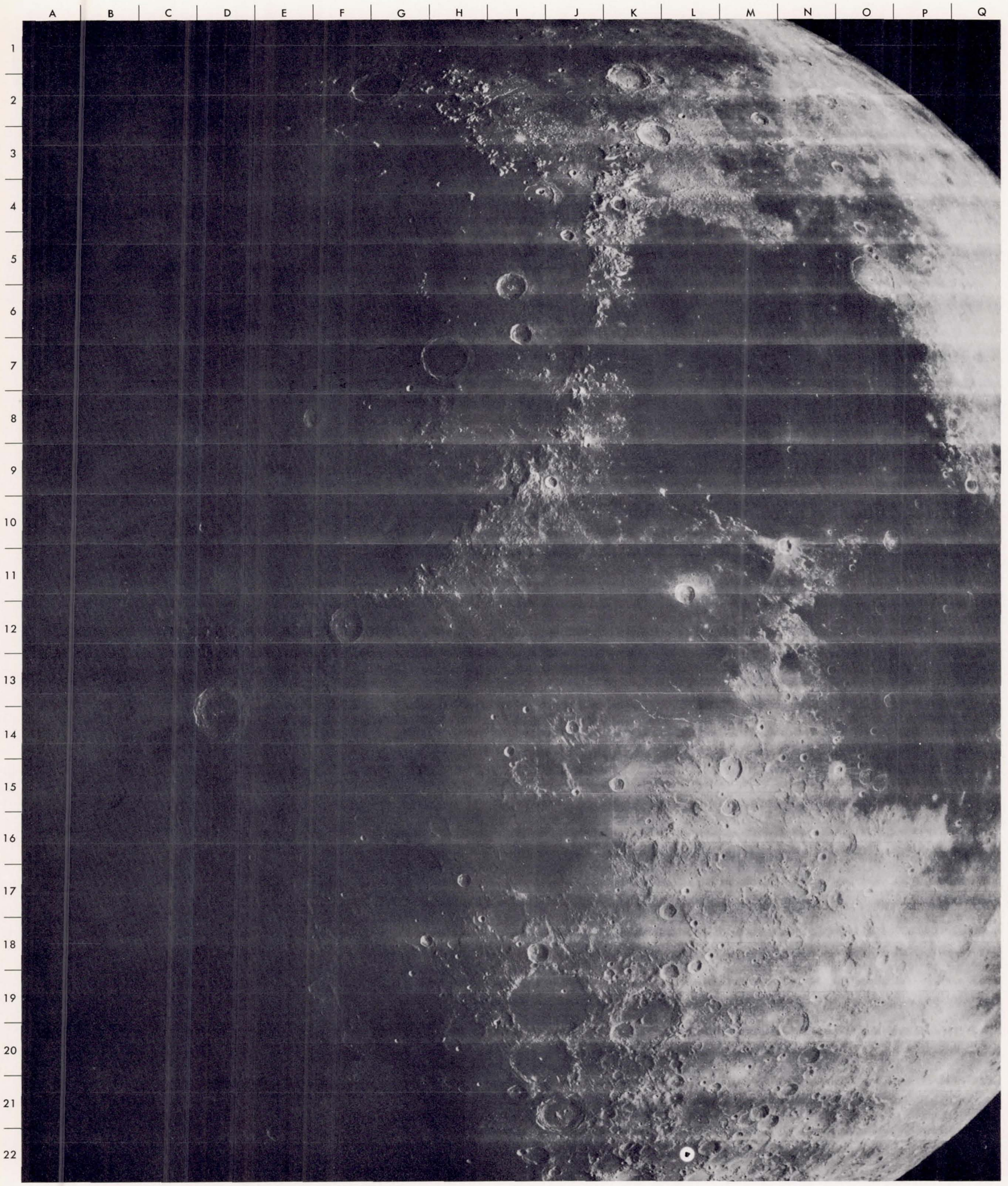

The central zone is here viewed from nearly the same direction as it is seen from Earth, but the perspective is different. Mare Imbrium, at upper left, is outlined by its great circular mountain rim. Mare Serenitatis (N7) is also circular, with a more subdued border. Below them is Mare Vaporum, with the crater Manilius at L11. The small patch of mare below that, at J16, is Sinus Medii, which is at the center of the frontside. The crater Ptolemaeus (J19) is 153 kilometers in diameter.

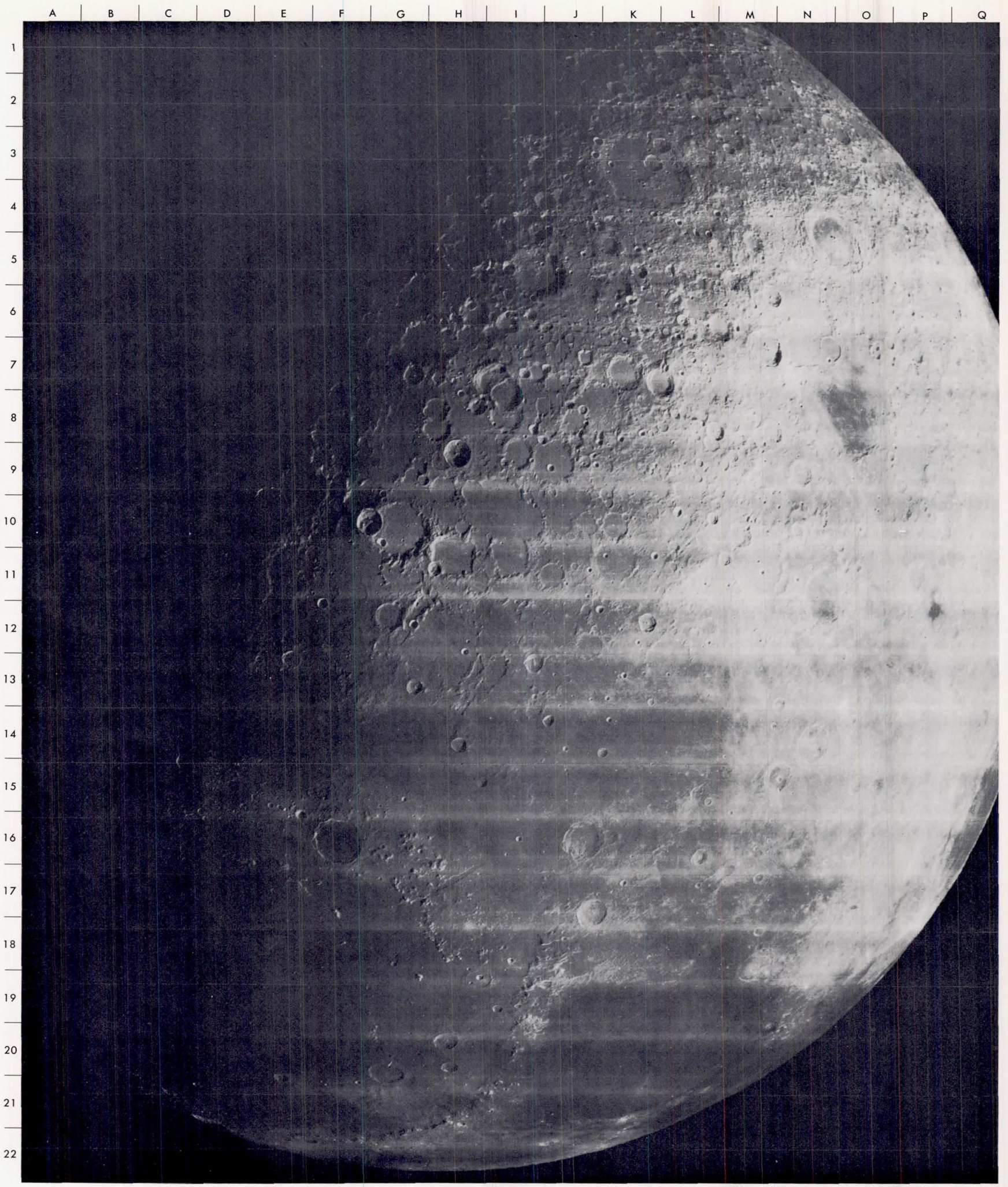

The north polar region as viewed from above. The sunrise terminator runs along the 31° West meridian, crossing (from south to north) Mare Imbrium and Mare Frigoris, the craters Philolaus (E10) and Mouchez (F8), and the north pole (G5), just outside the crater Peary. Beyond there, it becomes the sunset terminator, running southward along the 149° East meridian on the farside. The crater Nansen (I5) is 110 kilometers across. Barrow (H11) is a crater with a notably square outline.

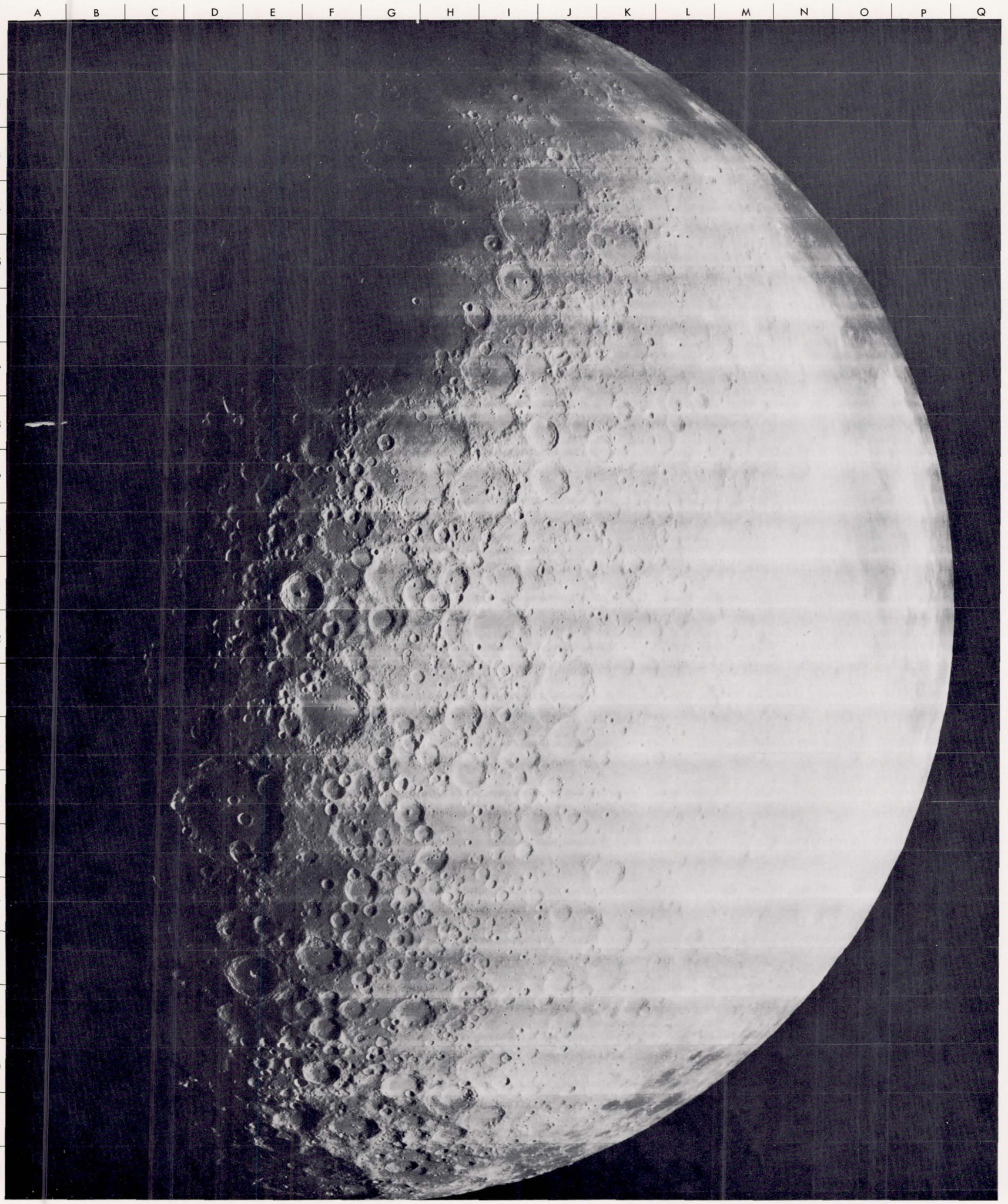

The south central region. The sunrise terminator is about 24° W. The 0° meridian crosses the craters Ptolemaeus (J4), Walter (I9), and Moretus (E18, located 70° S). The crater Pitatus (F7), marking the southern edge of Mare Nubium, the very fresh crater *Tycho* (F11), and the 225-kilometer-diameter crater Clavius (D15), lie to the west. To the east are the craters Maurolycus (J13), Manzinus (H19), Scott (E21), and Amundsen (E22). The south pole (D21) is near the last-named crater.

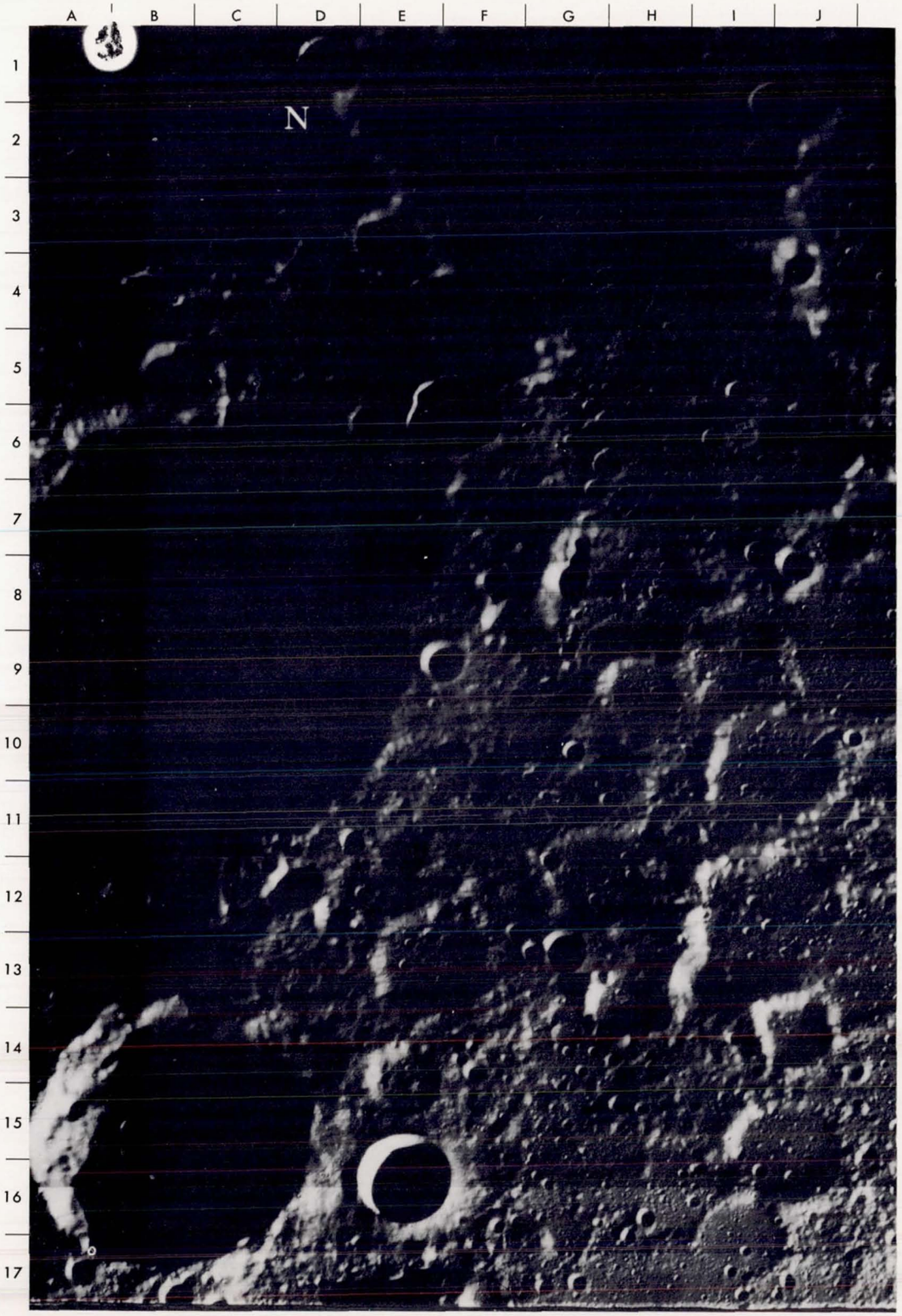

A closeup of the north polar area. The pole (D2, marked with an N) is in the shadow just outside the crater Peary (G2). The crater Hermite (C8), located about 86°N, 60°W, is 109 kilometers across. The very low solar elevation brings out the apparent squareness of the shallow depressions at E13, G12, and J14.

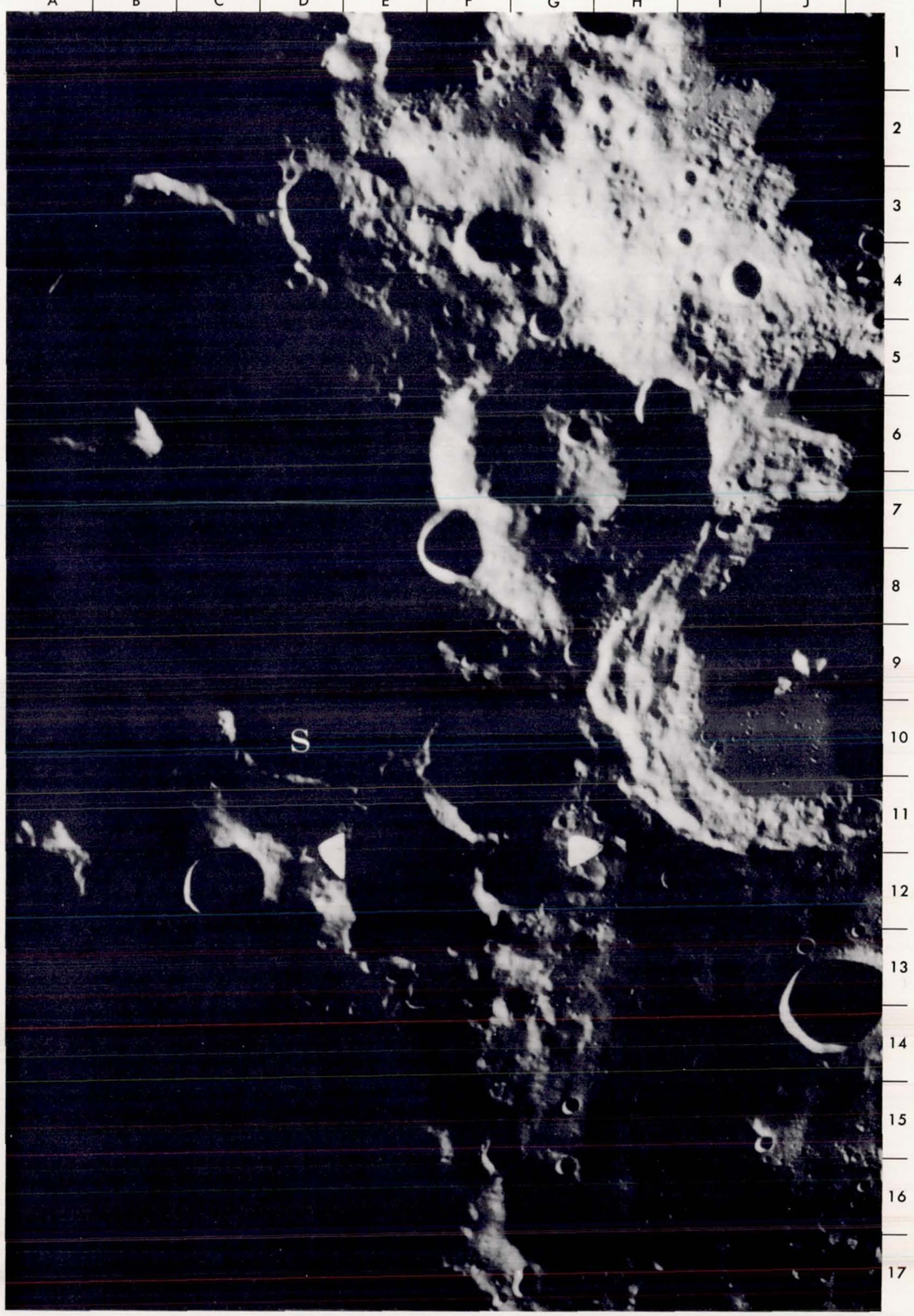

A closer look at the south polar area. The pole (D10, marked with an S) is in shadow. The crater Scott (J2), located about 82°S, 45°E, is 108 kilometers in diameter. The crater Amundsen (J9) is southeast of Scott. The two white triangular marks at D12 and G12 are processing blemishes.

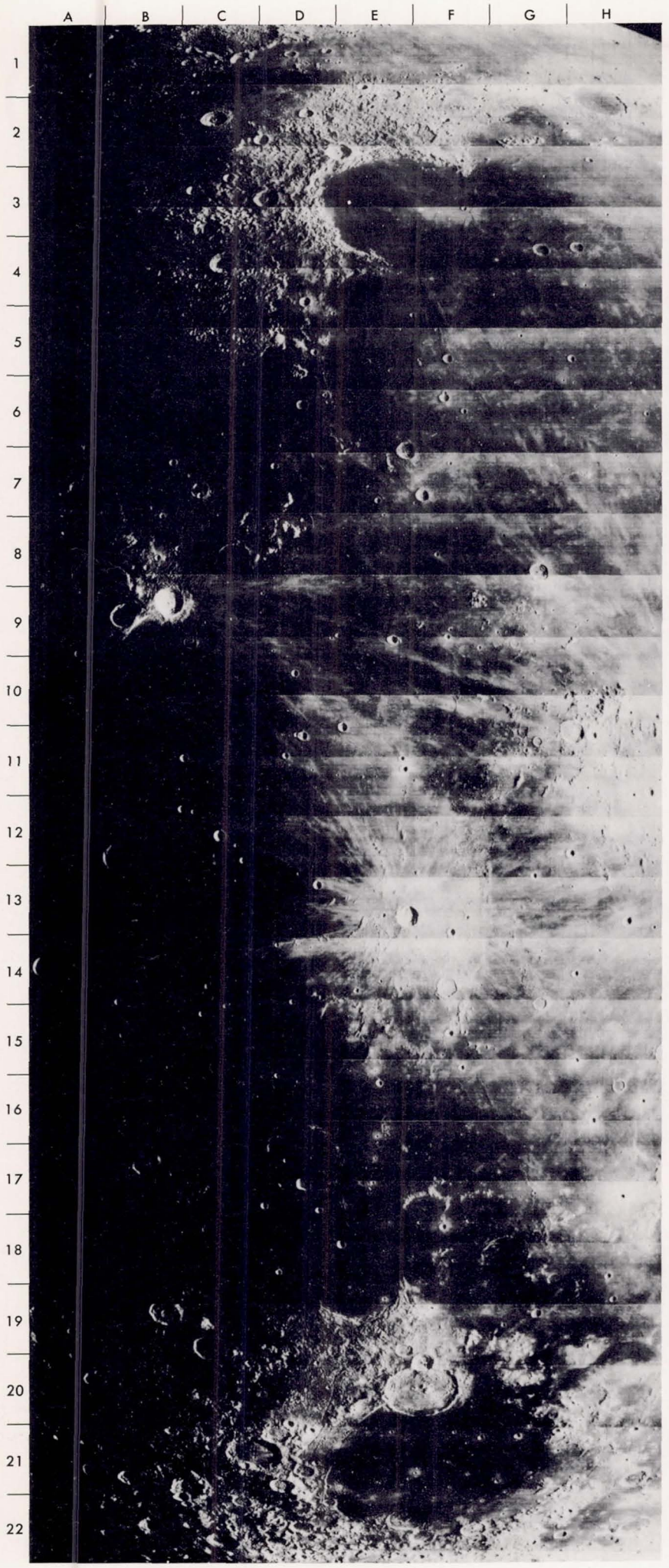

The zone along the 40° West meridian is mainly mare terrain. Oceanus Procellarum, with its widespread rays from *Kepler* (E13) and *Aristarchus* (B9), covers most of the picture. Sinus Iridum (E3) is the semicircular bay at the northwest edge of Mare Imbrium. The crater Euler (G8) is 27 kilometers in diameter.

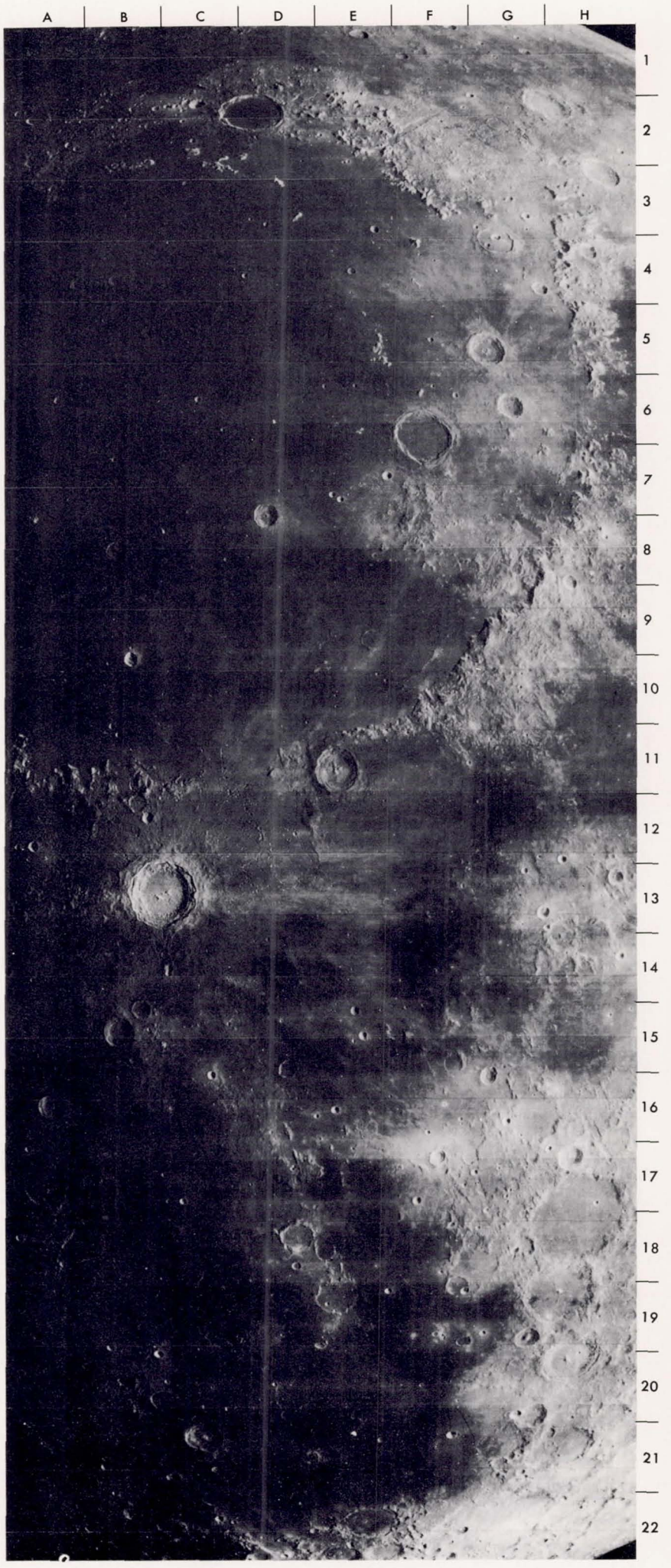

The 10° West meridian passes through the crater *Plato* (D2), which is 100 kilometers in diameter, and just east of the craters Eratosthenes (E11) and Pitatus (E22). Rays from *Copernicus* (C13) are spread across Sinus Aestuum to the east and Mare Imbrium to the north. The crater Lansberg (A16) is on the equator.

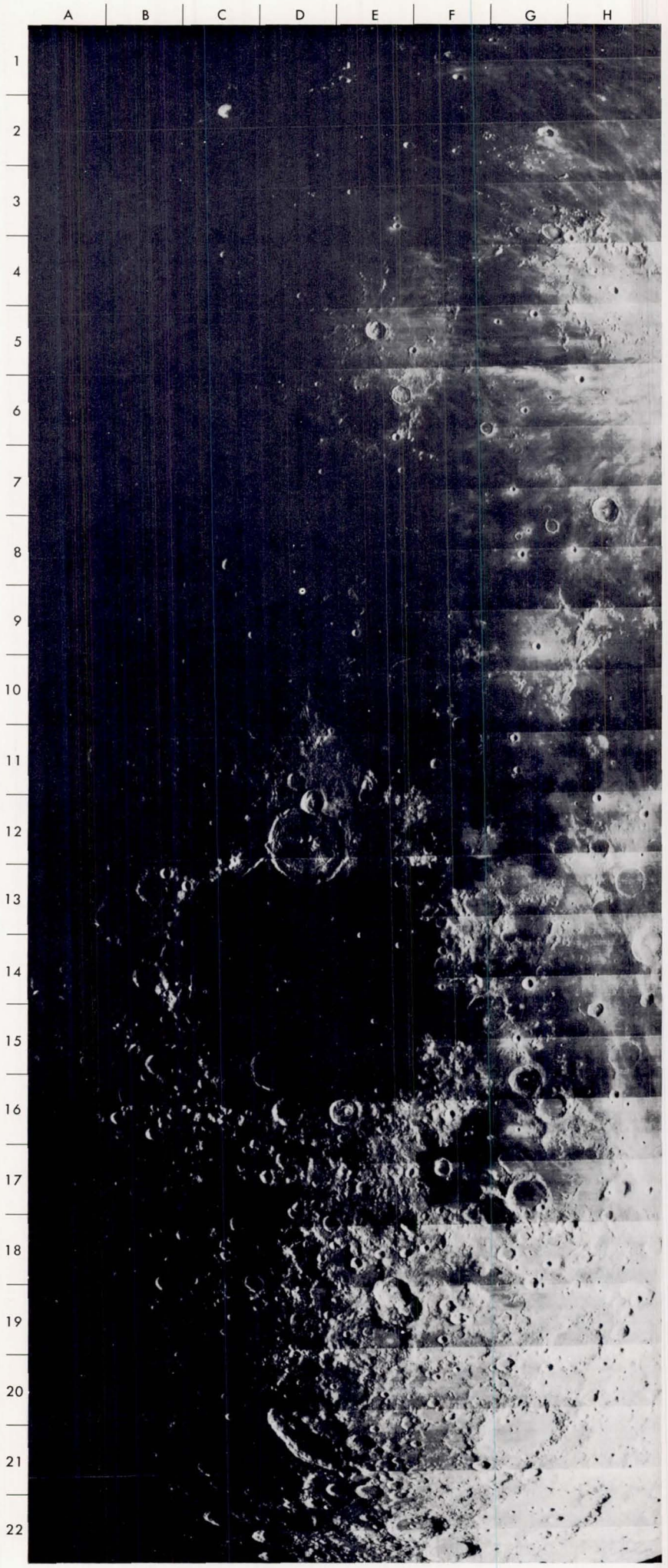

Running southward from the vicinity of *Kepler* (E5), the 40°W meridian crosses the crater *Gassendi* (D12), which is 64 kilometers across, then the circular Mare Humorum. In the highland region to the south, it crosses the crater Schiller (D21). Schiller, at 52°S, is distinguished by its footprint shape.

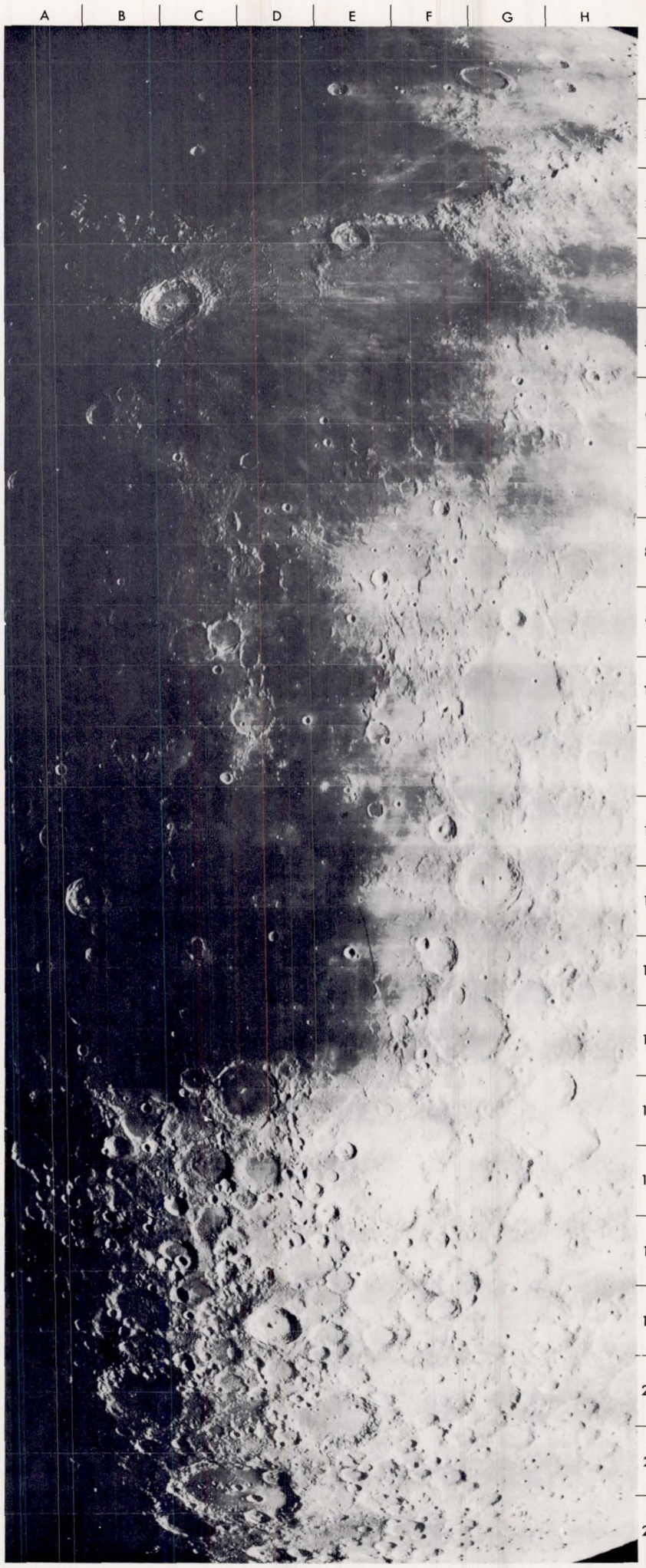

The zone just west of the center, mainly in the southern hemisphere. Within Mare Nubium are the *Straight Wall* (E14), 120 kilometers long, and the crater Bullialdus (B13). Ranger VII made the first closeup photographs of the Moon at B10, in Mare Cognitum. Ranger IX photographed the crater Alphonsus (G11).

The western limb area in the northern hemisphere. The sunrise terminator runs along the 98° West meridian, from the Cordillera Mountains (C22) to the north pole (A2). Note the intersecting rille patterns crossing the craters Repsold (D9) and Galvani (C10). The crater Pythagoras (D6) is 128 kilometers across.

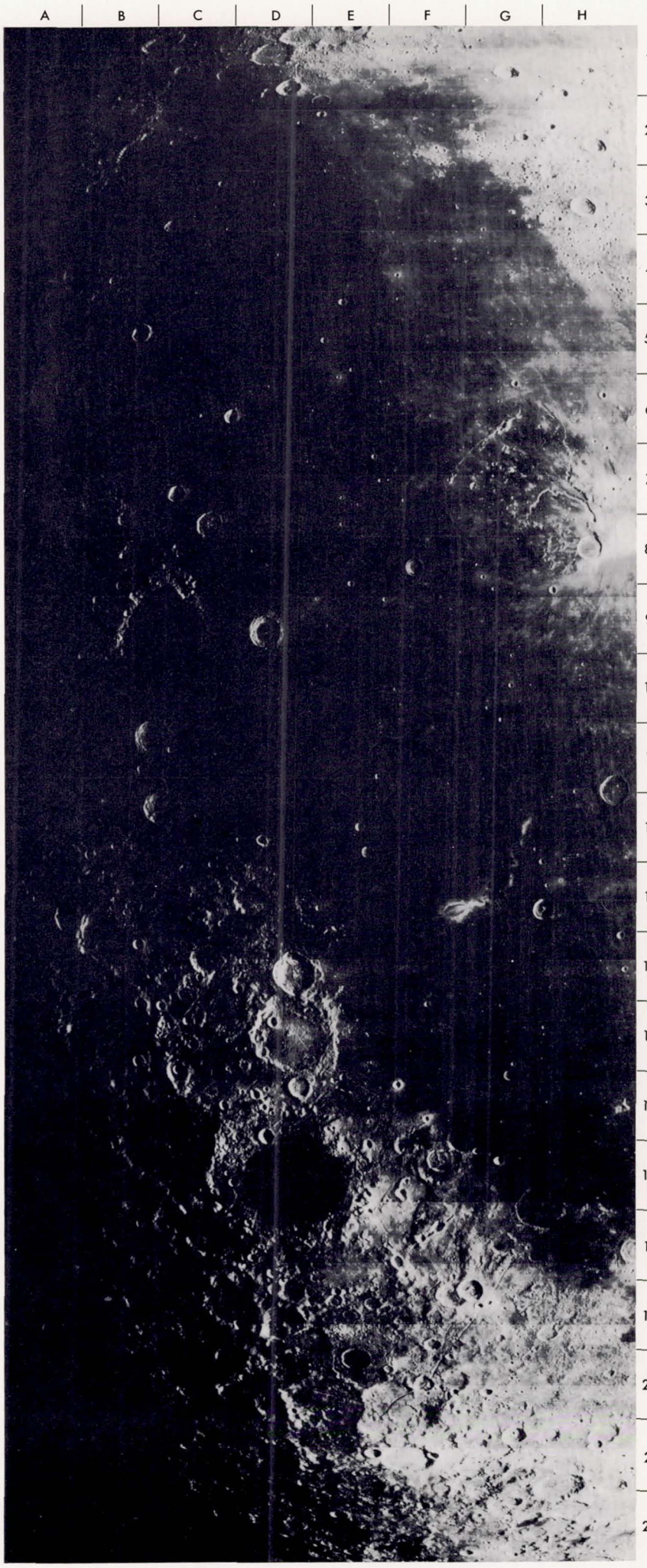

The western portion of Oceanus Procellarum, with its widespread, irregular bright markings near the craters Seleucus (D9) and Reiner (G13). The dark-floored crater Grimaldi (D17) is about 220 kilometers in diameter, and can be considered as a small circular mare. The terminator is at 80°W.

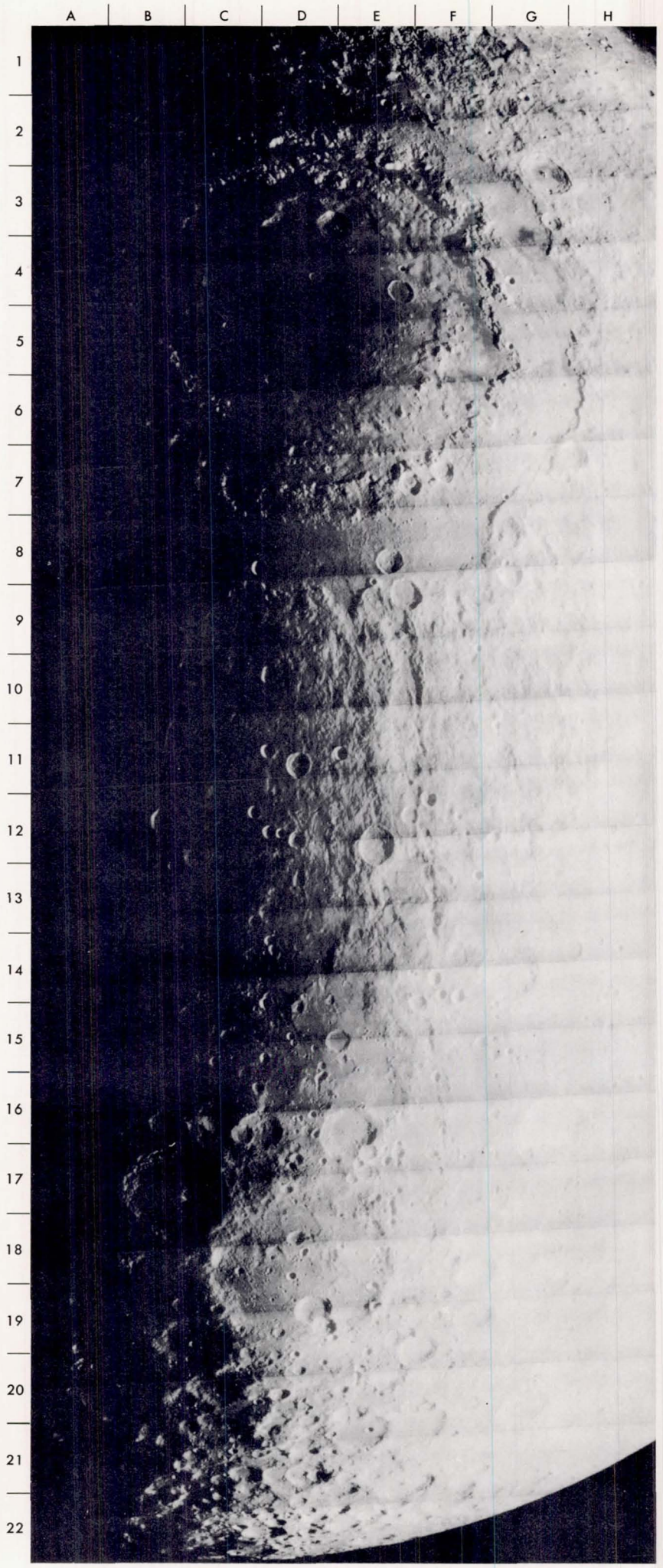

The western limb area in the southern hemisphere. The center of *Mare Orientale* (D5) is located about 20°S,95°W. The prominent crater Hausen at C17 is about 65°S, 90°W. The light-floored circular plain just southeast of it (D19) is Bailly, which is 300 kilometers in diameter.

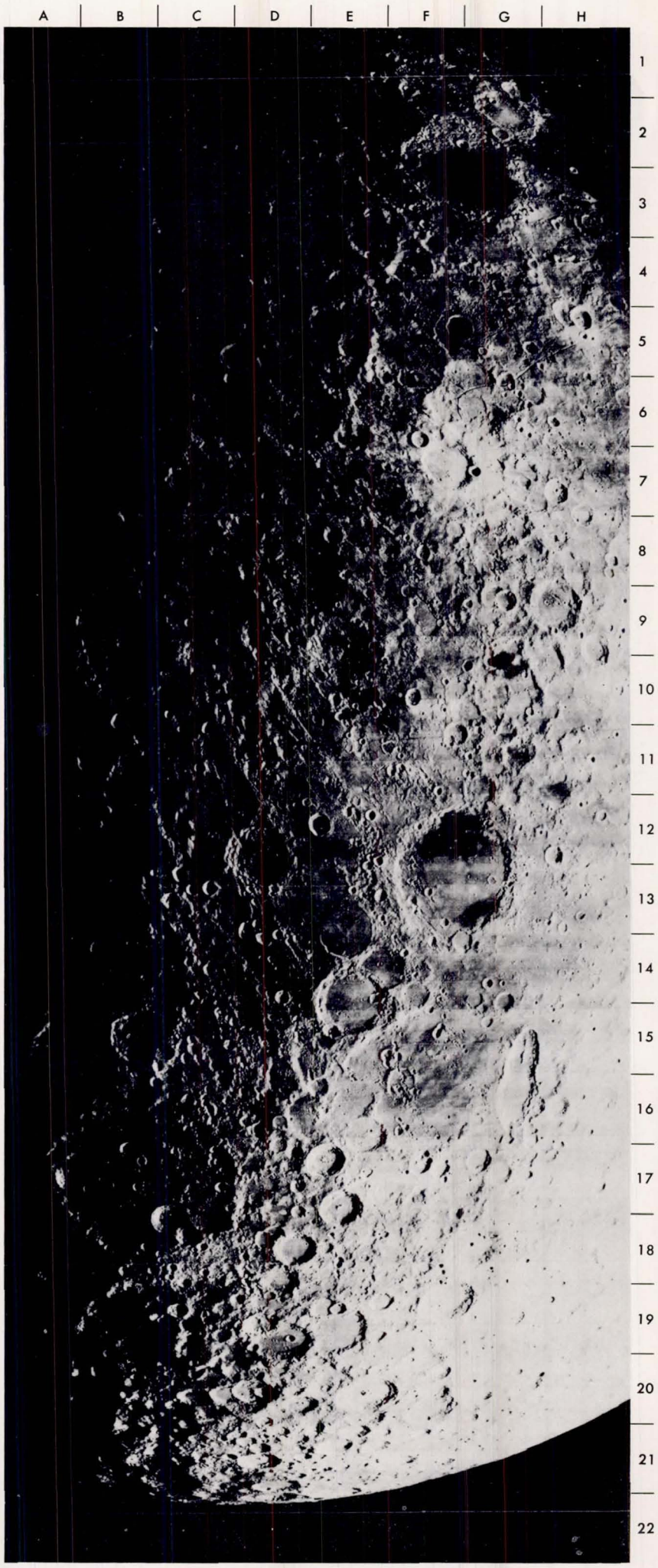

The southern hemisphere centered about 70°W. The elongated features of sculpture and deposition radiating from Mare Orientale are apparent at upper left. The dark-floored crater Schickard (F13) is 230 kilometers across. A very sharp rille runs between the craters *Byrgius* (F7) and Sirsalis (H5).

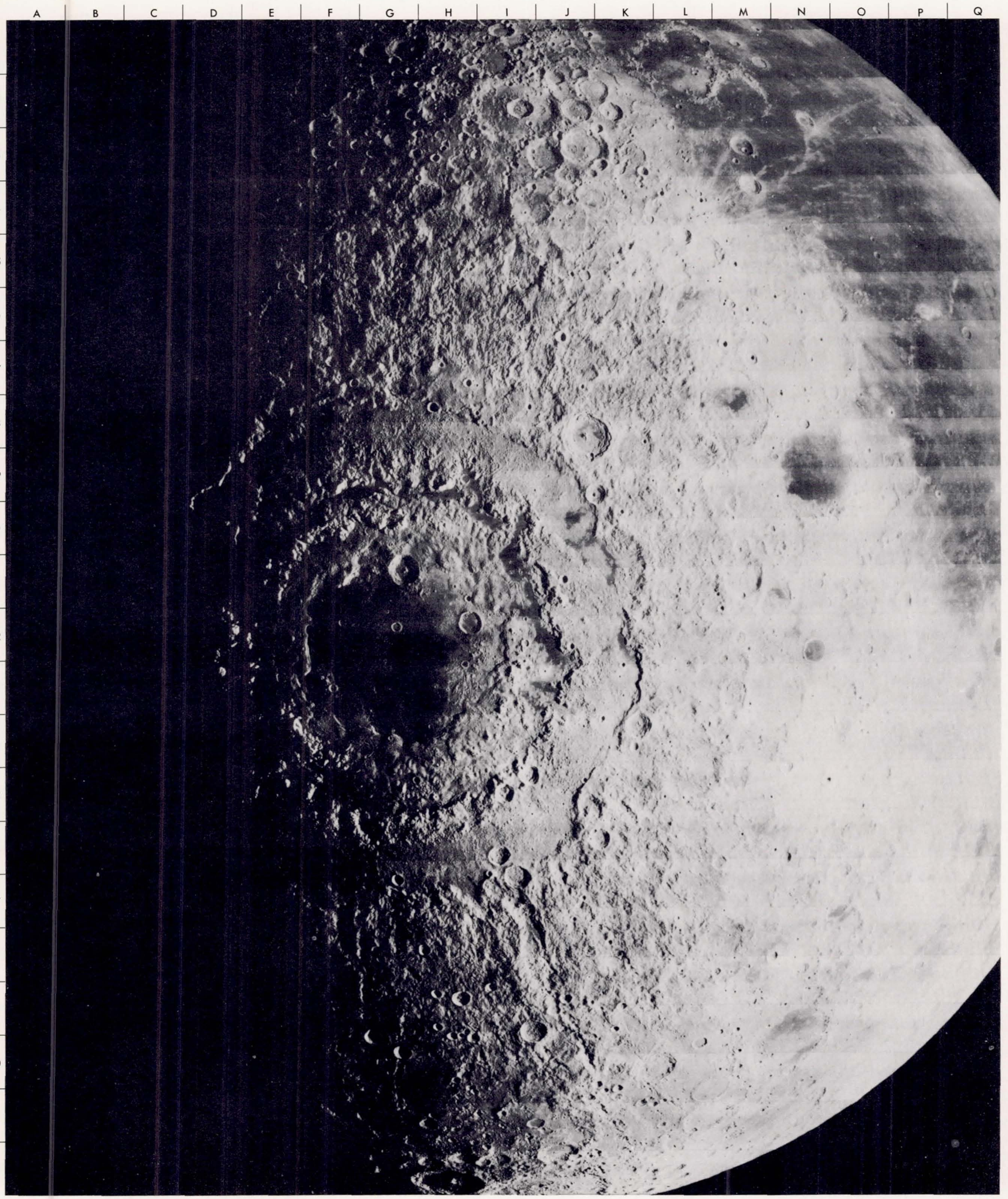

The "bull's eye" at the center of this spectacular view is the Mare Orientale basin (the name Mare Annulatum has also been proposed), on the extreme western edge of the visible side. Three circular scarps surround the inner basin, which is partially filled with mare material. The outermost is the Cordillera Mountain scarp, almost 900 kilometers in diameter. The craters Schlüter (J8), Riccioli (M8), and Inghirami (L20) are all located within the area that was blanketed by deposits of material ejected from Orientale. Detailed views of characteristic portions of the basin are shown on pages 125 through 131 .

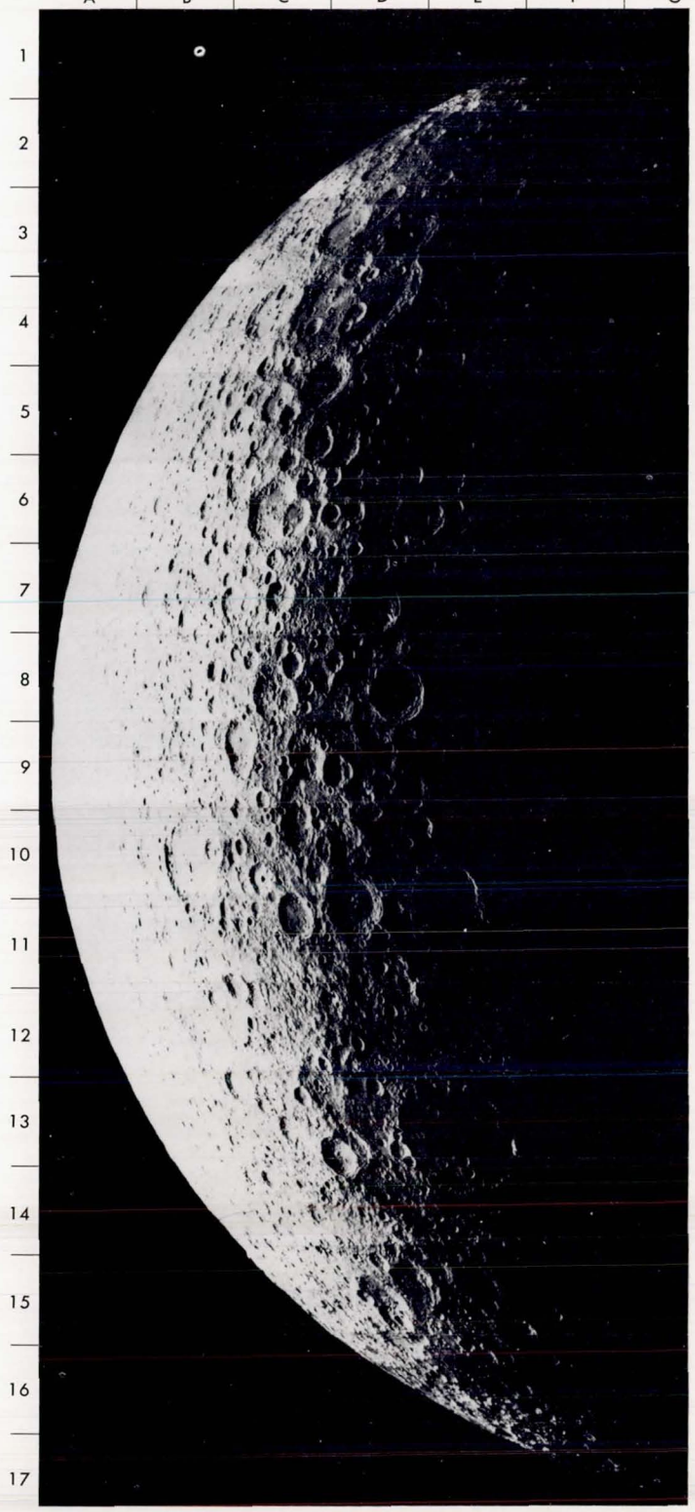

The equatorial zone of the eastern farside. The terminator is at 125°W. The sharply defined crater at D13 is located on the equator near the 140° West meridian, which also passes through the craters at C5 and C11.

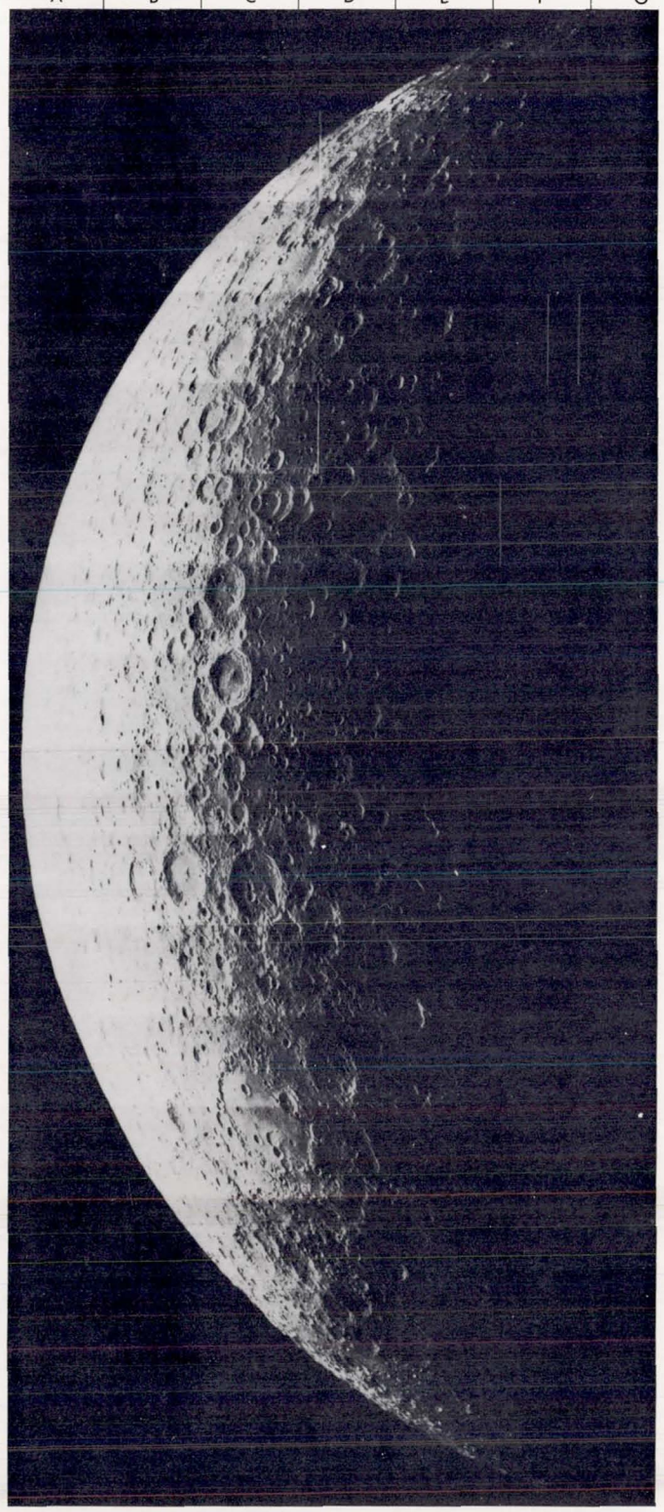

Equatorial zone of the eastern farside. The pattern of overlapping arcs of crater walls at C6, located about 43°N, 130°W, was produced by a series of successively (right to left) younger craters. The terminator is at 112°W.

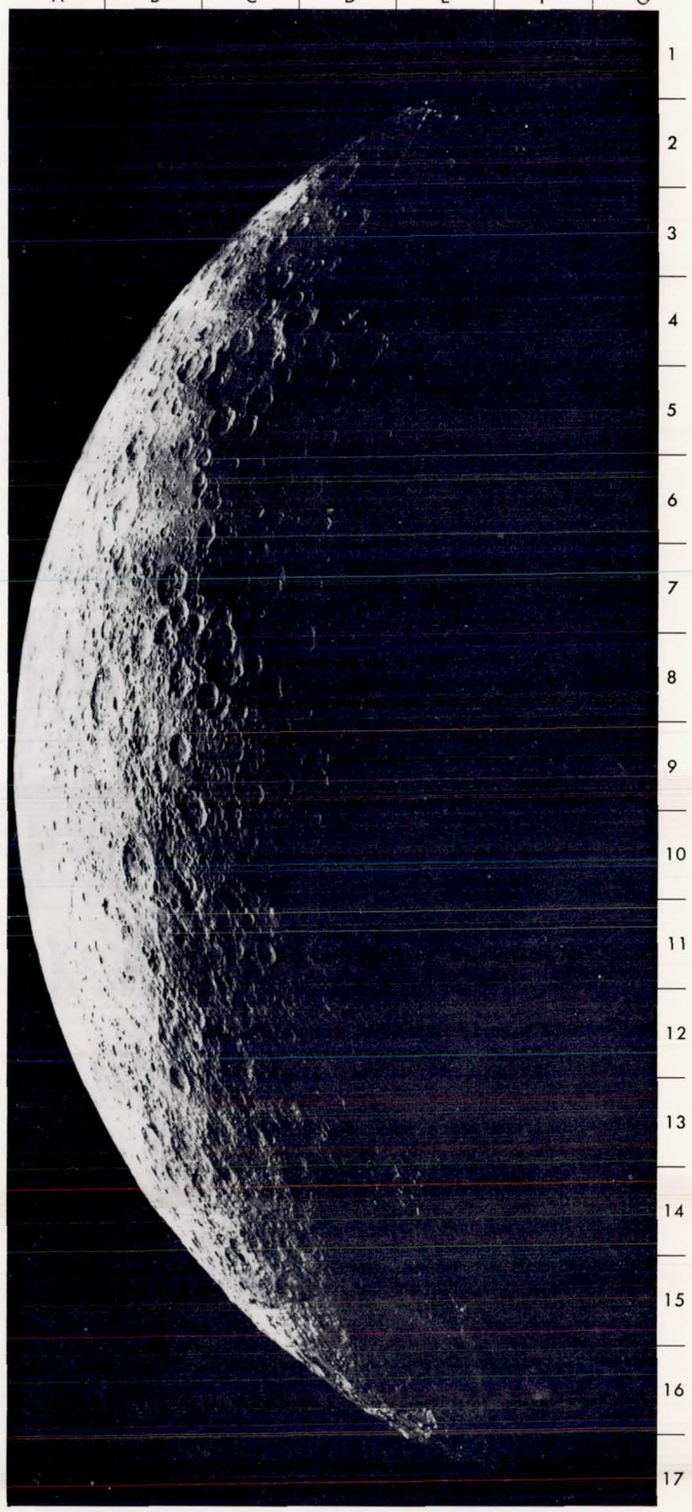

The equatorial zone of the eastern farside, just past the limb. Crater chains radiate from *Mare Orientale* (F14). Two of these chains end within the crater at B8, which is located about 18°N, 128°W. The sunset terminator is at 100°W.

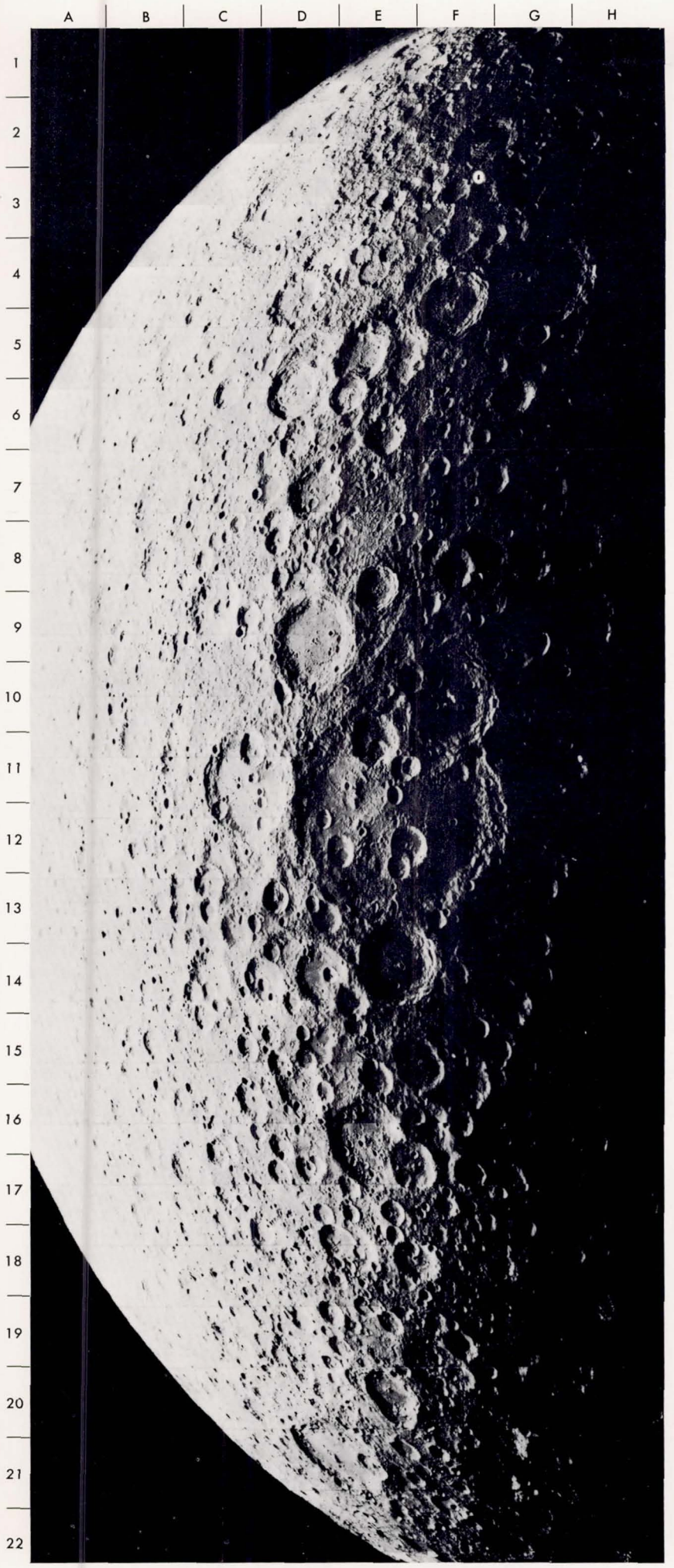

The northern region of the eastern farside. The large circular depression centered on E12 is more than 250 kilometers across, and is located about 58°N, 150°W. Its floor lacks the smooth dark-toned surface seen in maria. Such basins are somewhat more abundant on the farside than on the frontside.

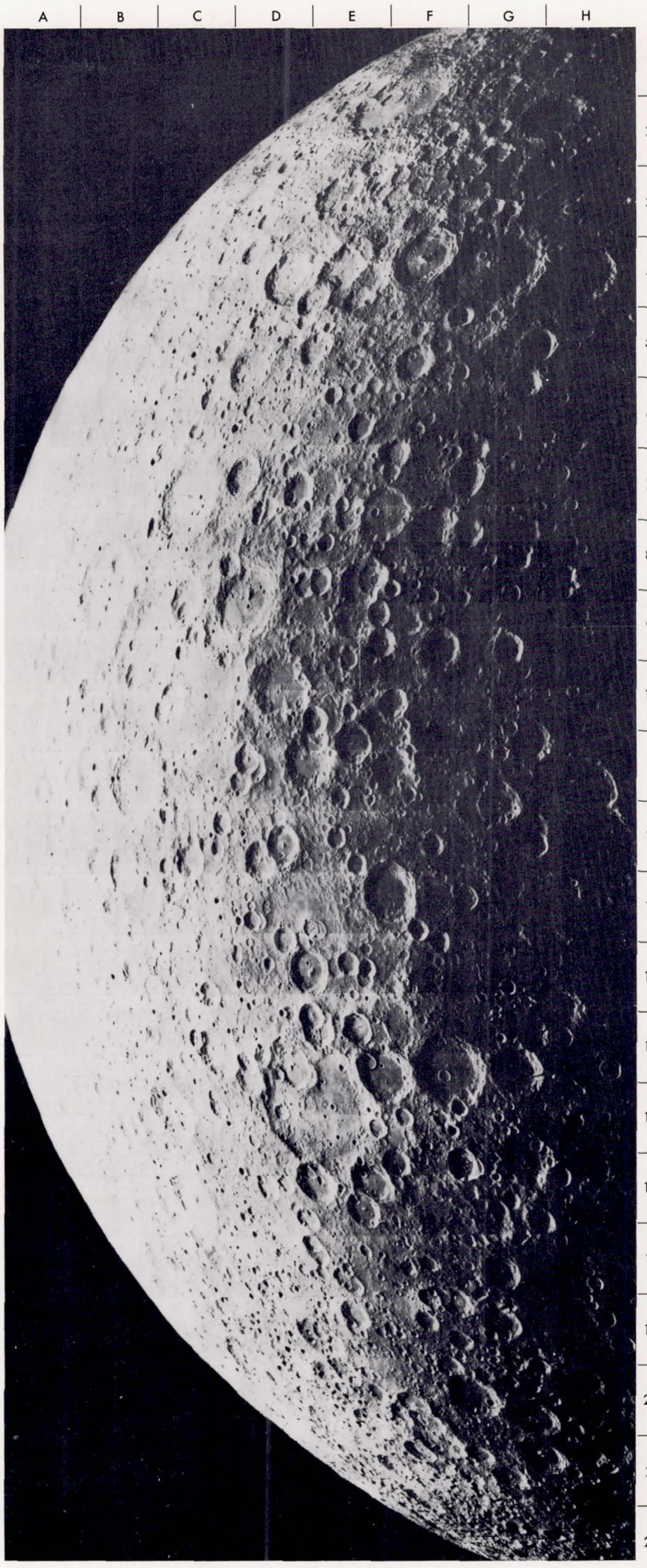

The northern region of the eastern farside. The north pole is at H3. The basin at C10 is quite inconspicuous in this photograph, where the terminator is at 99°W, although it was very distinct on the photograph to the left, where the terminator was 30° further west.

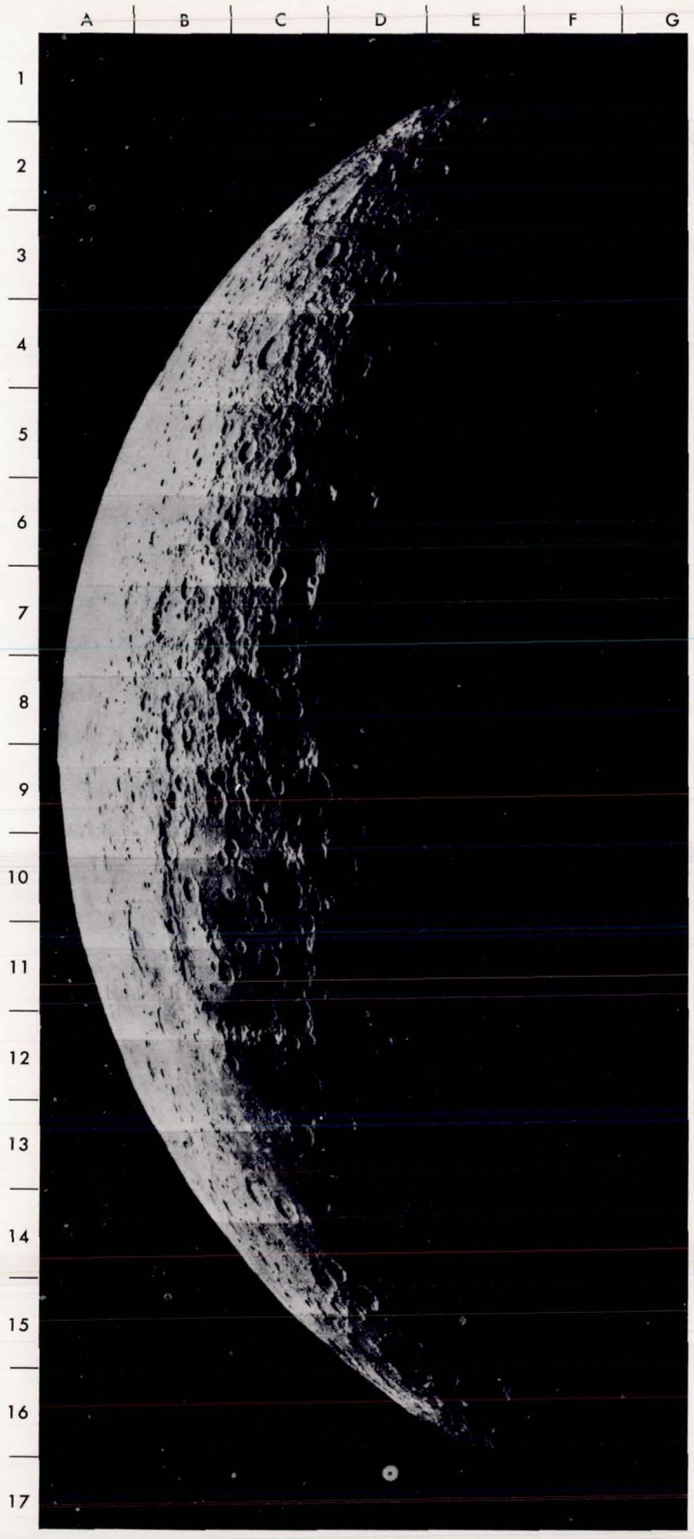

The basin at C11, which is about 350 kilometers across, is located about 37°S, 152°W. It resembles the much larger *Mare Orientale* (Mare Annulatum) in its concentric pattern, and in its partial flooding with dark-toned material. The terminator is at 131°W.

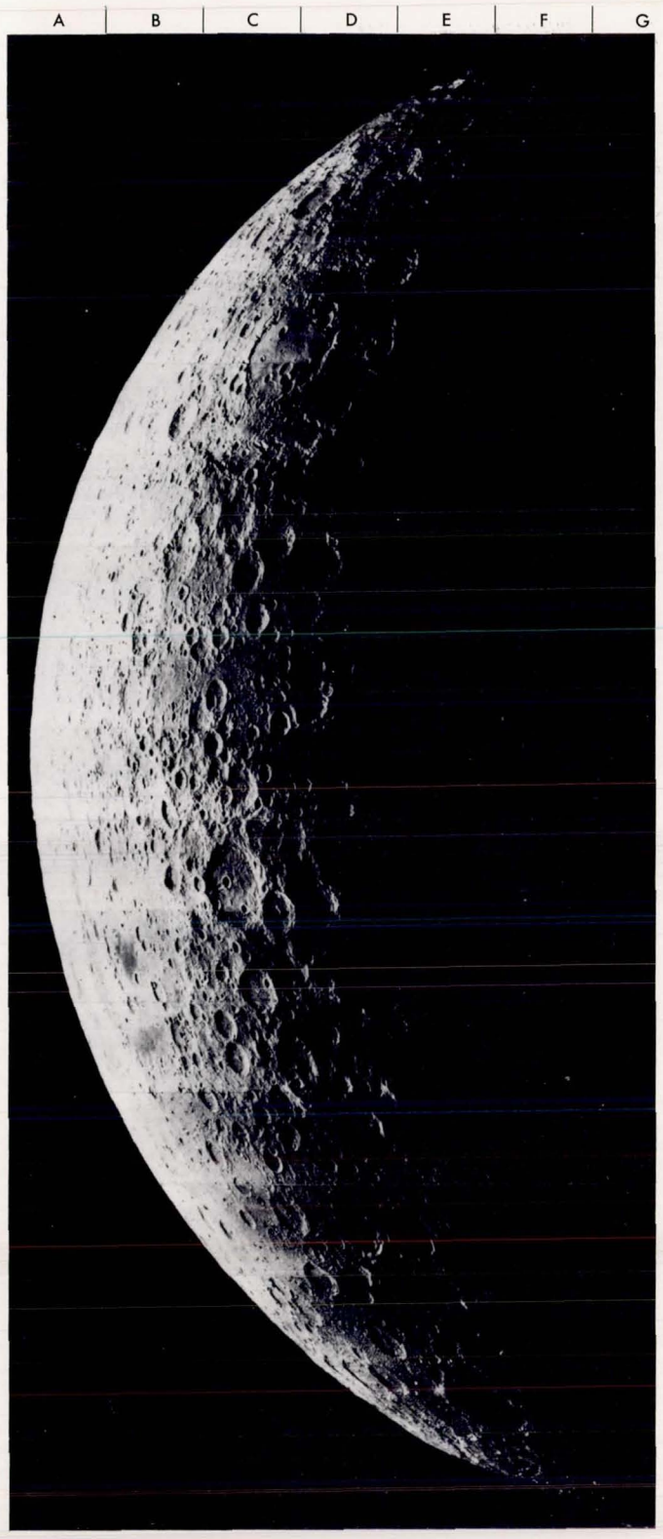

The terminator is at 120°W. The large light-floored circular depression (basin) centered at C4 is located on the equator, about 128°W. Its subdued outer rim is over 400 kilometers across. It is also visible in the middle photograph on page 20 .

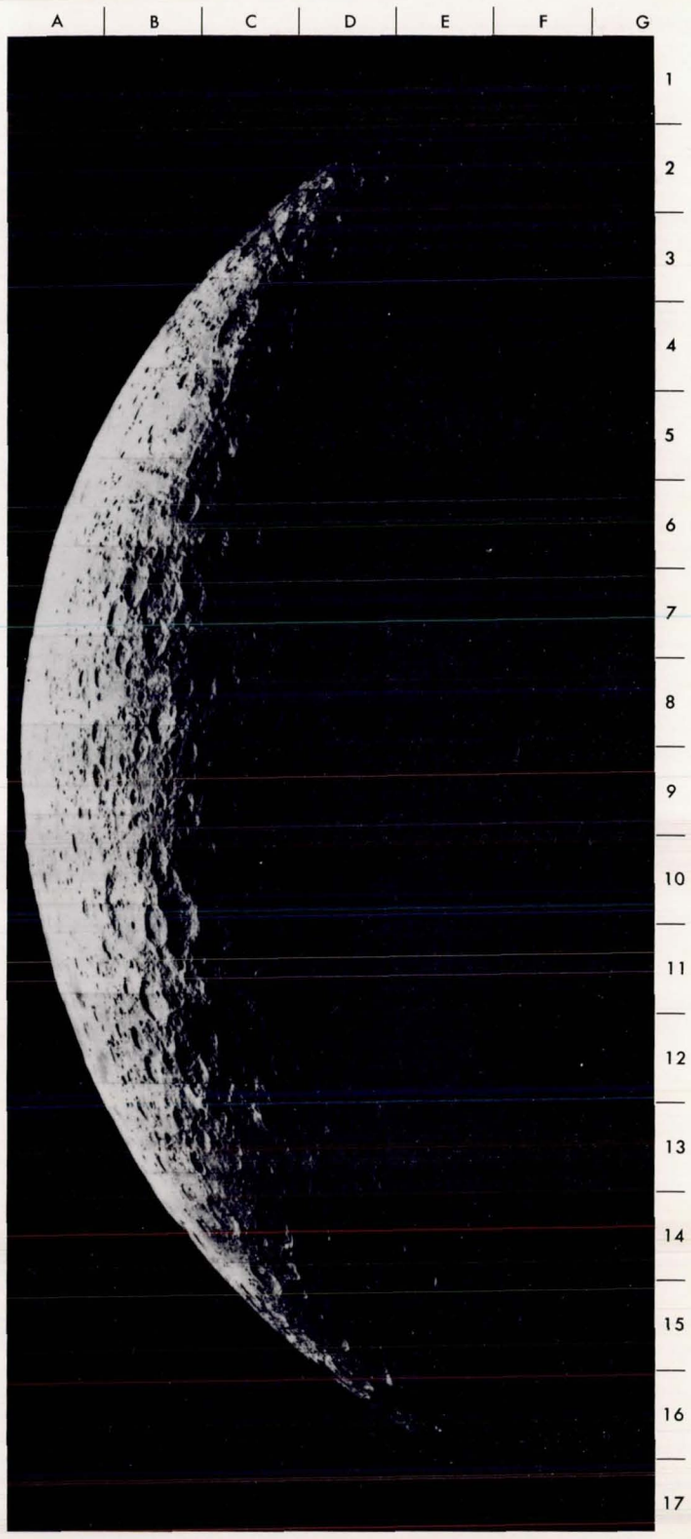

All three photographs on this page are in the southern zone of the eastern farside. The terminator here is at 106°W. Crater chains radiating from *Mare Orientale* dominate the picture . The irregular crater at B8 is located about 22°S, 125°W.

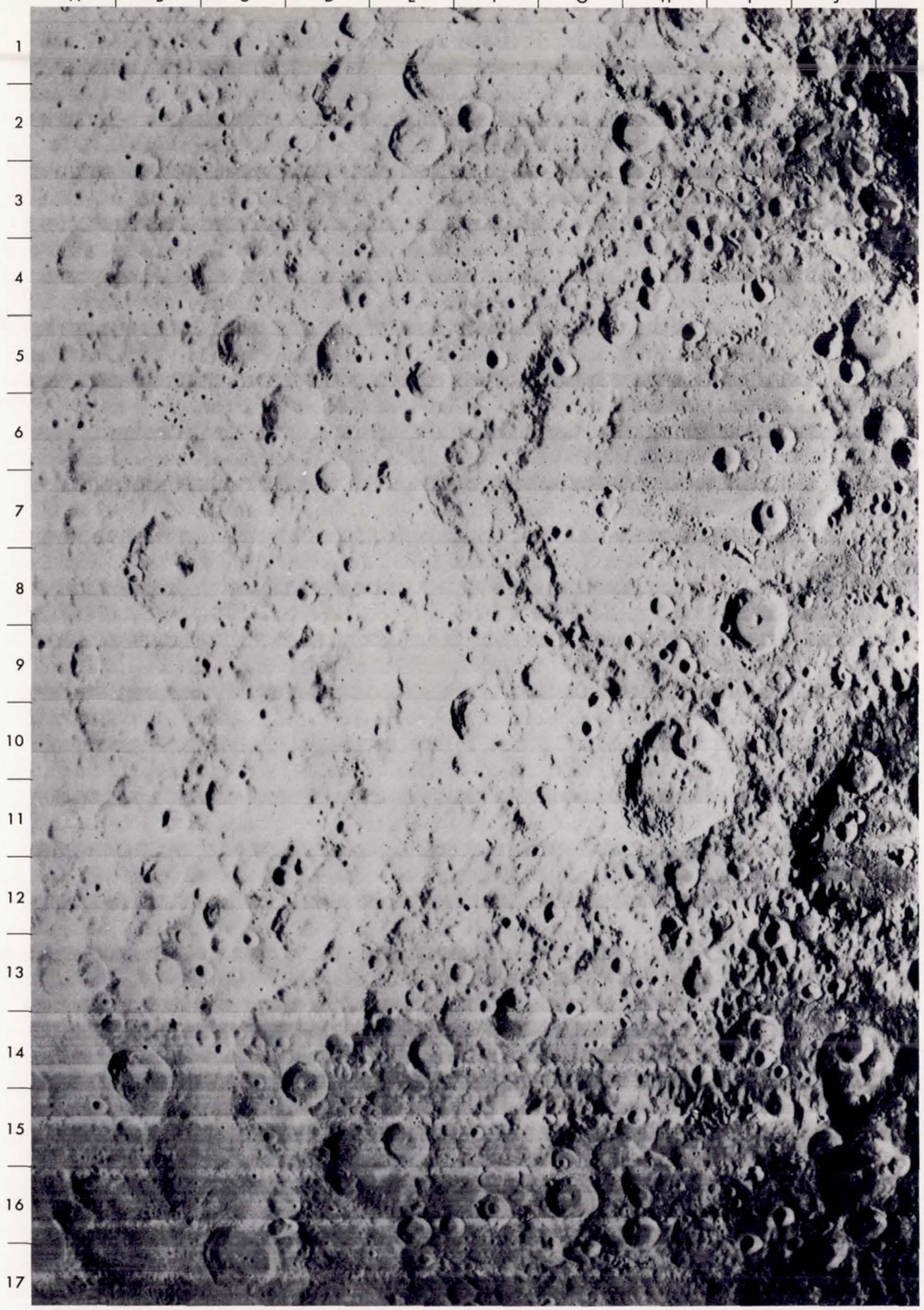

The equatorial zone of the eastern farside. Both of the photographs on this page were made by Lunar Orbiter I, with the terminator at 142° W. Although they overlap in coverage, they are not positioned here for best stereoscopic viewing. The crater with a central peak at B8 is located about 5° S, 174° W.

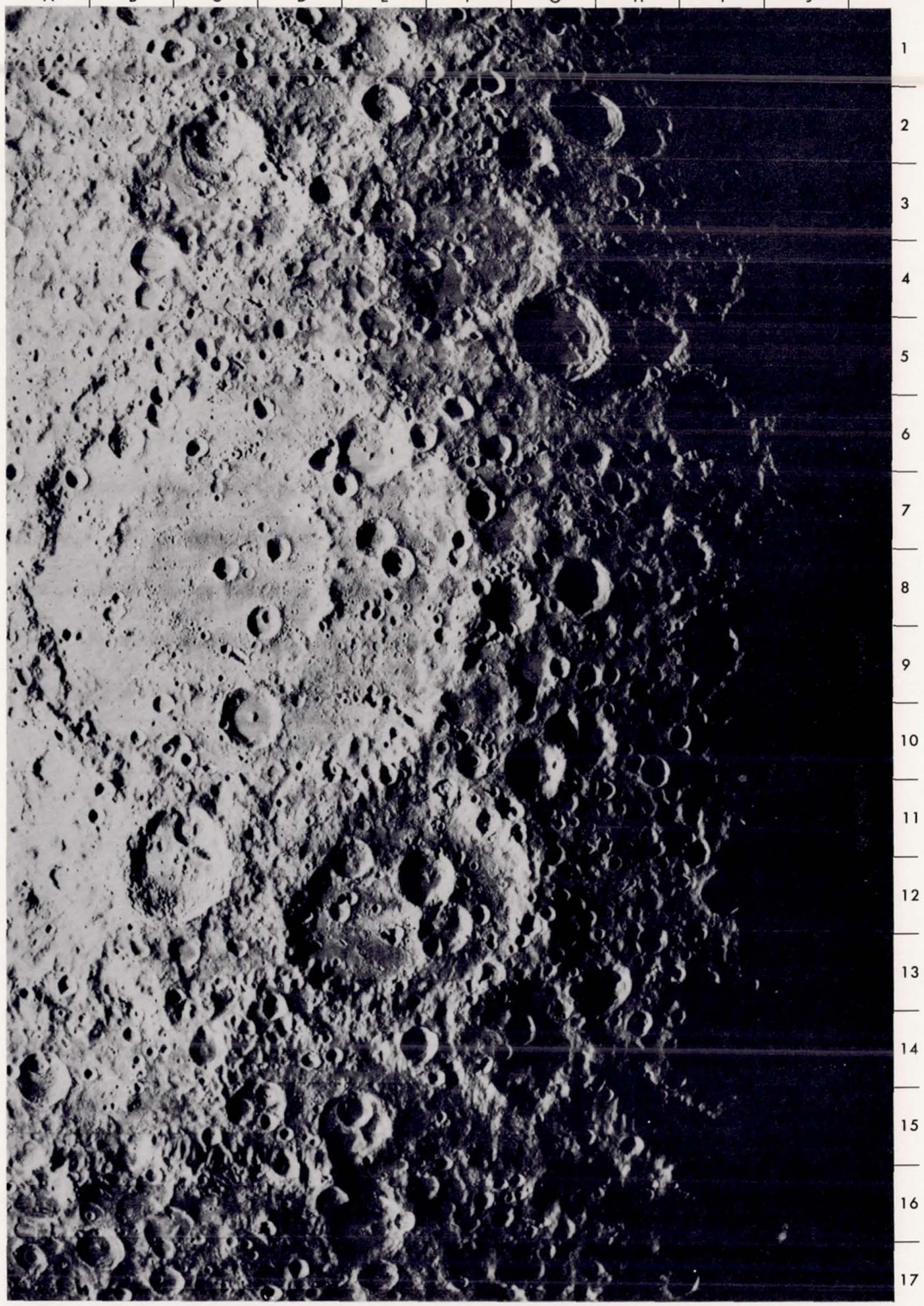

The most prominent large-scale feature of this region is the basin whose center is at C8. It is about 300 kilometers in diameter, and is located about 3° S, 158° W. It has a ring of subdued hills concentric with its outer rim. The many craters in its floor indicate that it is a relatively old structure.

Oblique view of the north central region of the farside, looking northward from an altitude of 1450 kilometers. The terminator is at 172°W. The large crater at L2 is located on the 180° meridian at 30°N. From there the meridian slants down to its intersection with the equator at P15. The crater with the central peak at E16 is on the equator about 163°E. With the exception of the small portion of *Mare Moscoviense* visible at A5, this entire region is one of highland terrain. The elongated crater at J4 resembles the frontside crater Schiller (see page 16) in having a line of central peaks along its longer axis.

The middle of the Moon's farside. The crater at J8, with the diagonal ridges and grooves on its floor, is located about 7°S, 172°E. The terminator is at 171°W. The crater at K16 (about 150 kilometers in diameter), whose floor is incompletely flooded with dark mare material, is an exceptional feature in this highland region of light-toned surface material. The cluster of bulbous-floored craters just east of its central peak is shown in more detail on page 136. Note also the area of darkish discoloration on the highland surface to the north of the crater at E6.

Northern zone of the western farside. *Mare Moscoviense*, C16, is shown again on page 132. The circular depression at D8, about 200 kilometers across, is located about 45°N, 150°E. Except for the patch of dark mare material on part of its floor, it resembles other farside basins. The terminator is at 172°E.

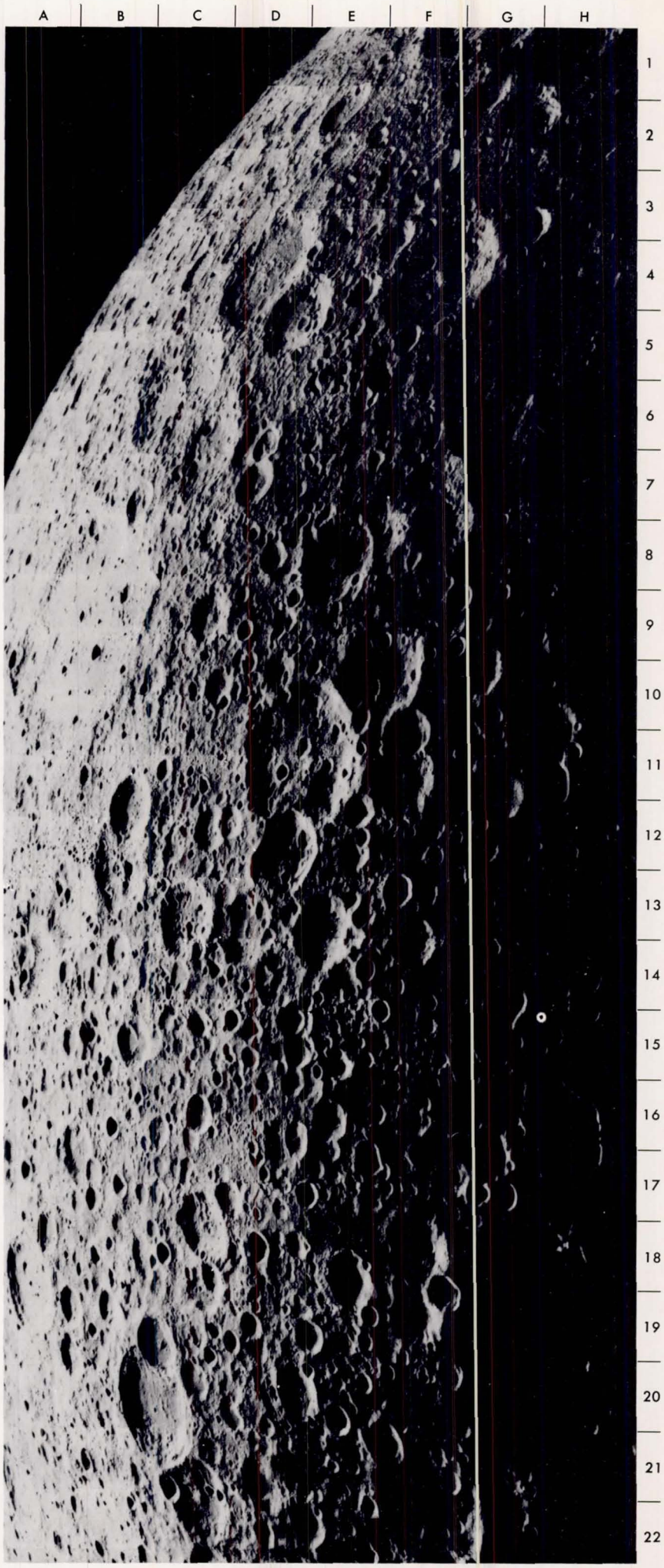

The northern zone at the middle of the Moon's farside. The chain of four craters at F3 runs along the 180° meridian about 65°N. The large crater at C20, which is about 100 kilometers in diameter, is located on the same meridian at 30°N. The terminator is at 164°W.

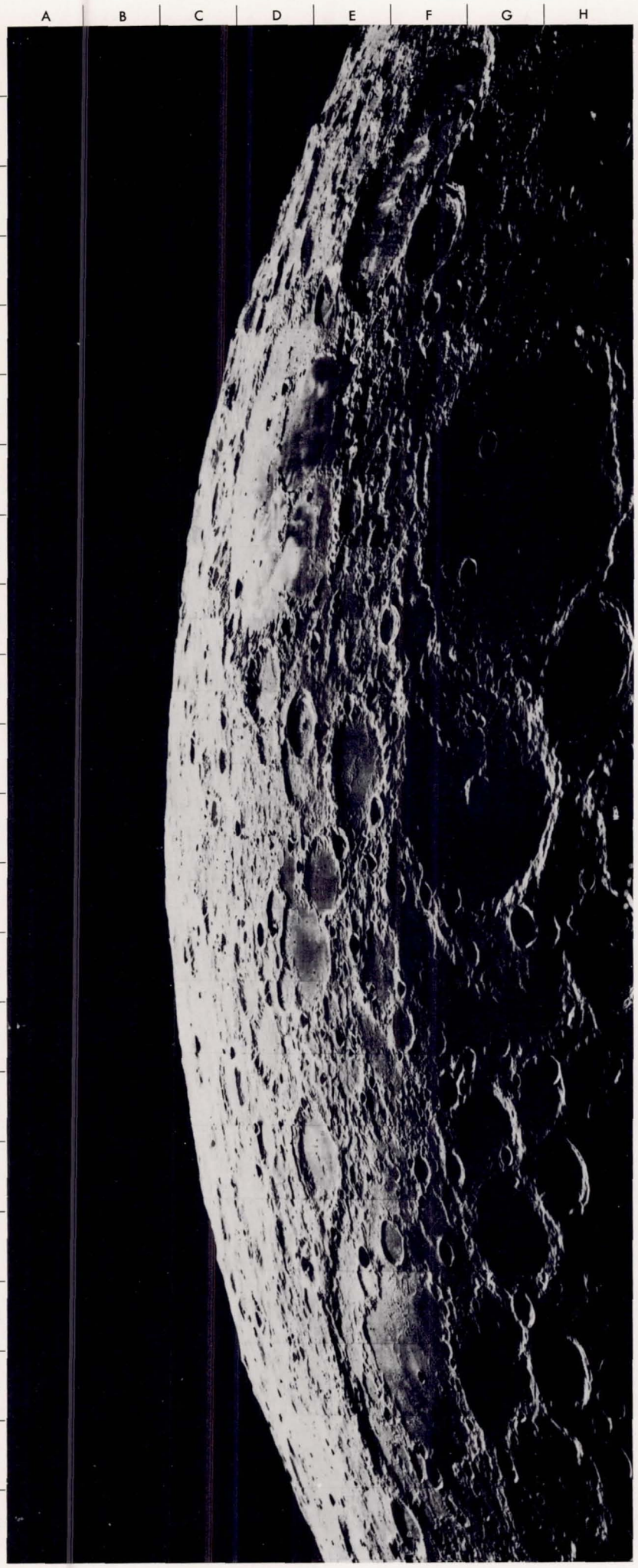

Southern zone in the middle of the farside. The crater at G12, about 200 kilometers across, is near 45°S, 175°E. The terminator is at 172°W. This region is unusual in the extent to which depressions are flooded with dark mare material. Note also the areas of bright discoloration in the maria, as at F2 and D8.

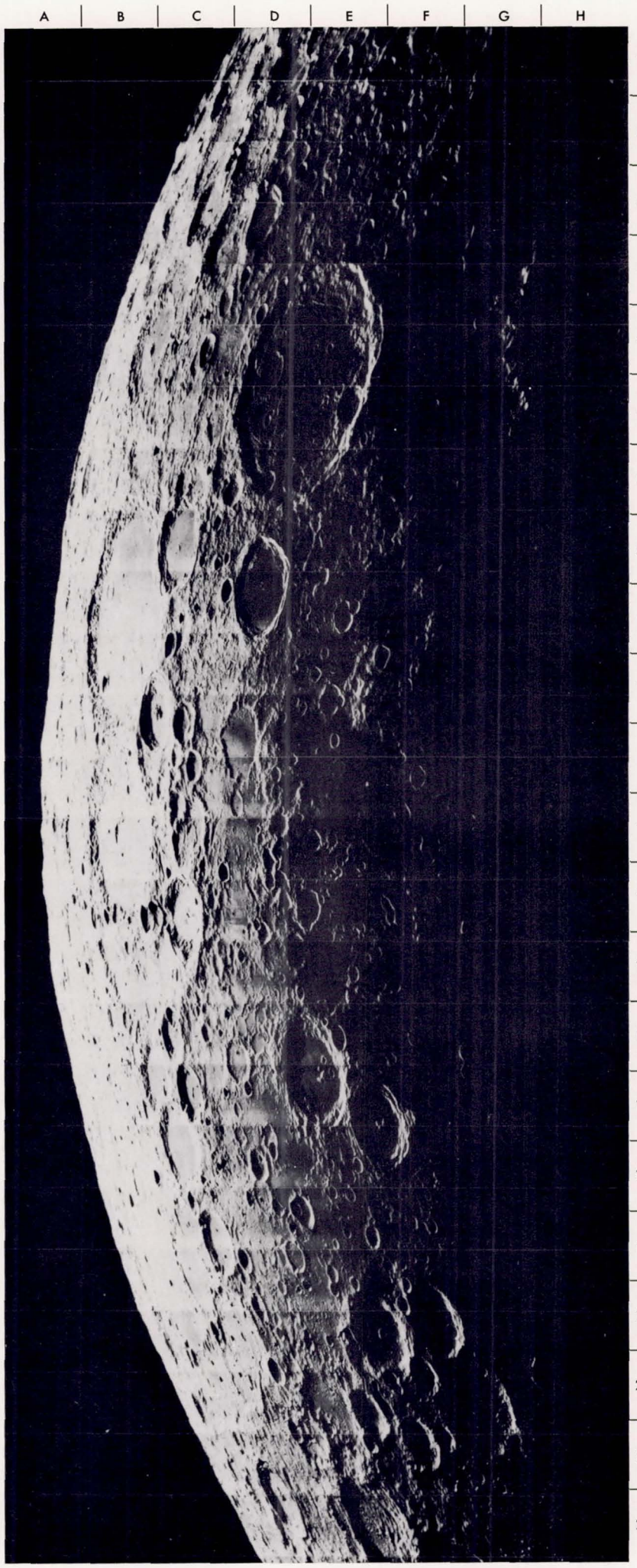

Southern zone just east of the middle of the farside. The crater at D9 is located about 40°S, 170°W. The apparent smoothness of its floor suggests a comparatively recent flooding. The crater with a central peak at E16 is located about 52°S, 170°W. The terminator is at 156°W.

The equatorial zone of the western farside. The crater at I11 is located about 5° S, 150° E. The terminator is nominally at 164° E, but the pronounced roughness of this part of the Moon produces great loops and indentations in the visible terminator. The basin at bottom center is about 270 kilometers across. Its floor is quite rough, and is itself devoid of mare material. However, the bottom of the crater excavated in that floor at H19 is flooded with mare material.

Southern zone of the western farside. Since this is an oblique photograph facing southward, it can be viewed in its natural perspective by holding the book upside-down. The terminator is at 174° E. The mare-filled crater Jules Verne (C16) is distinguished by the sharp escarpment near its eastern edge. This feature, which might be compared with the frontside's *Straight Wall* (page 105), consists of a number of straight segments with distinct changes in direction. The crater with a central peak at J3 is located about 10° S, 160° E. The concentric-ringed basin at I21 is 1400 kilometers to the south, at 55° S, 160° E.

The equatorial zone of the western farside. The prominent basin at O3 is located about 5° N, 140° E, and is about 300 kilometers across. Its floor, which is devoid of any mare filling material, is crossed by a chain of craters in a precise line. The line points to the crater *Tsiolkovsky* (J20), more than 800 kilometers away at 20° S, 130° E. The region between the two is marked by other crater chains. Some of these, as at I11, are radial to *Tsiolkovsky*, while others (e.g., J8) are not.

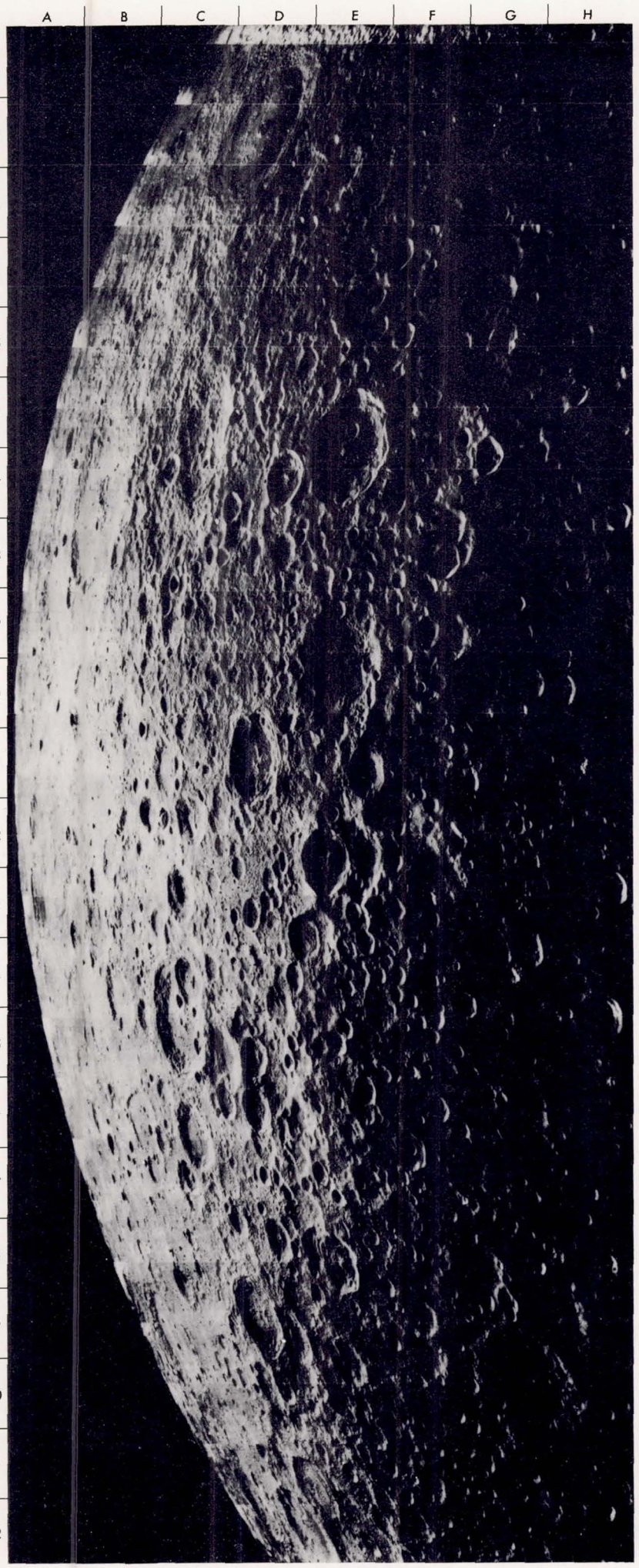

The northern zone of the western farside. The crater at D11 is located about 40°N, 120°E. The terminator is at 140°E. The large unnamed crater at D2, with rilles crossing the floor near the central peak, is located about 55°N, 105°E.

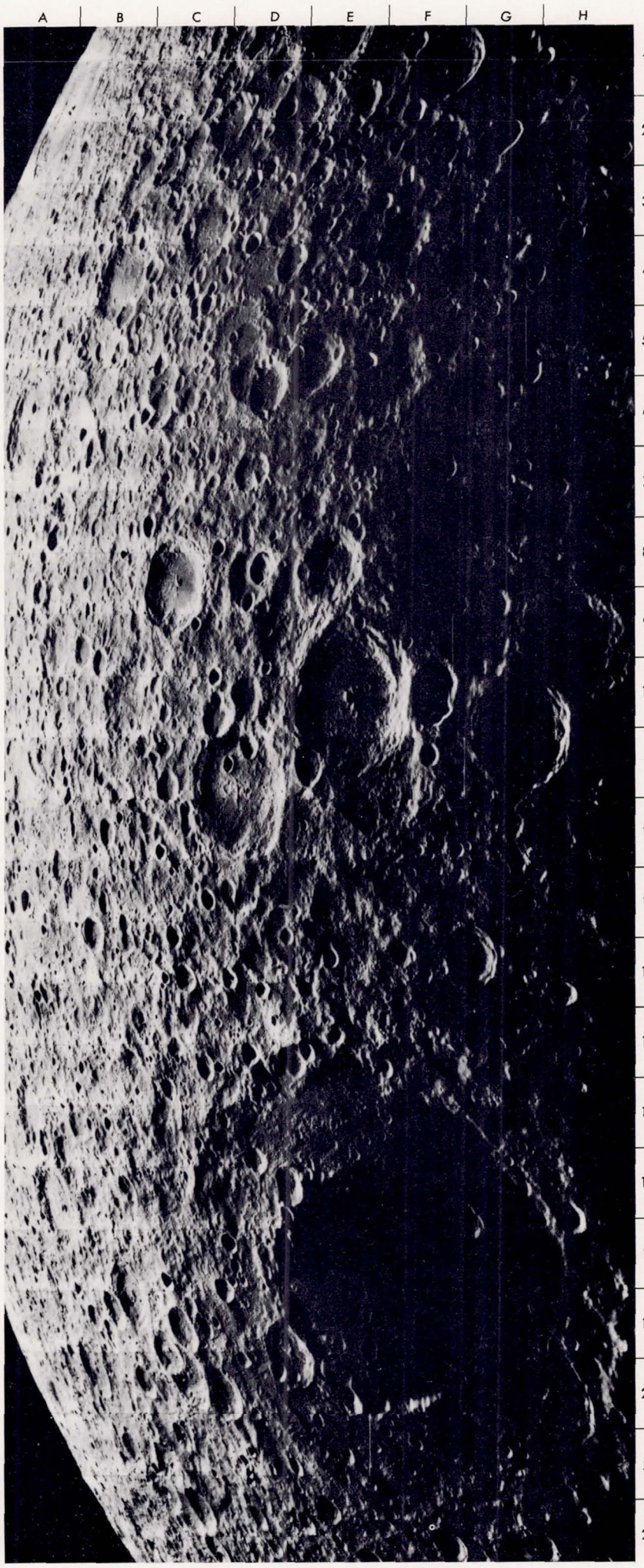

The northern zone of the western farside. The crater whose central peak is at E10 is located about 40°N, 145°E. The terminator is at 156°E. *Mare Moscoviense* (F19) is about 300 kilometers in diameter.

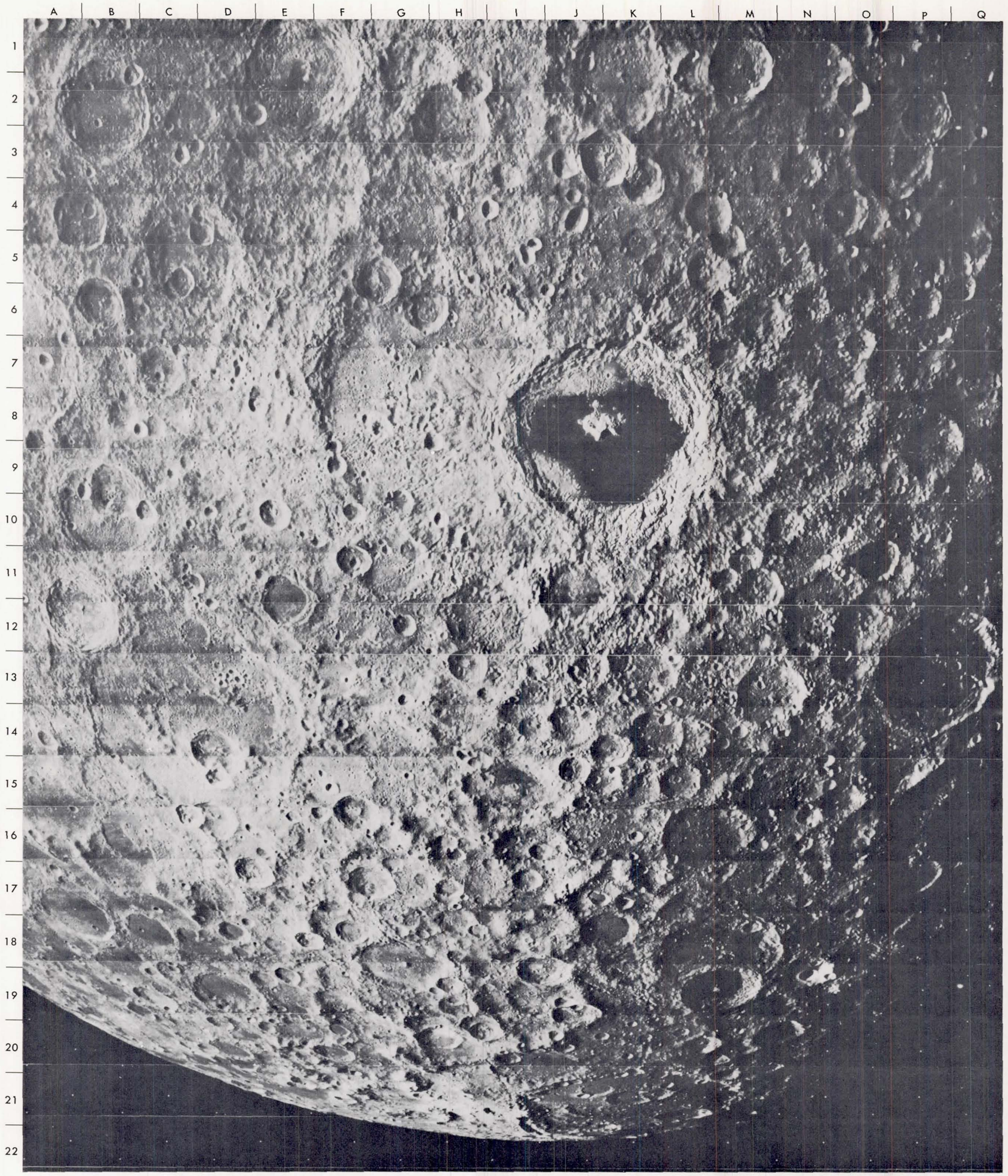

The southern zone of the western farside. The terminator is at 147° E. Like the other southward-facing oblique on page 29, this photograph shows correct perspective when viewed upside-down. The crater *Tsiolkovsky* (K8) is located about 20° S, 130° E. Some of the remarkable features of this conspicuous dark-floored crater are shown in detail on pages 133 and 134. The central-peaked crater at B12 is located about 28° S, 110° E. The large circular depression at K21 is centered about 55° S, 130° E.

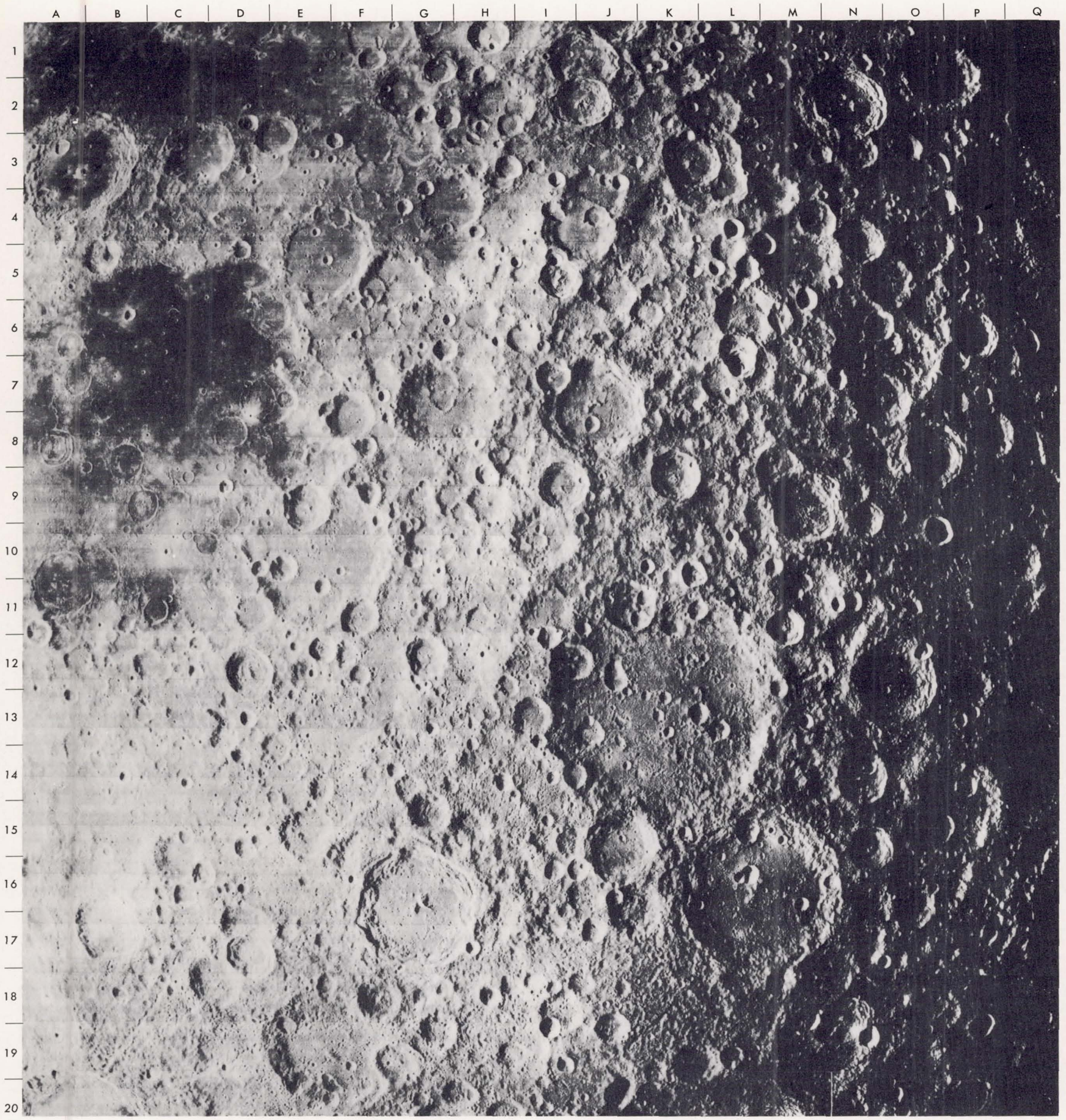

The equatorial zone just beyond the eastern limb area. The terminator is at 116° E. The left third of the photograph shows regions of the eastern limb that were pointed out at the beginning of this chapter. Mare Marginis is at the top. The crater Neper (A3), which is 142 kilometers in diameter, is located at 9° N, 84° E. Mare Smythii, centered at B7, resembles the frontside's Mare Nubium in having a considerable number of "ghost rings." The crater Gibbs (B17) is at the margin of the secondary crater chains and deposits of ejected material radiating from the large crater Humboldt, whose northern rim is seen at B20. The interior of Humboldt is shown in more detail on page 96.

The eastern half of this photograph covers the area seen so strikingly in the oblique picture on pages 34 and 35, with the Earth in the background. The basin centered at K13 (located about 12° S, 105° E) is exhibited here as a very distinct depression. It is about 250 kilometers in diameter. In the oblique view, where it occupies about half the length of the picture, the evident roughness of the floor almost completely obscures the height and continuity of the rim.

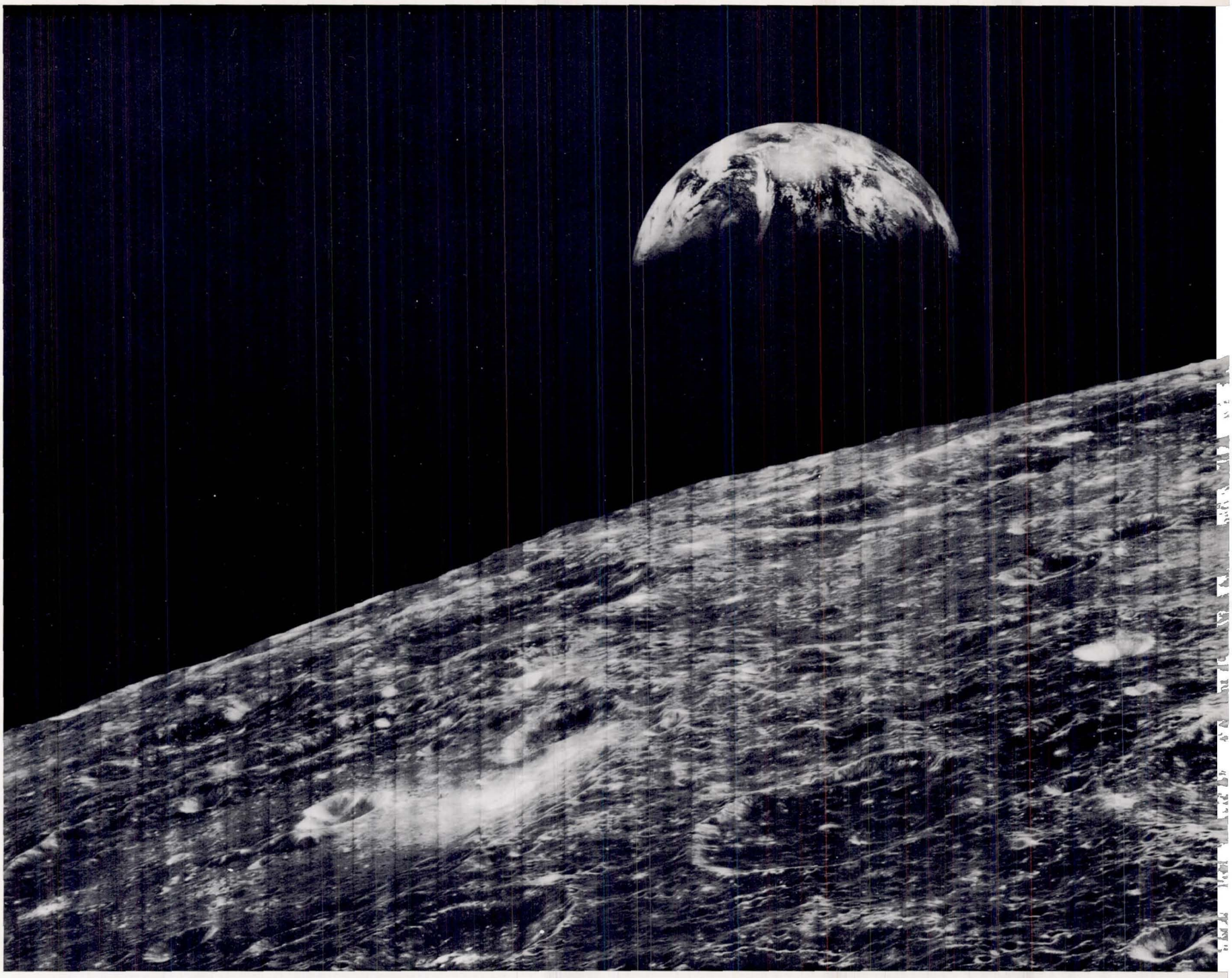

This Lunar Orbiter I photograph, taken August 23, 1966, at 4:36 p.m., Greenwich Mean Time, was our first view of the Earth from the vicinity of the Moon and also provided our first detailed oblique view of the lunar landscape. The spacecraft was 380,000 kilometers from the Earth and 1200 kilometers above the lunar surface. At that time the sunset terminator on Earth was near Odessa in the Soviet Union and Istanbul, Turkey, and passed slightly west of Capetown, South Africa. The Earth's South Pole was within the field of view but on the dark side of the terminator, as it always is in August.

The homeward look emphasizes the spatial relationship between the unmanned spacecraft and the farflung mission operations team that controlled it. It was midmorning at the Space Flight Operations Facility in Pasadena, California, and at the nearby Goldstone tracking station, where the Moon was not due to rise for another 3 hours. At the Woomera, Australia tracking station, where it was the middle of the night, the Moon had just set. The Moon was high in the midafternoon sky at the station

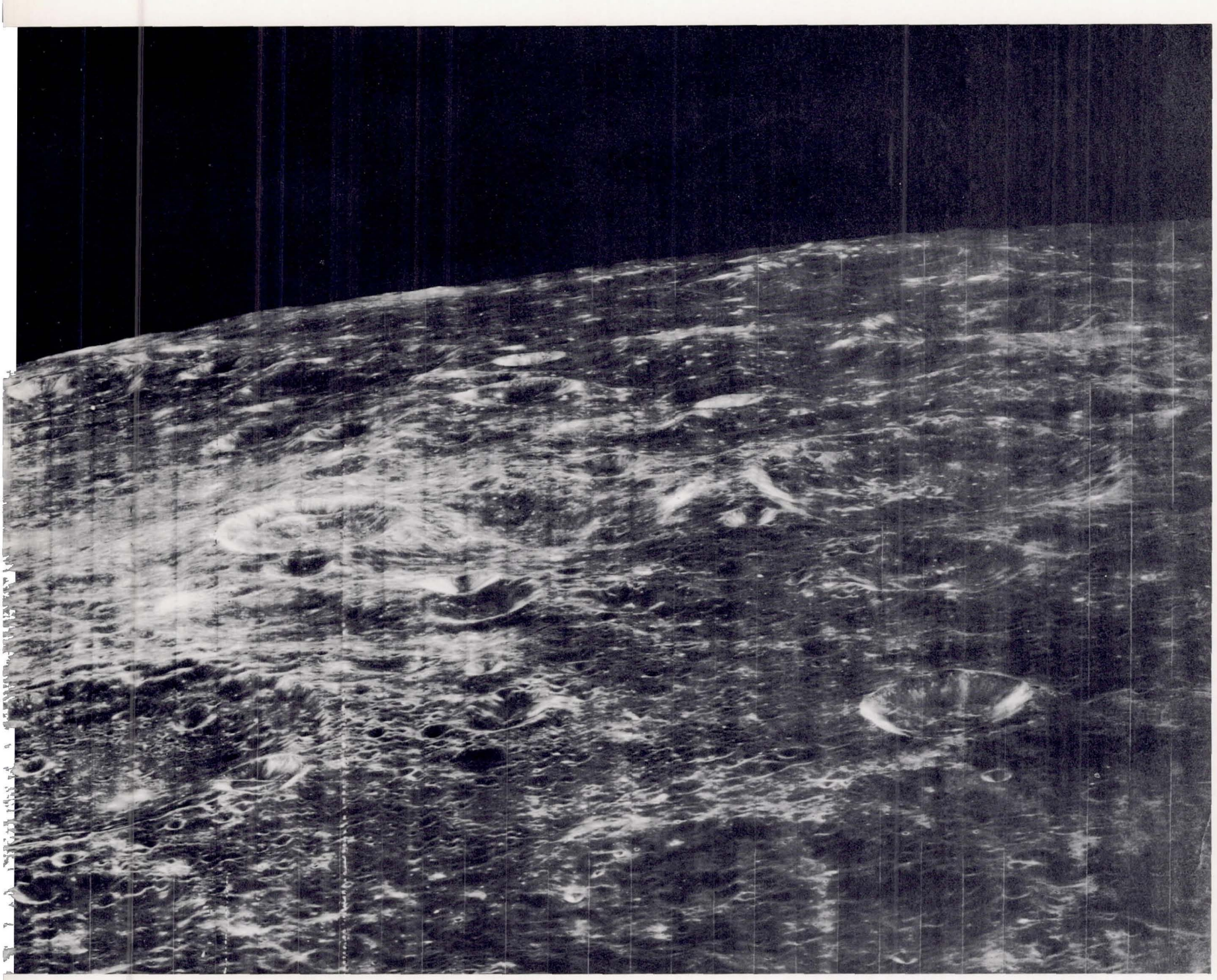

near Madrid, Spain, but the spacecraft was about to interrupt all communication by going behind the Moon.

The portion of the Moon seen in this photograph (which covers two-thirds of the original high-resolution frame) lies within the farside region that is shown in vertical view on page 33. The center of this photograph, located about 10° S, 105° E, corresponds to K12 in the vertical photograph. As the camera was facing westward, north is to the right. The horizon covers about 550 kilometers from north to south.

With the Sun nearly overhead, very few lunar surface features cast shadows. Even so, the oblique view conveys a strong impression of the roughness of the surface. The lighting on the interior walls of craters suggests a general relationship in this area between the apparent freshness of the craters and the reflectivity of their wall materials. Those craters that are not notably modified by later cratering or slumping generally have brighter walls. The upper part of the crater wall commonly appears as a darker horizontal band.

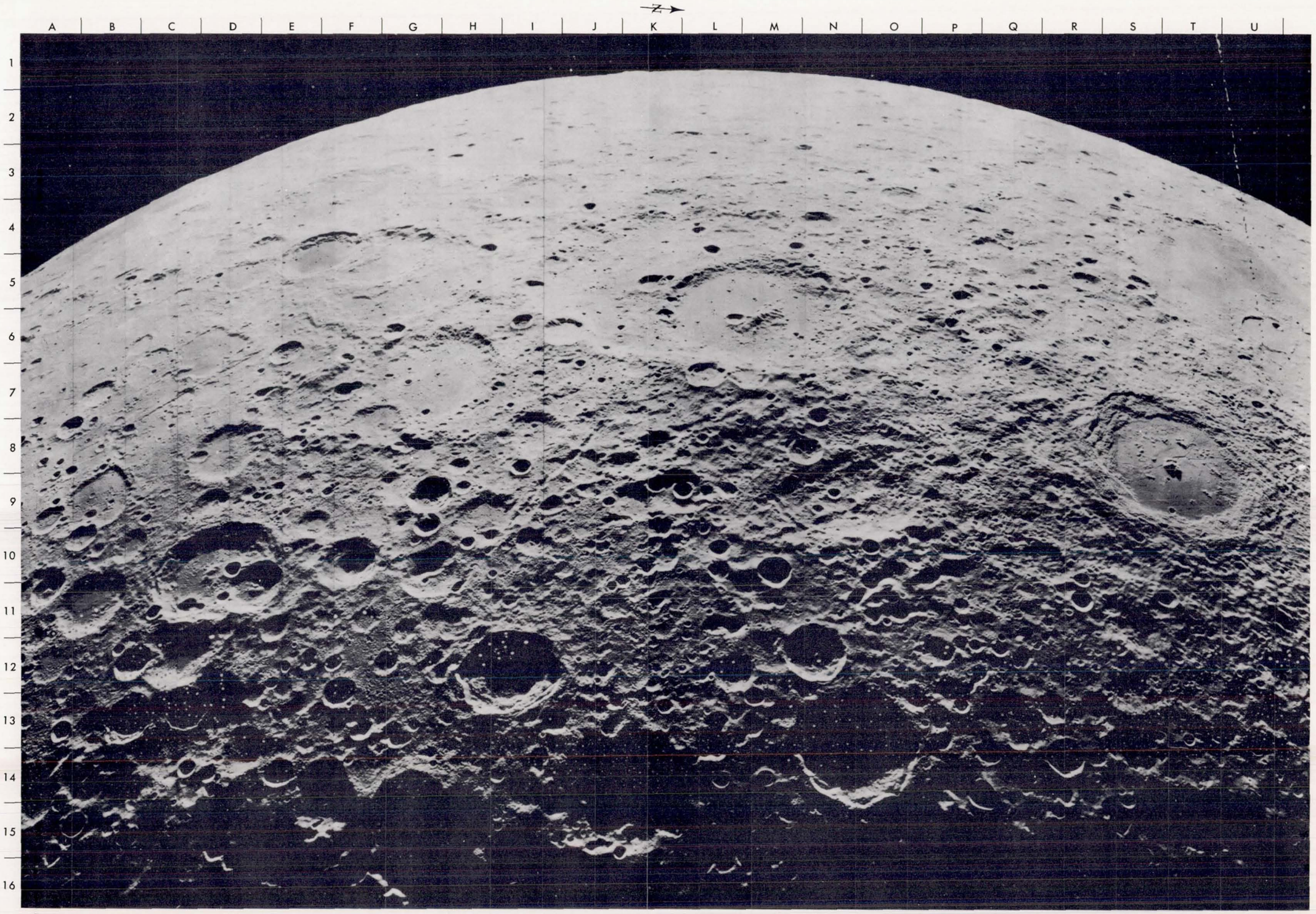

The northern zone of the western farside, looking westward toward the eastern limb region. North is to the right. The terminator is at 127°E. (The white "freckles" along the terminator are caused by a processing defect on the spacecraft film.) Mare Humboldtianum, centered at T5, is a frontside feature about 55°N. The crater Boss (O4) is located about 46°N, 90°E. The crater Lomonosov (E5) is the southernmost and youngest of three intersecting craters. The middle crater is second in age. This age relationship, which can be deduced from the manner in which their rims intersect, is supported by the relative smoothness of Lomonosov's floor and the sharpness of its rim features. Just west of Lomonosov is the large crater Joliot Curie (F3), located about 27°N, 95°E. The large unnamed crater with the multiple central peaks at M6 is about 180 kilometers in diameter. The southern half of the photograph contains three long, distinct crater chains which are roughly parallel. The southernmost chain is at B6, the middle one runs from D6 to B8, and the third runs from J8 to H10.

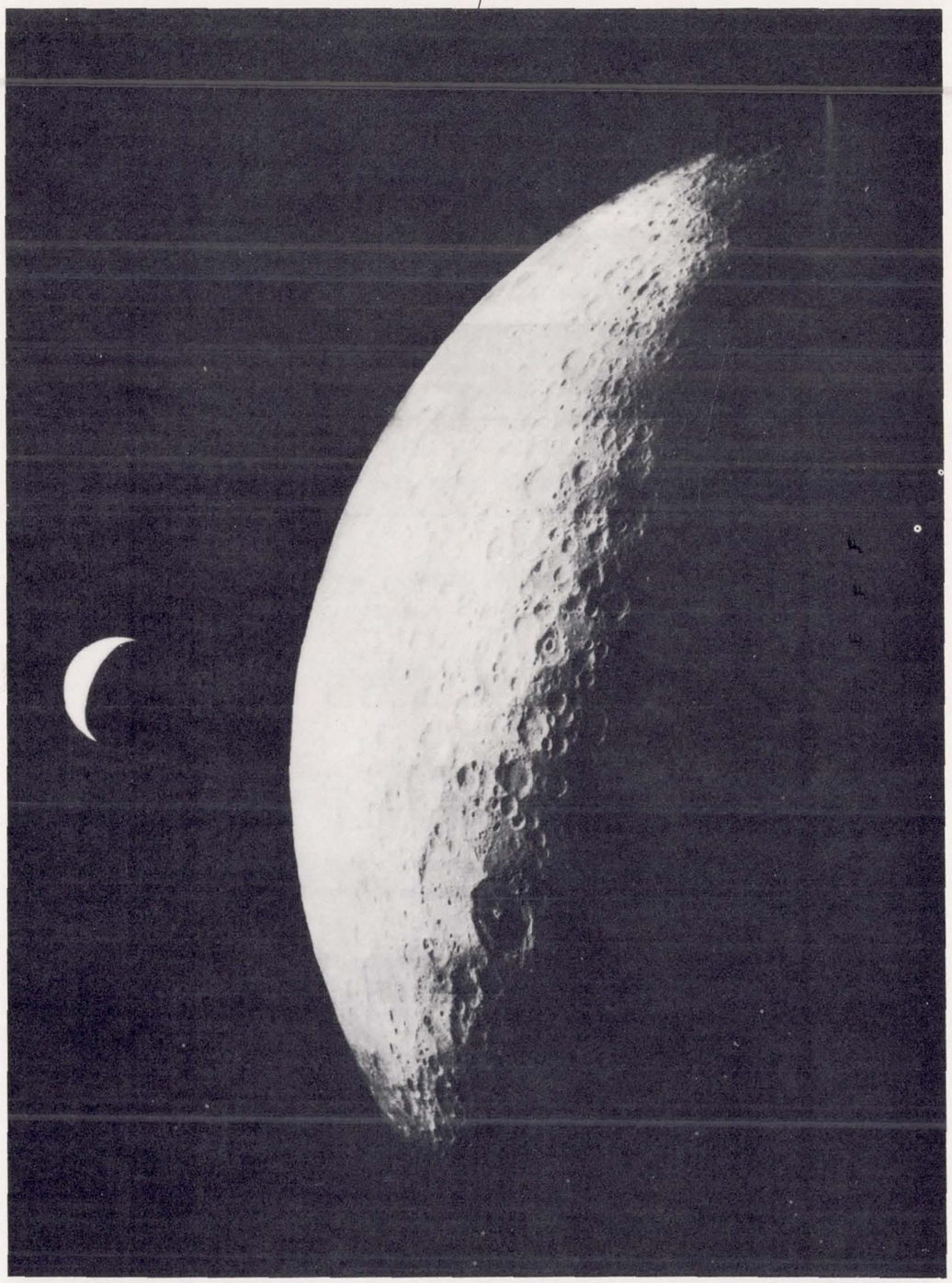

This Lunar Orbiter IV photograph, taken from an altitude of 6150 kilometers, conveys a different impression of the Earth's relation to its natural satellite from that given on pages 34 and 35. As seen from the Moon, the Earth goes through its apparent phases in a monthly cycle which is opposite the lunar cycle. Thus, this photograph, taken 4 days before the time of full Moon, shows the Earth as a thin crescent. The lunar sunset terminator was at 140° E, and the photograph covers the western portion of the farside between the latitudes 50° N and 50° S. The large, particularly dark-floored crater in the southern hemisphere near the terminator is Tsiolkovsky.

This photograph (the only one in the book not taken on a Lunar Orbiter mission) shows the Earth as it appears from one-tenth the lunar distance. It was taken by the spin-scan camera aboard the Applications Technology Satellite ATS III. Being in a circular equatorial orbit 35,800 kilometers high, the satellite had an orbital period of 24 hours, enabling it to hover above a point on the equator at 95° W longitude. The photograph, which was originally in color, covers nearly the entire Western Hemisphere. South America occupies most of the lower right quadrant. North America is at top center, with Mexico's Baja California and Yucatan peninsulas showing the greatest land-water contrast.

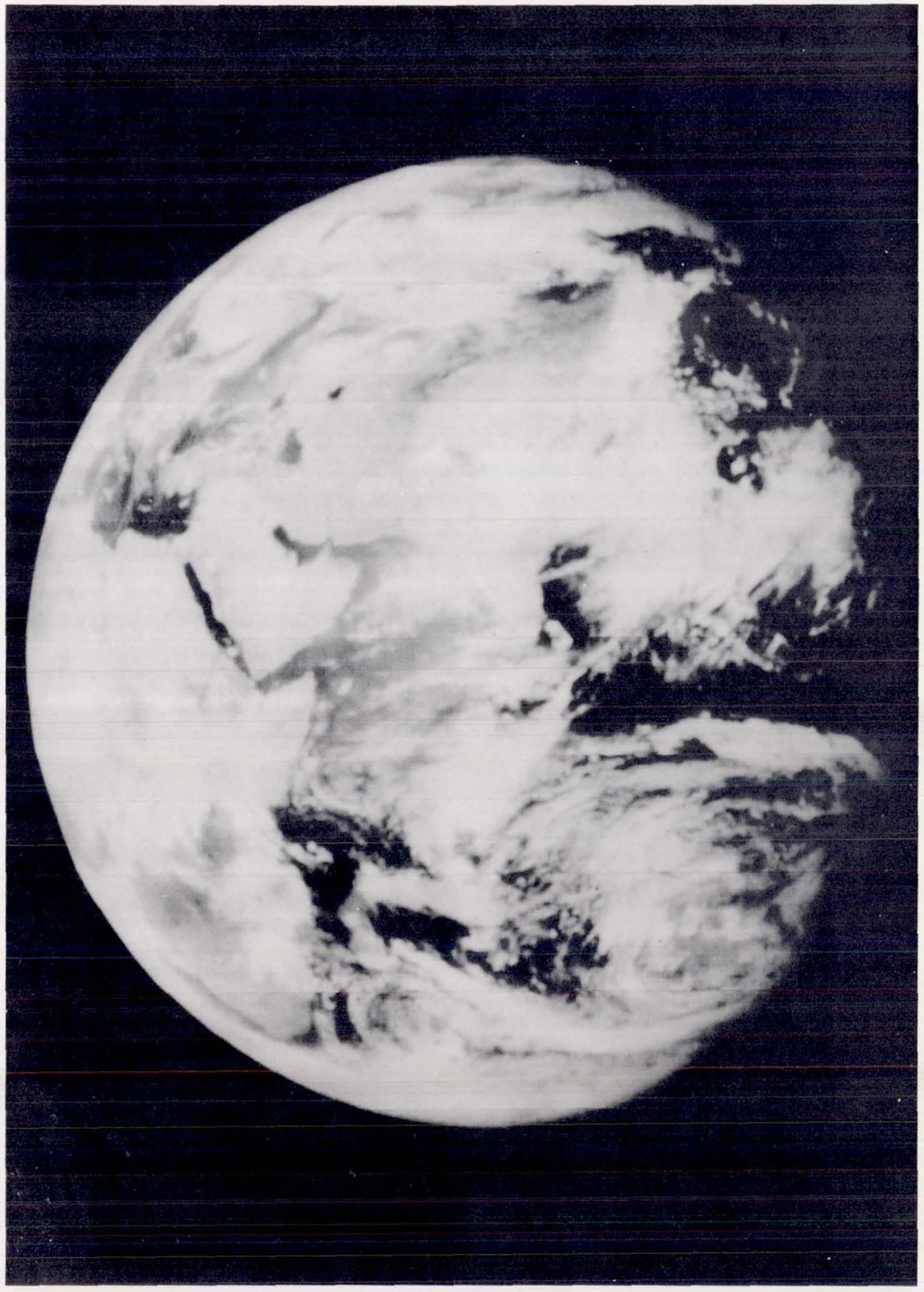

The Earth, photographed from a distance of 362,000 kilometers by Lunar Orbiter V's telephoto camera on August 8, 1967. Since the date was 2 days past the new Moon, the Earth (as seen from the lunar vicinity) is exhibited in the gibbous phase corresponding to 2 days past full Earth. The photograph is centered near the southern tip of India. The visible detail comprises both the large-scale cloud patterns and the land-water boundaries. The latter are delineated in the drawing at the right.

The latitude and longitude lines are drawn here at 30° intervals. At the time the photograph was taken (9:05 a.m., Greenwich Mean Time) the Sun was directly overhead in the southern part of the Arabian Peninsula, and the sunset terminator crossed the Equator about 136° E longitude. The portion of the Earth that was in darkness is drawn in dark shading.

CHAPTER 3

A CLOSEUP VIEW

Man's early interest in the Moon is recorded largely in mythology. Ancient Egyptians honored the Moon as their god Thoth (Dhouti), god of wisdom and magic. To the ancient Greeks the Moon was their goddess Selena, from whose name the term selenology (study of the Moon) is derived. Even those civilizations that did not worship the Moon fixed their religious festivals in terms of the 29½-day cycle of visible phases which constitutes the lunar month. With this awareness, a great deal of accurate information was accumulated in ancient times about the motions of the Moon with respect to other celestial bodies.

Galileo's application of the telescope to the Moon in 1610 marked the birth of a new area of science, selenography (study of lunar surface morphology). Observation of the Moon, using telescopes of various sizes and optical designs, has continued to the present time at many observatories around the world.

Two factors limit what can be accomplished by telescope observation. Instability of the Earth's atmosphere has prevented observations of lunar detail finer than a few hundred meters. Because the Moon always presents nearly the same face to the Earth, a fixed viewpoint is imposed on the observations. Within the past 10 years, photography from spacecraft has circumvented both of these limitations.

The photographs of the western farside transmitted to Earth from the Soviet spacecraft LUNA 3 when it flew past the Moon in October 1959 freed selenography from its fixed viewpoint. Man's first closeup view of the lunar surface was provided by the American spacecraft Ranger VII July 31, 1964. Photographs transmitted from soft-landed spacecraft, particularly the Surveyor missions, more recently have shown us local details at the millimeter scale. The Lunar Orbiter photography represents the largest single advancement in selenography to date.

To display all that was revealed by Lunar Orbiter photography is beyond the scope of this book. A modest photo collection of lunar surface details is presented, beginning with closeup views of the frontside, grouped in sections under four headings: Maria; Highlands; Craters; and Faults, Rilles, and Domes. These sections are followed by a selected group of detailed views of the farside.

MARIA

Since the 17th century, when they were actually considered to be oceans, the dark areas of the Moon have been called *Maria* (plural of the Latin *mare*, sea). Lunar surface materials have been found, in general, to be poor reflectors of light, with the brightest spots on the Moon reflecting about 20 percent and the darkest regions as little as 5 percent of the incident sunlight. A quantitative basis for differentiating between the two major surface units of the Moon, the relatively dark mare regions or seas and the relatively bright terrae or highlands, is provided by comparisons of their *albedo* (the ratio between the light reflected from an unpolished surface and the total light falling on it).

Oceanus Procellarum, the maria Crisium, Fecunditatis, Frigoris, Humorum, Imbrium, Nectaris, Nubium, Serenitatis, and Tranquillitatis on the Moon's frontside and the maria Orientale, Moscoviense, Australe, Marginis, and Smythii on its limbs and farside, together with several smaller regions, constitute the dark, relatively flat and smooth areas of the lunar surface. Many of the maria are approximately circular. Mare Imbrium, the largest of these features, is about 1300 kilometers across and can easily be seen with the naked eye when the Moon is full. There does not appear to be any sharp distinction between the circular maria and individual craters with mare-filled floors, such as Grimaldi.

The photographs provided on the following pages display some of the salient characteristics of mare surfaces, with special emphasis on those observed near the candidate Apollo landing sites.

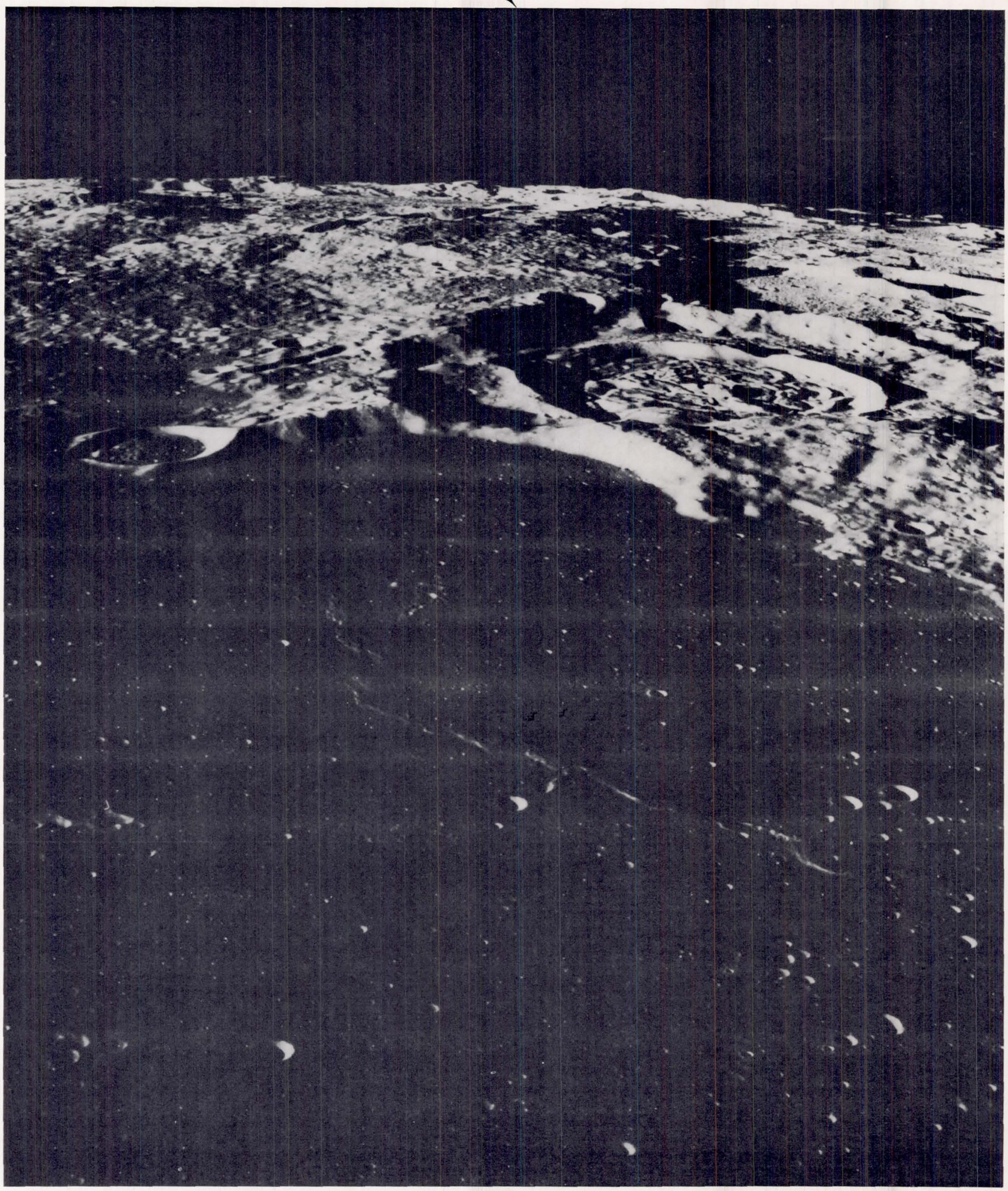

This oblique view to the southwest shows part of the extensive mare of Oceanus Procellarum. The smooth plain is pitted with sharp-walled craters in the foreground. A wrinkle ridge is visible extending diagonally across the mare to the small crater Damoiseau L. The arcuate cliffs (up to 1300 meters high) at the mare-highlands boundary in the middle background are markedly evident. Behind the right-hand cliff is the crater Damoiseau, located about 5°S, 61°W. This crater, with its intricately cracked floor 37 kilometers across, is seen to be in the middle of a larger crater, about 65 kilometers across.

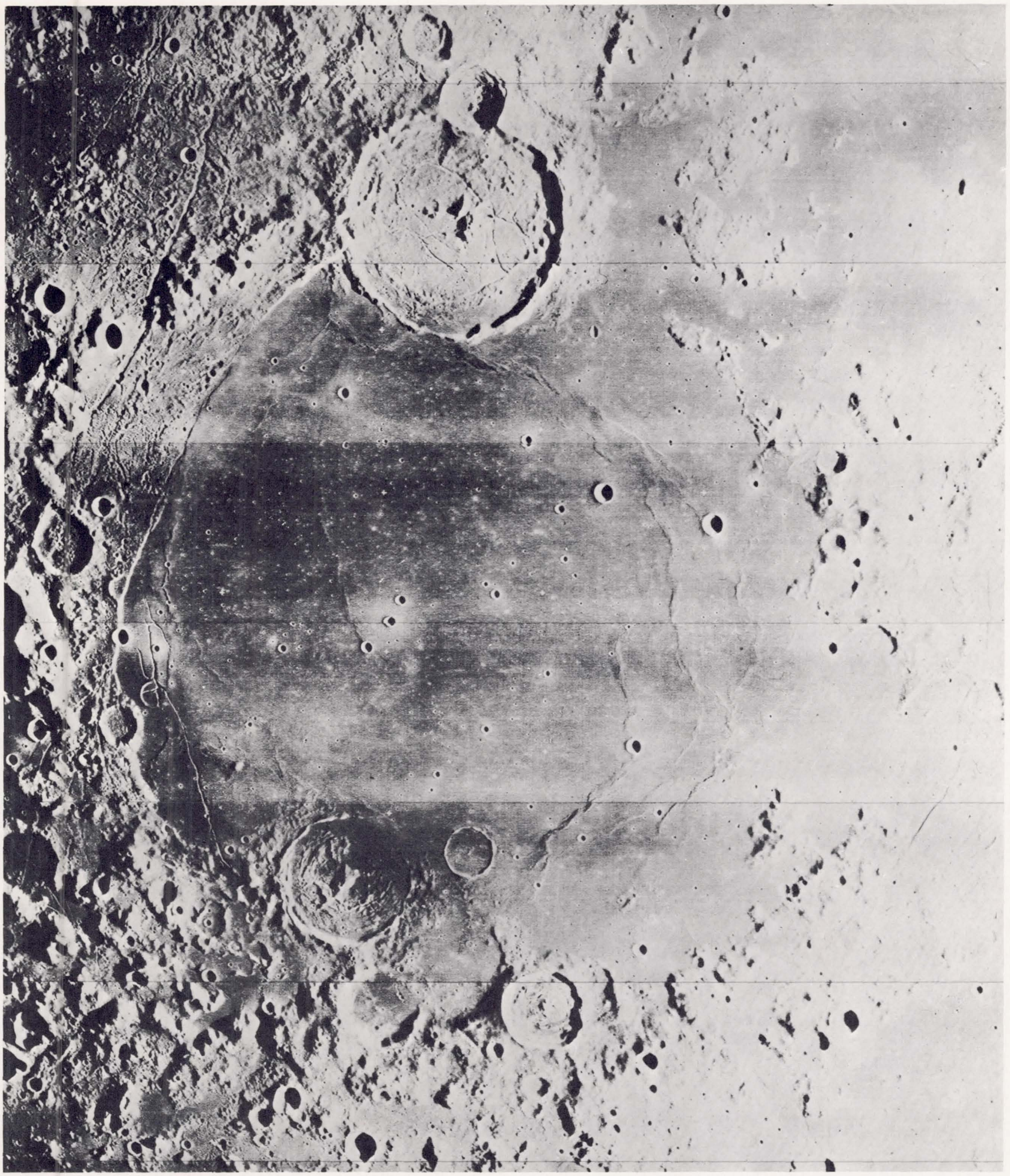

A series of long, arcuate, branching ridges is evident in the right half of Mare Humorum, which is about 350 kilometers in diameter. These ridges extend across the mare plain from the crater Gassendi in the upper center almost to the crater Vitello in the lower center. The left-hand ridge is about 200 kilometers long, but only 8 to 16 kilometers wide. The dark mare material filling the basin nearly obscures one crater in the lower center. The arcuate rilles close to the lower right edge run approximately concentric with the basin borders. Location: 23°30′S, 38°30′W. Framelet width: 86 kilometers.

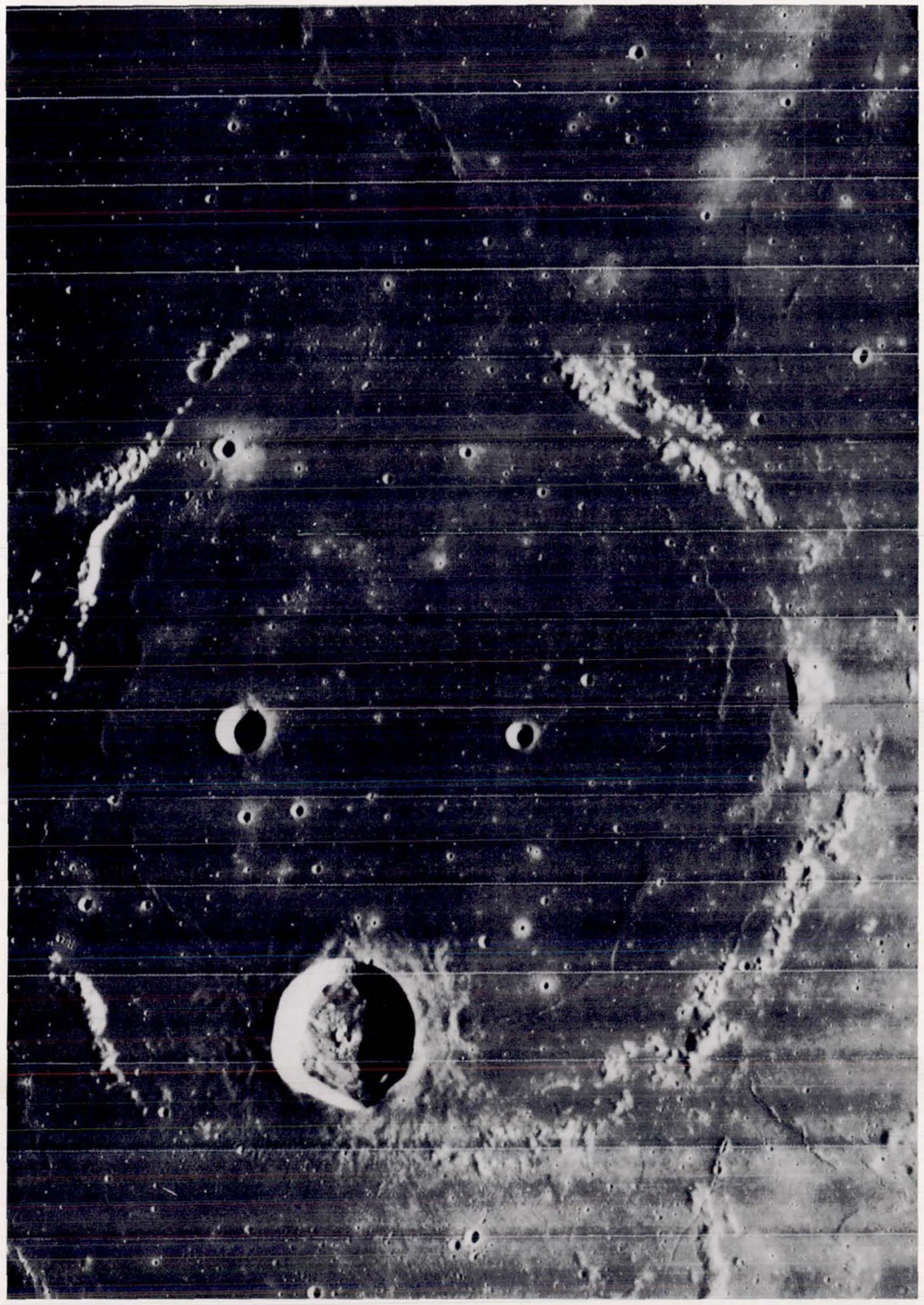

This broken ring (100 kilometers in diameter) of bright ridges has been interpreted as the rim of an old, flooded crater or, by some, as an igneous intrusion similar to terrestrial ring dikes. The Surveyor I spacecraft landed on this mare material in the upper right sector of the ring. The large crater surrounded by hummocky ground, near the lower part of the ring, is Flamsteed, about 20 kilometers in diameter. A concentric wrinkle ridge is evident within the ring. Location: 3°S, 44°W. Framelet width: 11 kilometers.

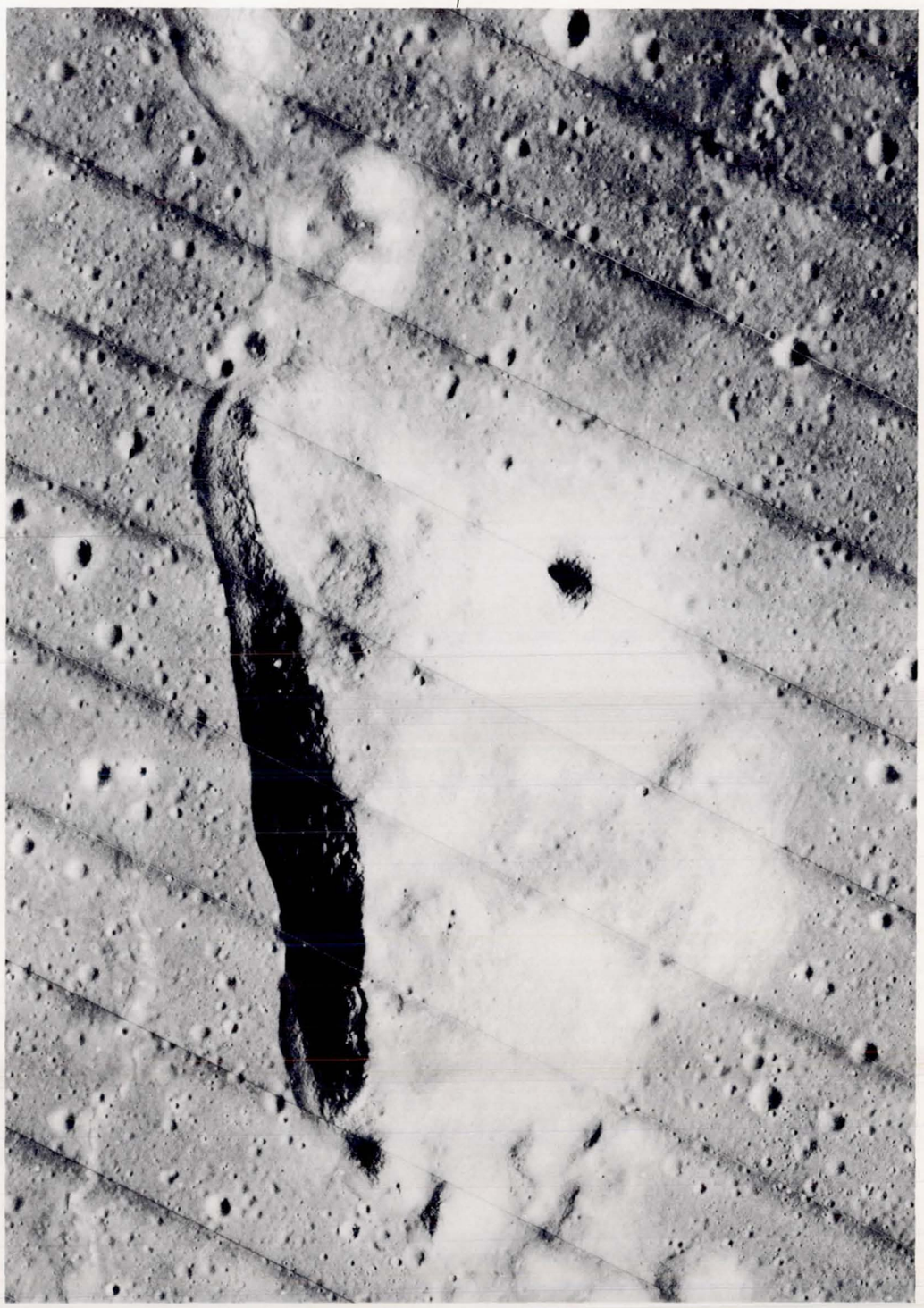

This steep-sloped, bright ridge is part of the right center of the ring illustrated at left. The large bright crater on the upper right side of the ridge is funnel-shaped with no visible flat floor, in contrast to most craters in this field. The ridge has a steep scarp on the left side and gentler slopes on the right. A distinct bulge extends along the toe of the scarp, which is shown in greater detail on page 58. Location: 2°40′S, 42°30′W. Framelet width: 1700 meters.

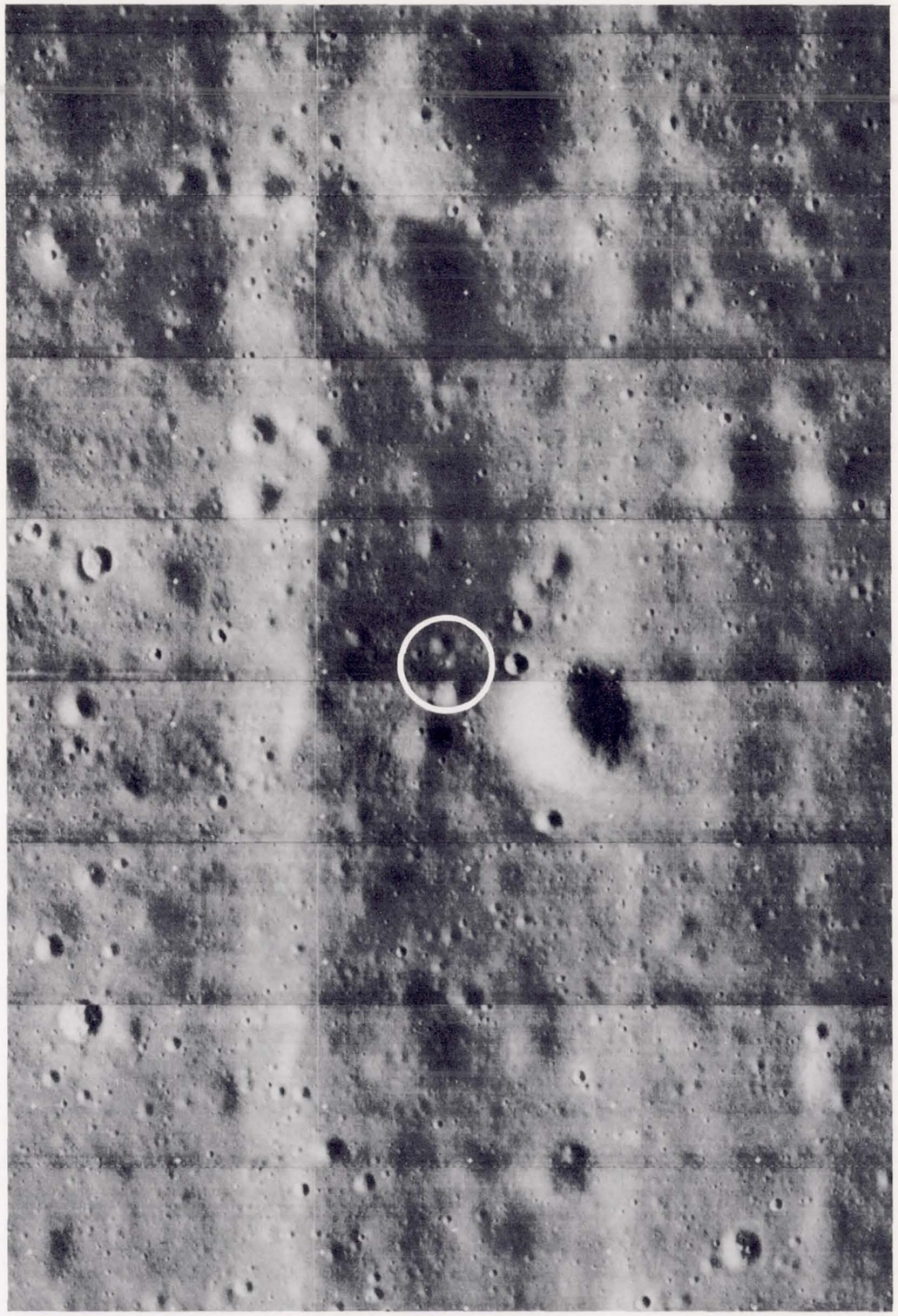

The landing site of Surveyor I is shown in this high-resolution photograph of the mare plain within the Flamsteed ring in Oceanus Procellarum. The spacecraft, which can be identified by the long shadow cast by its purposefully oriented solar panels, is visible in the circled area in the center of the picture. Location: 2°30′S, 43°20′W. Framelet width: 220 meters.

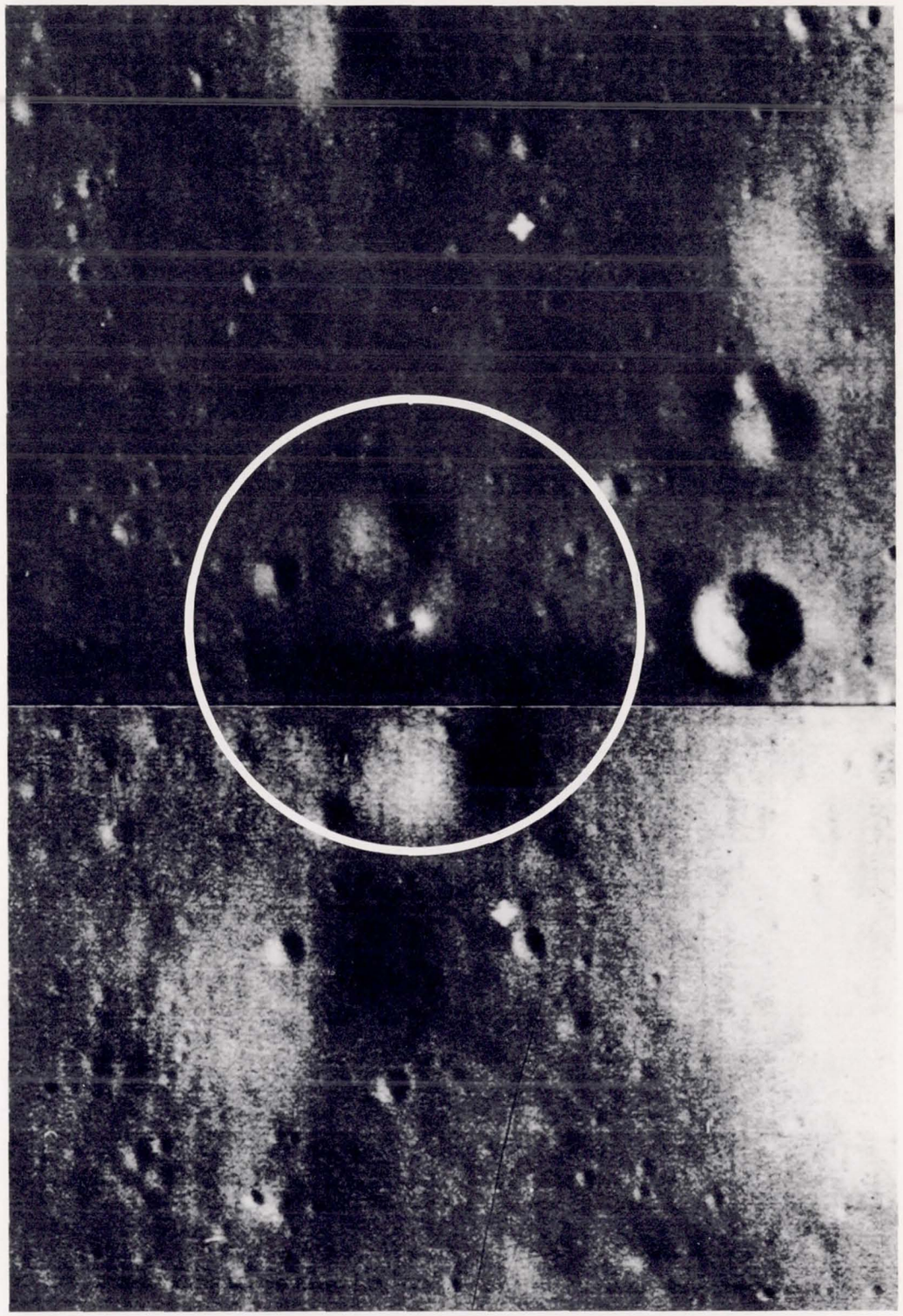

The Surveyor I spacecraft can be seen better in the circled area in this enlarged print of the opposite photograph. The spacecraft is the bright spot; the shadow of the solar panels (1 meter wide) is clearly visible. The size of the circle in this picture is directly proportional to the ratio of enlargement of the two photographs.

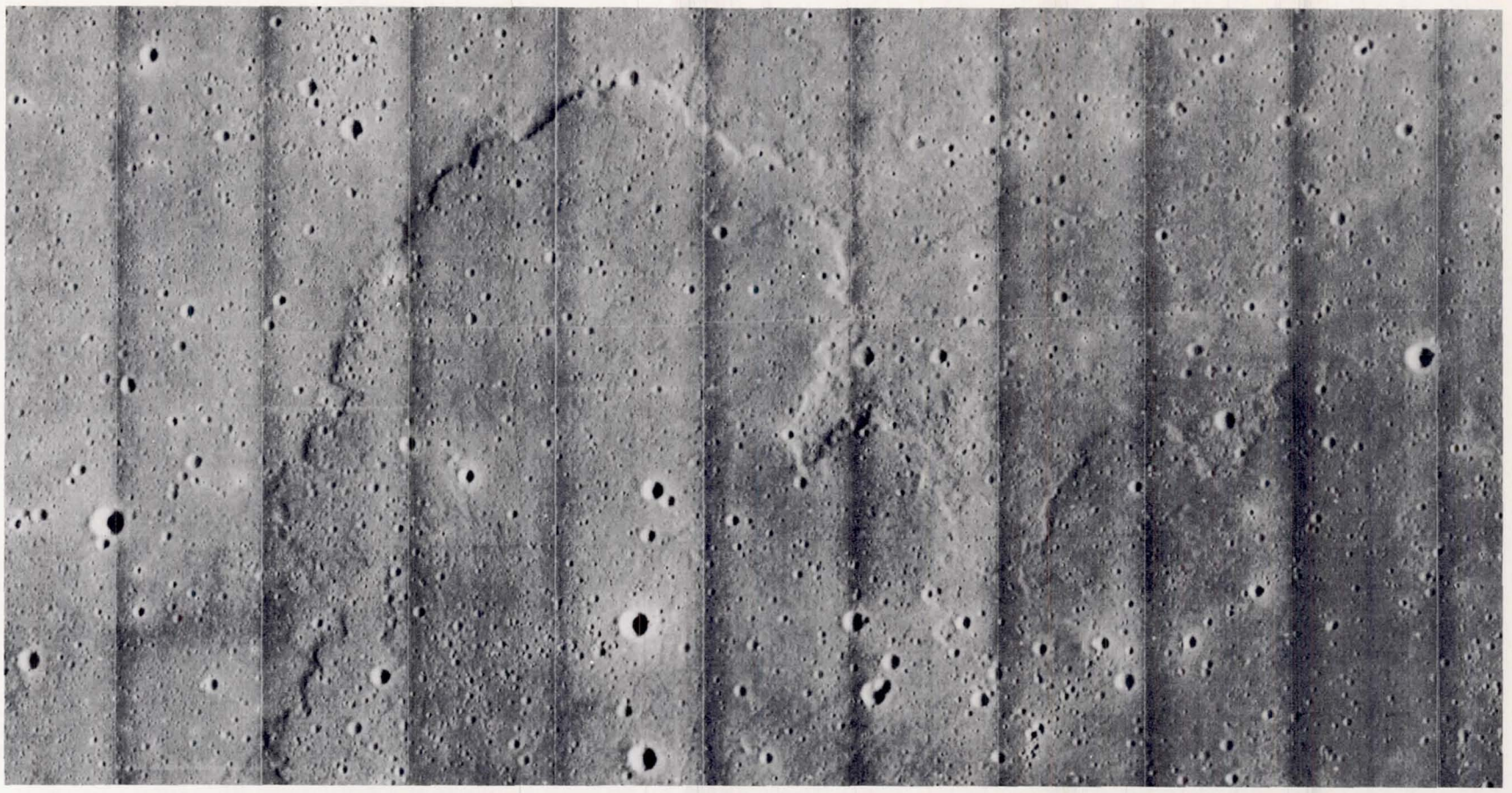

A highly sinuous, locally steep scarp can be seen along the scalloped edge of a flat-topped plateau in the middle of Mare Imbrium. The lobate shape of the plateau is similar to that of some terrestrial lava flows and is so interpreted by lunar scientists. The crater density on the flow appears to be the same as that on the bordering mare plain, and sharp-walled craters are common on both. Location: 32° N, 21°50′ W. Framelet width: 5 kilometers.

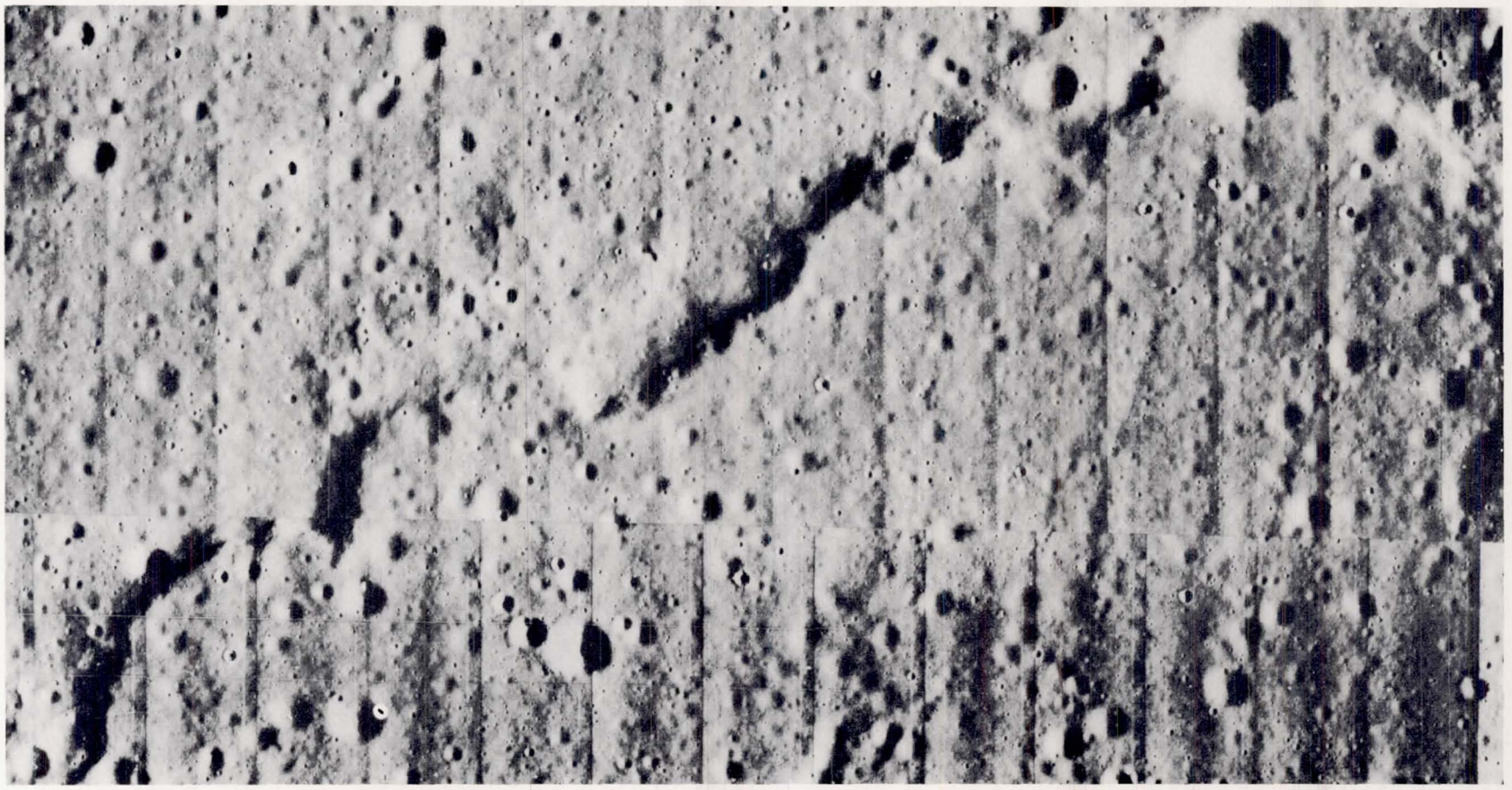

This high-resolution mosaic shows part of the steep scarp of the flow front illustrated above. The scarp for its entire length appears to be somewhat rounded and smooth in profile. No outcrops or rock ledges are visible along the scarp, nor are any blocks of rock evident around the many small sharp-walled craters along the rim of the scarp. Details of the flow front appear to be well preserved. Location: 32°20′ N, 22° W. Framelet width: 650 meters.

The broad, smooth wrinkle ridge along the left side extends southward for many kilometers through Mare Serenitatis. The thin, sharp ridge along the upper part of the left edge appears to be genetically related to the broad ridge. A shallow, forked rille is evident along the right side of the picture. Many small subdued craters, and two large sharper ones, are visible in the dark mare plain in the middle. Location: 23°40′ N, 29°00′ E. Framelet width: 4 kilometers.

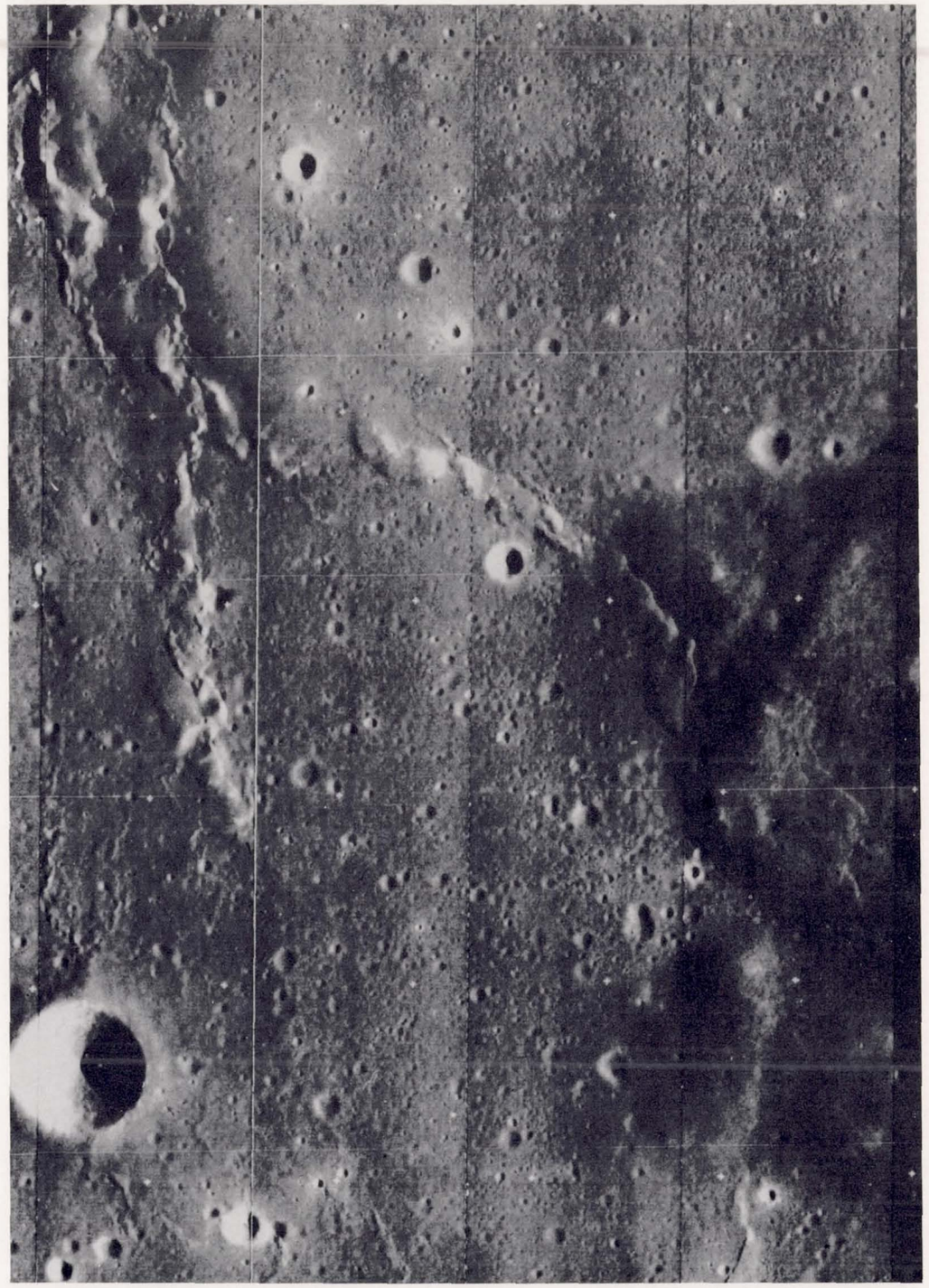

The ropy, fresh-looking mare ridge visible in the upper left corner is the southern end of the ridge shown in the opposite picture. This ridge forks near the picture center; the right-hand branch is partly obscured in the lower right sector by a thin mantle of smooth, extremely dark material, which is uncratered in contrast to the lighter mare material. Location: 21°30′ N, 29°00′ E. Framelet width: 4 kilometers.

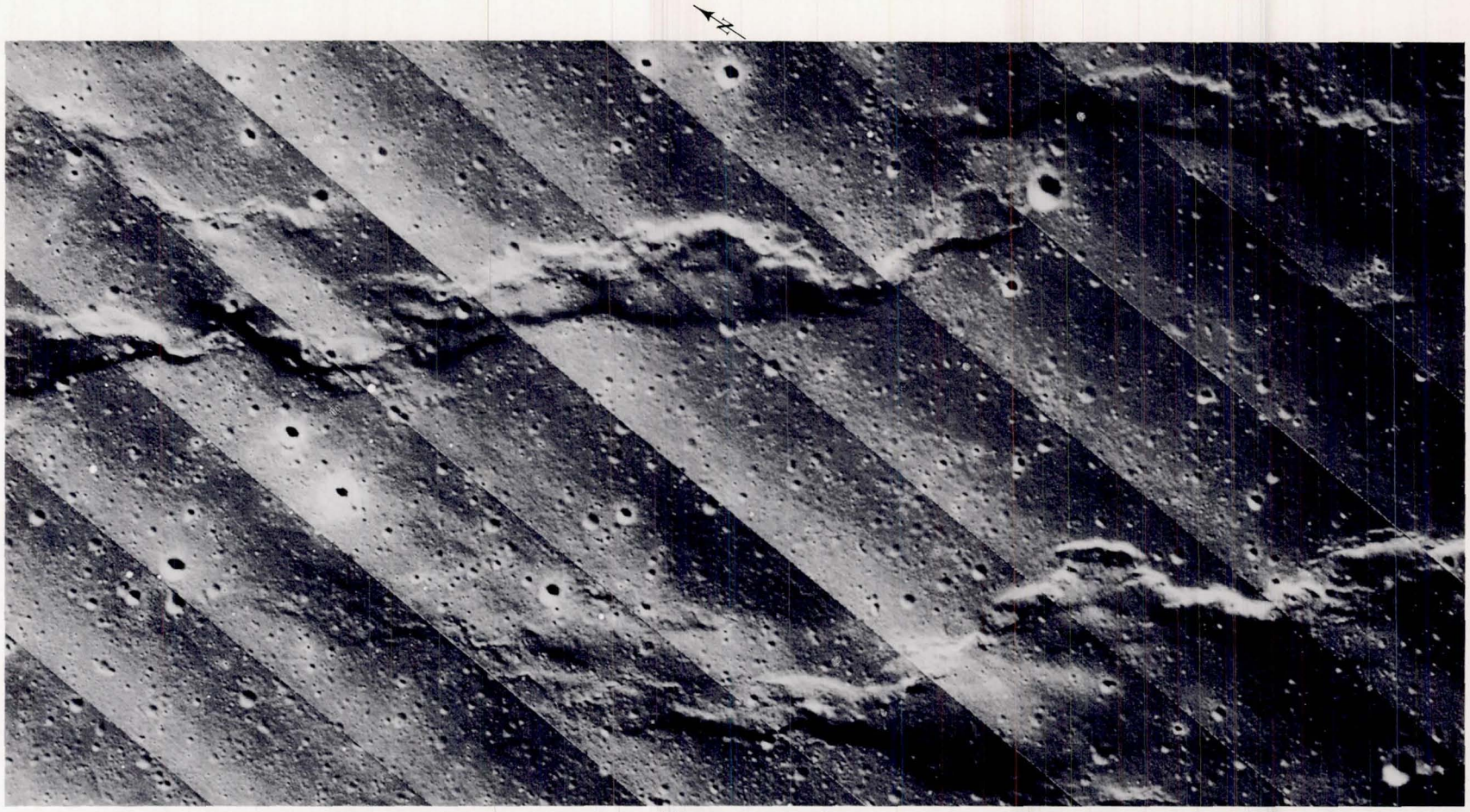

The wrinkle ridges extending across the picture are near a candidate Apollo landing site in Oceanus Procellarum. This moderate-resolution photograph shows the ridges as smooth, rounded features, with some local areas of steeper relief. The ridges broaden and thin irregularly, but all decrease in breadth near the ends. Crater density is about the same on the ridges as on the mare plain, and bright, sharp-walled craters are common on both. Location: 3°50′ S, 36° W. Framelet width: 3.4 kilometers.

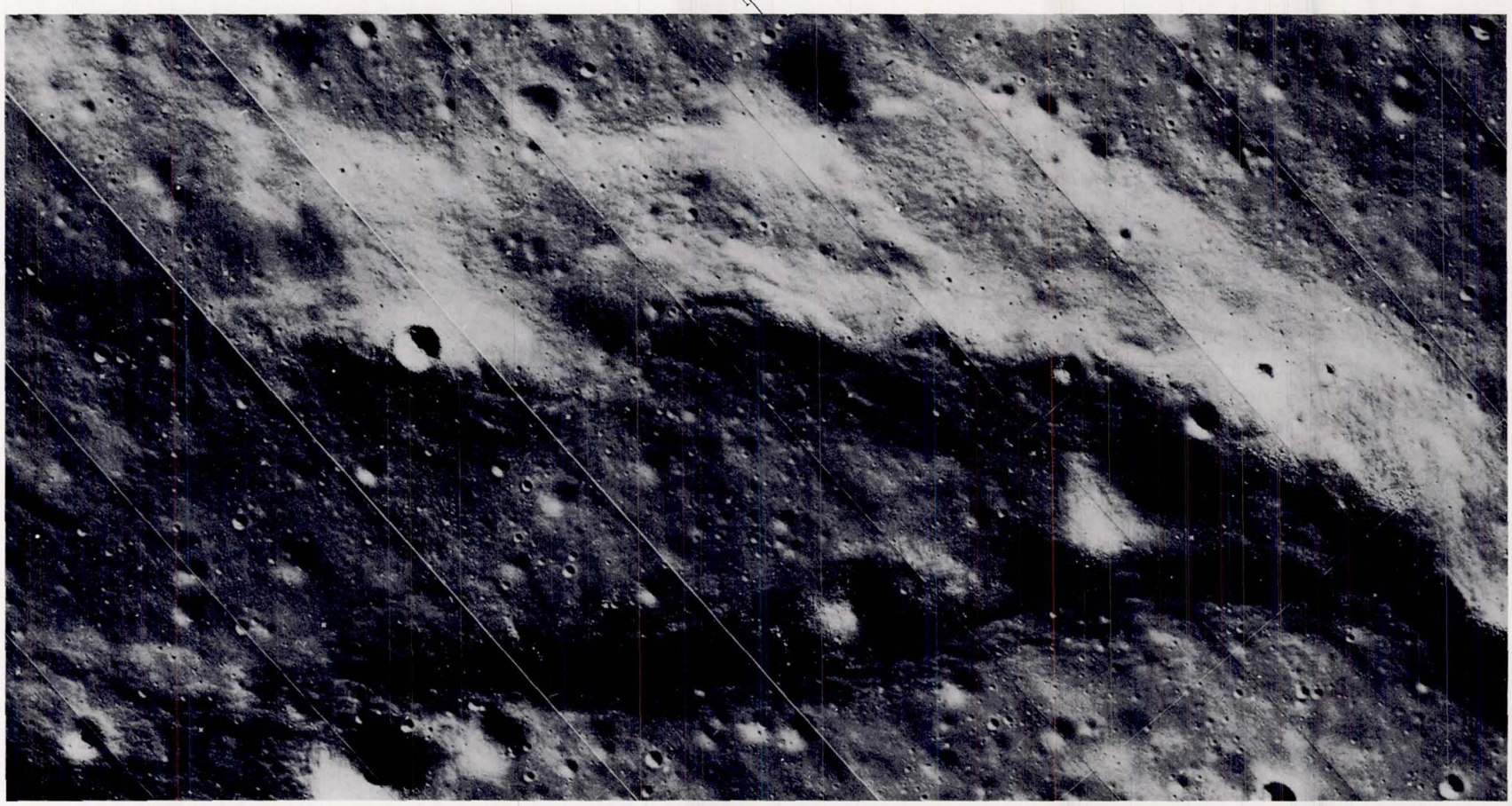

A high-resolution photograph of the wrinkle ridge visible at the extreme left side of the picture above. The ridge top is generally smooth and rolling, but its crests and sides are steep and abundantly strewn with blocks of rock. Blocks are concentrated around several craters on the upper ridge crest, especially the bright, sharp-walled crater at the left center of the picture. In this case, the blocks appear to be a product of the cratering event. Location: 3°20′ S, 36°10′ W. Framelet width: 450 meters.

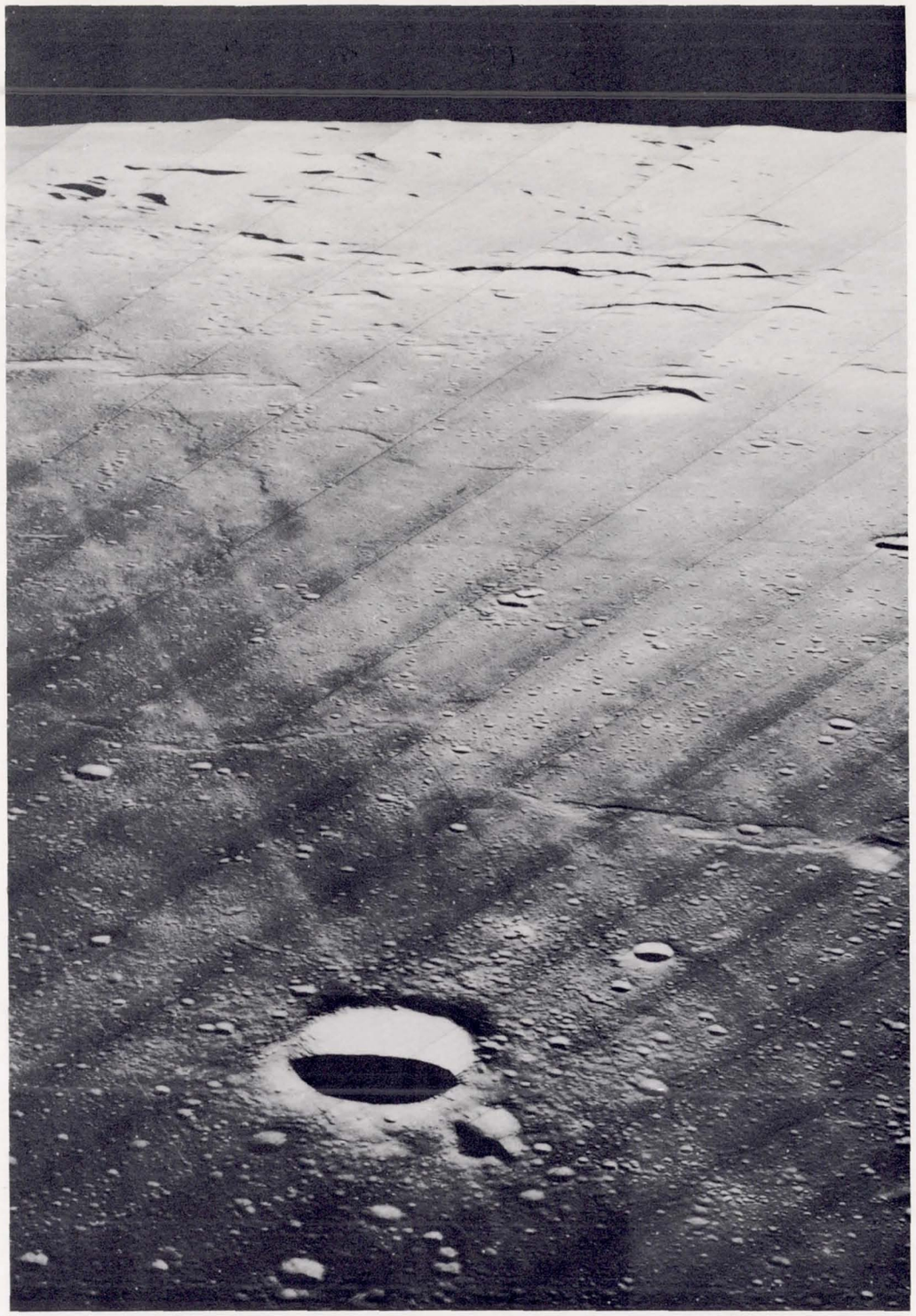

A westward oblique view of a broad expanse of mare plain in Sinus Medii. The large crater in the foreground is Bruce, about 7 kilometers across and 800 meters deep, located 1°N, 0°30′E. Several wrinkle ridges extend across the mare plain, especially in the middle ground. Higher highland ridges can be seen in the background. This is the view an astronaut would have while descending for a landing in Sinus Medii.

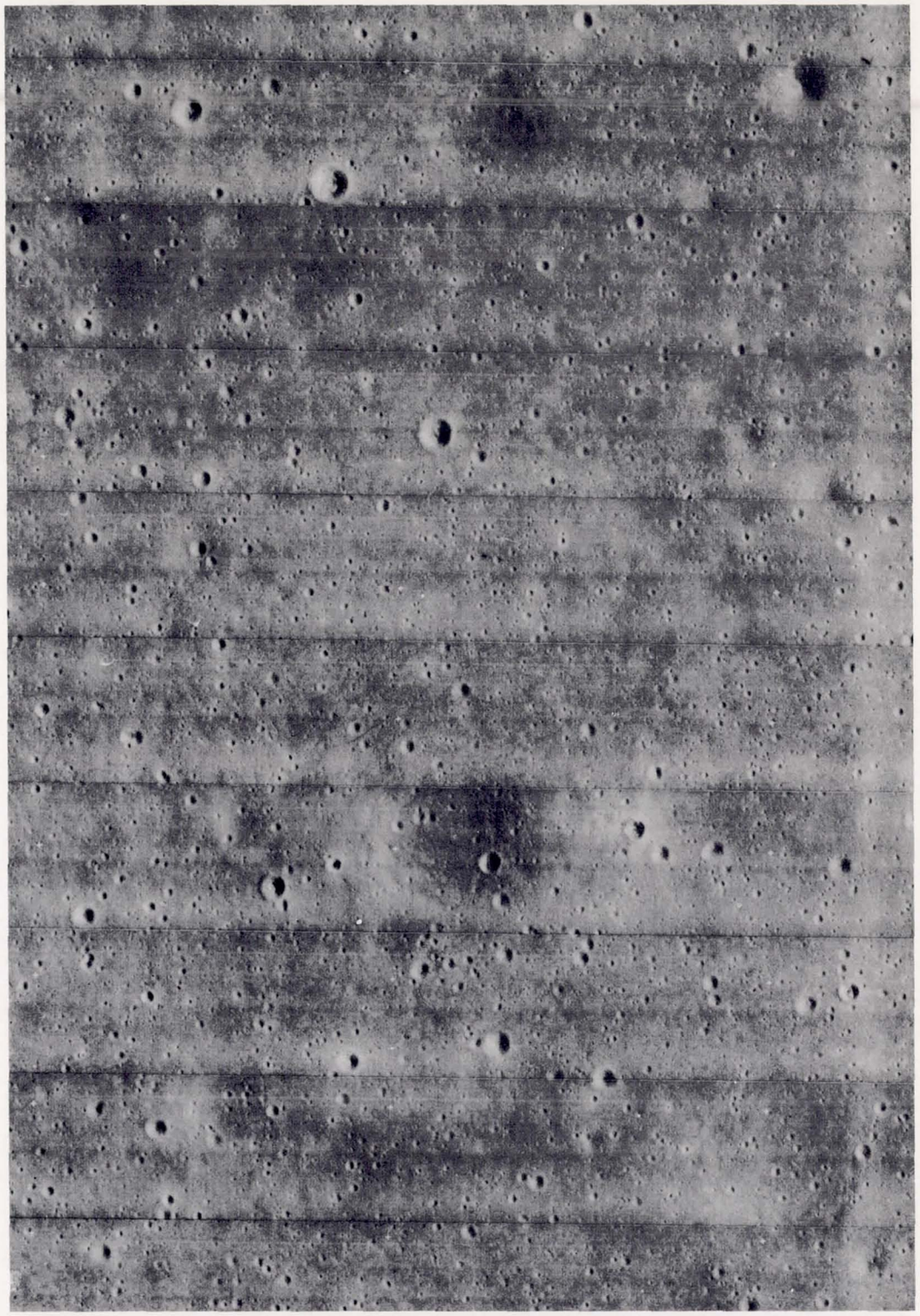

The smooth, light-toned mare plain shown in this high-resolution photograph of an area in Mare Tranquillitatis is a favorable type of terrain for an Apollo landing. Nearly all of the craters in the picture are small, shallow, and subdued; the few larger craters are essentially smoothed out and show only as darker circles. Few significant obstacles to a spacecraft landing are visible. Location: 0°50′N, 23°40′E. Framelet width: 210 meters.

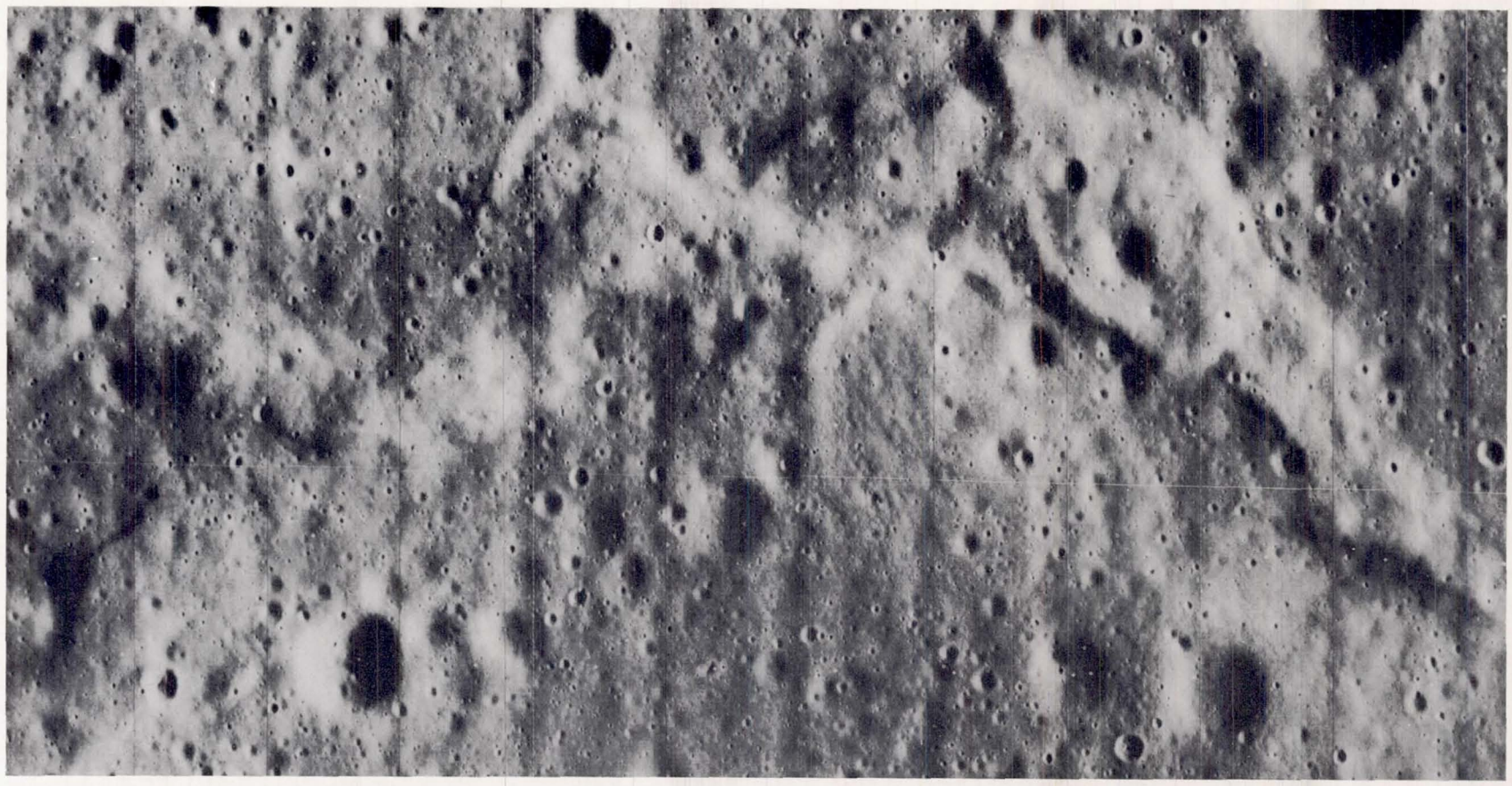

In the vicinity of this sinuous mare ridge lies a candidate Apollo landing site in Sinus Medii. The ridge is rounded and subdued with practically no steep slopes. No blocks of rock are visible around the few sharp-walled craters on the ridge. The crater density on the ridge appears to be equal to that on the adjacent mare plain. Most craters are subdued, and some below the ridge are essentially smoothed out. Location: 0°10′N, 0°50′W. Framelet width: 440 meters.

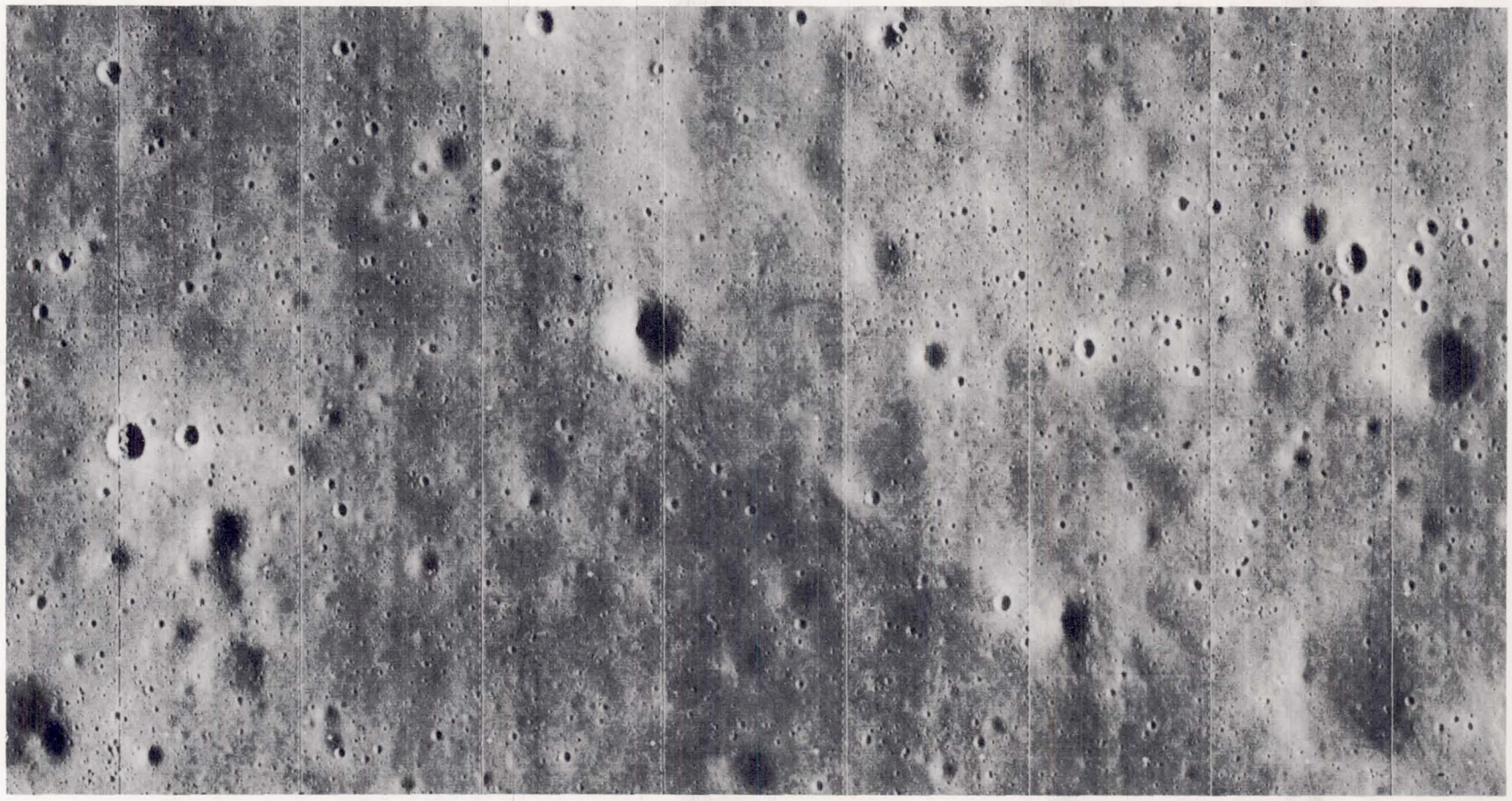

A wide diversity of crater forms is evident in this high-resolution photograph of a candidate Apollo landing area in Mare Tranquillitatis. Craters of all degrees of sharpness are visible in the picture; many are faint, ghost craters, as in the lower right corner, and only a few craters have sharp walls and appear fresh. Two craters, one in the upper right center and the other near the left edge, display sharp rims and rough floors; the one to the left appears to have an internal terrace near floor level. Location: 2°10′N, 34°10′E. Framelet width: 440 meters.

A faint pattern of lens-shaped mounds can be seen in the walls and floor of the shallow depression extending diagonally across this photograph of a site in southwestern Mare Tranquillitatis. This pattern is lacking on the mare plain in the upper right and lower portions of the photograph. Such patterned ground may indicate consolidated material just beneath the lunar surface. Location: 4°30′ N, 21°20′ E. Framelet width: 200 meters.

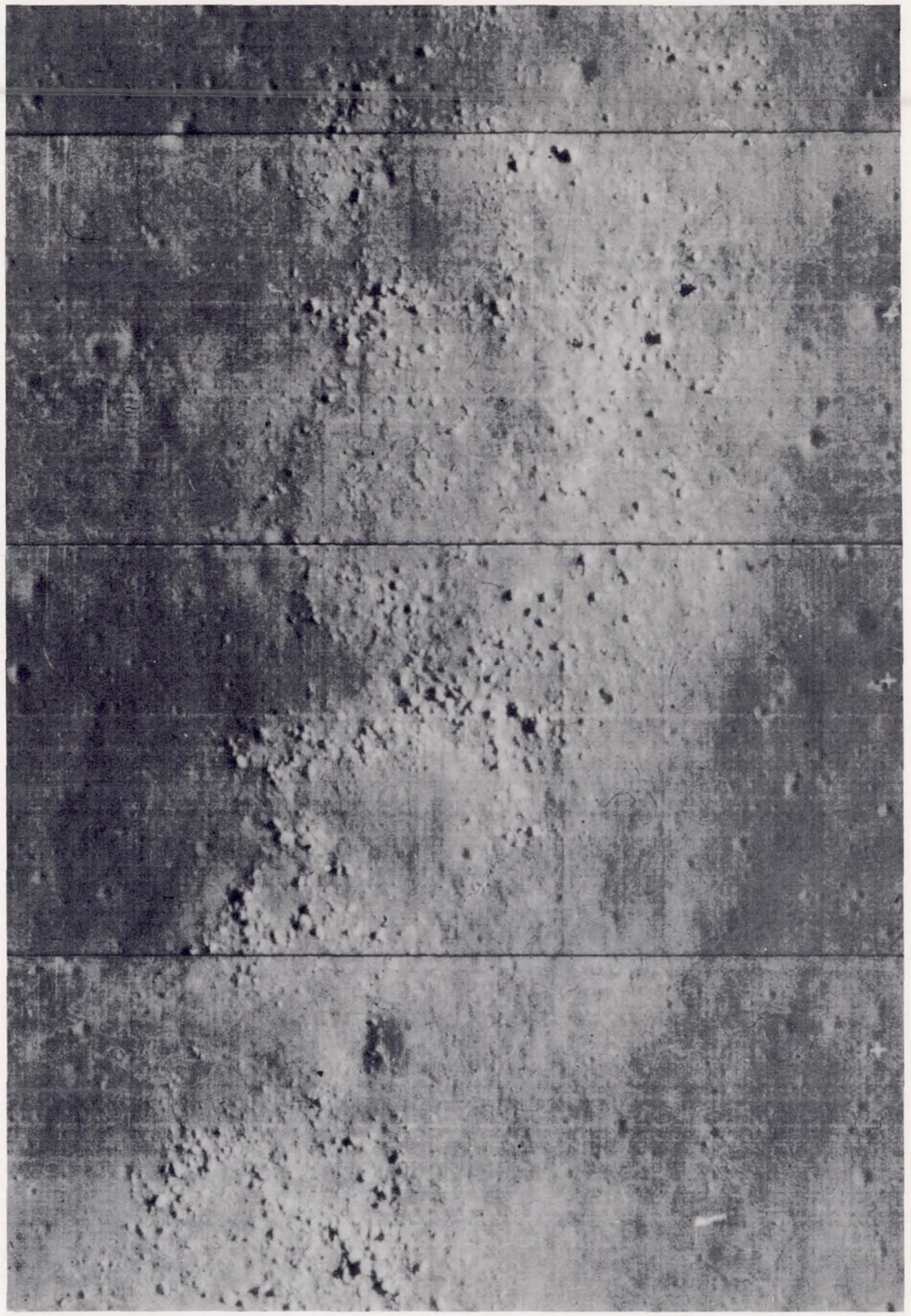

An enlargement of a high-resolution photograph depicting part of a low ridge just east of a candidate Apollo landing site in Mare Tranquillitatis. The surface, which is here sloping toward the right, is strewn with blocks, some of which are roughly arranged in form of incomplete rings. Most of the blocks are quite large, and many appear to have rounded outlines. Few craters are evident in this field. Location: 2°30′ N, 34°30′ E. Framelet width: 190 meters.

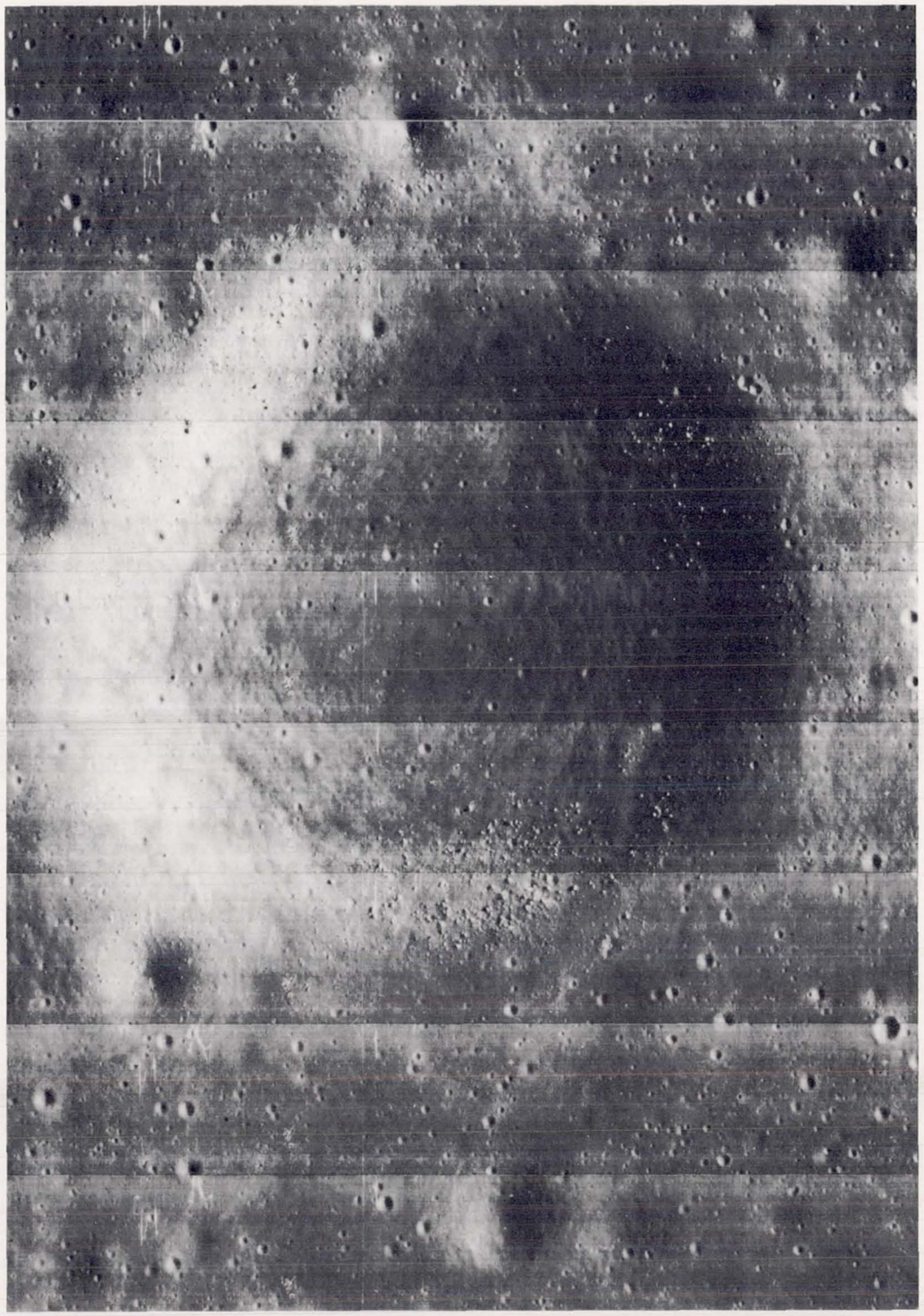

The large subdued crater evident in this photograph of a portion of Mare Tranquillitatis exhibits gently sloping walls and a fairly flat floor. The unusual feature of this crater is the abundance of blocks of rock visible on the walls, with fewer blocks on the floor. Blocks can be seen on the plain only in or near smaller craters close to the main one, as at the top center of the picture. These blocks may indicate consolidated material at shallow depth beneath the mare surface. Location: 2°40′N, 24°40′E. Framelet width: 180 meters.

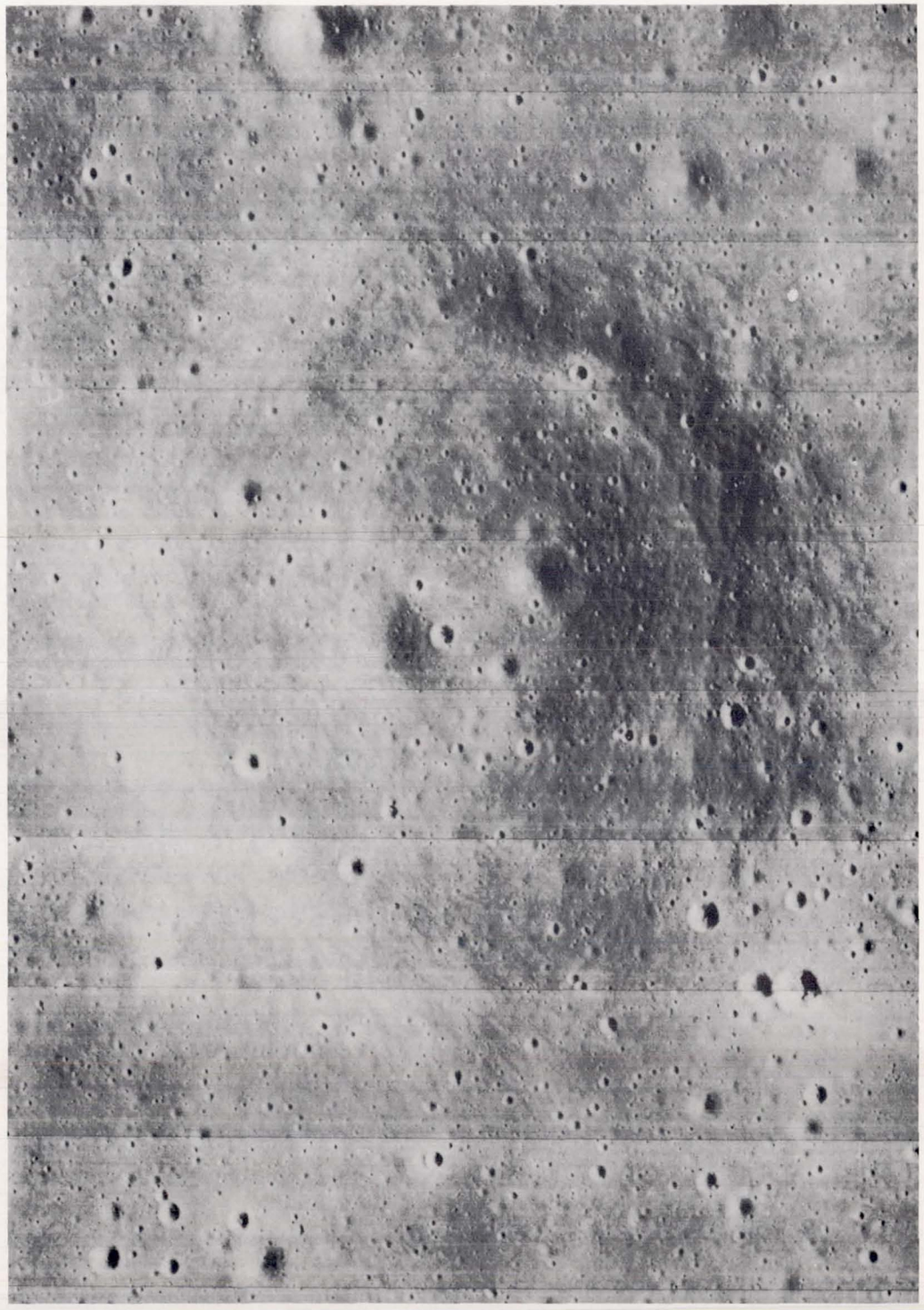

The circular depression visible in this high-resolution photograph of a mare plain in Mare Tranquillitatis is a ghost crater. The lack of any definite rim and the gently sloping walls indicate a high degree of smoothing out of this feature. Despite the subduing, traces of a low central mound and of a terrace at the base of the walls can be seen. The density of small craters in the depression is about equal to that on the adjacent mare plain. Location: 3°30′N, 41° E. Framelet width: 190 meters.

The sharp, double-walled crater at the center of this high-resolution photograph of densely cratered mare plain near the middle of Oceanus Procellarum is an uncommon type of mare crater. The inner wall appears to be formed of blocky material, as indicated by the shadows on the left side walls of the crater. Concentrations of blocks of rock mixed with secondary impact craters are visible as rays extending from this crater for distances of 2 to 3 crater diameters. Location: 1°40′N, 42°20′W. Framelet width: 230 meters.

Another example of a rayed, irregular crater near a candidate Apollo landing site in Oceanus Procellarum. In contrast to the opposite example, this crater has no distinct sharp rim. Central mounds, segments of an inner wall, and a ring of hummocky ground are visible, as is a rubble mantle of blocks on the crater. Rays formed of blocks of rock and small impact craters surround the main crater. Many large blocks can be seen within 1 crater diameter of the outer rim crest. Location: 2°10′S, 44°10′W. Framelet width: 260 meters.

HIGHLANDS

The relatively bright, rough, and elevated lunar surfaces are referred to as terrae or highlands, to distinguish them from the relatively dark, smooth, and low-lying maria. Much of the highland area, though rough, is actually a much modified plain. Morphologic features that originally were sharp commonly have become subdued with time. In part, this subdual is ascribed to the movement of loosely consolidated material from higher positions to lower levels on the surface under the influence of lunar gravity, possibly with the aid of moonquakes. The resulting texture, where it is gentle and does not involve large debris flows, is referred to as patterned ground. Several examples of patterned ground, which is visible only on high-resolution photographs, are shown in this section.

Mountain ranges exist on the Moon in the form of arcs, associated with the major circular basins and bounded on the side facing the basin by steeper slopes or scarps. They form a continuous border around basins such as Mare Crisium. Others form a discontinuous array, as exemplified by the Jura, Alps, Caucasus, Apennine, and Carpathian Mountains bordering Mare Imbrium. Still other arcs, such as the Altai Scarp, are in the highlands but appear to be concentric with a nearby mare basin, in this case Mare Nectaris. Many mountains of lesser magnitude occur as isolated blocks or peaks.

Concerning the relative age of the highlands and the maria, most scientists believe that the highlands represent older segments of the lunar surface. Age dating (by isotope abundances) of representative samples from both types of terrain is planned following the return of samples by the Apollo astronauts.

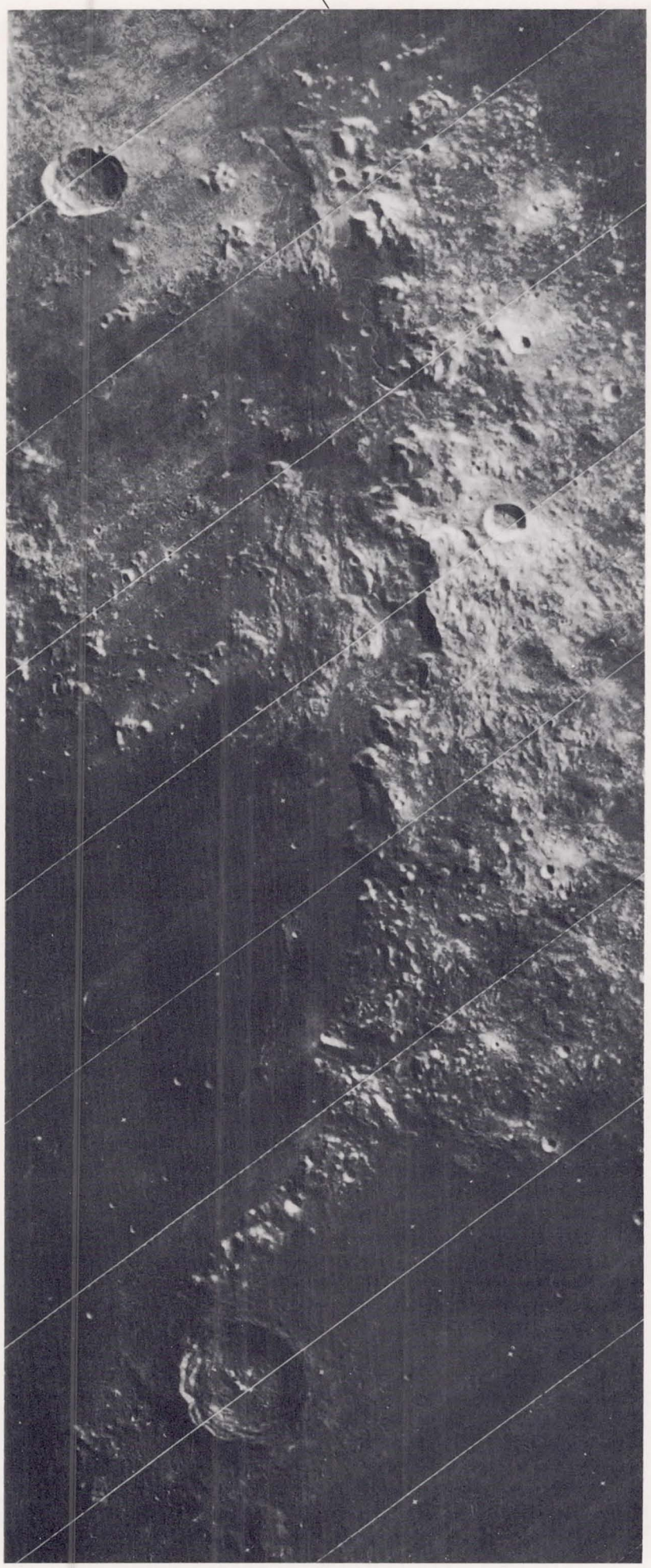

General view of the Apennine escarpment at the southeastern border of Mare Imbrium. Resolution in this view is roughly equivalent to that obtained with a large telescope on Earth on a night with good seeing conditions. Some of the peaks in the escarpment rise more than 2000 meters above the mare floor. Location: 20°30′N, 3°30′W. Framelet width: 89 kilometers.

View of the Caucasus Mountains (lower center) and the craters Eudoxus (upper center) and Aristoteles (top). The rugged Caucasus peaks, up to 4000 meters high, are a continuation of the Apennine Mountains (opposite) and border the eastern side of Mare Imbrium. Location: 42°30′N, 10°35′E. Framelet width: 97 kilometers.

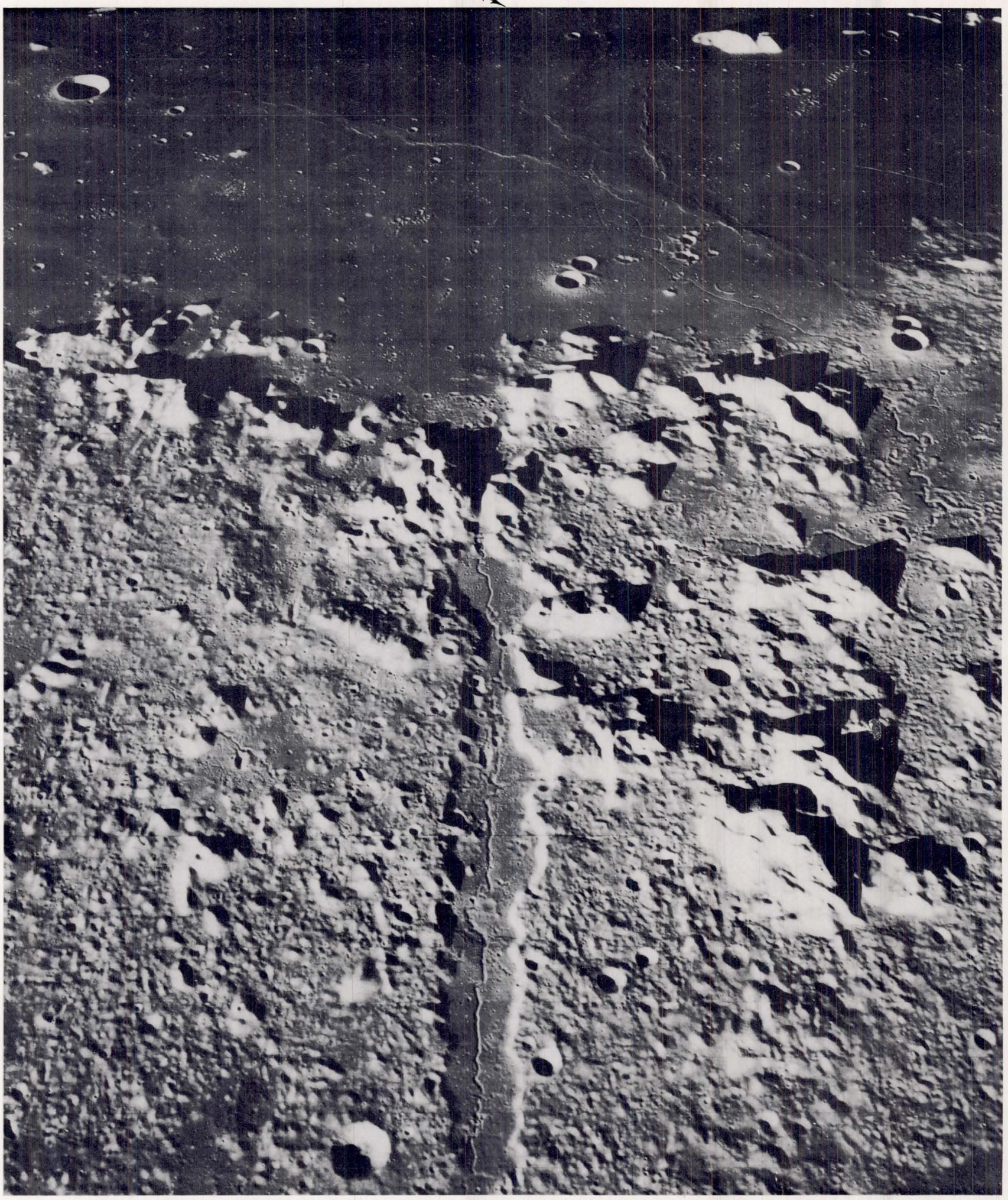

Oblique view toward the west showing Alpine Valley and Mare Imbrium (top) and the isolated mountain block Pico (top right). Alpine Valley, about 150 kilometers long and 8 kilometers wide, is a unique feature on the visible face of the moon and gives the appearance of a terrestrial valley cut by a winding river (sinuous rille). The genesis of this feature will undoubtedly provoke considerable discussion in the future. Location: 48°15′N, 1°E.

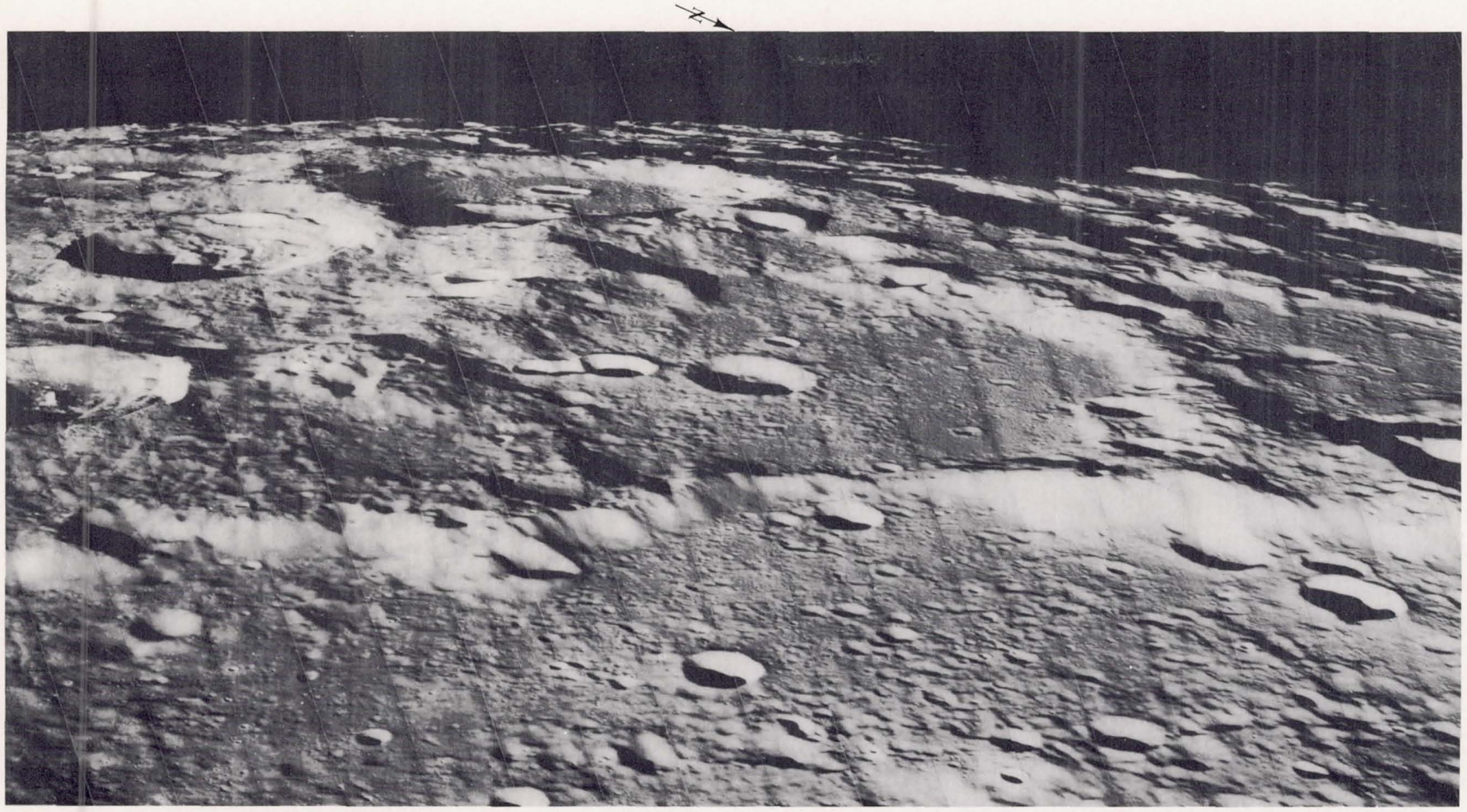

Oblique view, looking southwest, of the eastern side of the Altai Scarp. This portion of the scarp, seen in the middle foreground, rises above its base an average of 1000 meters. Brightness of the slopes facing the camera makes it difficult to observe the detail on much of the scarp. Location: about 26°E, 28°S.

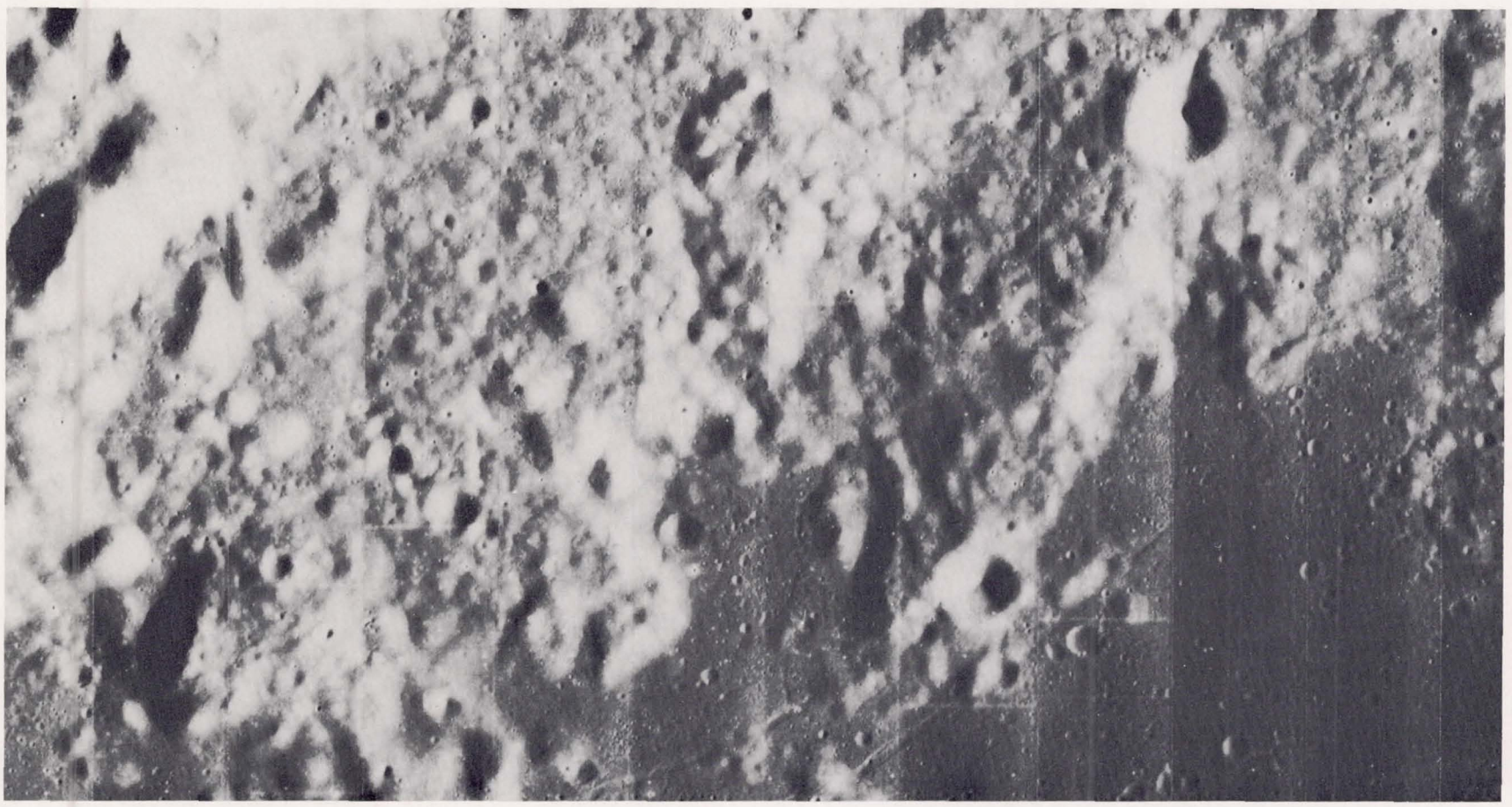

Representative details of the northern borders of Mare Serenitatis. The upper portions of the photograph show hillocks and hummocky terrain of unknown origin composed of light-toned materials. Part of the Calippus Rille extends northeastward from the lower center in the darker, smooth mare material. Location: 37°50′N, 13°55′E. Framelet width: 6 kilometers.

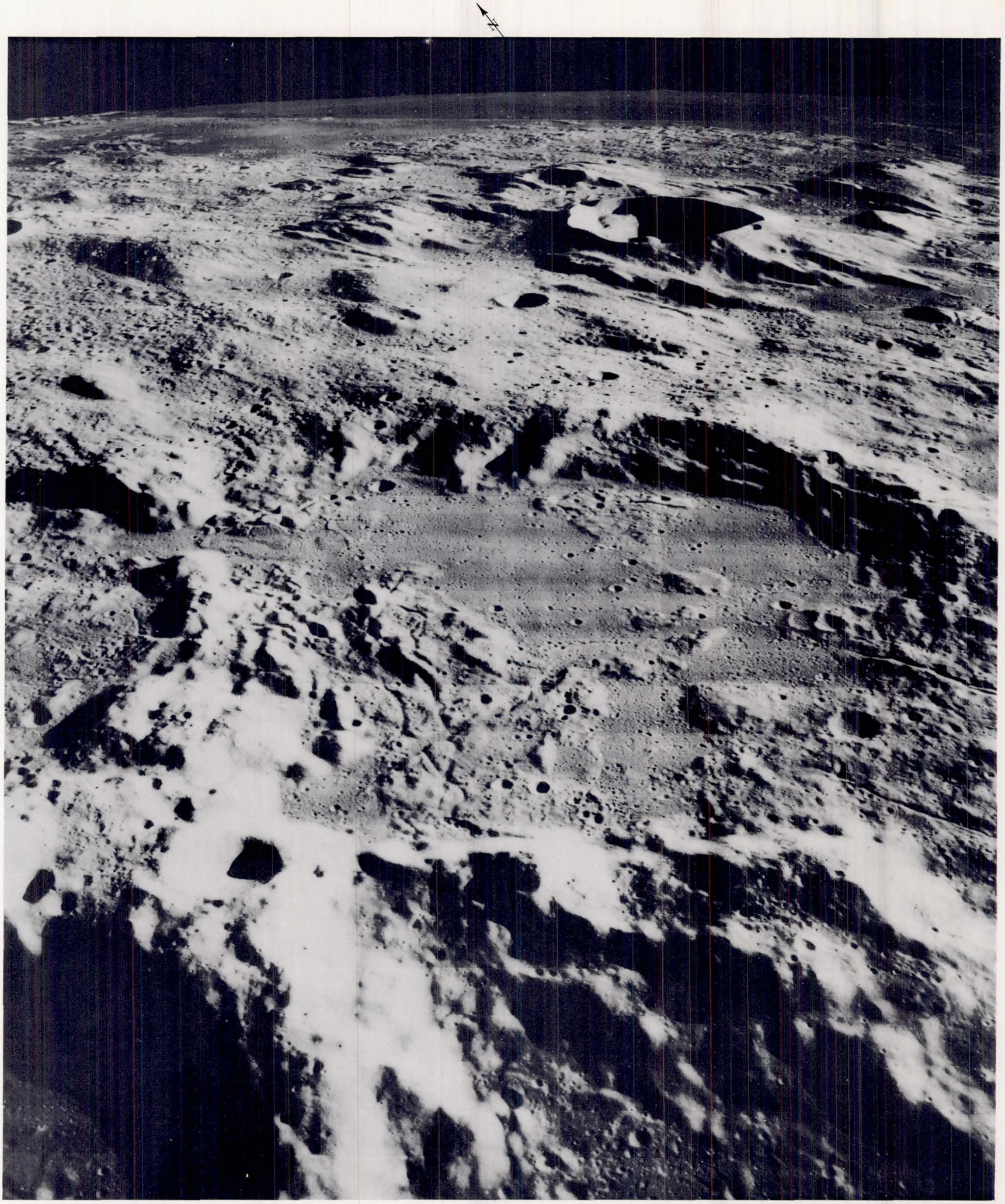

View of the crater Murchison, center (58 kilometers across) and Ukert, upper center, looking north toward the southern edge of Mare Vaporum in the background. The many irregular positive features on the floor of Murchison, which may be attributed to volcanism, are dissected by a network of rilles. Some of the rilles are sinuous and others linear. The prominent lineations which may be observed near Ukert have a pronounced northwest-southeast trend; these have been attributed to throwout (ejecta) from the Imbrium event farther to the northwest. Location: about 5° N, 0°30′ W.

Portion of a crater chain close to the southern rim of the crater Abulfeda. The shadowed area in the lower center of the photograph is part of a small rille connecting the elongate craters Abulfeda T, to the left, and Abulfeda X, to the right. This part of the "Southern Highlands" has a very subdued look, and the patterned ground is not strongly developed. An almost complete absence of large blocks is characteristic of this chain, for which an internal origin has been suggested by some lunar geologists. Location: 15°S, 13°55′E. Framelet width: 410 meters.

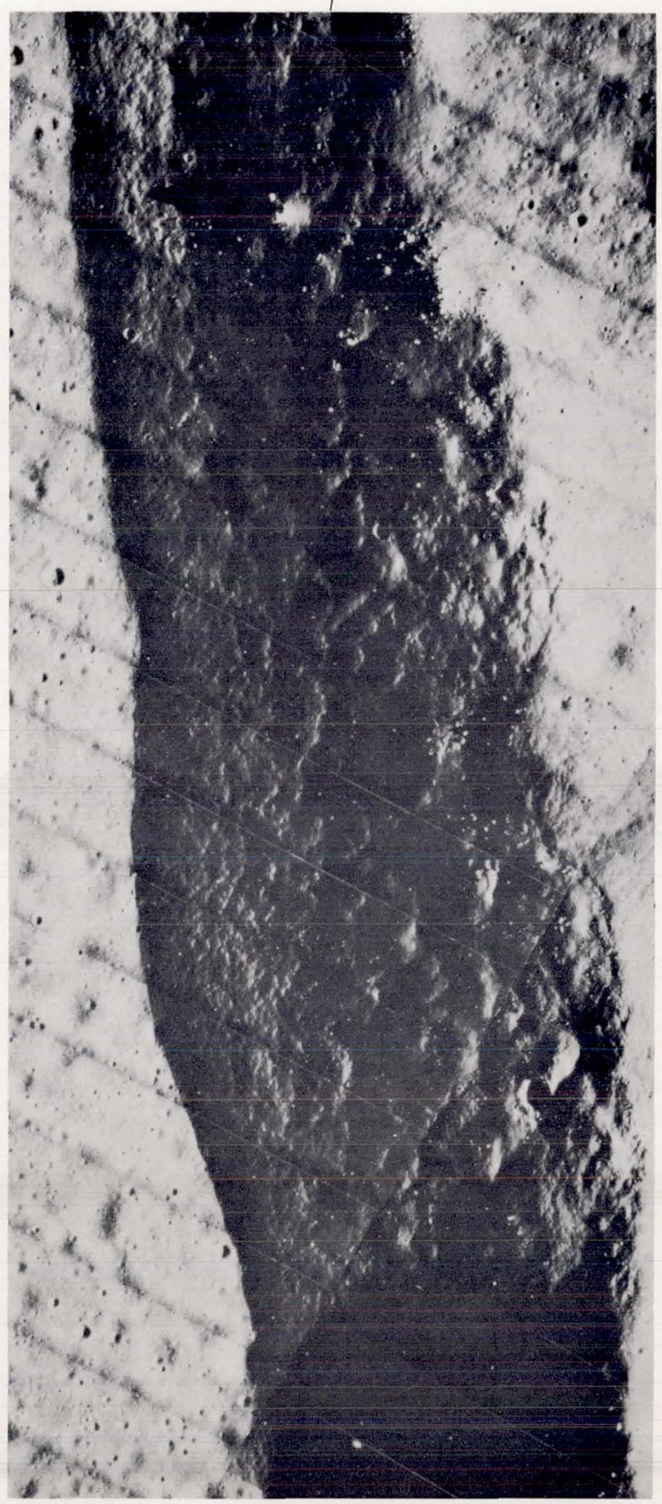

Fine details of a part of the Flamsteed Ring, a nearly circular pattern of ridges in Oceanus Procellarum. These three photographs show details of the westward escarpment of the ridge illustrated on page 42. Starting with the picture on the left, they cover the entire escarpment (about 9 kilometers long and 300 meters high) from north to south. Note the difference in crater density between the ridge material east of the escarpment and the mare surface to the west. Large blocks of rock can be seen along the face of the escarpment. It is probable that these are *in situ* blocks that were exposed following an enormous down slope mass wasting of finer material. Location: 2°50′S, 42°40′W. Framelet width: 220 meters.

Patterned ground in the crater Gassendi. The textures are similar to other highland areas where the patterns are strongly influenced by the slopes. Note the increase in crater frequency in the shallow valley floor, at the middle left of the photograph, and also the abundance of large blocks on the crests of the hills in the upper right. Some of these blocks are more than 10 meters across. Location: 19°15′S, 40°05′W. Framelet width: 560 meters.

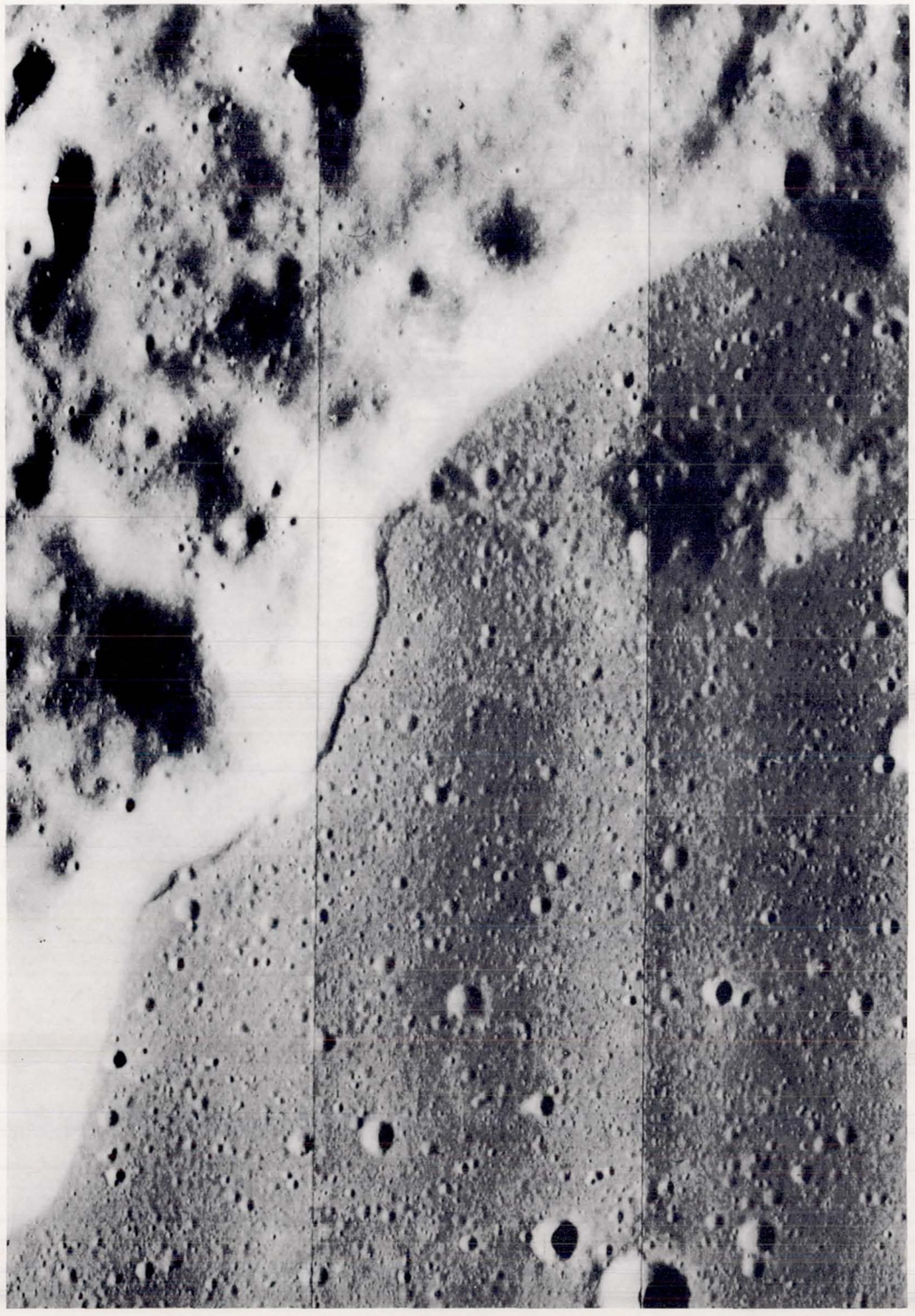

Mare-highland contact south of Gruithuisen γ dome at the northeastern rim of Oceanus Procellarum. The convex profile of the highland contact, which appears to bulge out in places over the mare, is of particular interest. In the center of the photograph, a depression or trench occurs at the foot of the slope. This may indicate that the contact at this point is controlled by faulting. Location: 36°N, 41°20′W. Framelet width: 5.5 kilometers.

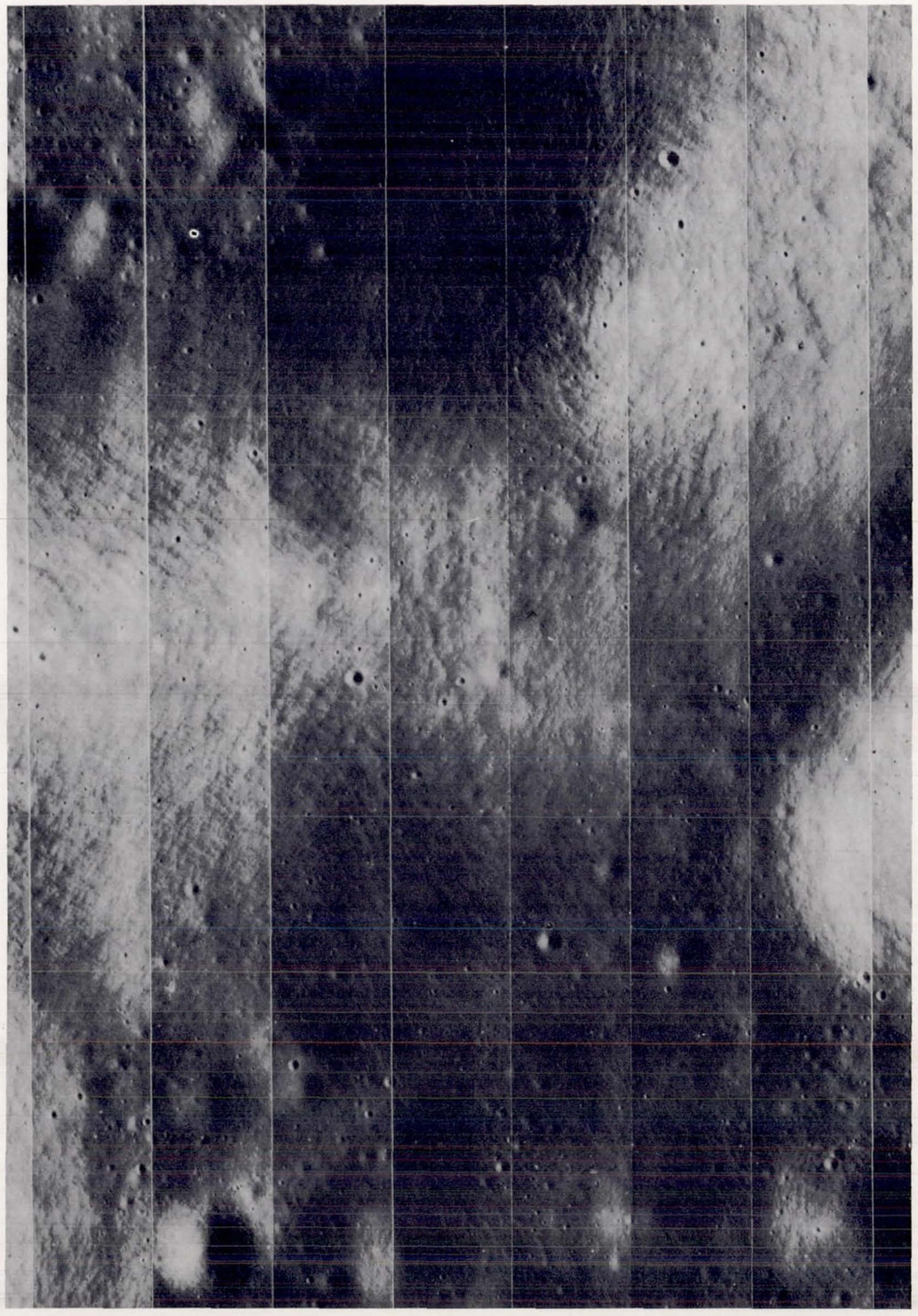

Patterned ground in the floor of the crater Alphonsus. This view shows the typical topographic expression of patterned ground in areas of gentle slopes, and the usual low crater density associated with such ground. Low crater density over most of the area shown can be compared with the higher density of the relatively flat area in the upper left-hand corner. Location: 13°50′S, 4°15′W. Framelet width: 490 meters.

Patterned ground in the Alpes Mountains north of Rima Plato II. This terrain has a notable northeast-southwest pattern in the surface topography. Note also the apparent change in coarseness of the pattern at the break in the slope. Crater frequency is significantly less on the ridge slope than on the flatter areas above or below the slope. A small circular feature, perhaps a ghost crater, can be seen in the lower left. Location: 49°15′N, 1°W. Framelet width: 1 kilometer.

CRATERS

A crater is a circular, polygonal, or elongate topographic depression, generally with steep inner slopes. Craters abound on the surface of the Moon and Mars and, to a lesser extent, the Earth. Lunar craters range in size from the microscopic up to more than 100 kilometers in diameter. The individual craters shown in this section are arranged in order of increasing size, starting with one nearly 4 kilometers in diameter.

Although scientists have generated a voluminous literature on the subject, the origin of craters is still controversial. Prior to the availability of closeup photography, many scientists believed that most craters were formed by the impact of meteorites and comets, while others felt that most of them were the products of volcanic activity. While the Lunar Orbiter photography has provided seemingly incontrovertible evidence for the existence of both impact and volcanic craters, the relative importance of the processes is far from settled.

Lunar craters abound as single features, randomly distributed on the surface. However, many others occur as pairs, clusters, and chains. Some examples of these are presented at the end of this section.

The relative ages of lunar craters are hypothesized from their shapes and the appearance of their rims, walls, and floors. What are thought to be young impact craters may display a sharply raised rim, steep inner slopes, and a deep, sculptured floor. Older craters may show subdued and rounded rims, gentle inner wall slopes, and evenly filled floors. Some apparently young craters, believed to be of volcanic origin, also display subdued rims. Geologists recognize other structural details by which they may infer the relative ages of craters. In the following examples, reference will be made to some of these structural and textural details as they were disclosed by the five Lunar Orbiters.

The crater Mösting C (3.8 kilometers in diameter) is a very fresh crater with abundant blocks on the rim. The ejecta blanket is hummocky, braided, and dunelike, i.e., similar to those of larger, fresh lunar craters. Secondary impact craters abound near the outer edges of the ejecta blanket. The crater is more nearly circular than it appears in this somewhat oblique view. Location: 1°30′ S, 8° W. Framelet width: 1.7 kilometers.

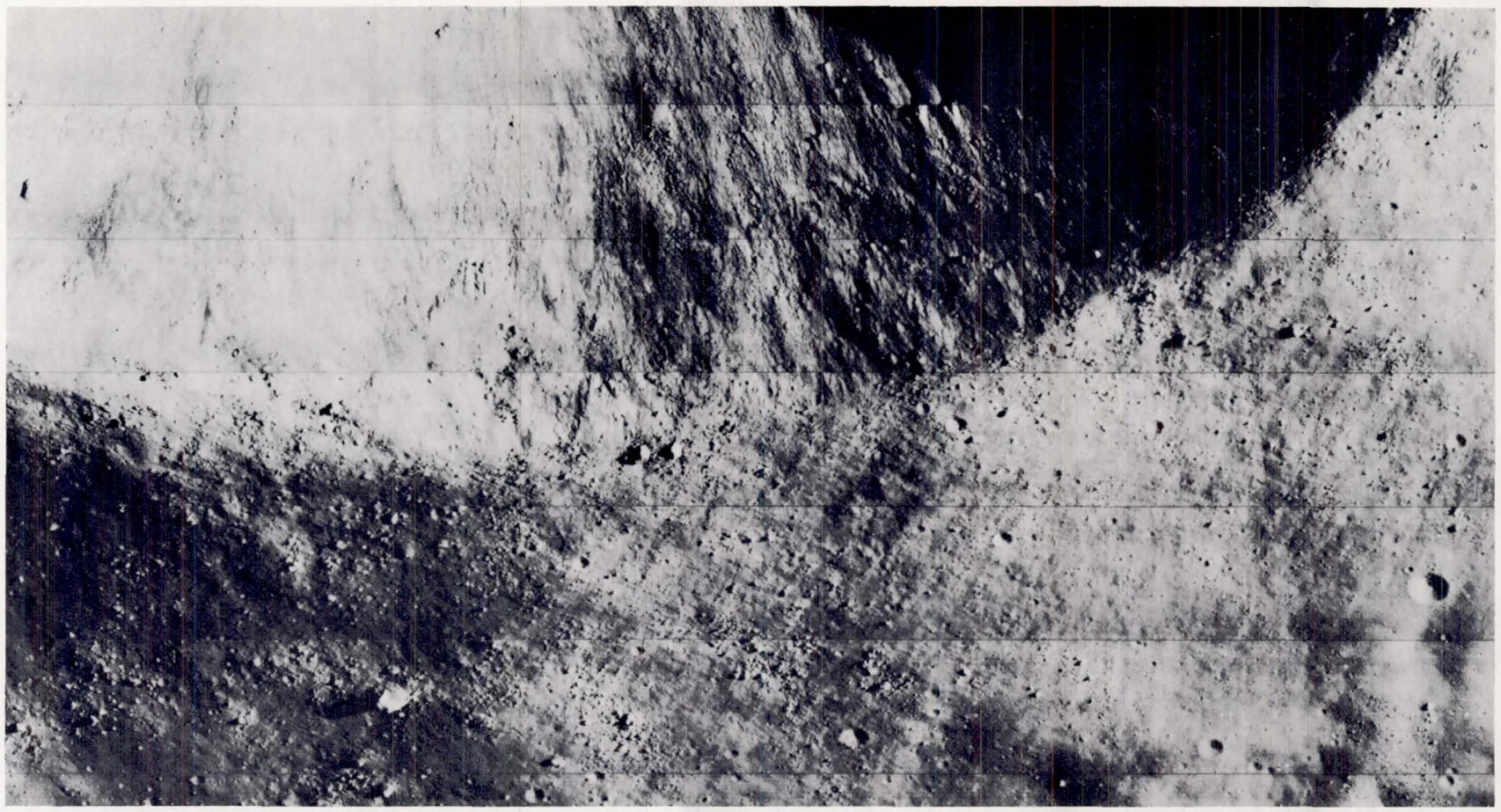

Part of the rim and walls of Mösting C. Large blocks up to about 60 meters in length occur near the rim. The steep crater walls are characterized by talus slopes and outcrops of broken rock. They resemble many steep terrestrial slopes, including those of some man-made craters produced by explosives. The freshness of the materials exposed in Mösting C was predicted on the basis of Earth-based infrared studies. Framelet width: 220 meters.

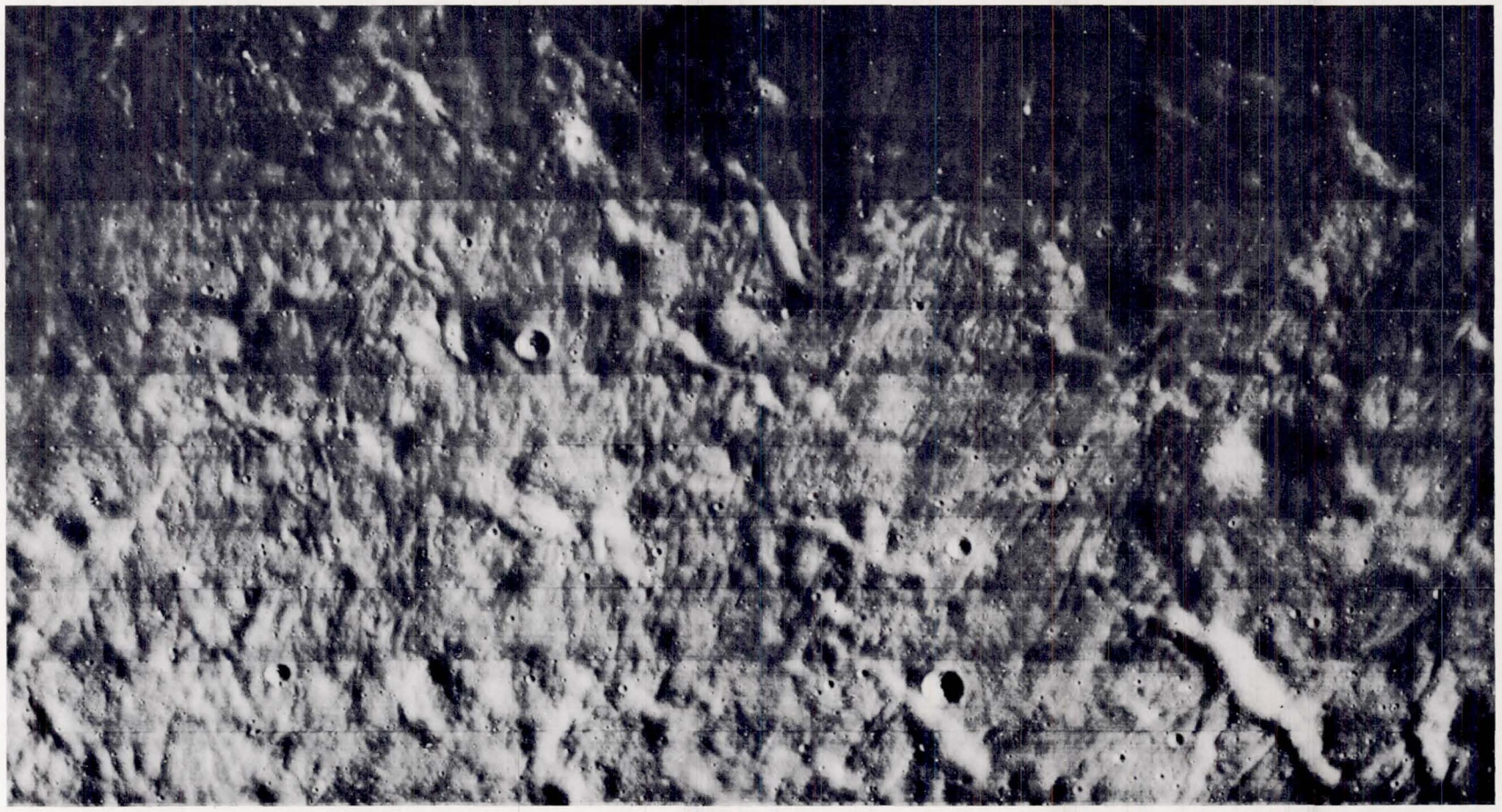

Transverse and radial dunelike textures north of the crater Mösting C. These are similar to base surge deposits produced on Earth by chemical and nuclear explosions and to those around some volcanos. Well-developed, discrete flows, such as those observed around larger craters (e.g., Aristarchus), are lacking. Framelet width: 220 meters.

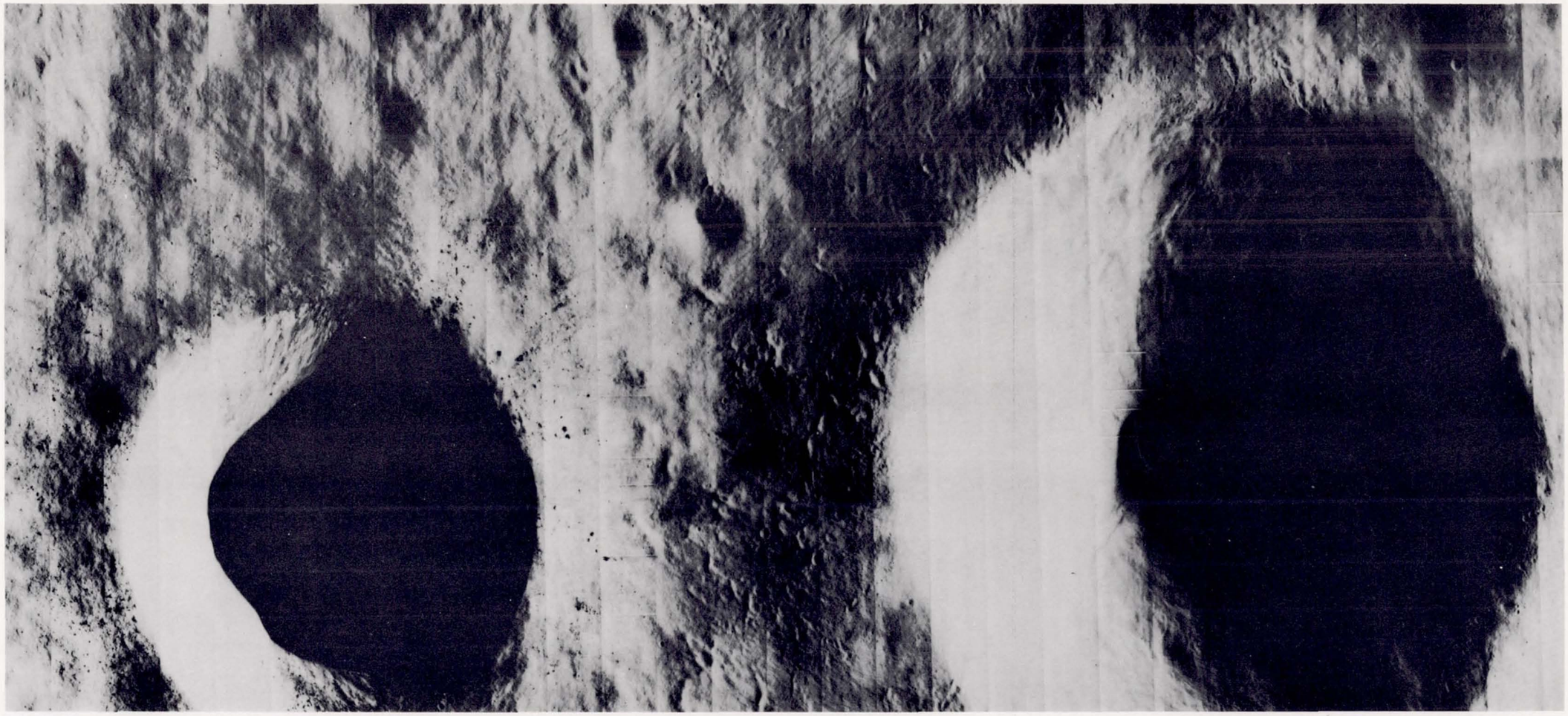

Censorinus (left) is a small crater, approximately 4 kilometers in diameter, on the uplands south of Mare Tranquillitatis. It is a fresh, young-looking crater with a well-developed system of bright rays. Its morphologic characteristics indicate that it is much younger than the neighboring crater, Censorinus A (the larger crater on the right), since ejecta from Censorinus have left marked imprints in the mantled wall of Censorinus A. Abundant blocks lie immediately adjacent to the rim of the crater Censorinus, and scattered blocks extend some distance from it. At the center of the photograph, near the rim of Censorinus A, several blocks have left tracks as they moved down and across apparently low slopes. The tracks are visible as fine, dark, curved lines. Their curvature suggests that the blocks were deflected by the slope of the older Censorinus A. The pattern of ejecta originating from the crater Censorinus and its conspicuous effects on the surroundings suggest that it is most probably an impact crater. Location: 0°30′ S, 32°50′ E. Framelet width: 460 meters.

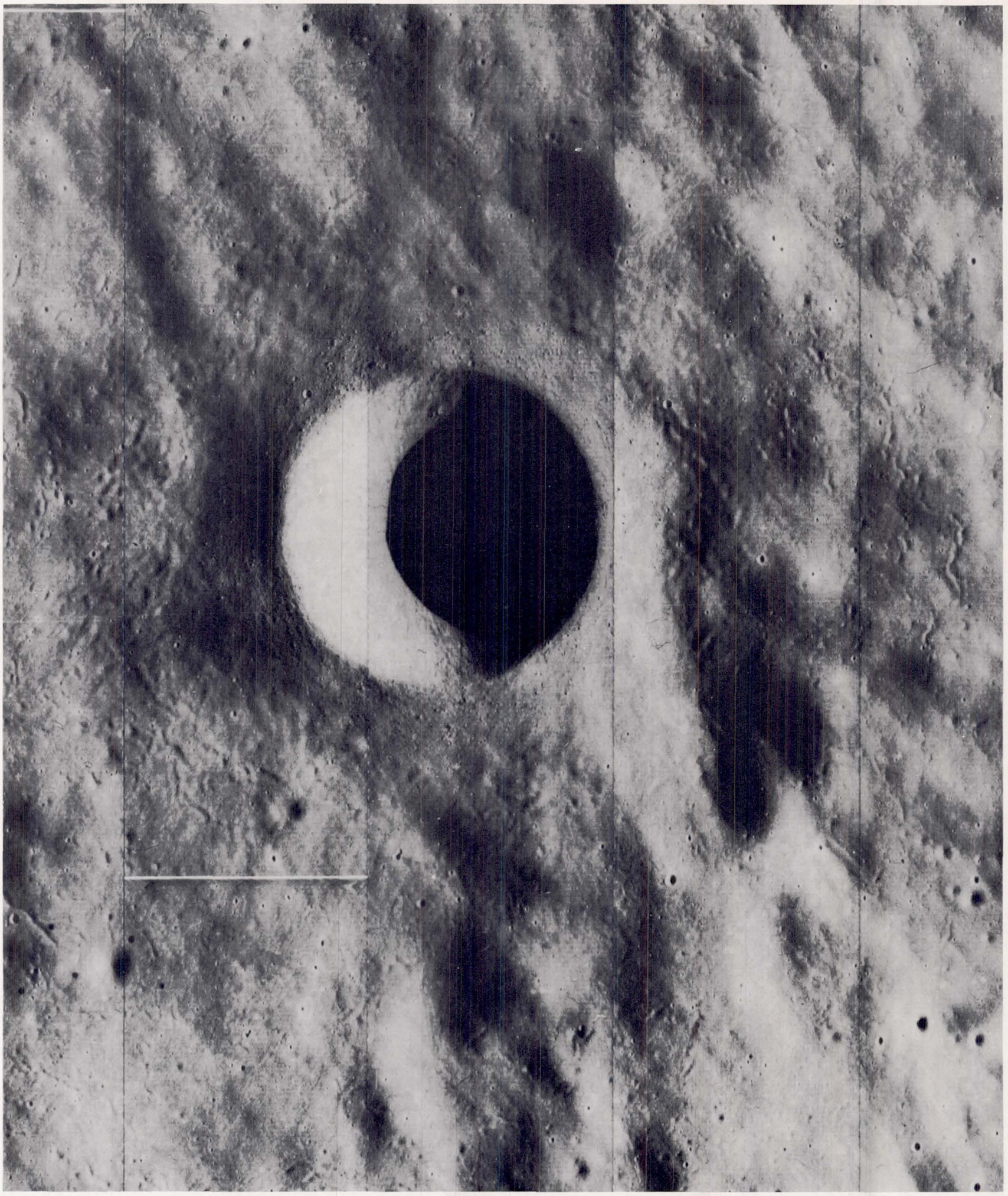

The crater Copernicus H, 4.6 kilometers in diameter, is superposed on the hummocky ejecta deposit outside the rim of the crater Copernicus. It is surrounded by an apron of material that is much darker than the bright ejecta blanket of Copernicus. The dark apron shows up best in full-moon photographs. The crater also has an anomalously high infrared emission signal during eclipse. Location: 6°50′ N, 18°30′ W. Framelet width: 3.3 kilometers.

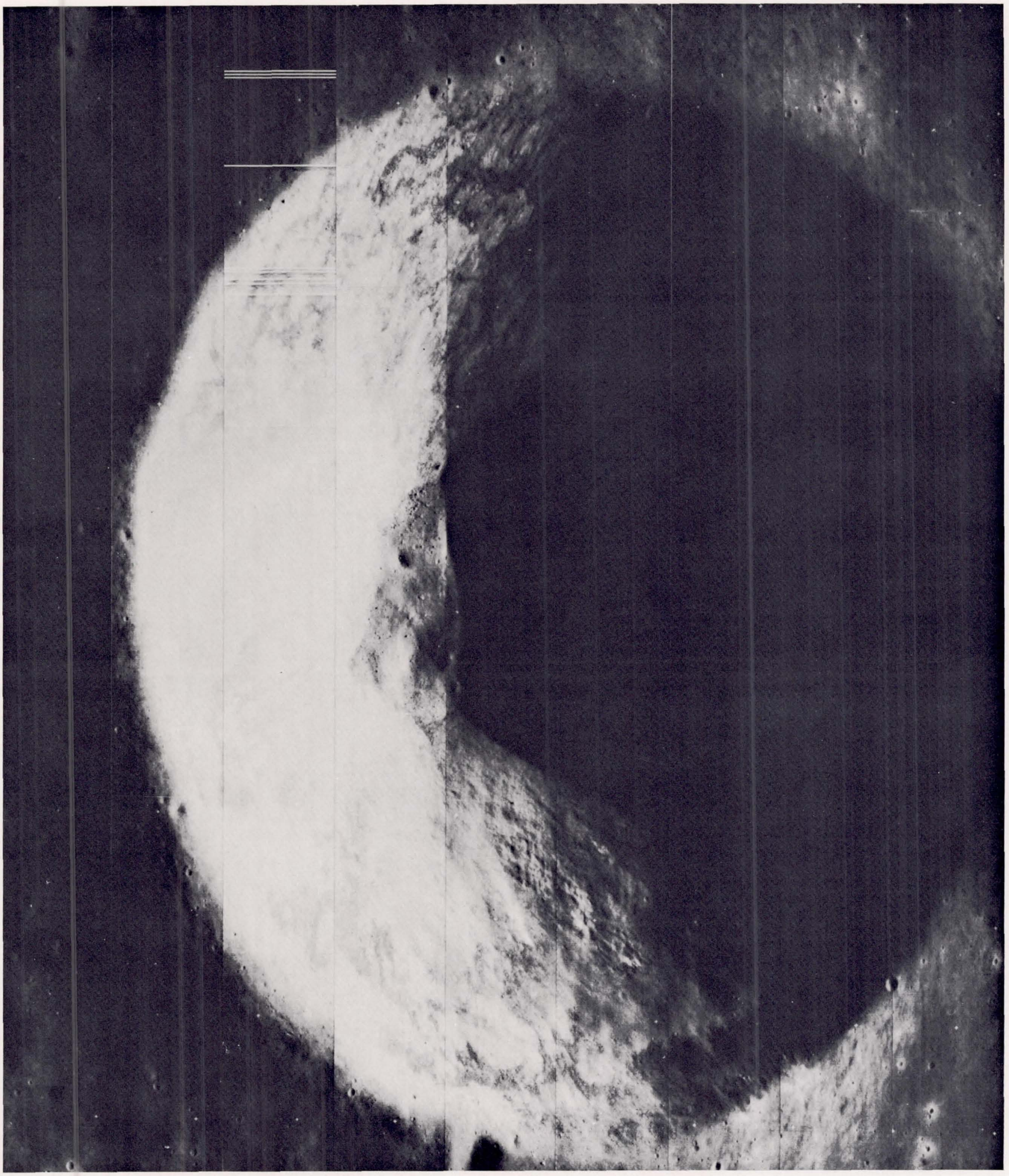

Secchi X, a small, young crater (5.6 kilometers across) near the western edge of Mare Fecunditatis. The striking mottling on the crater wall may be a result of differences in slope stability. The brighter areas appear to be steep surfaces from which fresh fragments may periodically slide downslope. The darker areas may be flatter benches on which material accumulates. Location: 1° S, 43°40′ E. Framelet width: 450 meters.

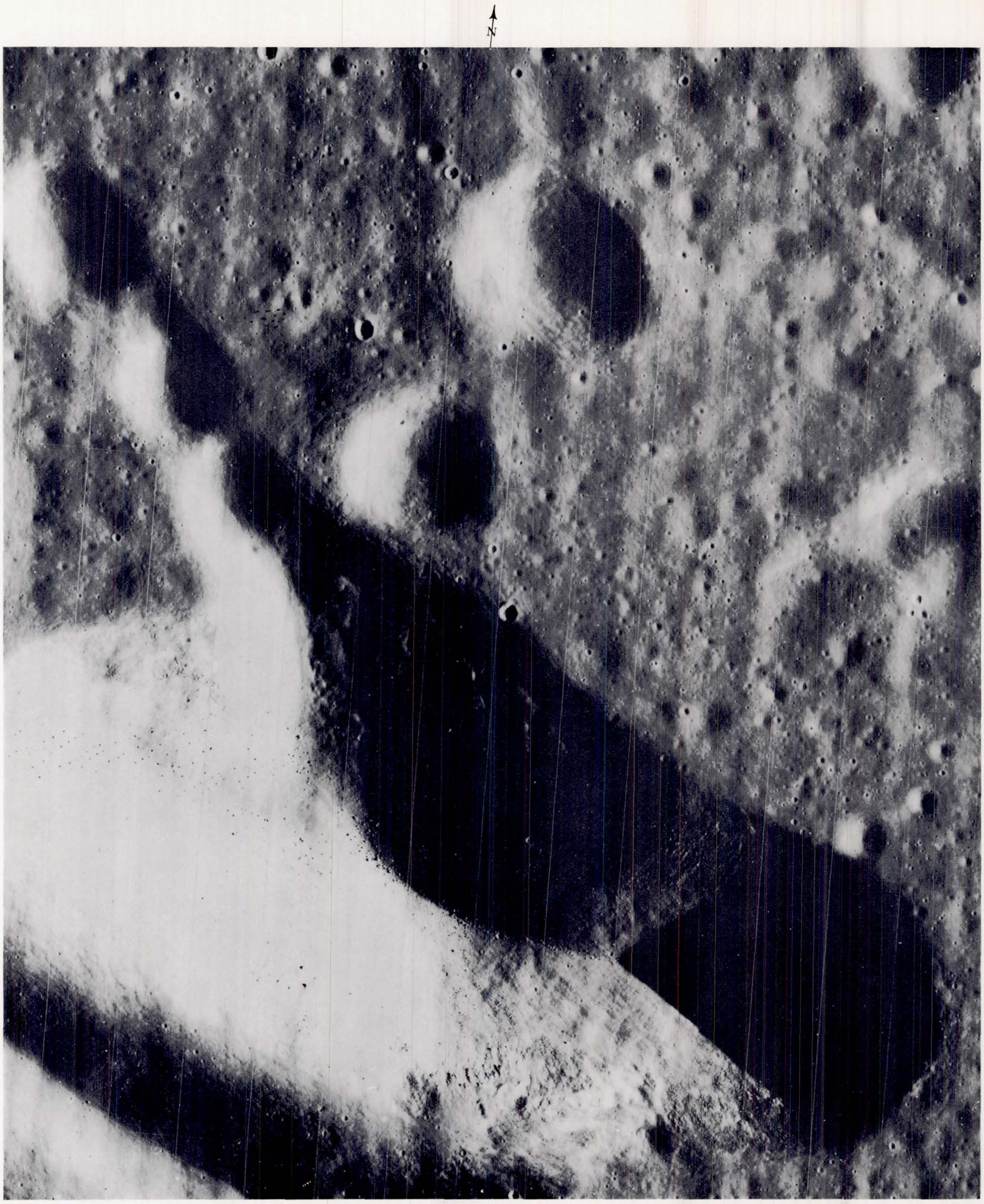

Unnamed crater, 6 kilometers long, next to Rima Bode II. The great number of fresh blocks suggest that the crater is relatively young. The elongate shape of this crater and the chainlike alinement of the smaller craters suggest a volcanic origin. The freshness of this crater was predicted from its high albedo on full-moon telescopic photographs and from its infrared properties. Location: 13° N, 4° W. Framelet width: 450 meters.

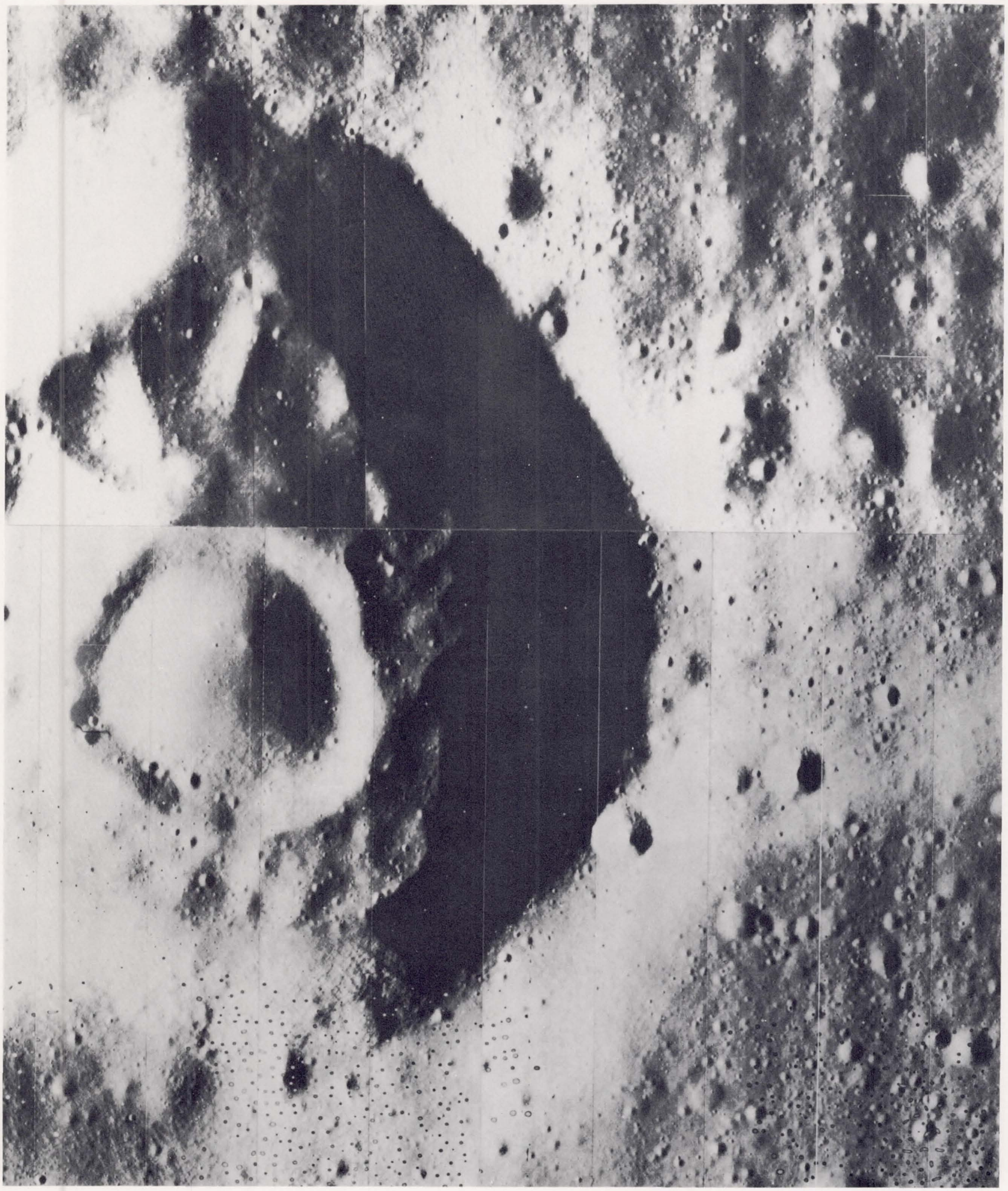

Gruithuisen K, a compound crater about 7 kilometers in diameter situated west of Mare Imbrium. It consists of inner and outer saucer-shaped depressions and an intervening ring of hillocks. Similar craters have been discovered in various parts of the Moon on Orbiter IV photographs. They were probably formed by volcanic processes. The "freckles" at the bottom of this mosaic are processing blemishes. Location: 35°20′ N, 42°40′ W. Framelet width: 700 meters.

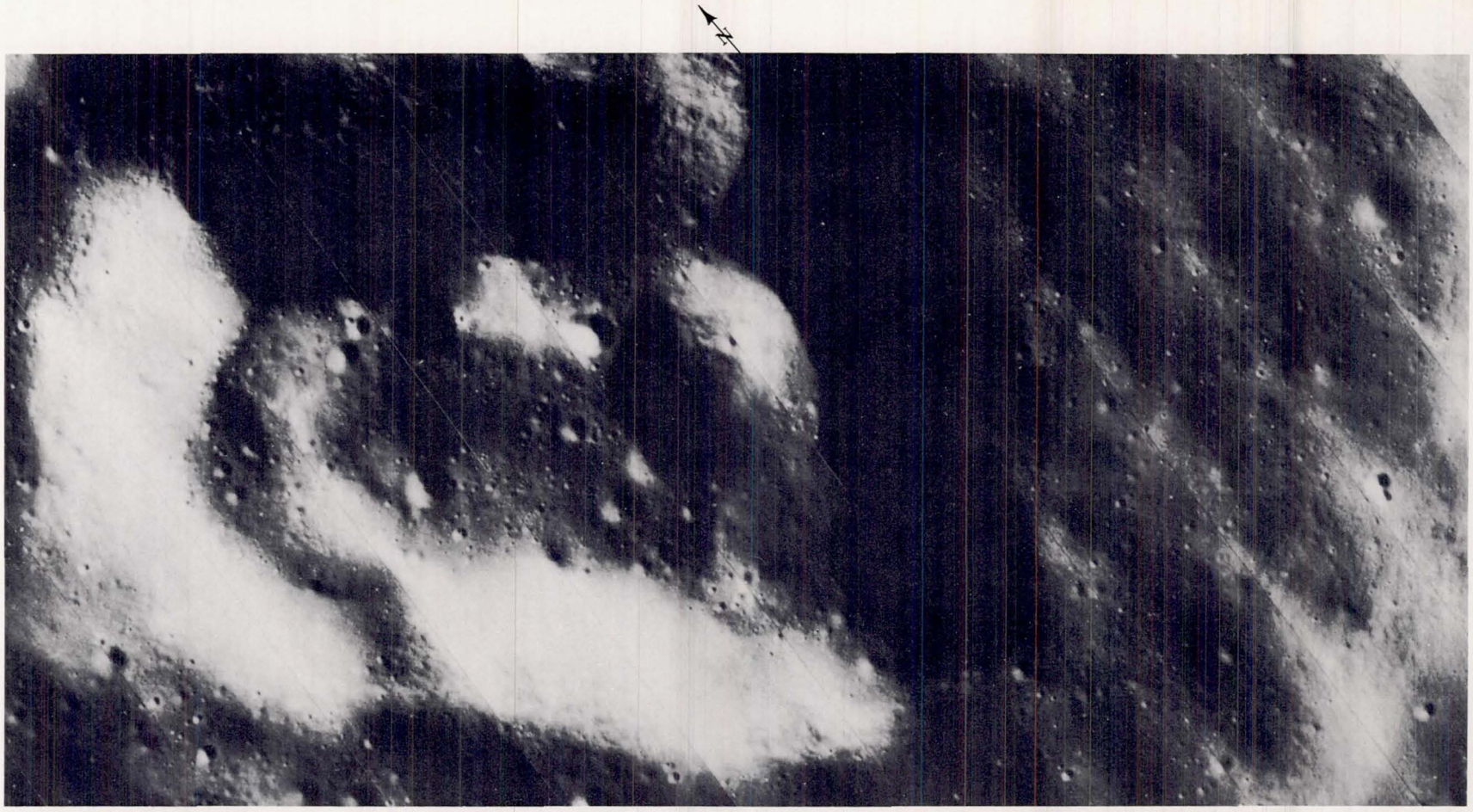

A crater near Gruithuisen K (and nearly as large) has internal domal structures like those of Gruithuisen K. The "domes" and the irregularly rectangular outline of the crater speak strongly for a volcanic origin. The crater floor also exhibits a number of sharp, funnel-shaped craters 100 to 200 meters across. Craters smaller than that are found with about equal frequency on the floor and on the surrounding terra surface. Location: 35°30′ N, 42°20′ W. Framelet width: 700 meters.

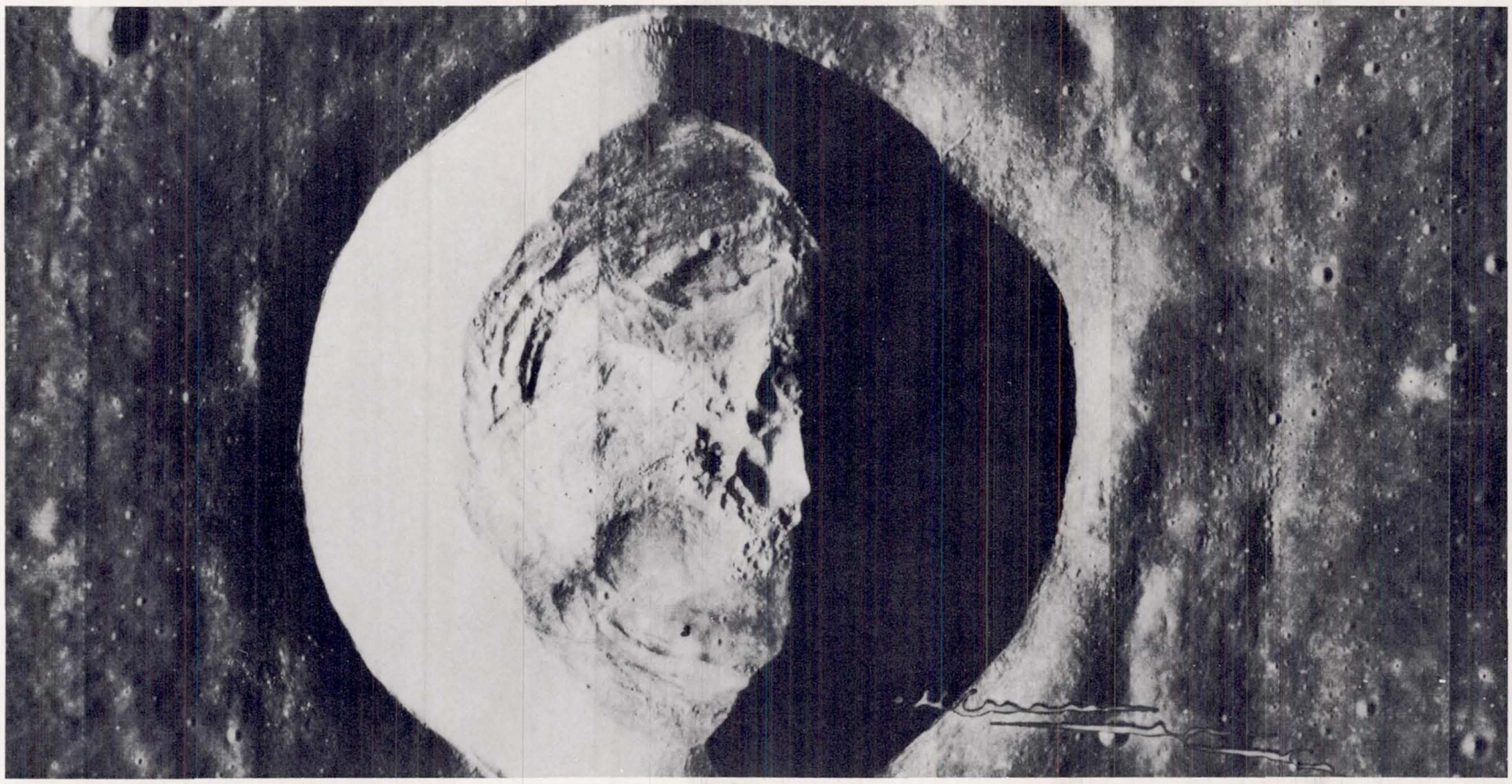

Dawes, a young, 18-kilometer-diameter crater between Mare Serenitatis and Mare Tranquillitatis, displays many features usually attributed to impact. Consolidated bedrock is exposed just below the rim crest; talus close to the angle of repose makes up the rest of the wall. Blocks up to 150 meters across occur on the sparsely cratered rim. A dense secondary crater field occurs beyond the rim, mostly outside the area of the photograph. The crater has an exceptionally high emission in the near infrared during eclipse. Location: 17°10′ N, 26°20′ E. Framelet width: 3.6 kilometers.

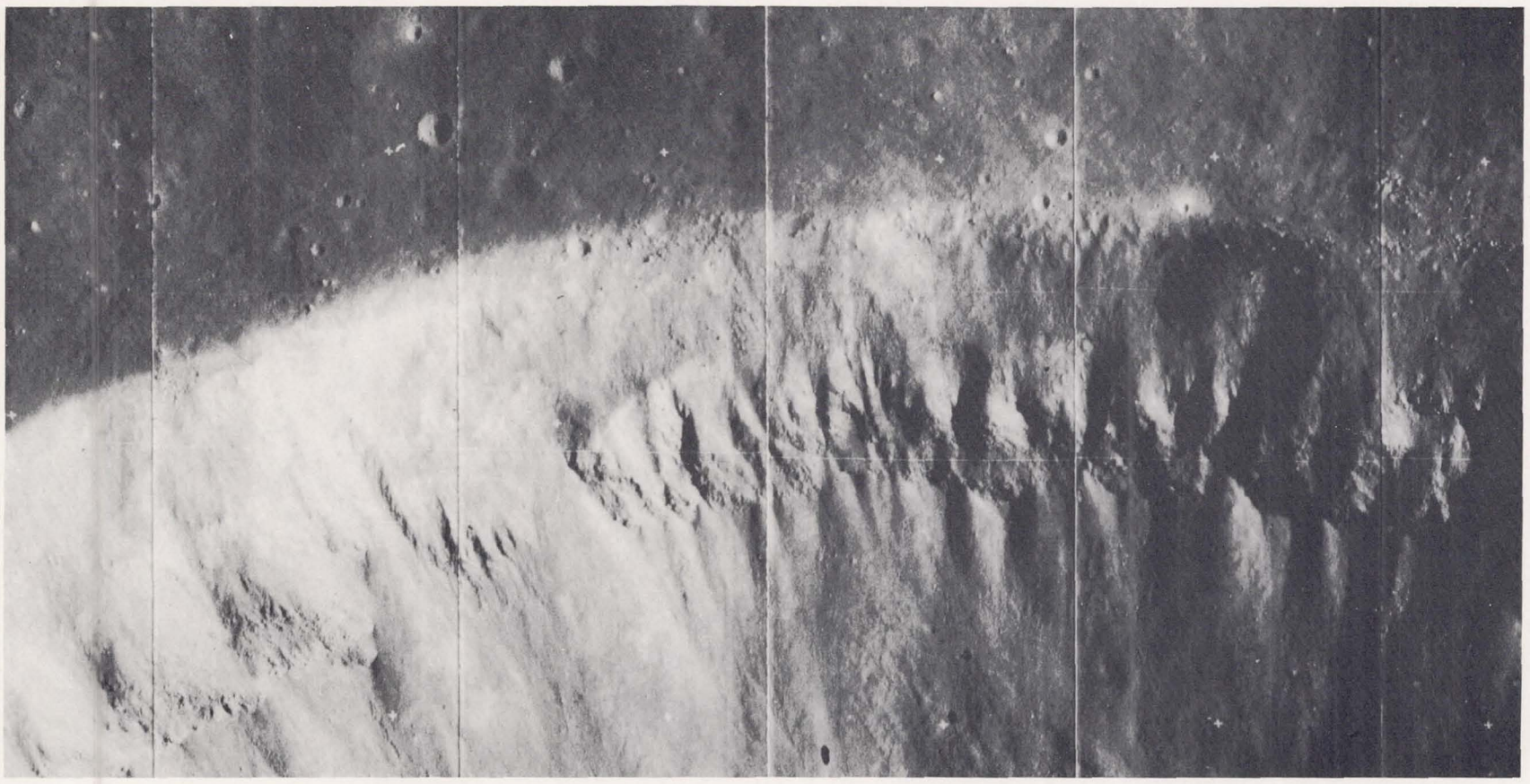

An enlarged view of the northern wall of the crater Dawes, shown at the bottom of the opposite page. Bedrock in place is clearly seen along the upper ledges of the wall. Talus close to the angle of repose makes the rest of the wall slopes. The blocks seen on the talus slope probably originated at the consolidated rock ledges. The tracks of their downslope movement are partly concealed by the fine talus. Framelet width: 470 meters.

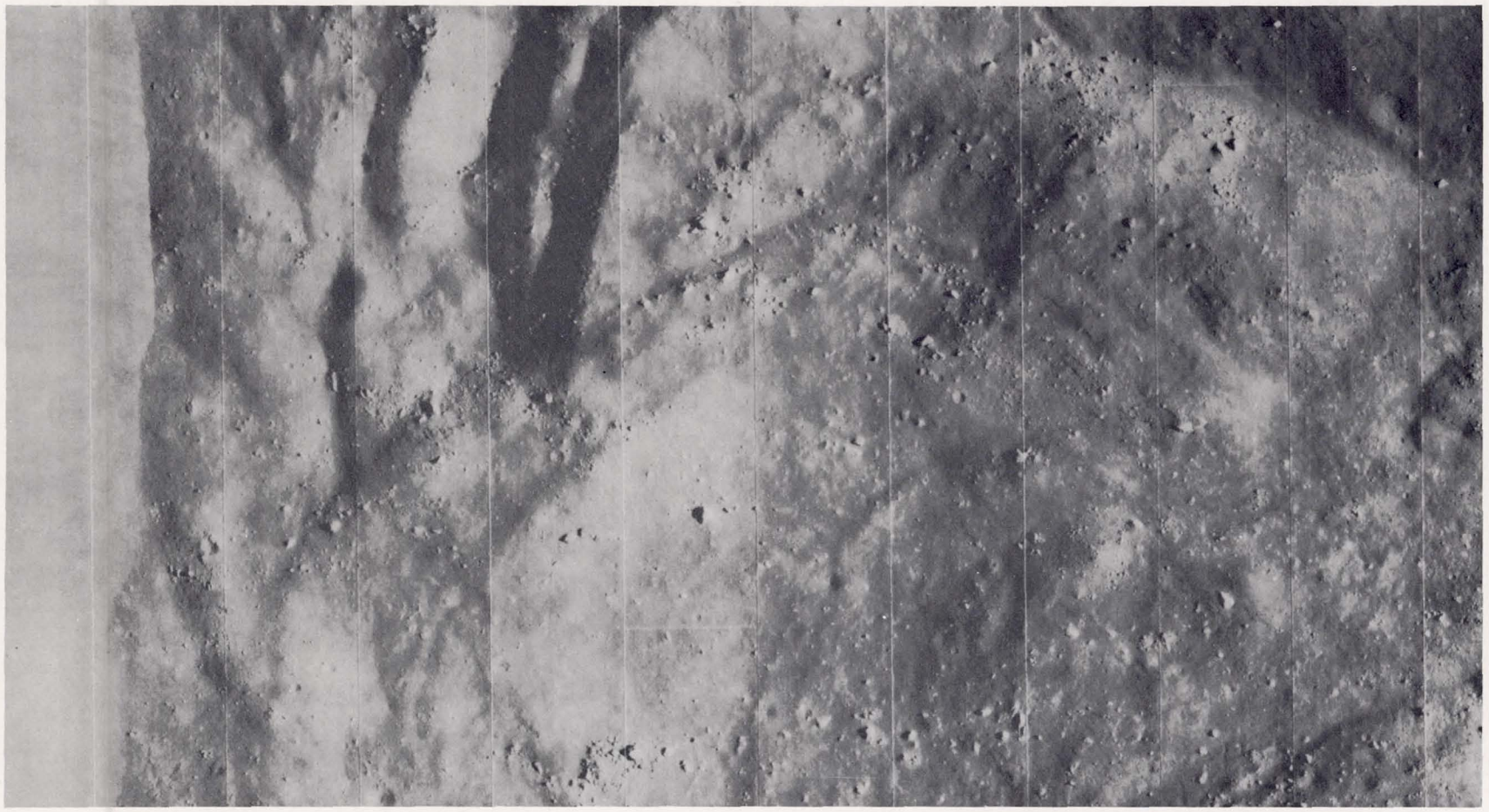

Detail of the floor of the crater Dawes. In the second framelet from the left is the contact between the floor and the wall talus. Several overlapping layers of notably blocky debris have slumped from the wall and now overlie the original floor of the crater. The arcuate structures near the wall may be the surface expressions of faults along which movement probably took place during the late stages of the crater formation. Framelet width: 470 meters.

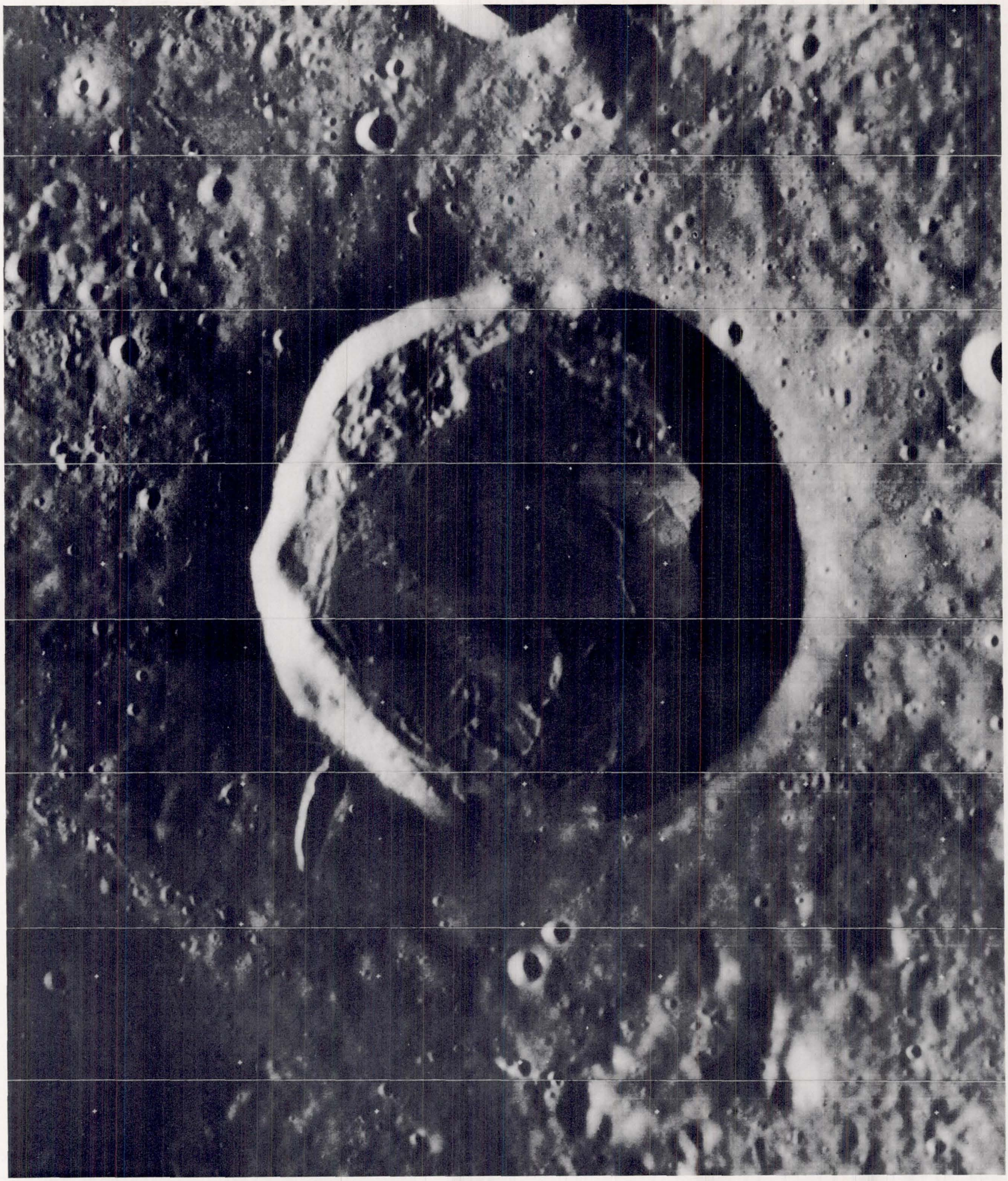

An unnamed crater about 35 kilometers in diameter, located within the Orientale Basin (see page 128). Both the crater and the basin materials are fresh, indicating that the crater is young. The rim flank is smooth, and it lacks the blanket of ejecta grading outward from hummocky to radial and the fields of secondary craters which are typical of young, probable impact craters of its size (for example, Aristarchus). These characteristics suggest that this crater is probably of volcanic origin, similar to those structures on Earth known as Calderas. Location: 18° S, 91° W. Framelet width: 11 kilometers.

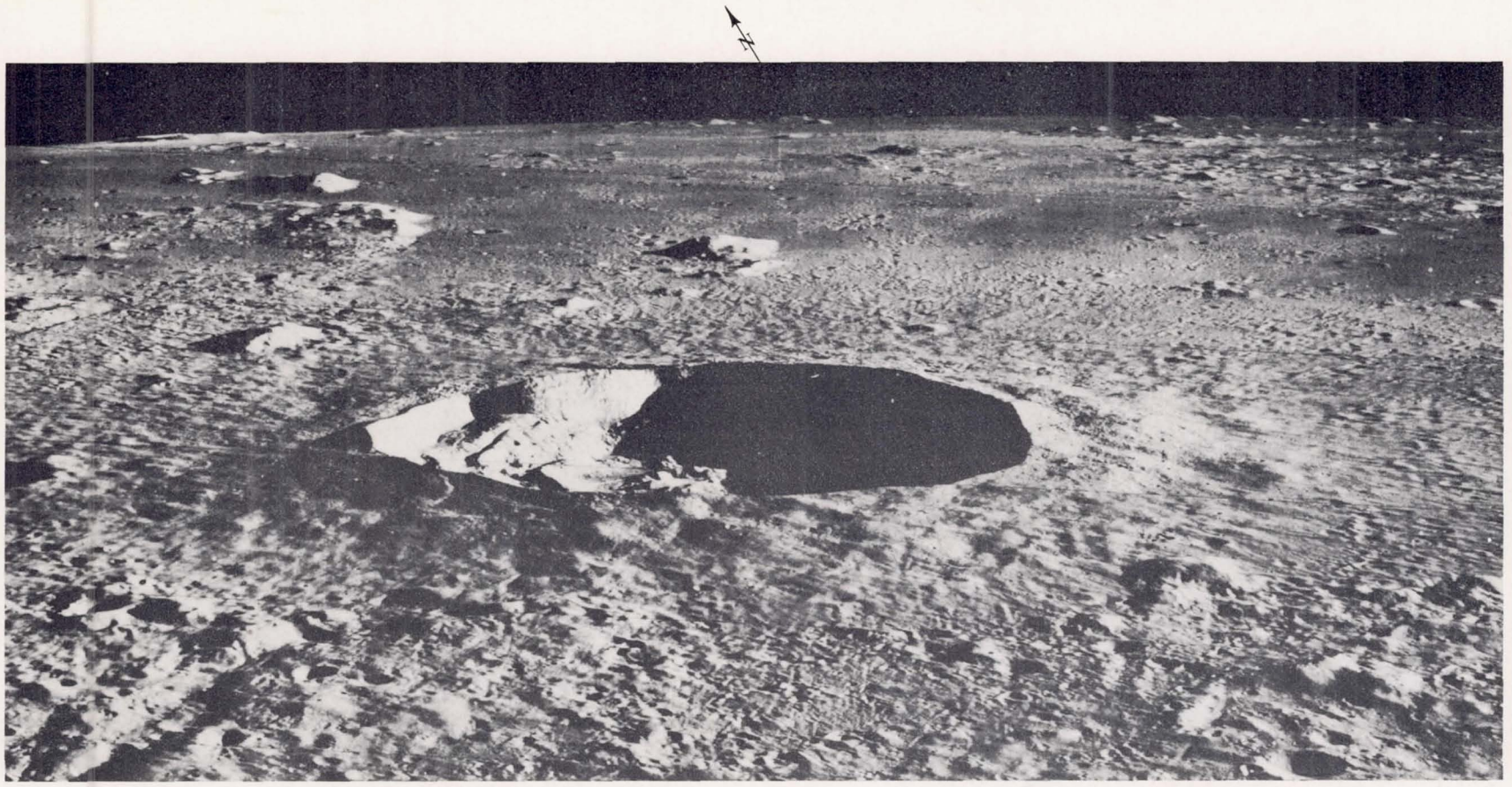

Oblique view of the crater Kepler, 32 kilometers in diameter. The blocky rim, radial ridges, and field of satellite craters are typical of relatively young craters of probable impact origin. Kepler and its related features are superposed partly on mare and partly on rugged terra that may be part of the outer rim of the Imbrium Basin. Location: 8° N, 38° W.

Crater Vitello (45 kilometers across), at the south edge of Mare Humorum. The cracks on the floor are relatively fresh and young, but the crater itself could be either young or old. If young, it is not of impact origin, because ejecta and secondary craters characteristic of young impact craters are not present on the mare just north of the crater. Location: 31° S, 37°40′ W. Framelet width: 5.4 kilometers.

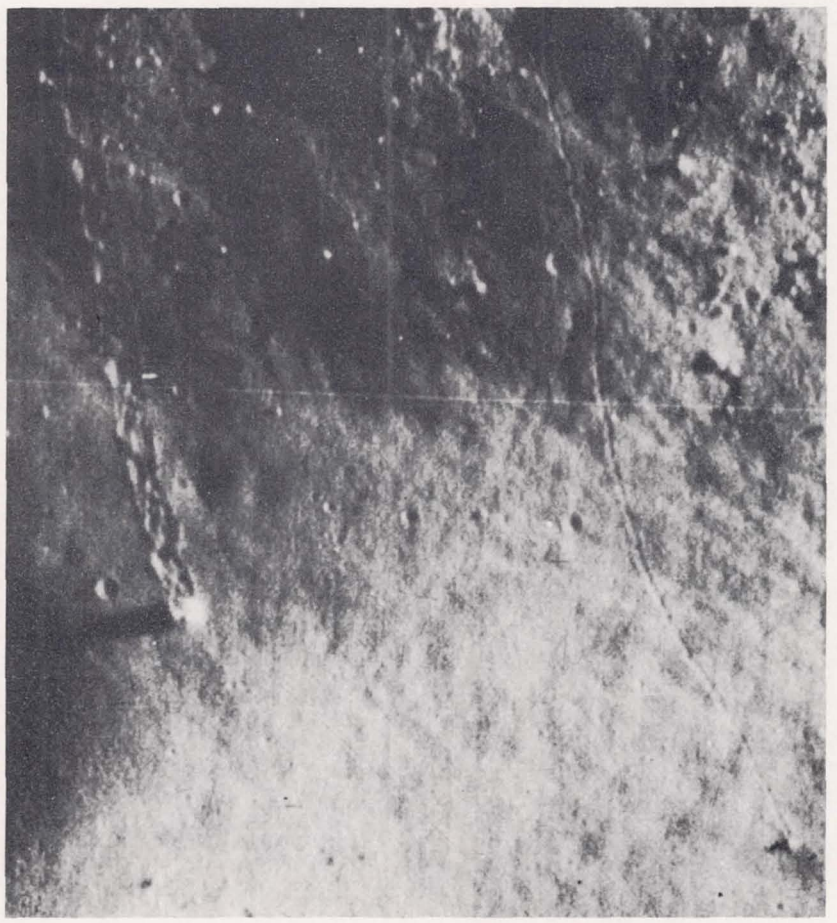

Tracks made by boulders, possibly set in motion by moonquakes, as they rolled downslope from the central peaks of Vitello. The larger track, which is about 25 meters wide, shows a repetitive pattern imprinted by the rolling of an irregularly shaped mass. Study of nearly 400 such boulder tracks noted to date is providing new insight into the mechanical properties of the lunar surface.

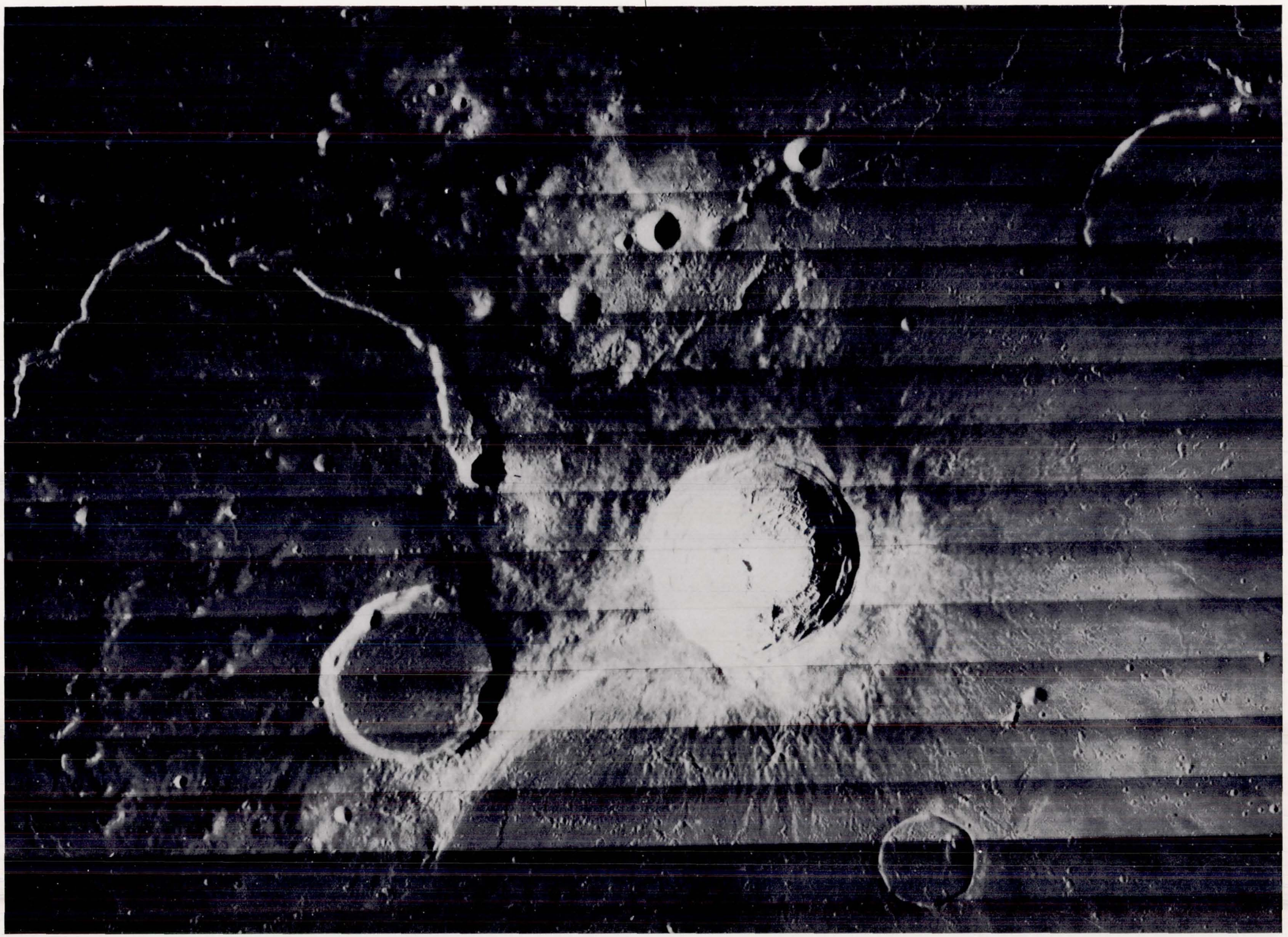

The bright crater Aristarchus (40 kilometers in diameter) is surrounded by an ejecta blanket and secondary impact craters. Superposition of the latter on surrounding materials shows that Aristarchus is younger than those materials. The meandering Schröter's Valley, 250 kilometers long, is shown in more detail on pages 113 and 114. It begins at the "cobra head," in a hill which rises about 1500 meters above the adjacent plateau. South of this is the flat-floored crater Herodotus (35 kilometers in diameter). Location: 24°40′ N, 48° W. Framelet width: 11 kilometers.

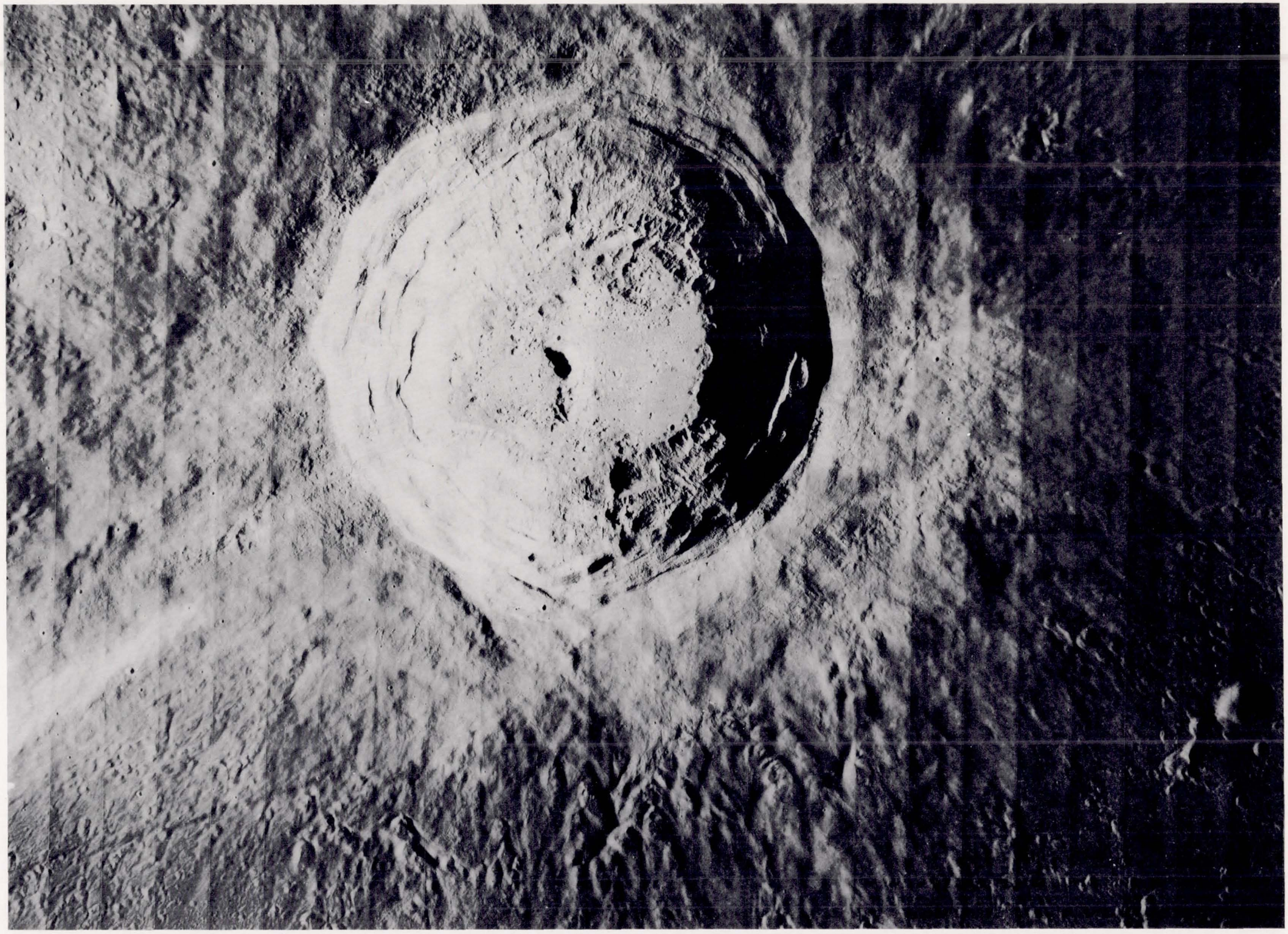

The crater Aristarchus is surrounded by blocky rim material, a hummocky ejecta blanket with radial ridges and braided appearance, and secondary impact craters at and beyond the limit of the ejecta blanket. Progressive softening and filling of the secondary craters near the limit of the blanket suggest that the latter was deposited later than these secondaries. Concentric and radial valleys on the rugged crater walls resulted from slumping and mass wasting. The crater depth from rim to floor is about 3.6 kilometers. Location: 23°30′ N, 47°10′ W. Framelet width: 4.4 kilometers.

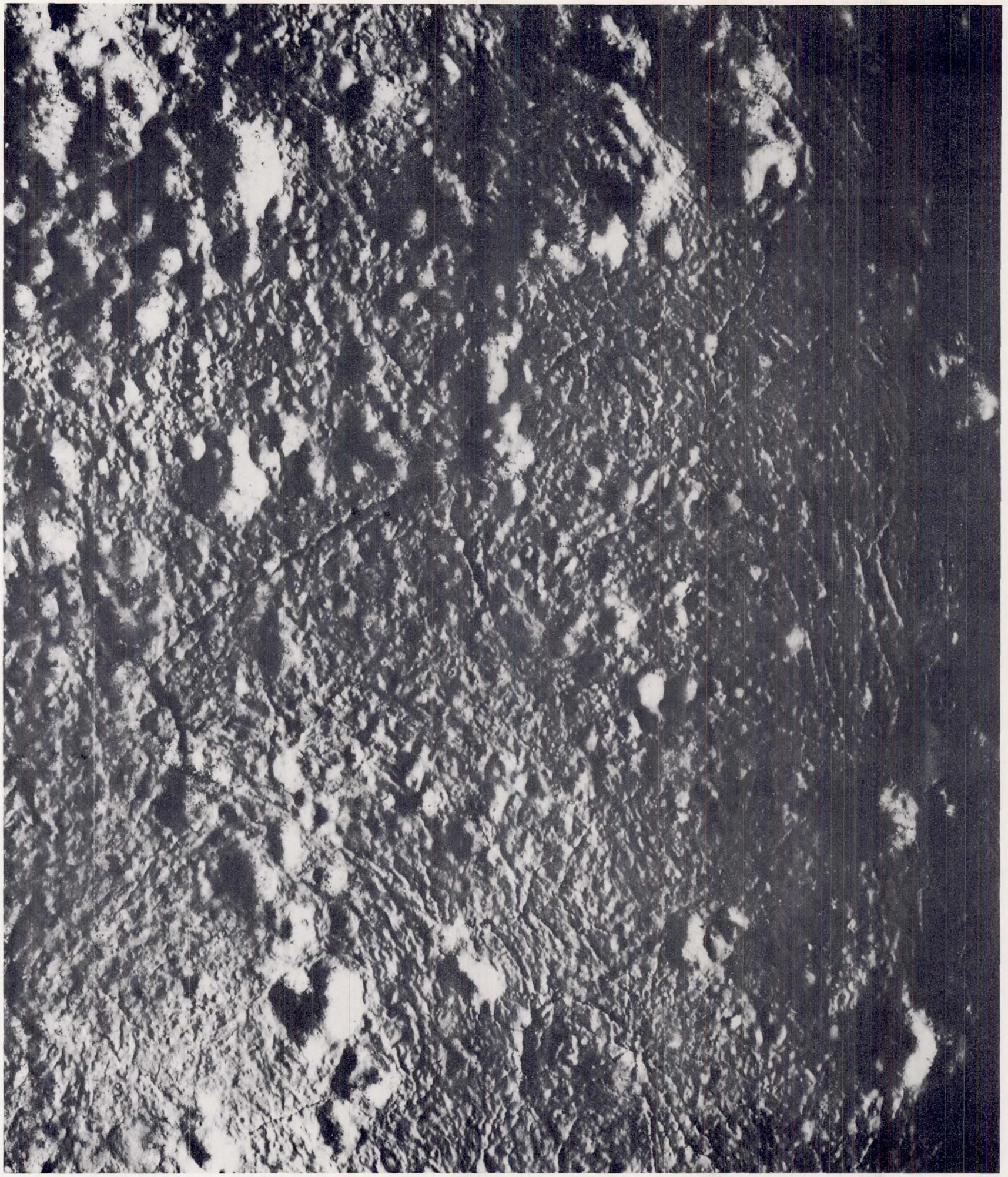

Part of the floor of Aristarchus which resembles, in many respects, the floors of some Hawaiian volcanos. Mounds, complex fissures, and large blocks appear very fresh. These could be either of volcanic origin (especially the flat, fissured material) or debris slumped from the crater walls. Location: 23°30′ N, 47°10′ W. Framelet width: 550 meters.

Concentric fault scarps and stepped surfaces are common features on the walls of large lunar craters. Here in Aristarchus, part of the original rim has been displaced downward toward the crater floor. Large blocks up to 115 meters long occur near the crater rim. Location: 23°50′ N, 47° W. Framelet width: 550 meters.

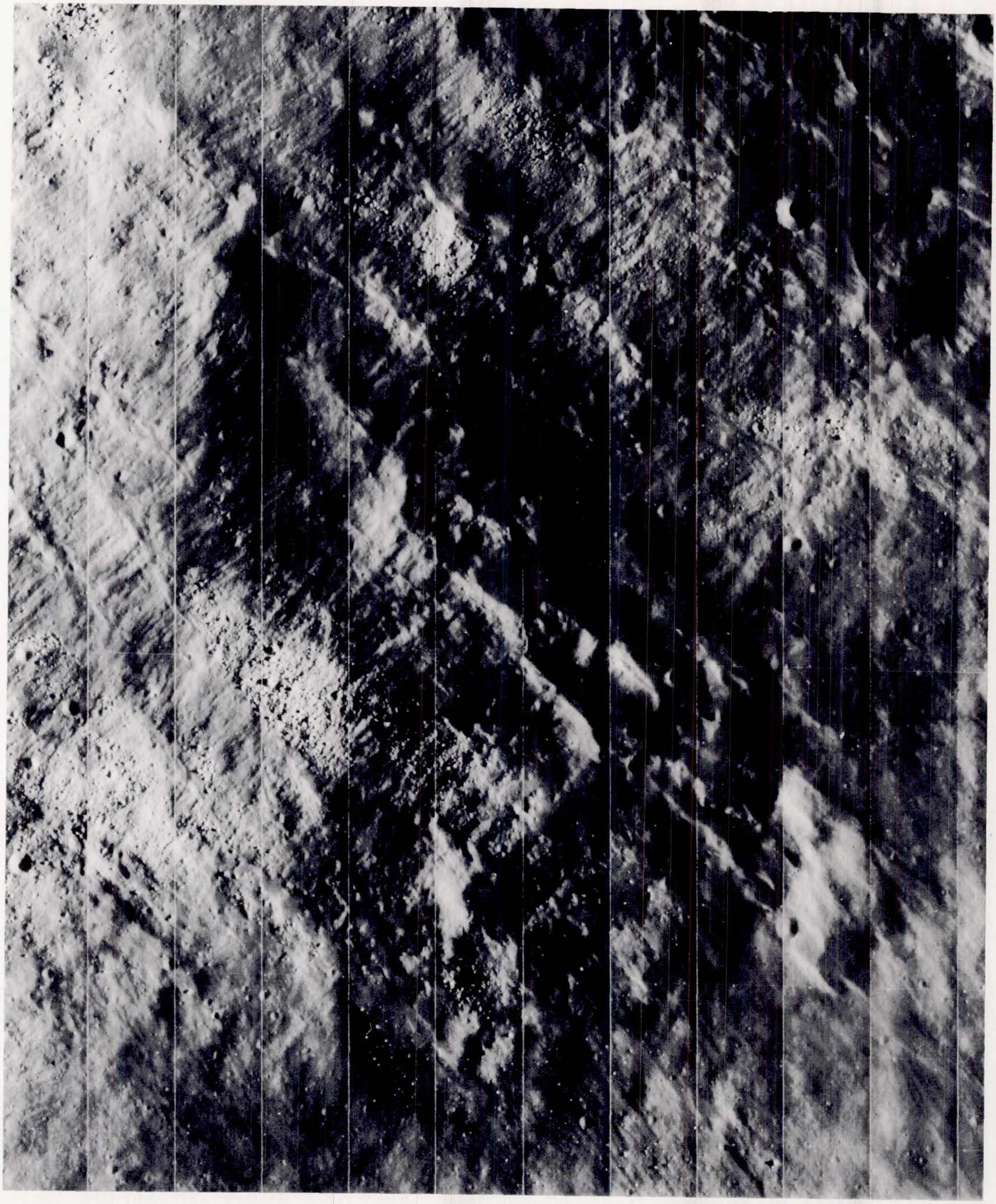

Large blocks, radial fractures, and concentric ridges characterize the surface near the rim of Aristarchus. This surface appears to be locally stripped of fine material (which is, however, present in the radial depressions) and radially channeled by materials ejected from the crater. Location: 22°50′ N, 47° W. Framelet width: 550 meters.

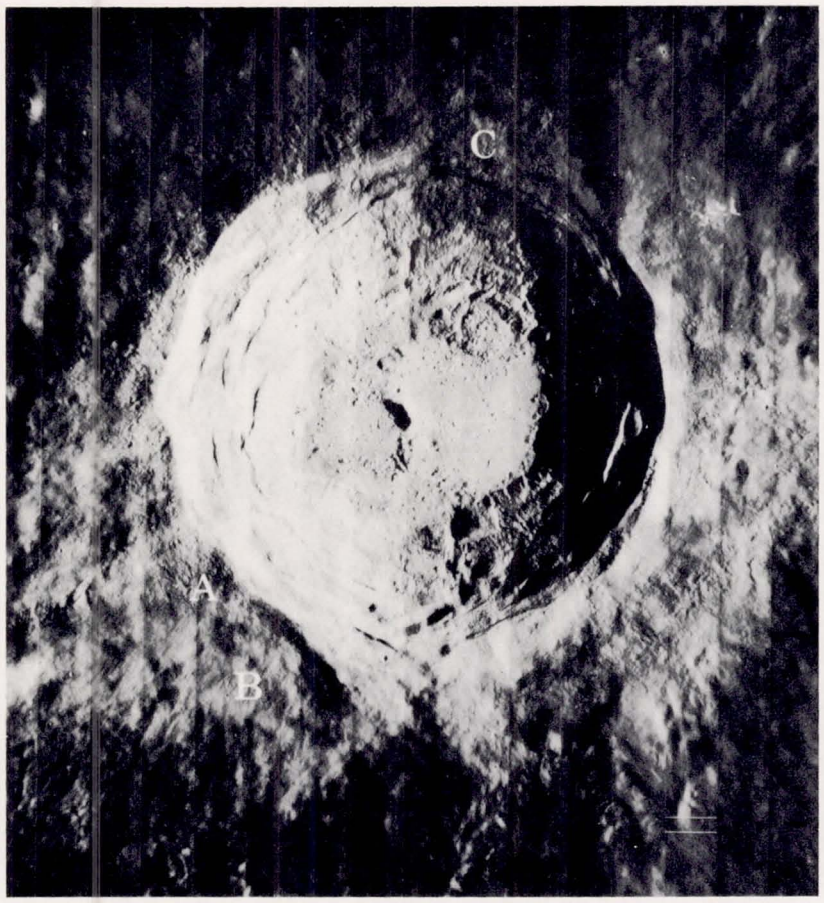

Index map of Aristarchus showing locations of the three flow features illustrated on this page. On all three photographs, the width of a framelet is 550 meters.

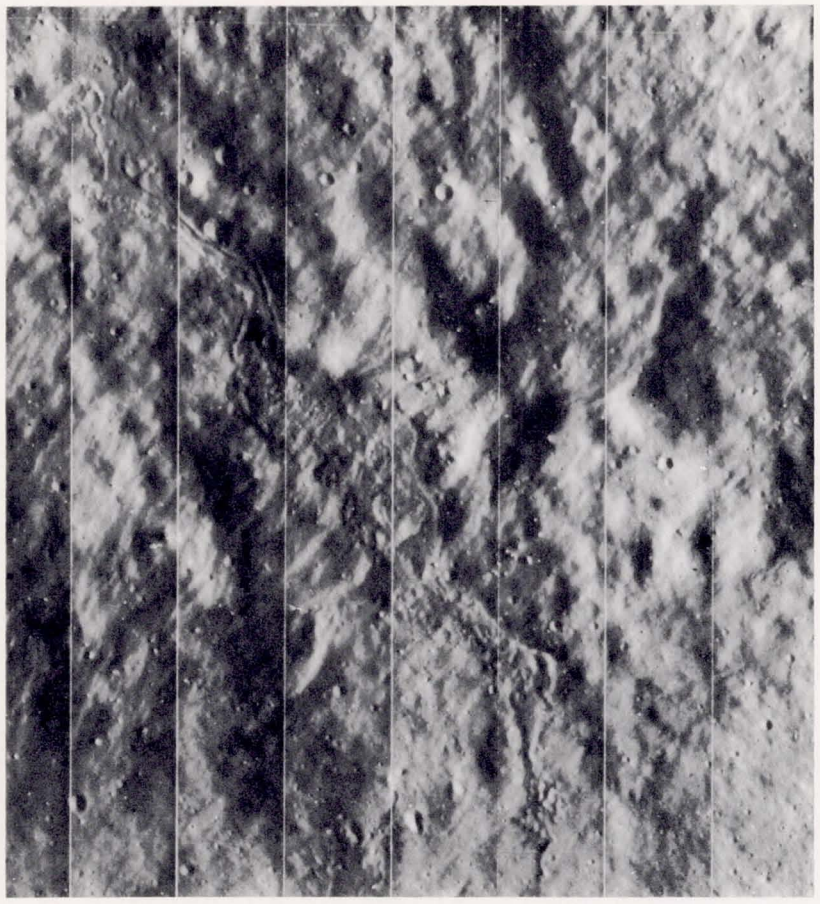

A. One of several flows near the south rim of Aristarchus that trends parallel to the crater rim. Here a leveed channel (upper left) disgorges bulbous ridges of flow material.

B. This hairpin-shaped feature is one of the many flow structures on the south flank of Aristarchus. It resembles superficially some secondary impact craters farther from the crater rim. Unlike secondary craters it is rimless, and one channeled leg has both a levee and a bulbous flow deposit.

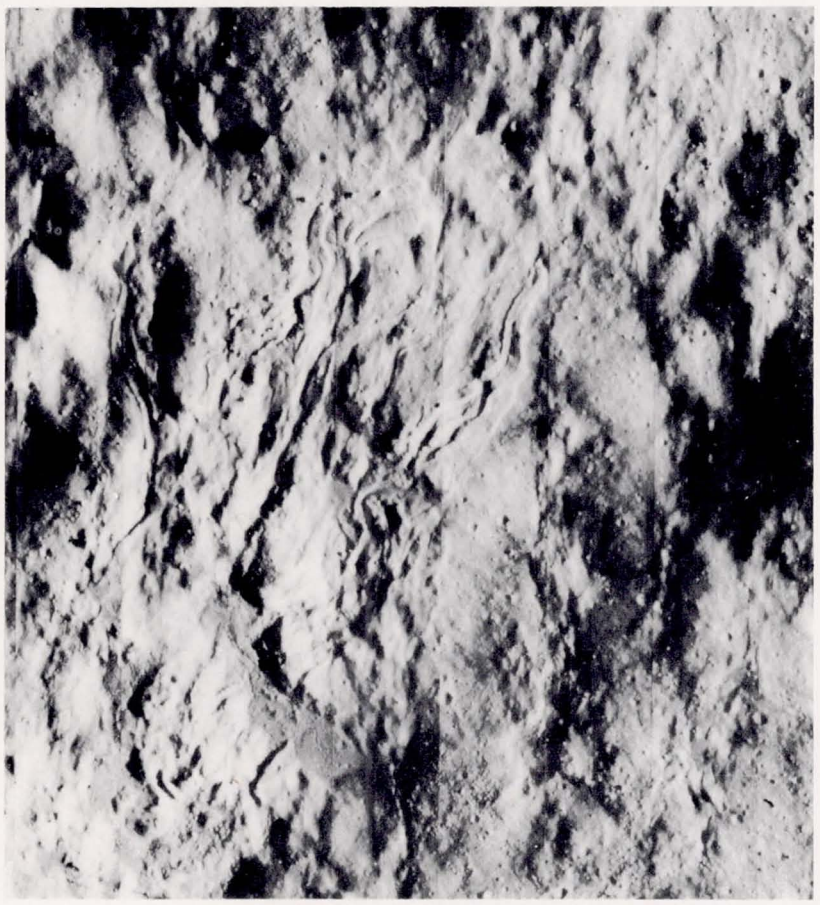

C. Flows with sinuous channels and marginal levees on the north rim of Aristarchus. The flows may be debris, volcanic materials, or shock-melted material generated by a hypervelocity projectile which produced the crater. The flows are demonstrably younger than the surrounding materials.

This photograph, one of the most interesting taken by Lunar Orbiter I, displays the crater Taruntius and its extensive field of satellitic craters. Taruntius (56 kilometers across) is anomalous because of its relative shallowness, its internal concentric ridges and rilles, and the large number and linearity of its satellitic craters. However, the long, linear, tangential trough at right center is probably unrelated to Taruntius. Location: 2°40′ N, 47°40′ E. Framelet width: 8 kilometers.

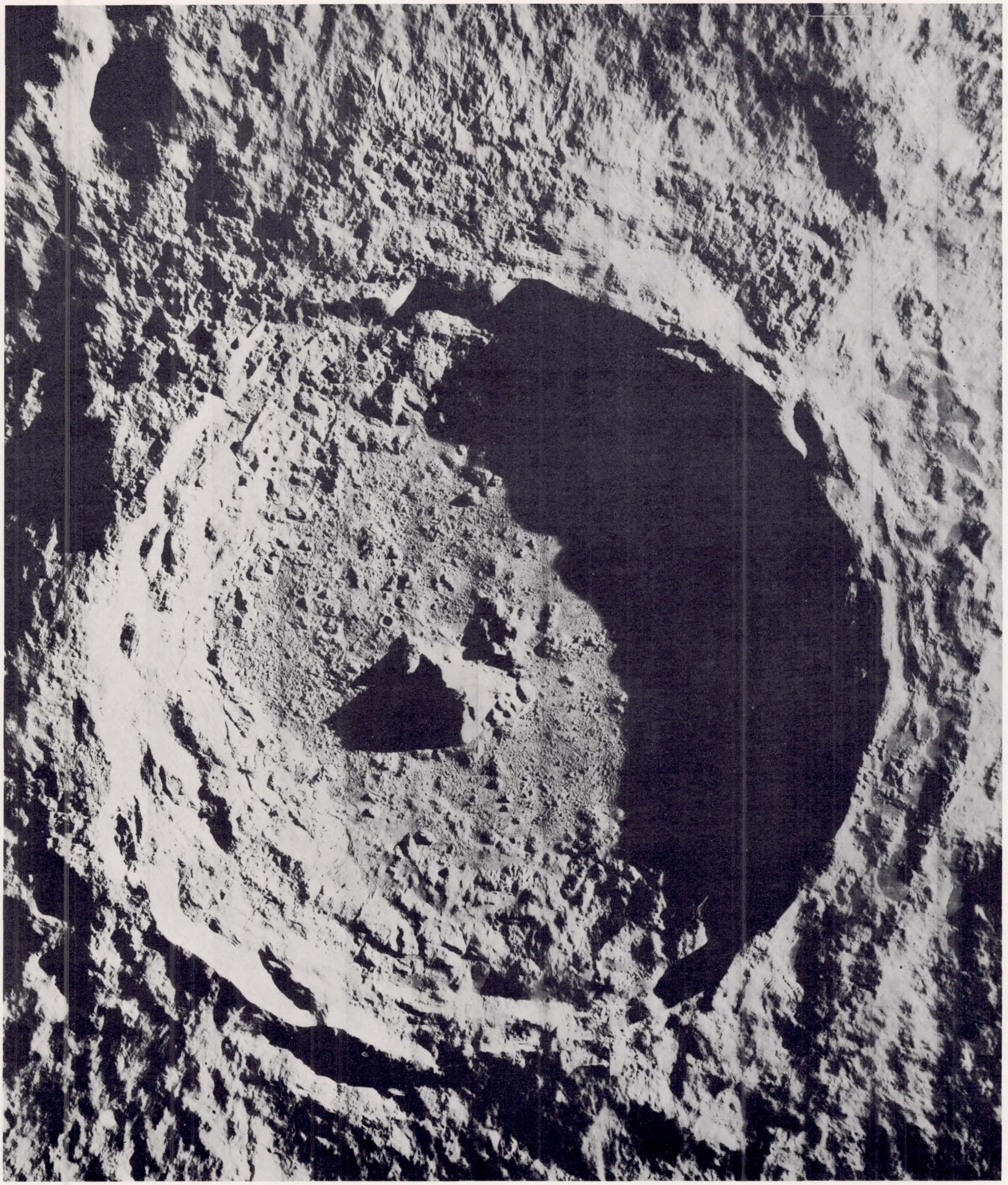

A general view of the crater Tycho, an excellent example of a young, fresh, lunar crater. A high central peak, slumped walls, and hummocky rim deposits are well-displayed typical features. In addition, the floor is extremely rough, with mounds and fissures, and the rim has prominent flow structures and a strong concentric texture in many places. Tycho, which is 85 kilometers across, is located at 43°10′ S, 11°10′ W. Framelet width: 7 kilometers.

Typical details of the floor and floor-wall contact of Tycho, including mounds, fissures, and blocks. Long fissures commonly parallel the floor-wall contact, while shorter, more irregular ones have variable directions. A flow lobe in the upper right corner has moved down the wall and "bulldozed" its way into the floor material. Framelet width: 940 meters.

A view of some of the roughest parts of the floor of Tycho. Some geologists consider the symmetrical rings or shells surrounding the large mounds to be due to the flowage of shock-melted rock off the surface of the mounds. Others interpret them as volcanic domes. Fissures and blocks abound in all parts of the floor. Framelet width: 940 meters.

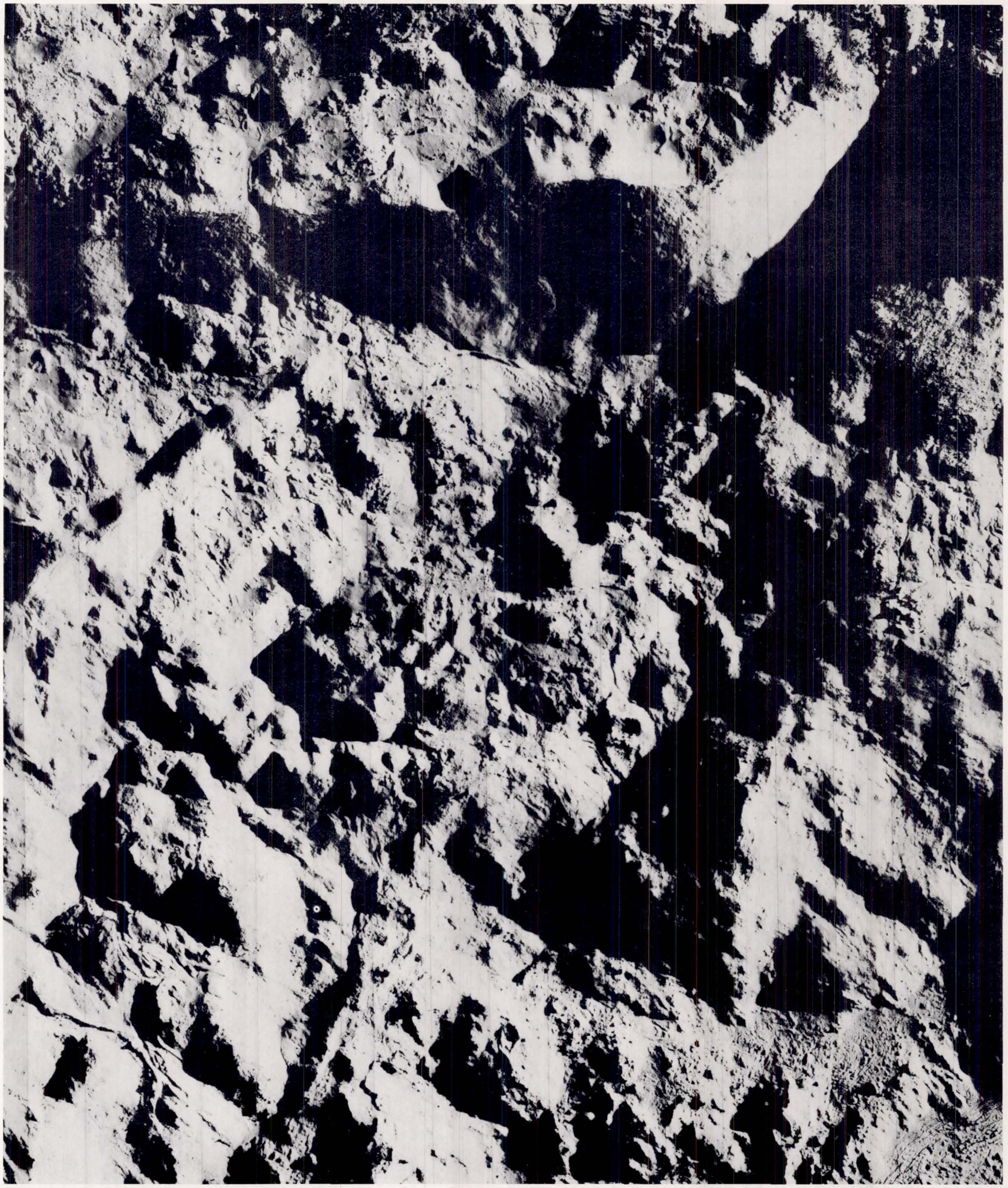

A representative segment of the crater Tycho's terraced wall and northern rim crest (located near the top of the photograph). As is typical of fresh craters, the uppermost wall scarp is the most pronounced. The level terrace surfaces are almost obscured by the abundant flow features, which are here probably debris flows. Blocks are particularly abundant on the rim, although they occur on all surfaces. Framelet width: 930 meters.

Well-developed flow features just outside the northern rim of the crater Tycho. Overlapping lobes, emanating from a large channel-and-levee system, flow northward away from the crater. The small-crater density variations on separate flows suggest different ages. The flows, themselves, may have been molten lava, volcanic debris, or partially fluidized impact ejecta. The cross at upper left marks the site of the Surveyor VII spacecraft landing. Framelet width: 920 meters.

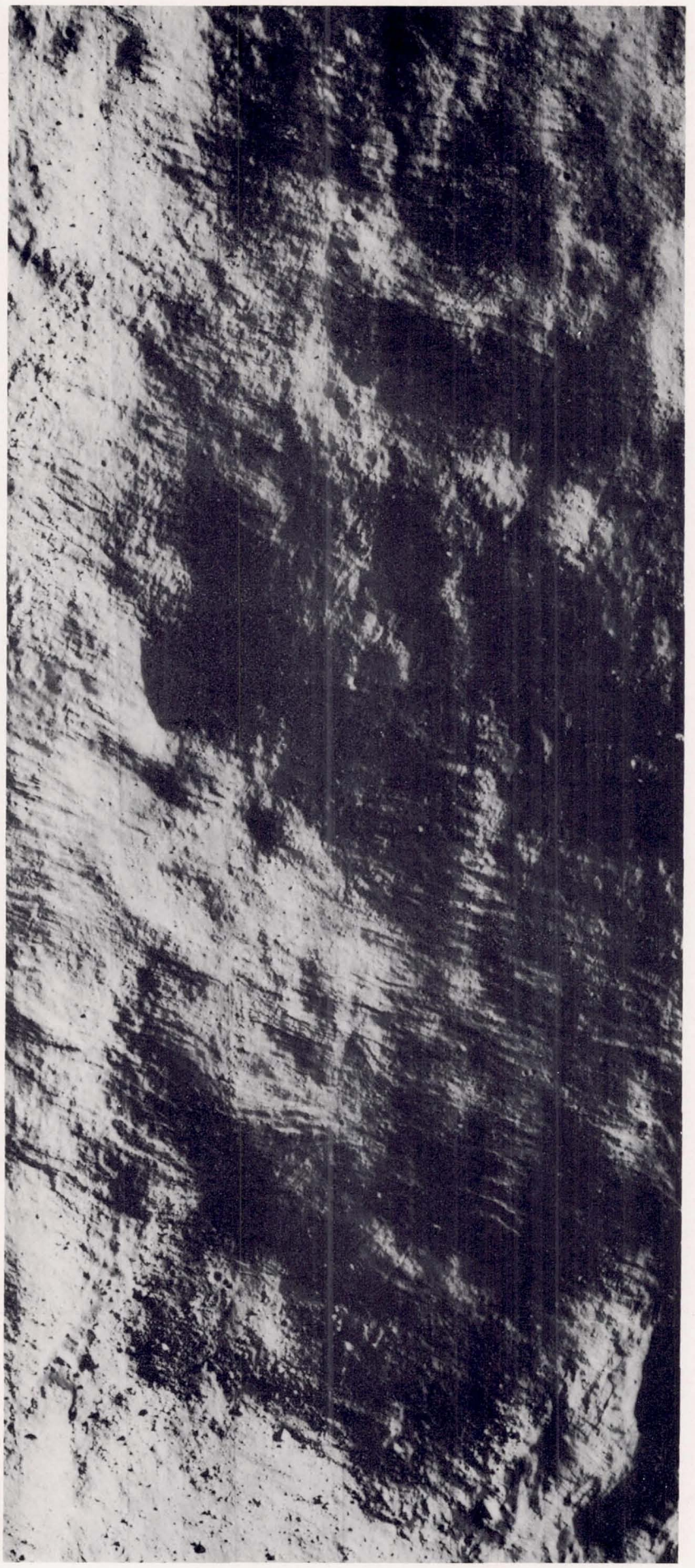

Part of Tycho's well-developed concentric rim pattern. The pattern may reflect a fracture system produced by the cratering event. Notice also the abundant blocks and the flat, smooth areas in topographic lows. The flat areas are "ponds" of either fine debris or volcanic materials that flowed and accumulated in the depressions. Located on the northern rim, directly east of the opposite photograph. Framelet width: 920 meters.

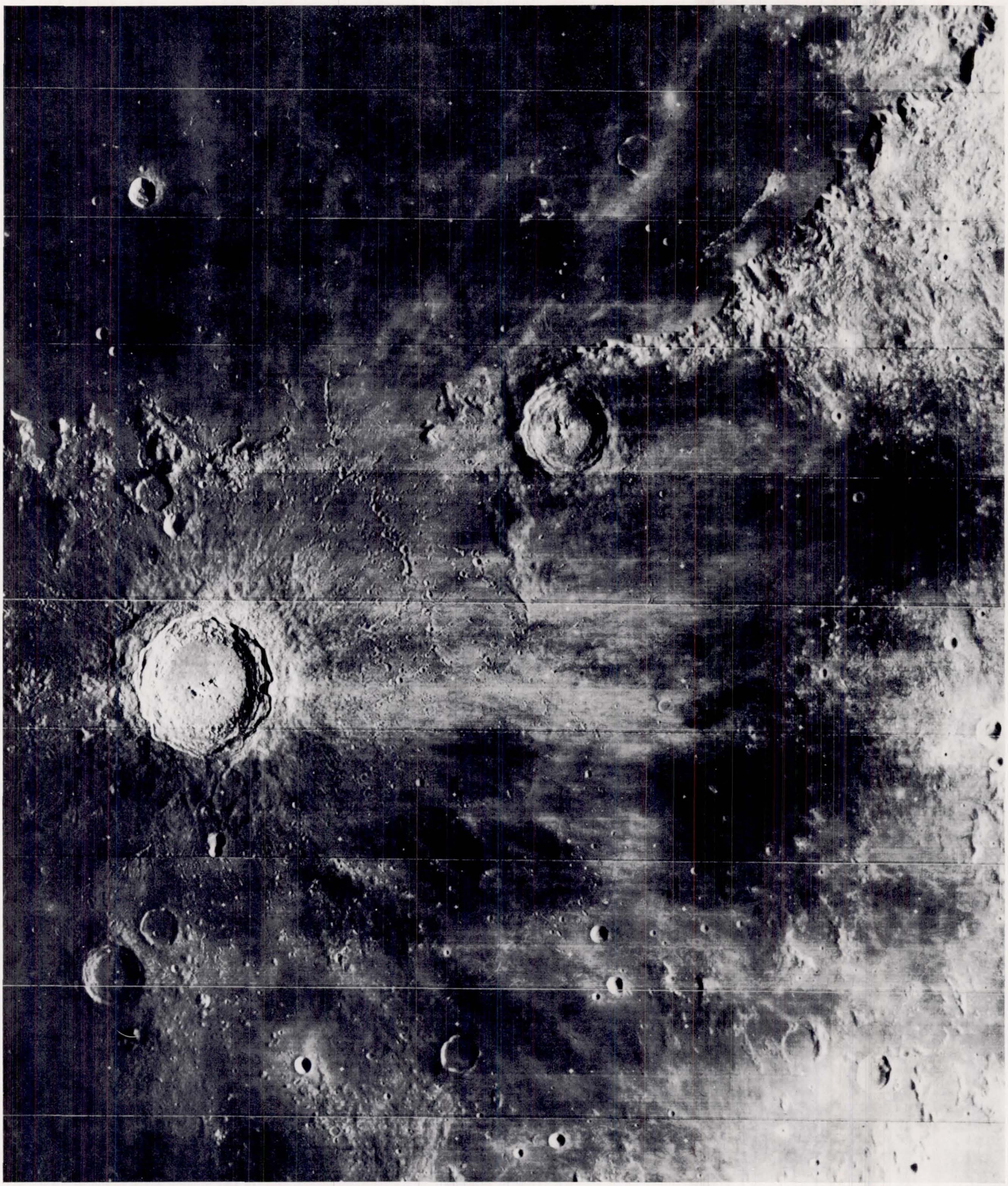

The rayed crater Copernicus, to the left, and the unrayed crater Eratosthenes. Both are relatively young, being superposed on the mare and having fresh and extensive ejecta blankets and satellitic crater fields; the superposition of Copernicus rays and secondary craters on Eratosthenes shows that Copernicus is the younger. Other craters in the picture are partly filled by mare material and are therefore older than the mare. The arcuate mountain chain is part of a ring surrounding the basin of Mare Imbrium. Location: 11° N, 13° W. Framelet width: 85 kilometers.

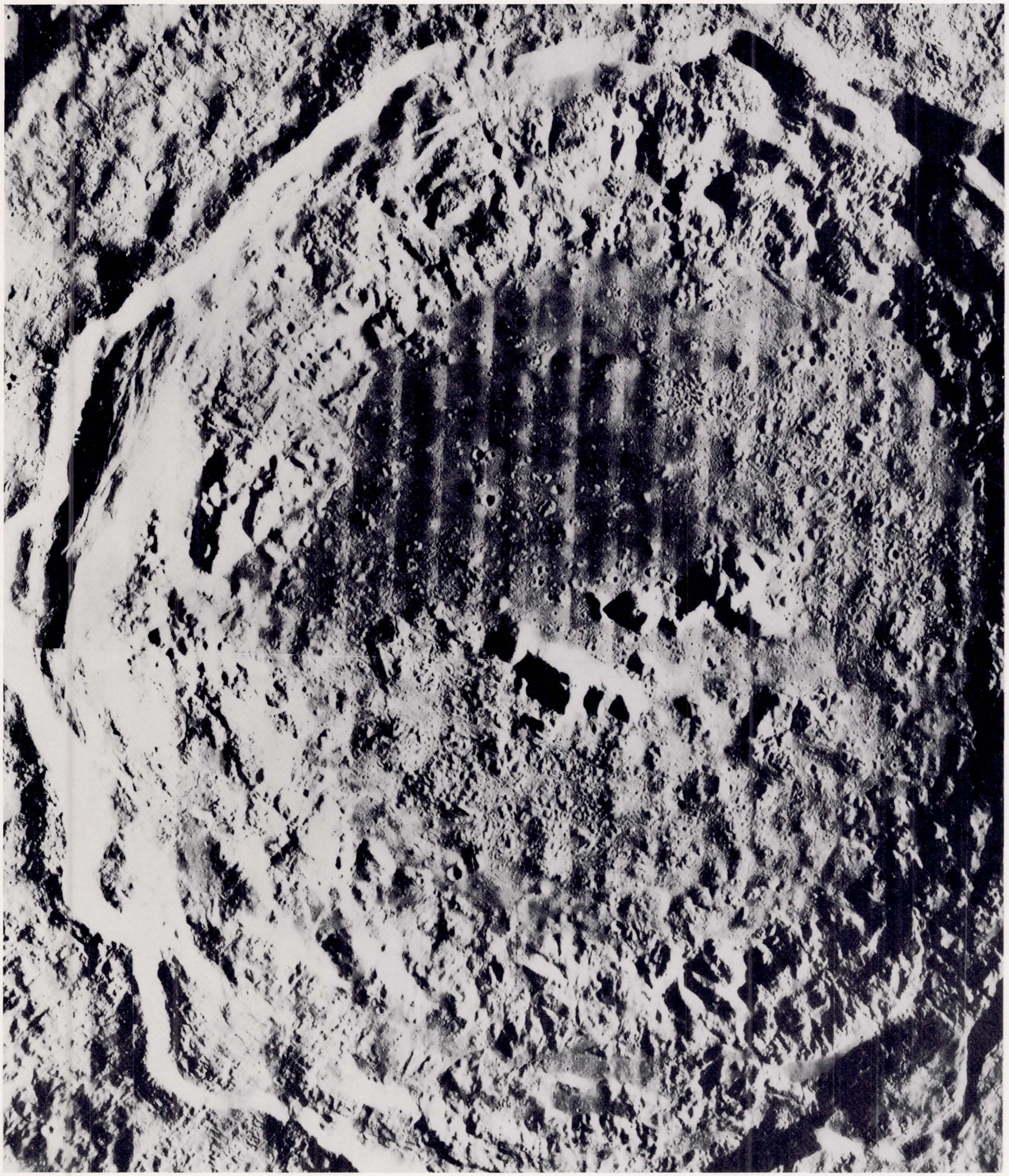

This mosaic composed of two medium-resolution frames provides a vertical view of Copernicus, a relatively young crater with an extensive ray system. The floor of Copernicus is covered with an intricate pattern of hills, ridges, troughs, and sinuous cracks. The less rugged northwestern part (upper left) has a lower albedo (i.e., darker tone) than the rest. The exterior rim displays a complex juxtaposition of concentric and radial structures and local smooth patches. Copernicus, 93 kilometers across, is located at 9°40′ N, 20° W. Framelet width: 3.4 kilometers.

Detail of the floor of the crater Copernicus. Hills are littered with blocks; some have summit depressions, which suggests the possibility of internal origin. The irregular cracks with crater-shaped enlargements along them may have formed by drainage of loose material into subsurface fractures. The floor is covered with swales and depressions which appear more subdued than those in the floors of Aristarchus and Tycho. Framelet width: 440 meters.

Wide-angle oblique view, looking due north, of the crater Copernicus. Blocky, rough ground just outside the rim crest is surrounded by a series of smooth ridges approximately radial to the center of the crater. The keyhole-shaped crater Fauth is superimposed on one of these ridges 60 kilometers to the south. In the foreground, a complex array of mounds, cones, and crater clusters mark the outer portions of the rim. The clusters appear to have been formed by the impact of fragments ejected from the large crater. The origin of the mounds and cones, however, is still a matter of controversy.

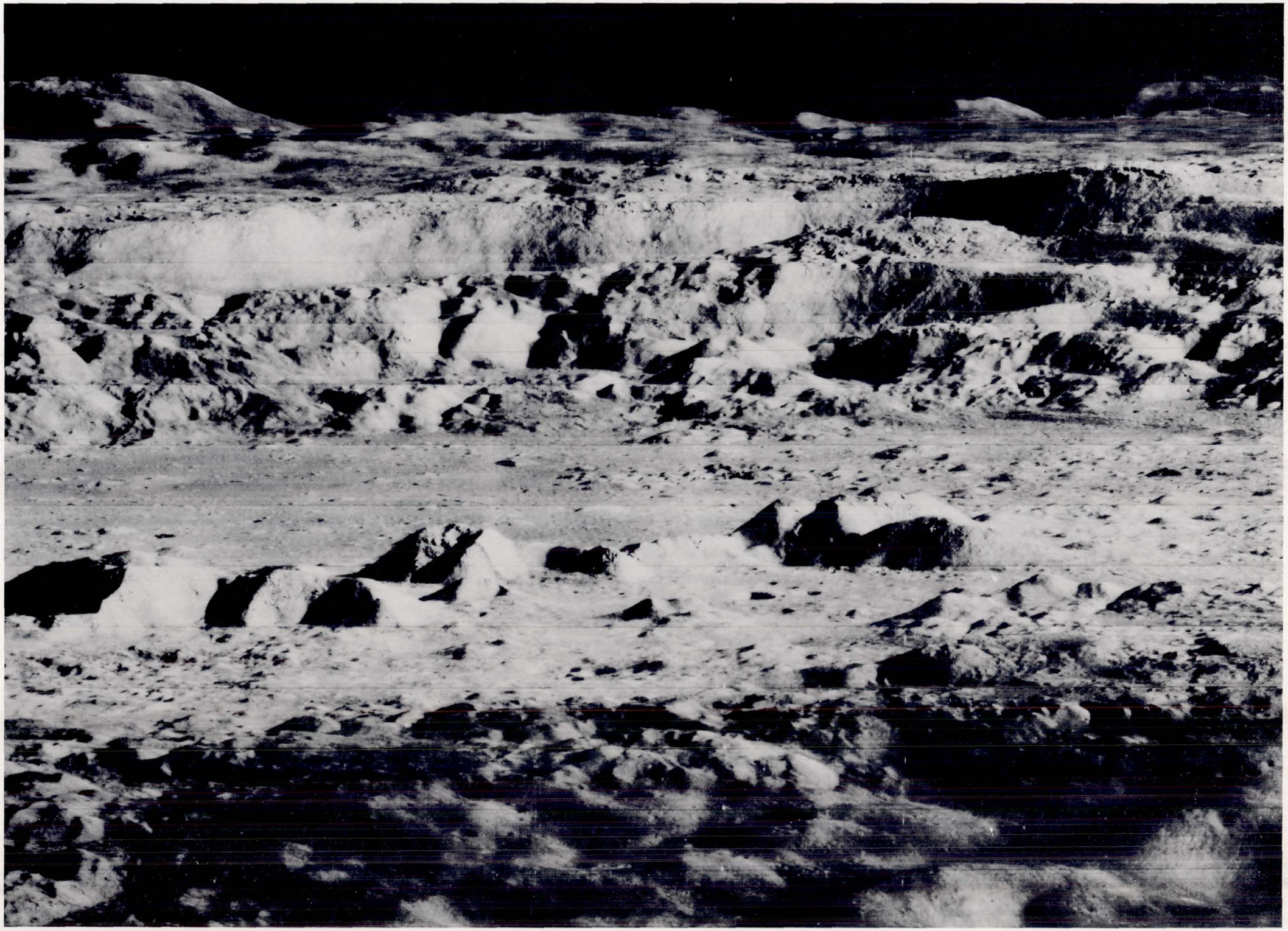

Close-up oblique view of the crater Copernicus showing details of the floor, the central mountains, and the northern wall. Flow lines, ridges, and troughs running down the far wall indicate that material has moved downslope, off the walls and onto the floor. Large blocks litter the slopes of the central mountains which rise 400 meters above the floor. The dark band dipping down the eastern side of the mountain near the center appears to be a ledge of lunar bedrock that has weathered under the influence of the space environment to produce some of the blocks.

Vertical view of the north wall of Copernicus. Patches of smooth material are perched at several levels. Two well-developed flows appear in the western half of the picture. The eastern flow extends onto the floor and the western one terminates abruptly at the floor in a nearly straight line. A comparison of this photograph with the oblique view of the same area is helpful in visualizing the three-dimensional relationships among the various features. Framelet width: 3.4 kilometers.

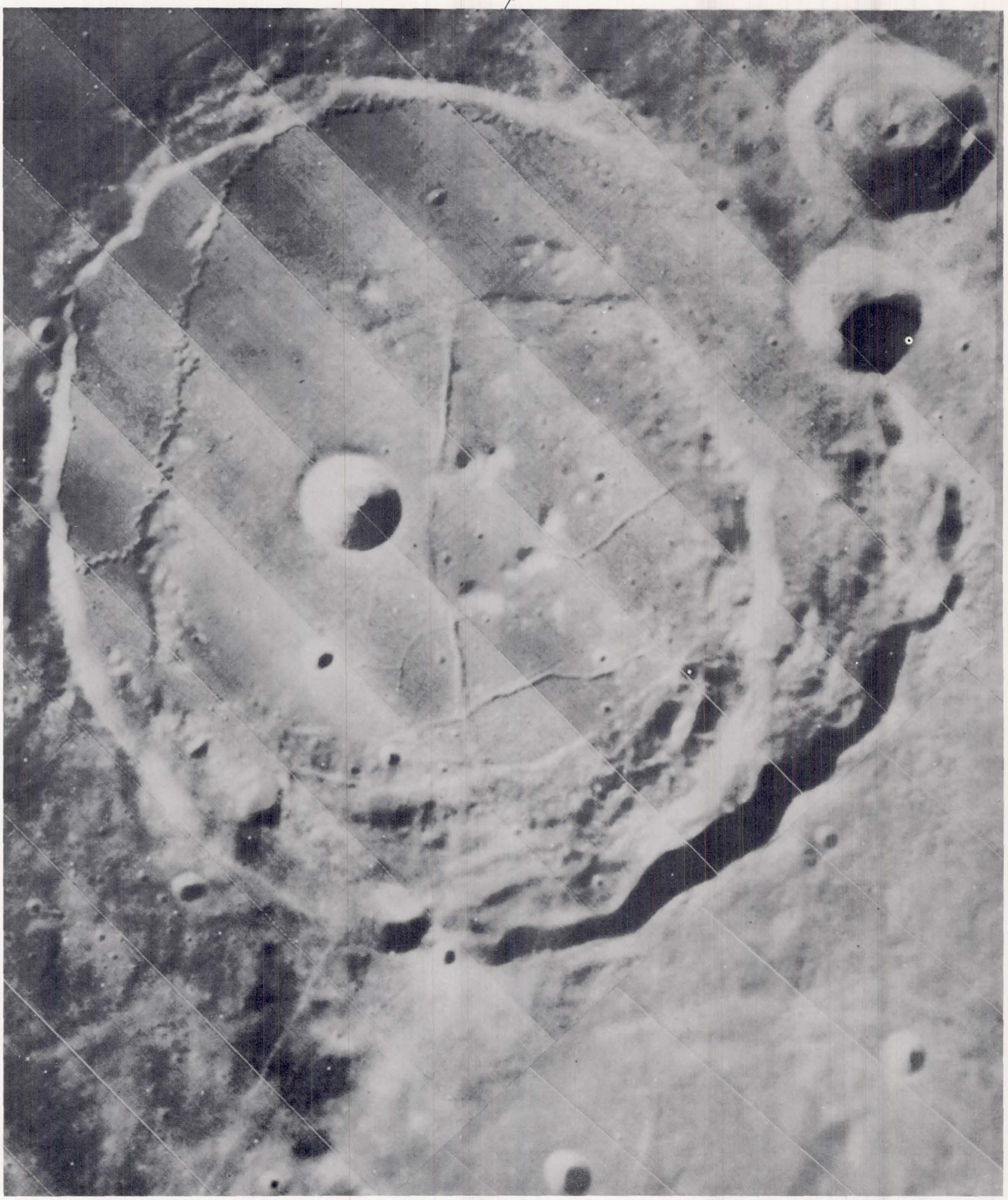

Posidonius, a 100-kilometer crater at the northeastern edge of Mare Serenitatis. The crater is partly filled and the rim partly covered with mare material. The existence of an inner ring suggests that the floor has been uplifted, probably by isostatic adjustment; the linear rilles may have formed by faulting due to tension associated with the adjustment. An intricately sinuous rille runs along the western edge of the crater floor. Location: 32° N, 30° E. Framelet width: 12 kilometers.

The mare-filled crater Plato, 100 kilometers in diameter, north of Mare Imbrium. The mare material in Plato is like that outside but is not connected with it at the surface, suggesting either local subsurface sources for the mare materials or a subsurface duct connecting the two. The sharp sinuous rilles that head near Plato (the one to the southwest is double) may or may not be genetically related to the crater. Location: 51°30′ N, 9° W. Framelet width: 12 kilometers.

Oblique view, looking south, of the crater Theophilus and part of the crater Cyrillus (right background). Although the two craters are nearly identical in size and gross form, landforms within the younger Theophilus are relatively angular while those within the older Cyrillus are smooth and gentle, having been modified by erosion and redeposition and by blanketing by a thin layer of ejecta from Theophilus. Theophilus, 100 kilometers across, is at 11°20′ S, 26°20′ E.

Gassendi, a 110-kilometer-diameter crater at the north edge of Mare Humorum. Gassendi is younger than the distinctly circular Humorum basin upon which it is superimposed, but older than the mare material that fills the basin and the peripheral depressions of Gassendi's floor. Considerable uplift of the floor, probably through isostatic adjustment, is suggested by the numerous cracks and the unusually high elevation of the floor and central peak relative to the rim crest (quite similar to Posidonius, page 92). Location: 18°50′ S, 39°50′ W. Framelet width: 4 kilometers.

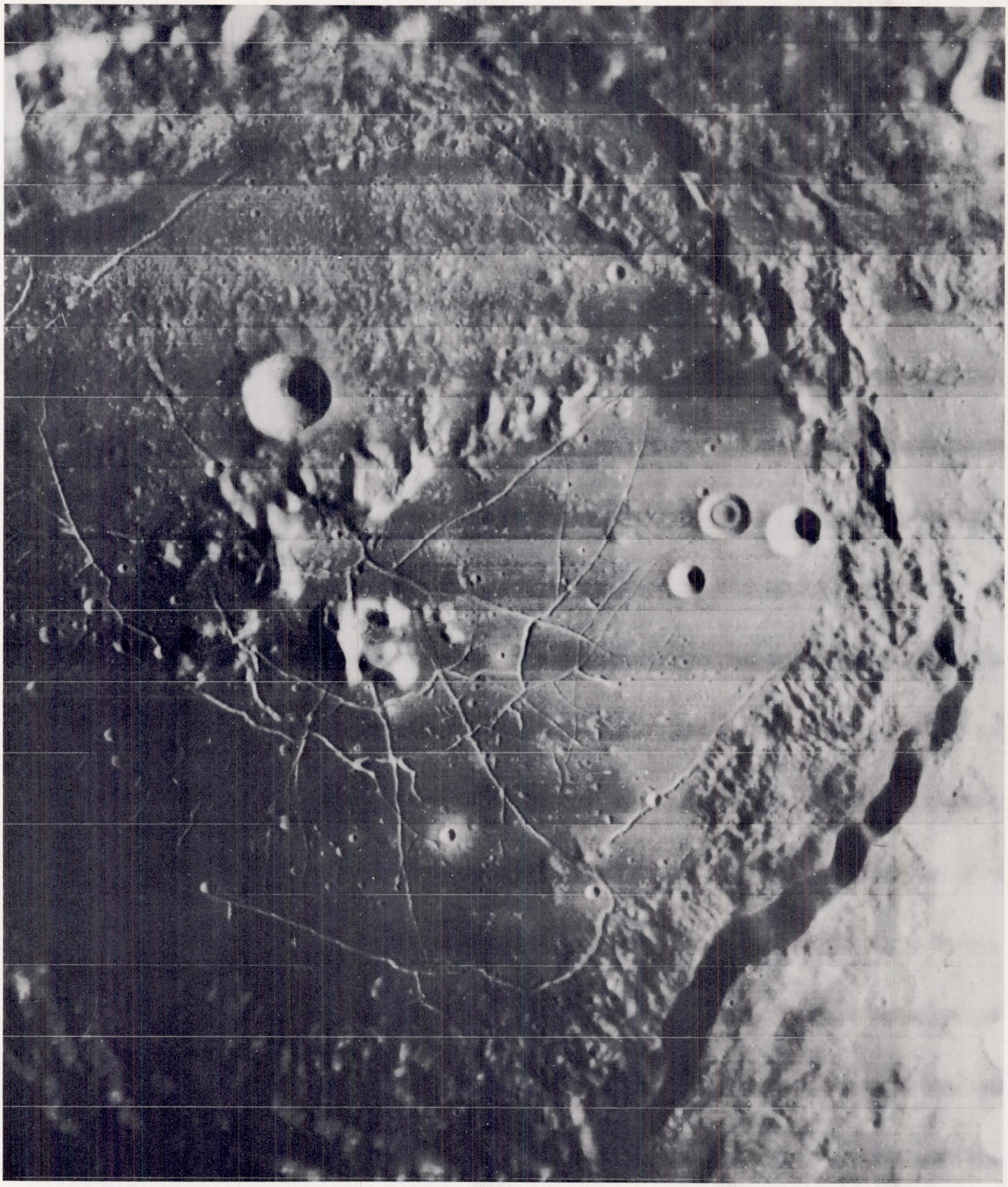

Humboldt, a large crater 200 kilometers across, having an unusually regular system of fresh-appearing rilles on its floor, resembling a spider web. The rilles cut across a complex of massive peaks near the center, a hummocky unit in the northwest part of the floor, and a light-toned plains unit covering the hummocks in the southeast. Some rilles are filled in by the dark mare material which occurs in patches around the periphery of the floor. The rilles may have formed as a result of slow isostatic rebound of the floor. Location: 26° S, 83° E. Framelet width: 12 kilometers.

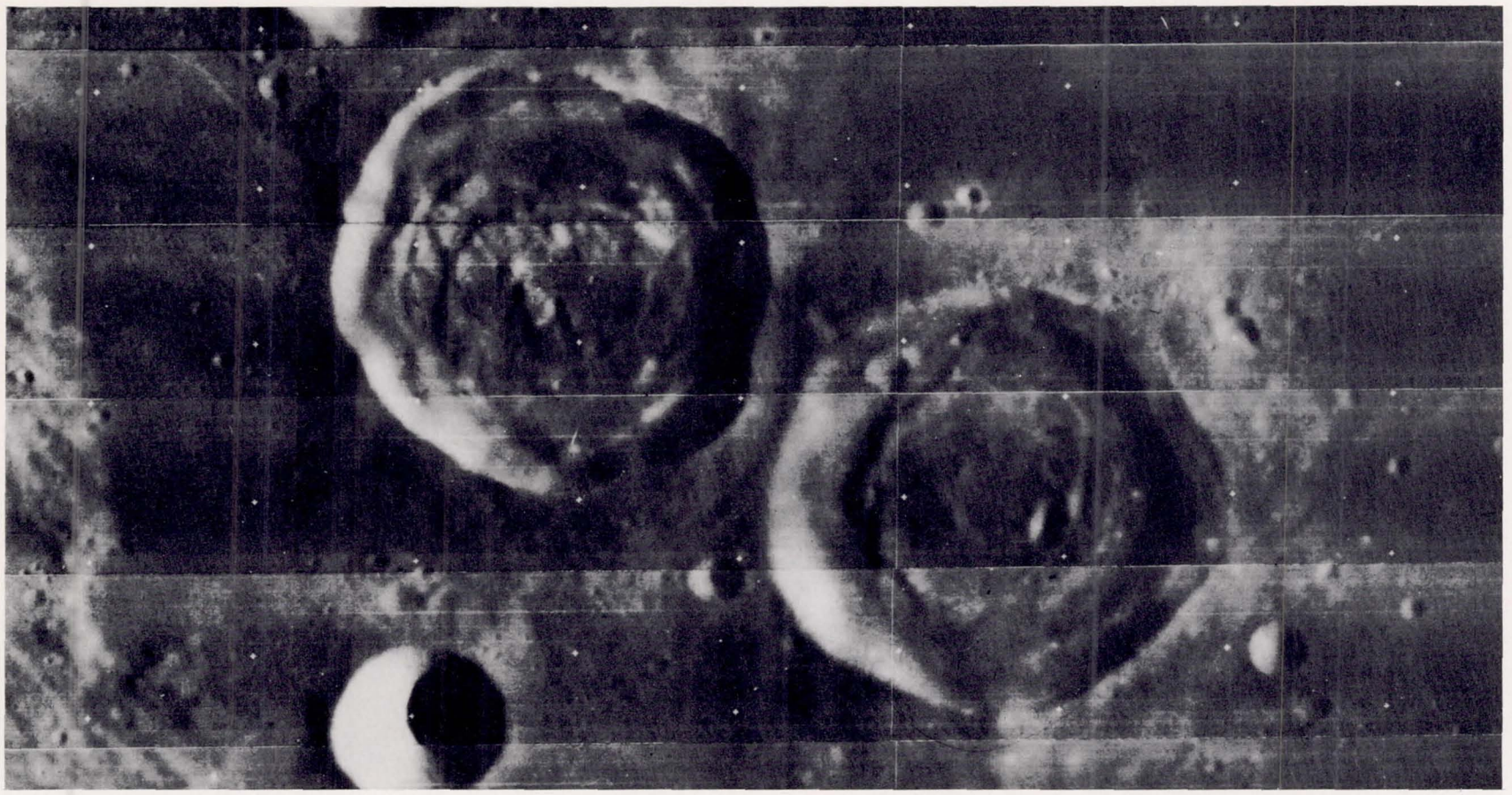

The unusual craters Sabine (right, 30 kilometers across) and Ritter, at the southwest edge of Mare Tranquillitatis. A possible volcanic origin for these craters is suggested by their relatively high floors, arcuate internal ridges, apparent lack of secondary craters, and close resemblance to each other. These characteristics resemble those of terrestrial calderas. Similar crater pairs exist on the Moon's farside (see page 135). Location: 1°40′ N, 19°40′ E. Framelet width: 12 kilometers.

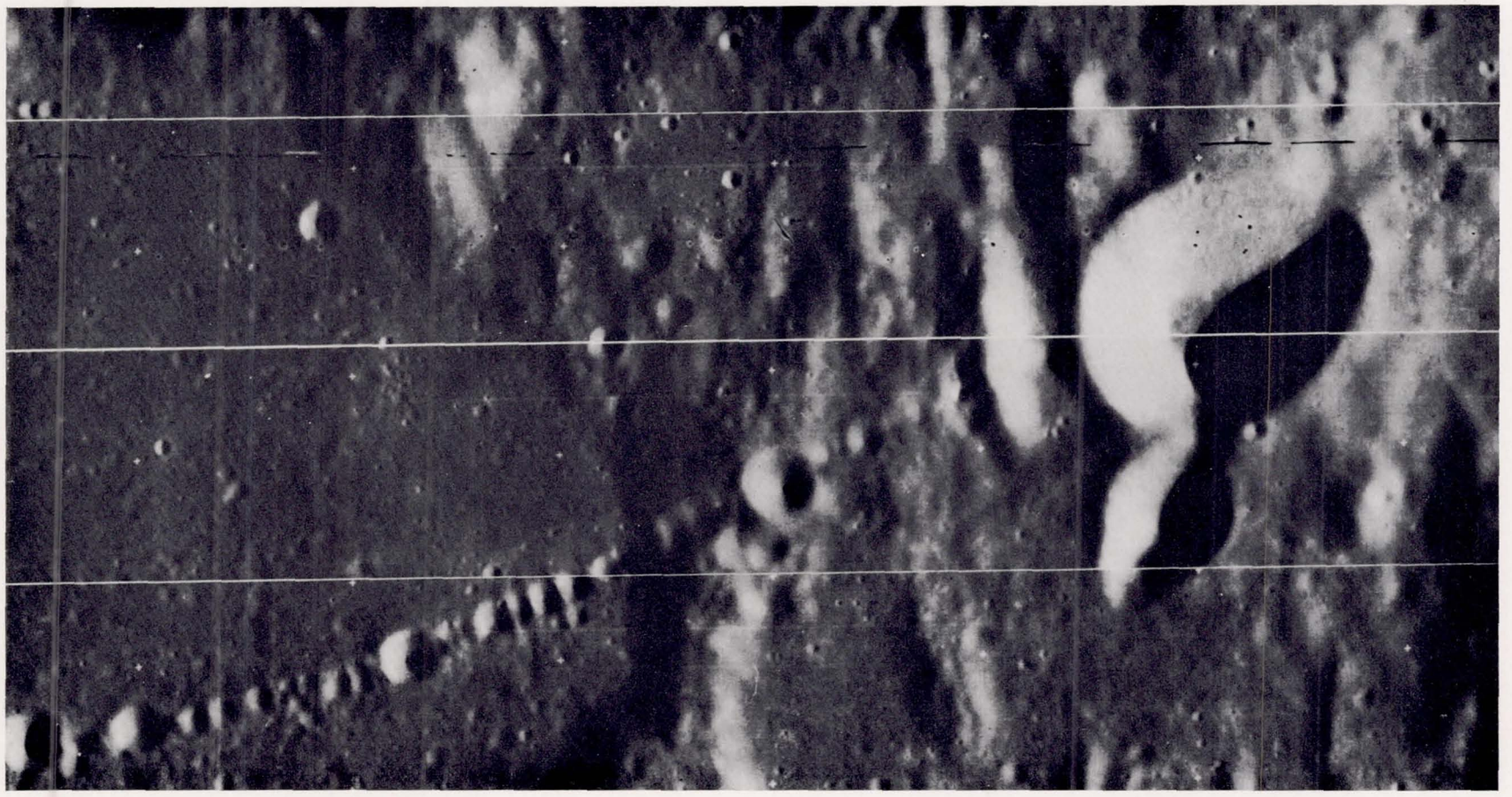

A crater chain that crosses light-toned plains-forming material in the large old crater Davy Y (left) and continues eastward into the adjacent rugged highlands where it culminates in the bright crater Davy G (15 kilometers across). Note the markedly uniform width and spacing of the craters in this chain. Davy G cools anomalously slowly at eclipse and appears to be a fresh volcanic crater at the intersection of two fractures. Location: 10°40′ S, 6°10′W. Framelet width: 12 kilometers.

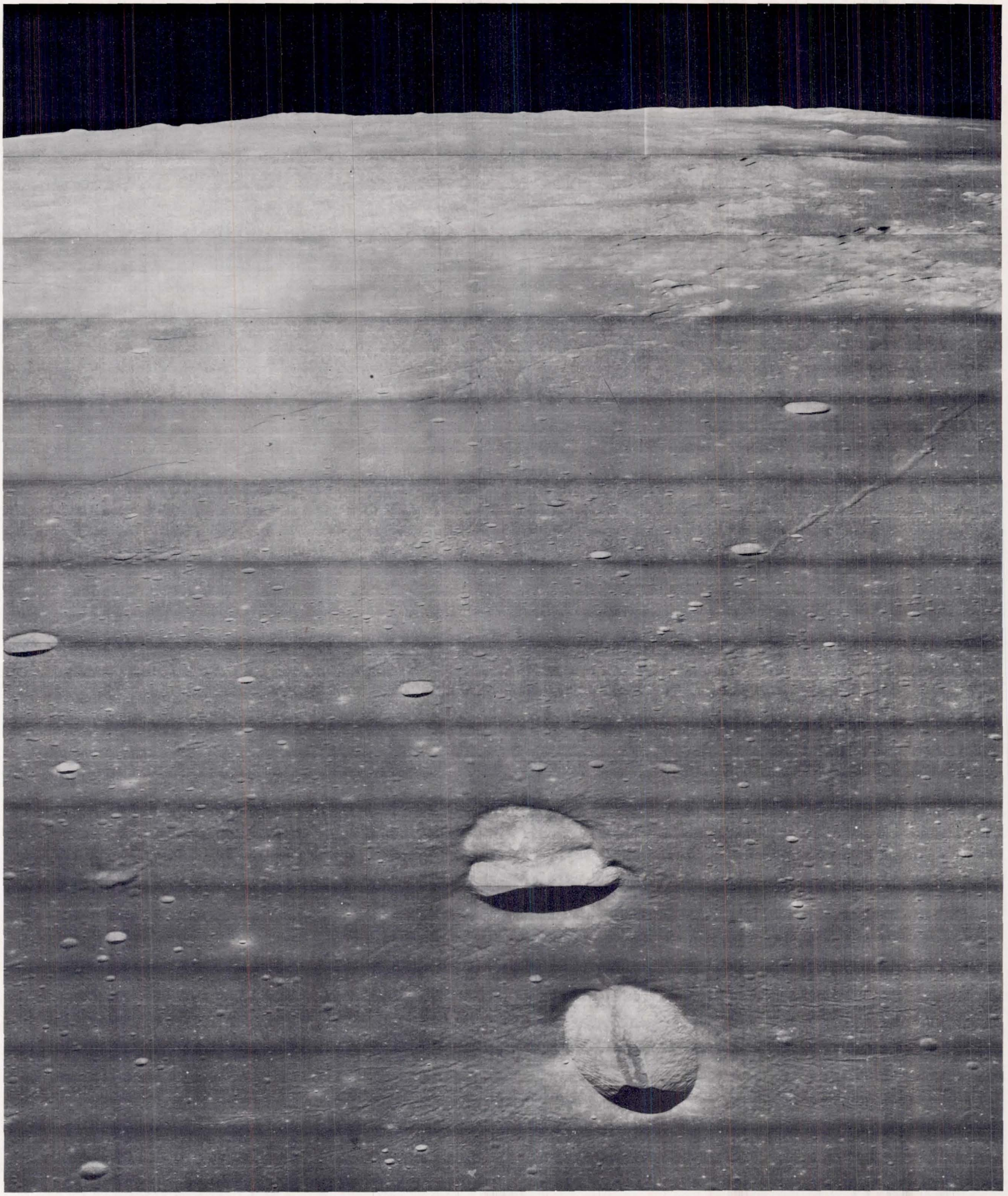

Oblique view looking westward across western Mare Fecunditatis showing the craters Messier (foreground) and Messier A, both approximately 12 kilometers in the longest dimension. Messier is a single, elongate crater. Messier A consists of two circular craters; the nearest one is young and superposed on an older deformed crater. The two faint rays in line with these craters extend some 120 kilometers and are very prominent in an Earth-based telescope view at full moon.

Detail of the crater Messier. Fresh blocks and possible outcrops of ledges occur along with slump structures on the walls. The dark material in the elongate depressions on the floor could be accumulated debris from the walls. Messier and the rays shown in the photograph on the opposite page may have been produced by a low-angle impact, but the coincidence of the asymmetric rays and the crater triplet remains to be fully explained. Messier is located at 1°50′ S, 47°40′ E.

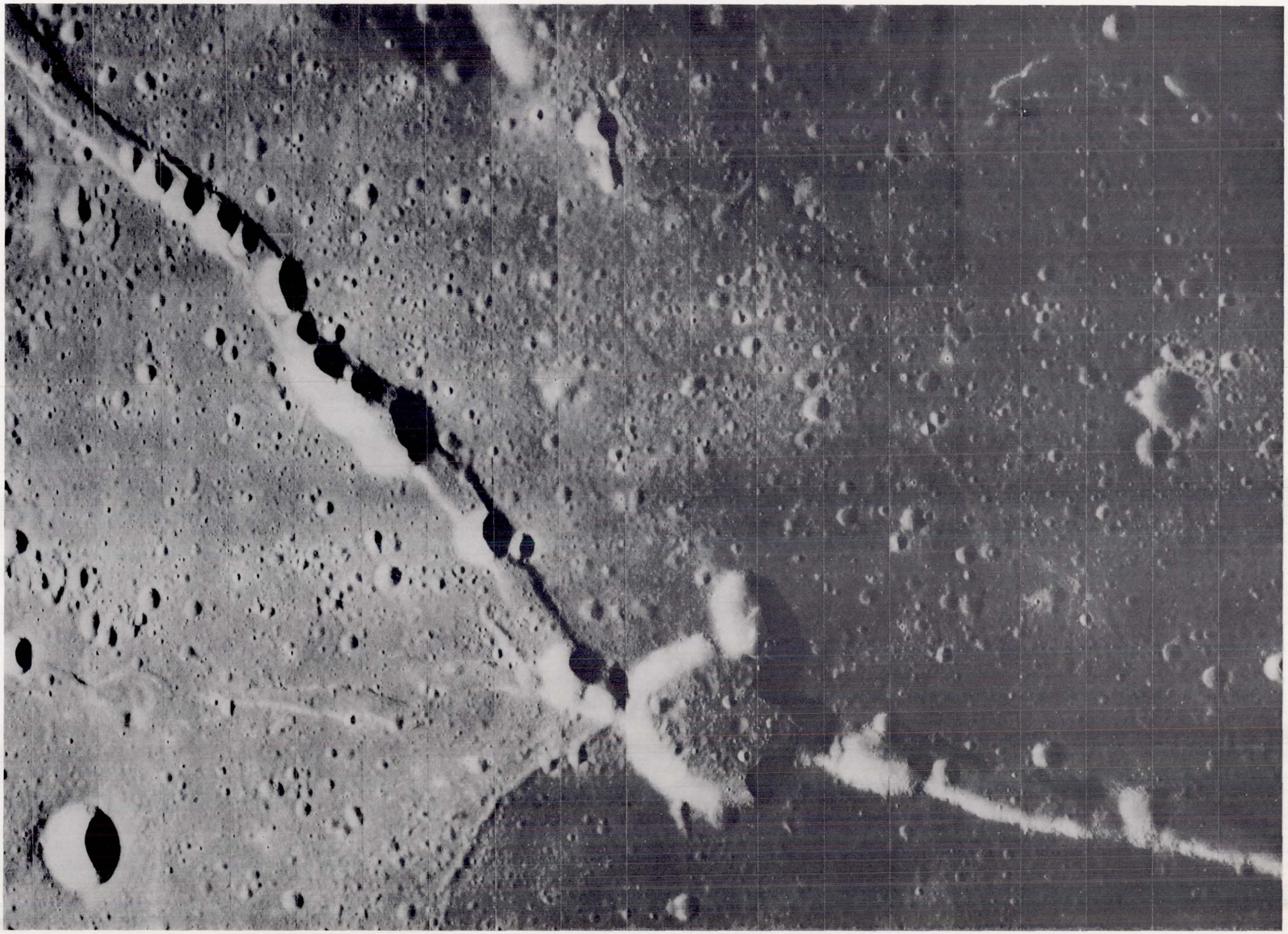

Crater chains along the Hyginus Rille (Rima Hyginus). Hyginus is the large crater (11 kilometers in diameter) at the junction of the two segments of the rille. The disconnected crater chains are clear evidence of lunar volcanism; so many similar and evenly spaced craters situated along an obviously fault-produced rille could hardly have been formed by impact. Note the small domes in the floor of the crater Hyginus. The dark material on the mare surface south and east of Hyginus may have erupted from that crater. Location: 8°N, 6°10′E. Framelet width: 3.3 kilometers.

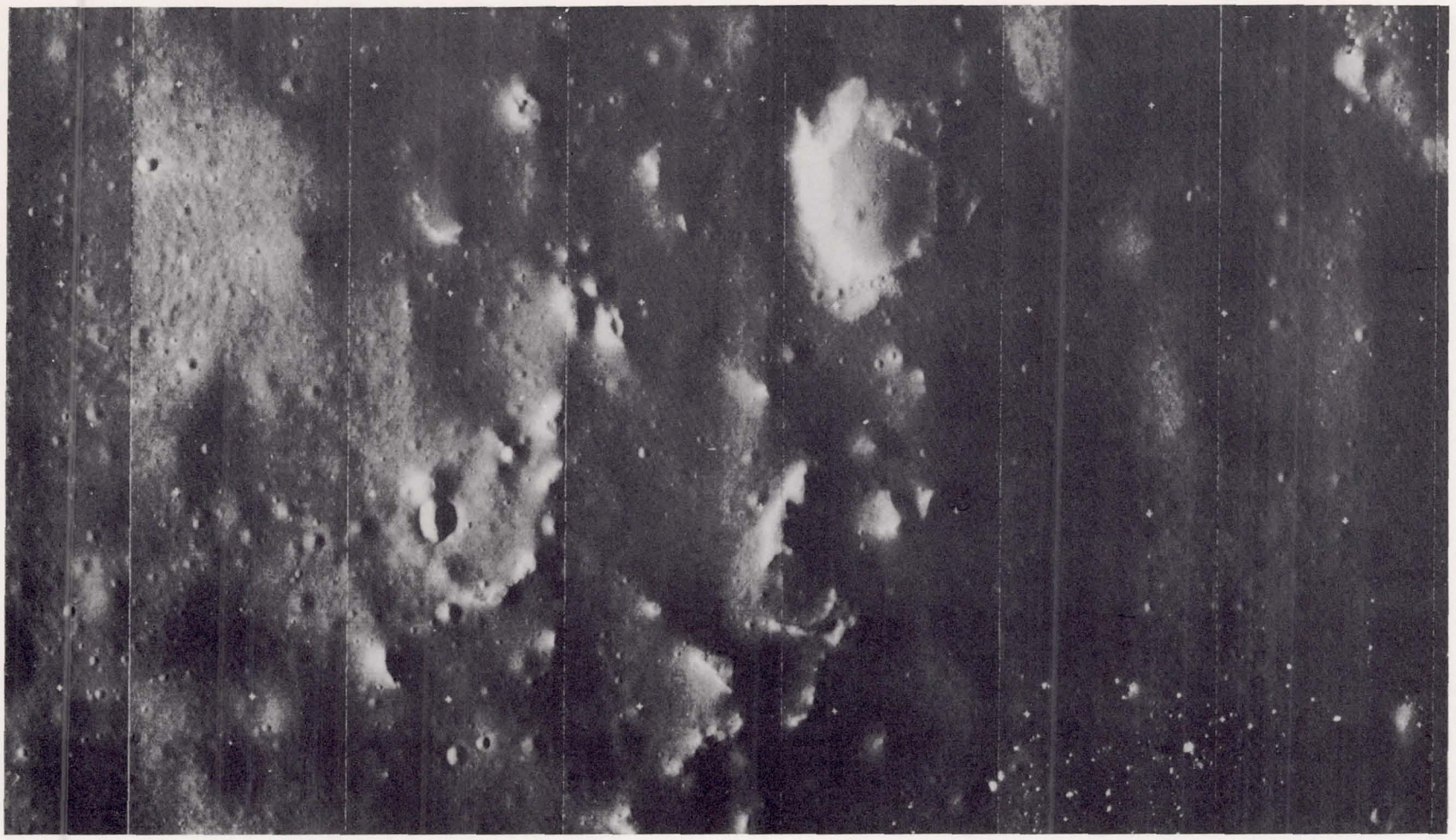

Detail of the floor of the crater Hyginus. The origin of the irregular depressions is not clear, but their form suggests the subsidence of a solid crust into a weak substratum. Framelet width: 440 meters.

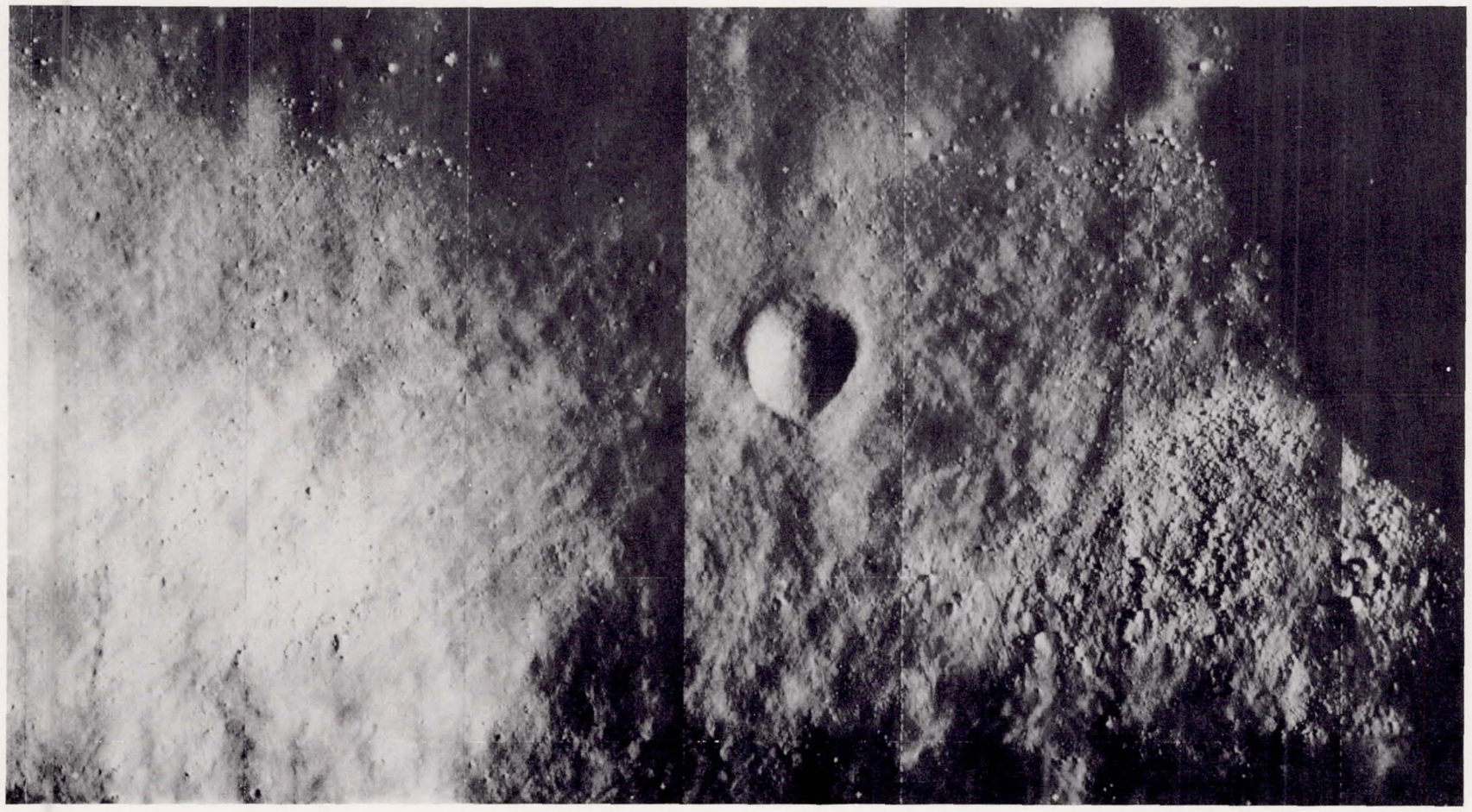

Fresh blocks on the south wall of the crater Hyginus, including many that have rolled and left trails of their downslope movement along the crater wall. Hyginus is located at 7°40′ N, 6°20′ E. Framelet width: 440 meters.

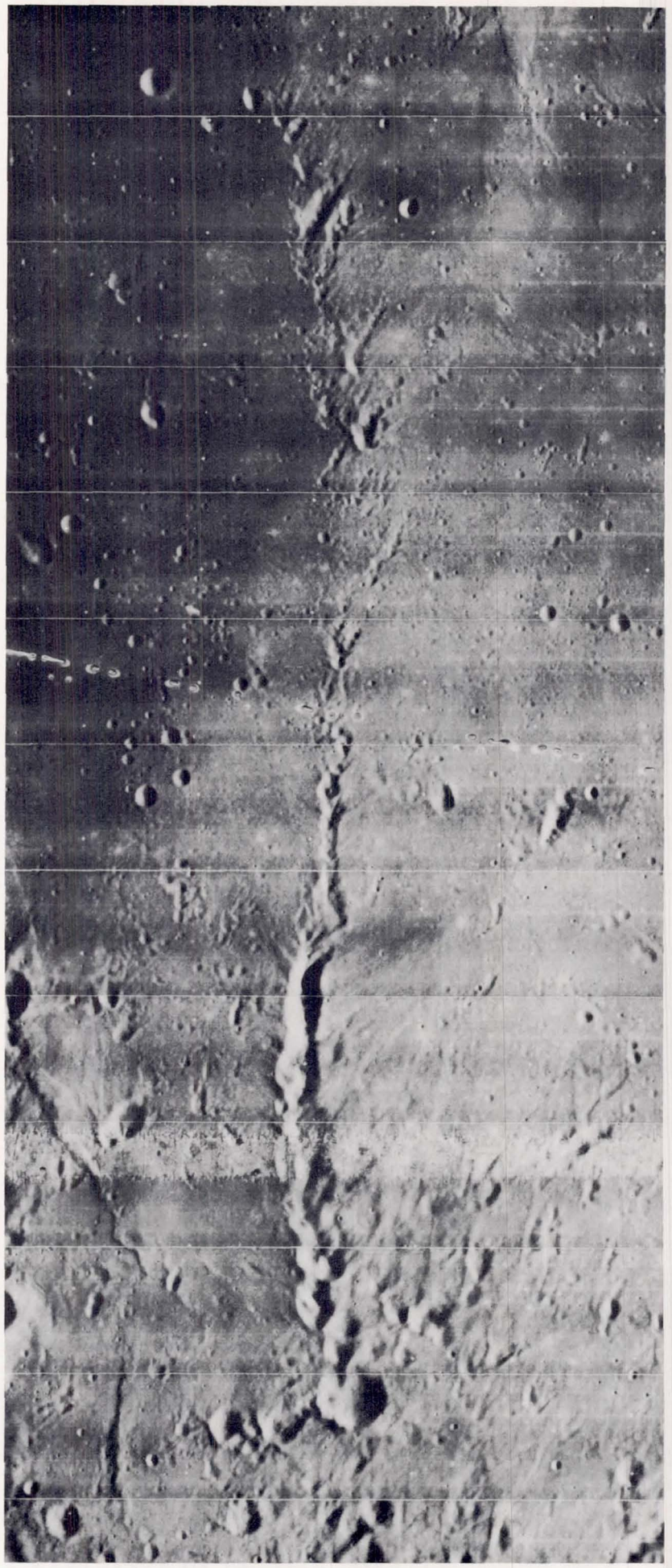

Rima Stadius IV, a chain of craters that is part of the field of abundant satellitic craters surrounding Copernicus. Narrow ridges and troughs, and strings of small craters form an irregular herringbone pattern with the "V's" pointing southward in the general direction of Copernicus. This pattern is seen in the small craters that surround many large, bright-rayed craters. Location: 16°30′ N, 16°20′W. Framelet width: 450 meters.

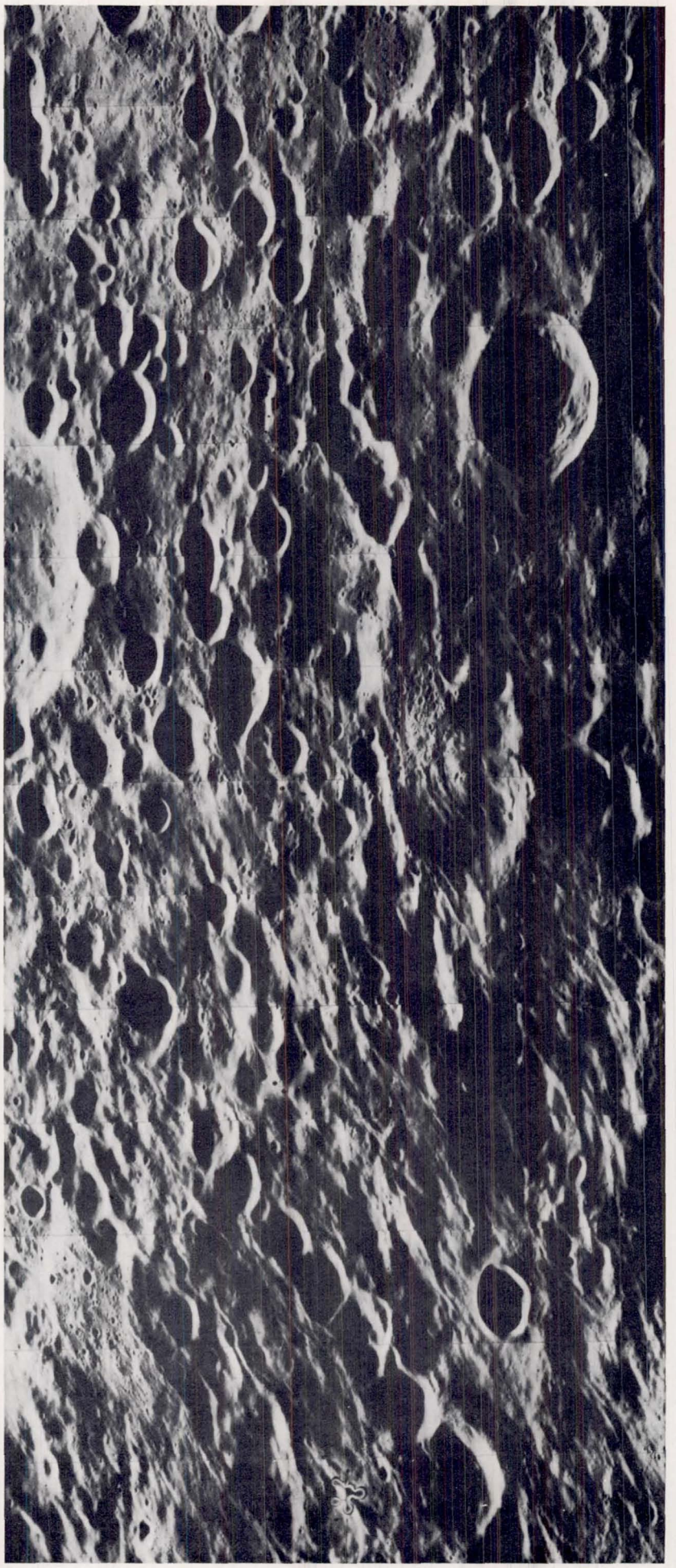

Terrain northwest of the Orientale basin, including radially streaked material and numerous equisized, somewhat irregular craters. Such craters are commonly arranged in chains radial to Mare Orientale. They may be secondary impact craters of the Orientale basin or volcanic craters along impact-opened fractures. Approximate location: 8° N, 113° W. Framelet width: about 25 kilometers.

FAULTS, RILLES, AND DOMES

The three previous sections have included several examples of such structural features as wrinkle ridges, fractures, shrinkage cracks, and slump blocks. This section is devoted to three other prominent types of structural features.

Faults: A fault is a plane along which rock masses have been shifted. The displacement may be horizontal, vertical, or diagonal. At places, the lunar surface gives visible evidence of such displacement structures. The Straight Wall (Rupes Recta) is a prominent example whose long, continuous escarpment displays a vertical component of displacement of over 250 meters.

Rilles: These are depressions on the lunar surface that bear some resemblance to terrestrial valleys. Two general types are recognized: linear and sinuous rilles, with a few combining the features of both types. Many linear rilles appear to be depressed rock masses bounded by parallel faults. Large linear rilles are as wide as 10 kilometers and half a kilometer deep and may extend for hundreds of kilometers across the lunar surface with complete disregard for the preexisting surface features. Sinuous or meandering rilles usually are smaller though often as long. Commonly they head at a crater or similar depression. They are common in some mare areas and rare in highland areas. Sinuous rilles are generally similar in form to terrestrial stream channels, and many scientists believe that they were formed through the action of particles carried by a fluid flow.

Domes: Circular, raised structures up to 20 kilometers wide and several hundred meters high abound on the Moon's surface, particularly in mare regions. Although most previously known domes were thought to possess smooth, flat surfaces, Lunar Orbiter photographs have revealed that many are characterized by steep-sided, rough, and cratered surfaces. Both types of surface are displayed by the volcanic domes found on the Earth.

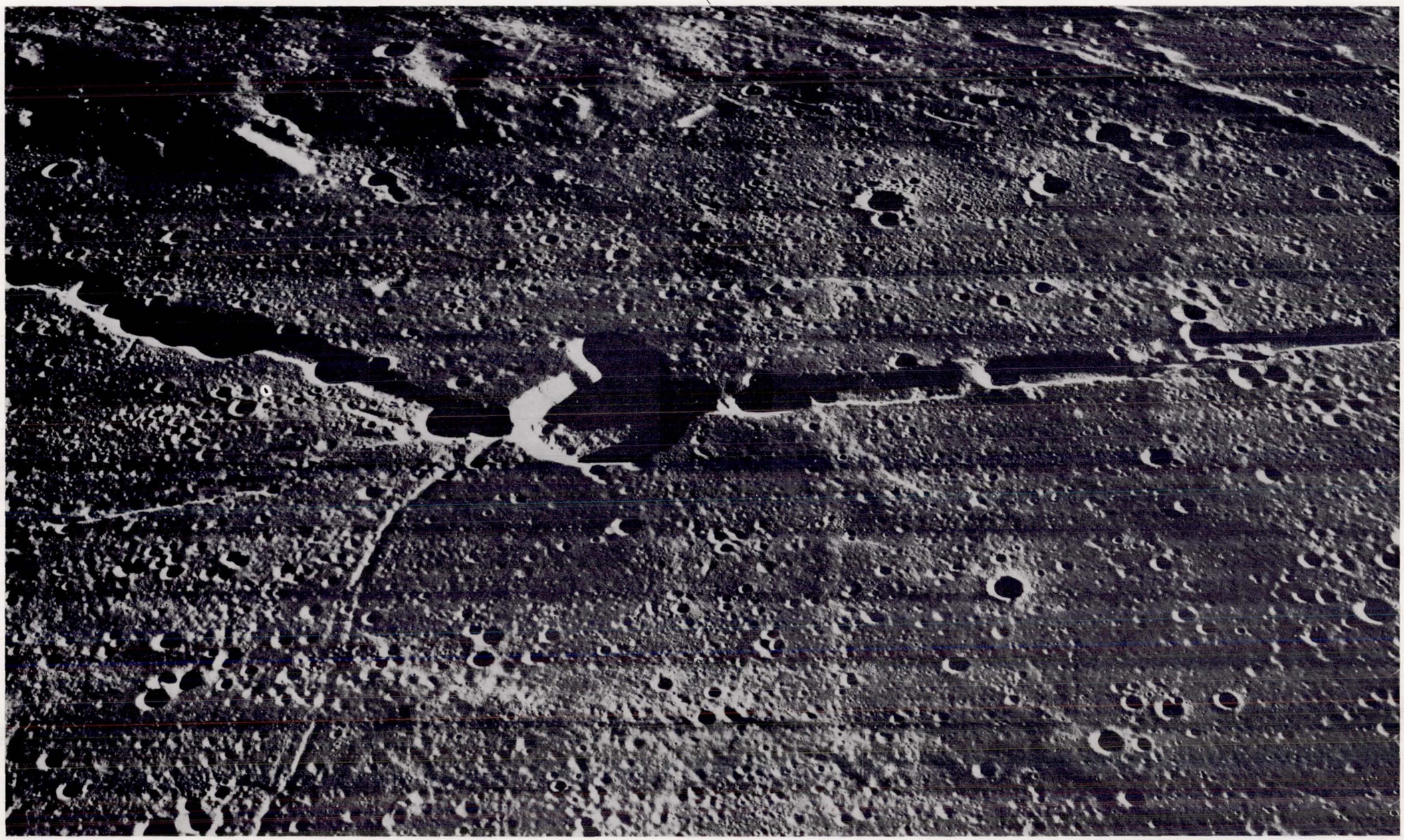

Oblique view, looking northward, of the crater Hyginus (11 kilometers in diameter) and its associated rille, Rima Hyginus. The rille changes direction at the crater. From this view it is clear that the eastern branch of Rima Hyginus extends west of the crater, but that this extension is much shallower than the rille to the northwest. Another rille, much narrower, extends southwest from the crater. The vertical view of this area (page 100) shows clearly the chain of craters aligned precisely along the northwest branch. The eastern branch is interrupted in a few places by cross-ridges. The darker-toned material surrounding the crater Hyginus has fewer small craters than the remainder of the mare surface. Location: 8° N, 6°20′ E.

The Straight Wall is a unique scarp on the eastern side of Mare Nubium. It originated as a fault some 120 kilometers long, with a vertical displacement of about 250 meters. This simple type of fault scarp is less common on the Moon than the graben which results from the downward displacement of the rock mass between two roughly parallel faults. Rima Birt I (left) is an irregular trough or rille, and not necessarily a graben. Location: 21°50′S, 8°10′W. Framelet width: 12 kilometers.

A portion of Rima Sirsalis (lower left to upper right), a graben which forms one of the longest lunar rilles. The rille is clearly younger than the large crater De Vico A (center), but older than the small crater De Vico AA (in the floor of the former), which indents the rille's adjacent side. The intersecting rilles (lower left) are part of the Rimae Darwin system, which is older than Rima Sirsalis. Location: 18°30′S, 63°40′W. Framelet width: 12 kilometers.

The existence of this large trough, on the farside near the south pole, was unknown prior to this photograph, taken by Lunar Orbiter IV on May 11, 1967. The trough extends northward for more than 250 kilometers from the rim of a large, as yet unnamed, crater. It displays raised rims and in places is as wide as 8 kilometers. The trough cuts across several older craters without regard for the preexisting structures. The sharpness of its features indicates that it is much younger than similar features on the front side. Location: approximately 65°S, 110°E.

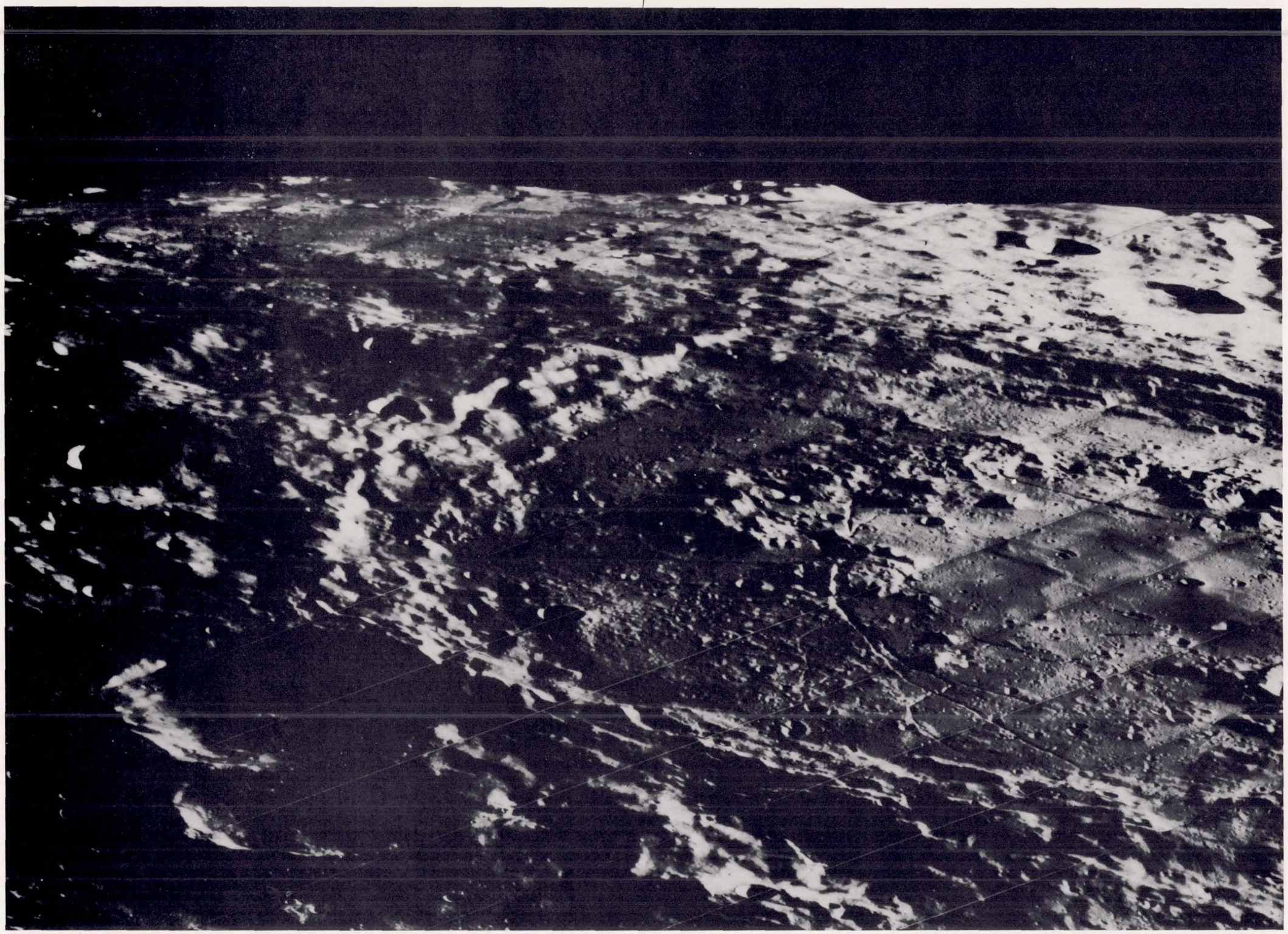

Oblique view of part of the area illustrated on the previous page. The southern third of the trough enters the photograph at the left, a half inch below the horizon, and ends at the outer rim of the large crater. The crater, which is located about 70°S, 130°E, is made conspicuous by the widespread terracing of its wall and the remarkable system of fractures and linear rilles which dissect its floor. A broken circle of peaks on the floor constitutes an inner rim. Within this circle, near the right side of the photograph, is a tear-shaped crater surrounded by a halo of very dark material.

This photograph illustrates part of a system of branching rilles (rimae) dissecting old features of the Moon's earthside. Cutting across the common boundaries between the crater Fra Mauro, which occupies the upper half of the photograph, and the craters Parry (lower right) and Bonpland (lower left), are Rima Parry I and Rima Parry V-VI, respectively. A portion of the latter rille within Fra Mauro is nearly obliterated by a deposit of darker-toned material derived from a line of presumably volcanic domes and cones along its west bank. Location: 7°10′S, 16°40′W. Framelet width: 3.3 kilometers.

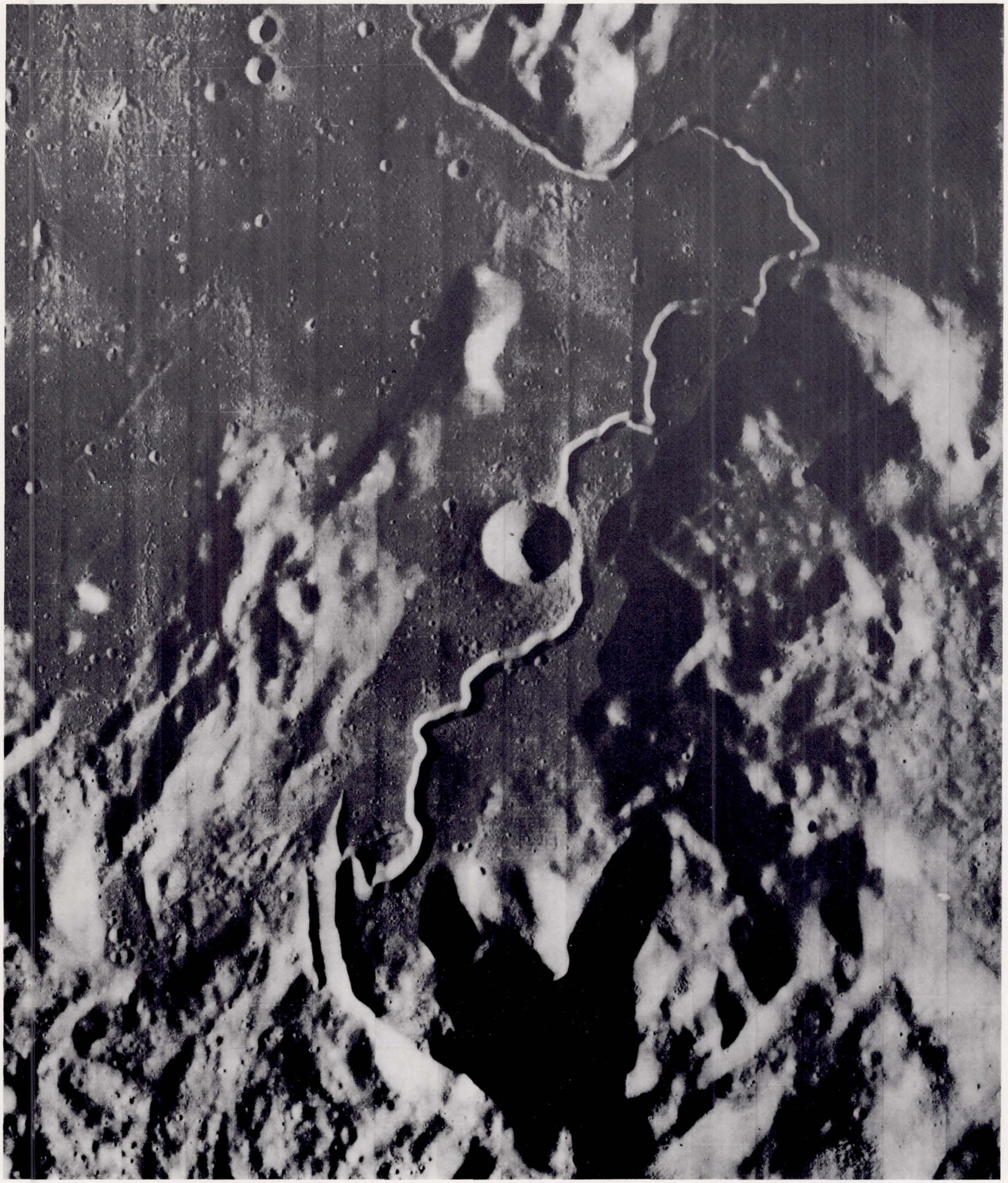

Rima Hadley, the sinuous depression illustrated above, is one of the most conspicuous lunar rilles when viewed with Earth-based telescopes. Its southern end is a very deep, elongate depression, which is interpreted by some as its source. The rille meanders through the mare material of Palus Putredinis in a northeasterly direction, approximately parallel to the margin of the Apennine Mountains which rise from 1 to 2 kilometers above the adjacent mare surface. The relatively large, circular crater in the center of the photograph is Hadley C. Location: 25°20′ N, 2°50′ E. Framelet width: 4 kilometers.

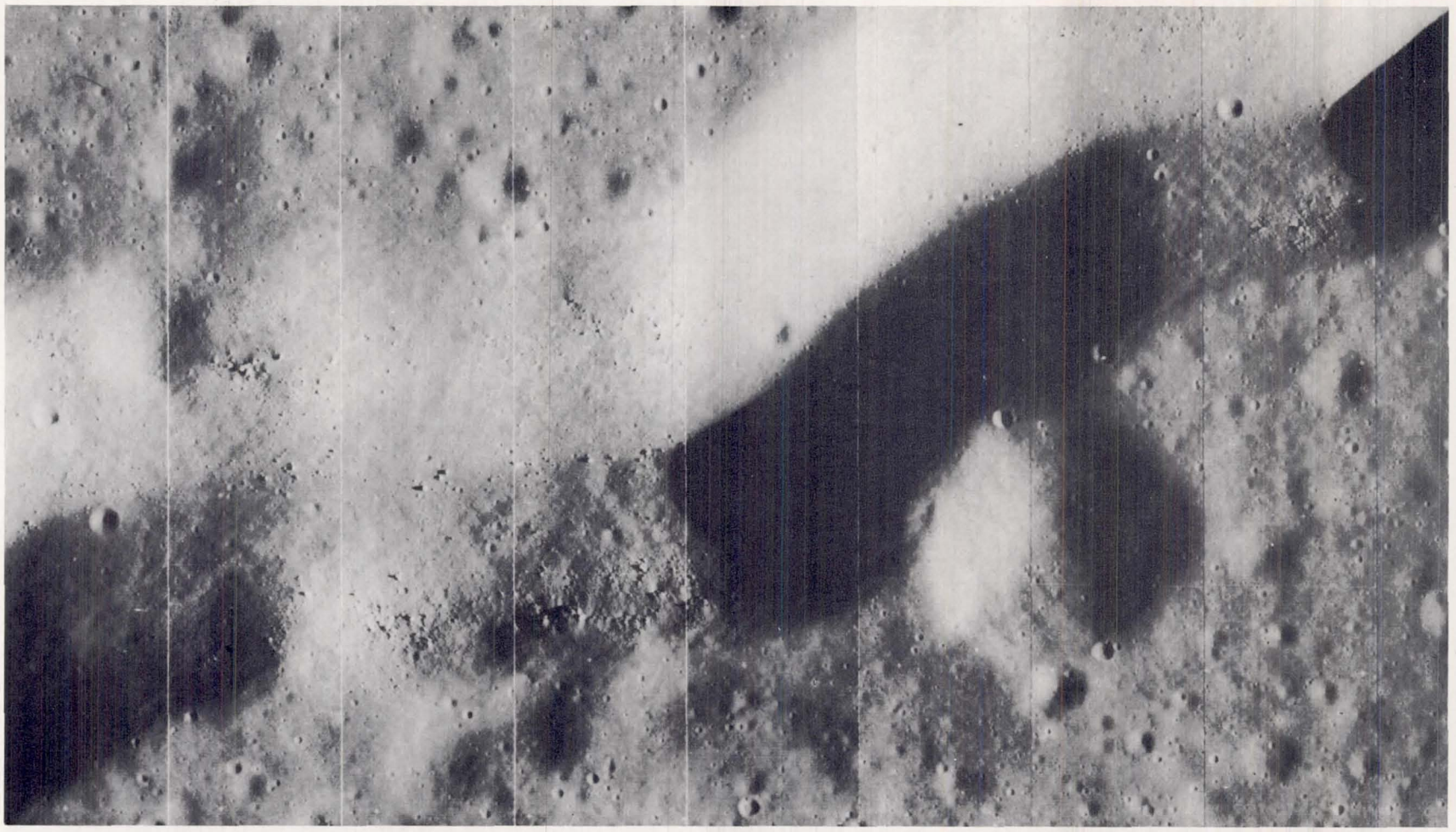

Telephoto lens views of two parts of Rima Hadley. The rille is a depression in a moderately cratered mare terrain. It has a V-shaped cross section, measuring between 1 and 1.5 kilometers from rim to rim. The inner walls of the rille have an average slope of about 20°, and are typically block strewn. Blocks at the bottom appear to be derived from ledges of bedrock along the walls, especially on the upper parts. The origin of Rima Hadley is still a matter of controversy, but apparently is related to some sort of flow of fluid material. Framelet width: 550 meters.

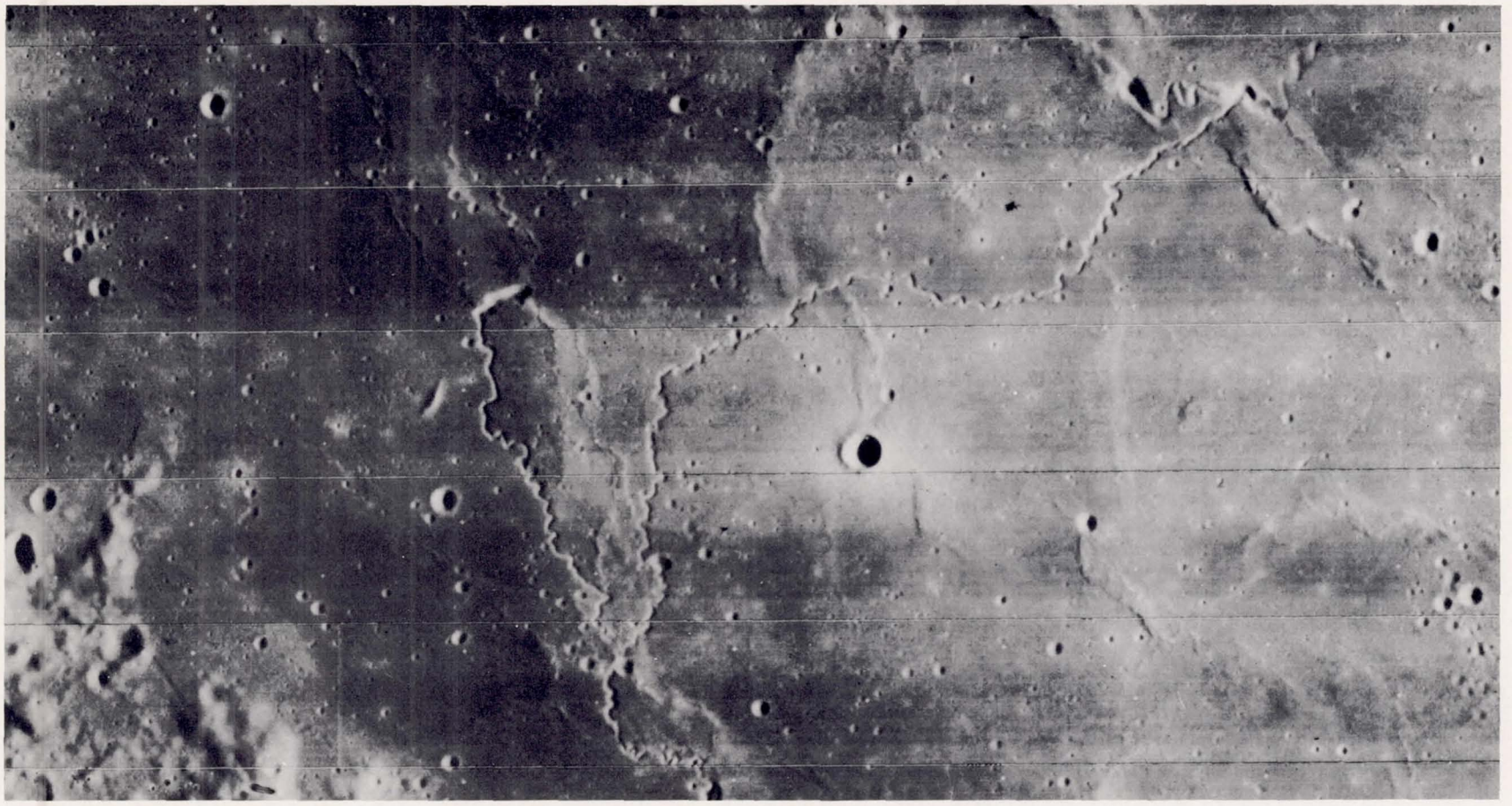

Part of a remarkable sinuous rille system in southern Oceanus Procellarum, northeast of the crater Gassendi. The rille cuts across several mare ridges, and some of its branches originate in elongated depressions. The branching is found in other sinuous rilles of the same type, such as Rima Plato II. The circular crater with a sharp raised rim near the middle of the photograph, Herigonius Ec, is about 3.5 kilometers in diameter. Location: 11°50′ S, 38° W. Framelet width: 12 kilometers.

This is part of a sinuous rille southeast of the crater Plato in the Montes Alpes region. The rille, Rima Plato II, forms a meandering, V-shaped depression. Its walls display some lamination that suggests the existence of layering in the incised material. The loop which the rille makes at the upper left of the photograph may represent a cutoff flow channel in the early stages of formation. Location: 49°30′ N, 2°50′ W. Framelet width: 1 kilometer.

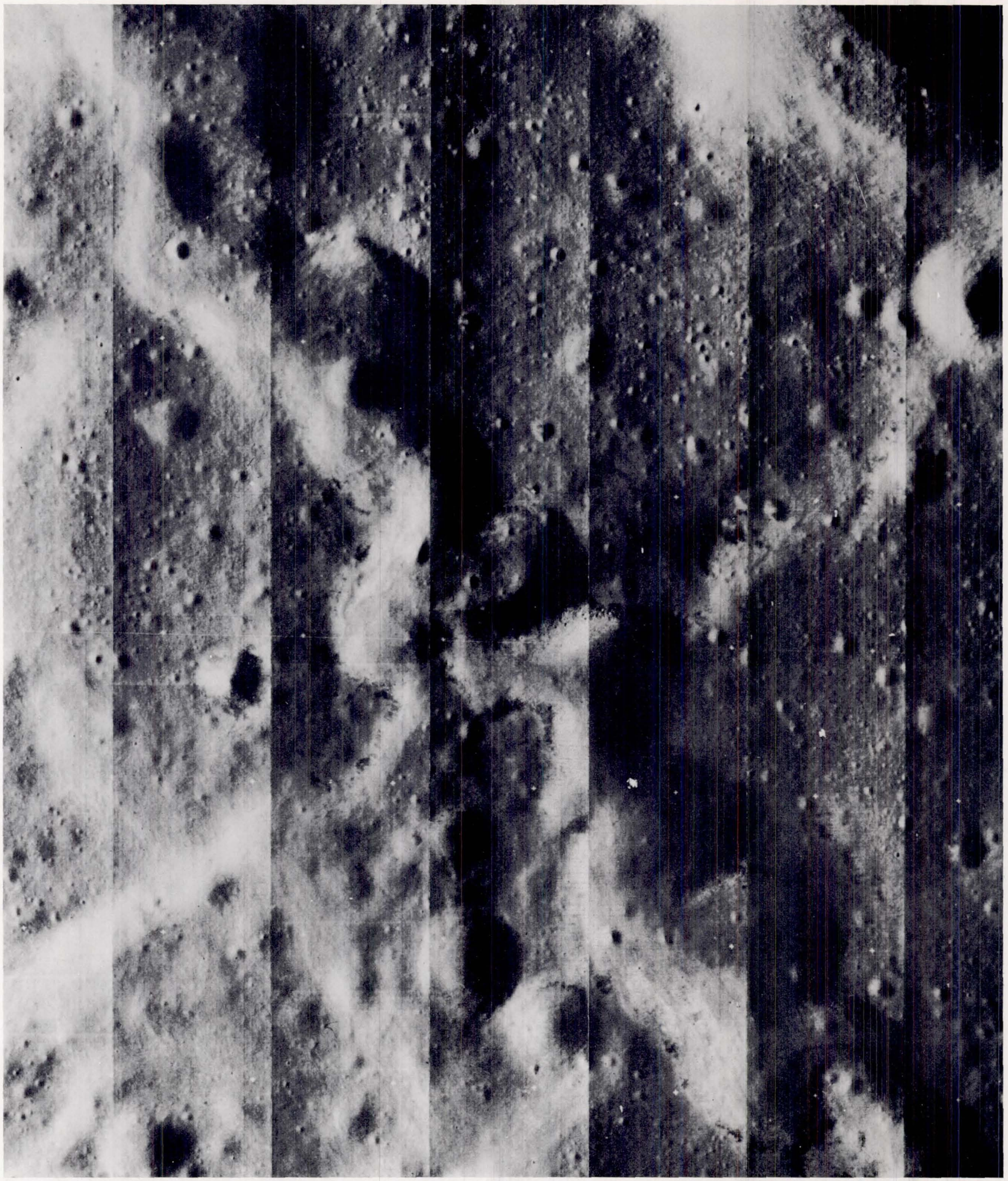

Part of Rima Plato II, a sinuous rille southeast of the crater Plato. The rille occurs in what here appears to be stratified mare material in a plainslike terrain. Indications of stratification exist on the rille walls, especially toward the top. Dark rock exposures abound on the walls, and the larger blocks appear to originate at the upper layers. As in most other rilles, there is evidence of downslope movement and "mass wasting" along the rille walls. The two irregular white spots in the lower right quadrant are processing blemishes. Location: 49° N, 1° W. Framelet width: 1 kilometer.

This photograph illustrates a lunar valley, named after the renowned German selenographer, J. H. Schröter (1745–1816). Schröter's Valley, which is about 1300 meters deep, has the Cobra Head (center right) at its southeastern end. This is interpreted as the source of the fluid material that eroded the valley. The north rim of the crater Herodotus appears at the lower right. Much of the surface sculpture in this area is caused by ejecta from the crater Aristarchus, situated to the southeast. Location: 24°58′N, 50°02′W. Framelet width: 4.3 kilometers.

Detailed telephoto view of part of Schröter's Valley. Within the valley is a meandering rille which also emerges from the Cobra Head. The rille meanders from wall to wall across the valley floor, and forms a cutoff channel near the center of this view. Note also the numerous blocks along the walls and on the floors of both the valley and the rille. Some scientists believe that the valley and the meandering rille were eroded by a dense mass of particulate material carried by a flow of either liquid or gas. Location: 25°40′N, 50°W. Framelet width: 570 meters.

This area is part of the Harbinger Mountains plateau in north central Oceanus Procellarum. Many sinuous rilles cut across the mare materials, and one cuts the highland mass near the center of the view. The north rim of the crater Prinz is just visible at the bottom. Photographs such as this provide stream hydrologists with data for the study of the geometry of sinuous rilles and their relations to the surroundings. This work is aimed at establishing the properties of channel materials, the flowing fluid, and the transport load, if any. Location: 27°10′N, 43°40′W. Framelet width: 4.5 kilometers.

This mosaic is a telephoto view of the head of the westernmost rille in the previous photograph. It lies on the flank of the old, partly flooded crater Prinz. Its relation to the rille (Rima Prinz I) is similar to that of the Cobra Head to Schröter's Valley. In both cases there is an inner sinuous rille which originates in a deep circular pit within the shallower and larger head. Location: 26°10′ N, 43°40′ W. Framelet width: 580 meters.

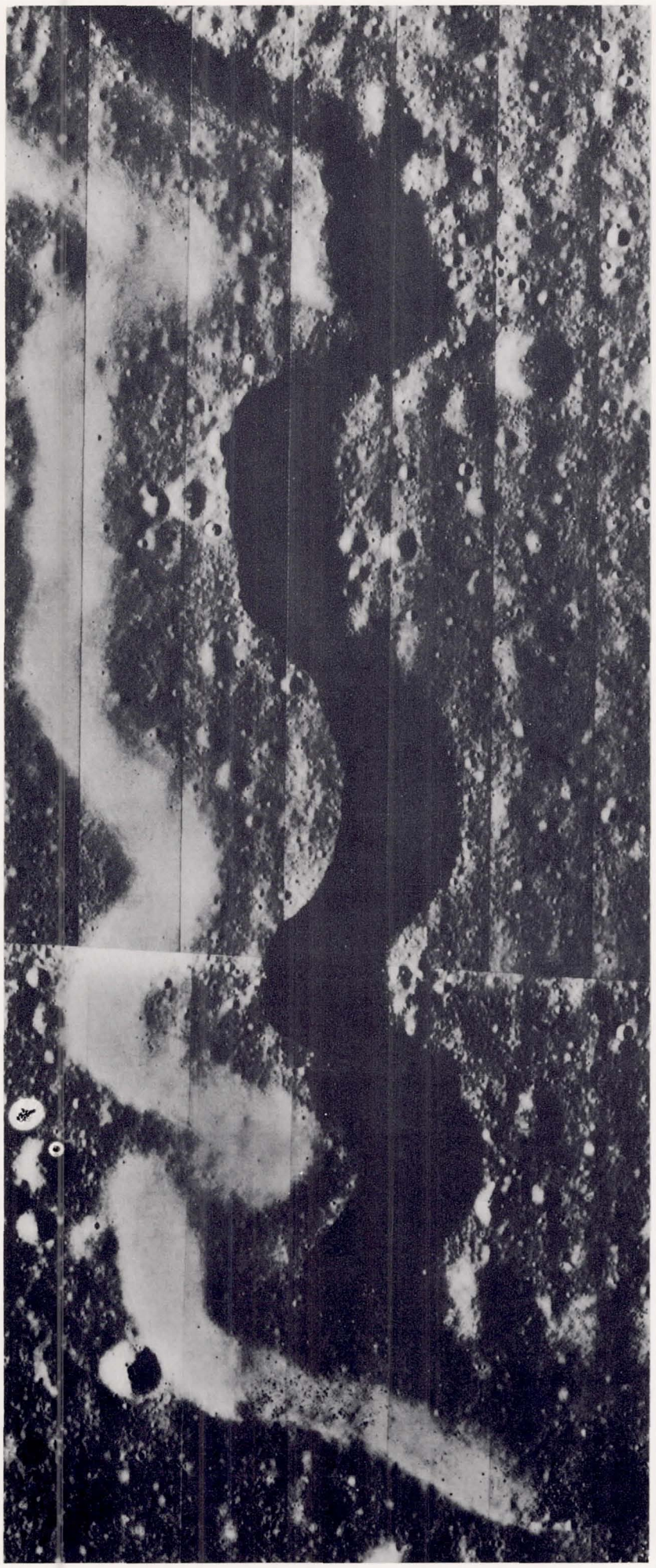

Part of Rima Prinz II, a sinuous valley in the Harbinger Mountains region with parallel walls and nearly constant width and depth. Blocks abound at places along the walls. Small craters are equally abundant on the rille floor and the surrounding areas. Location: 26°40′N, 43°40′W. Framelet width: 580 meters.

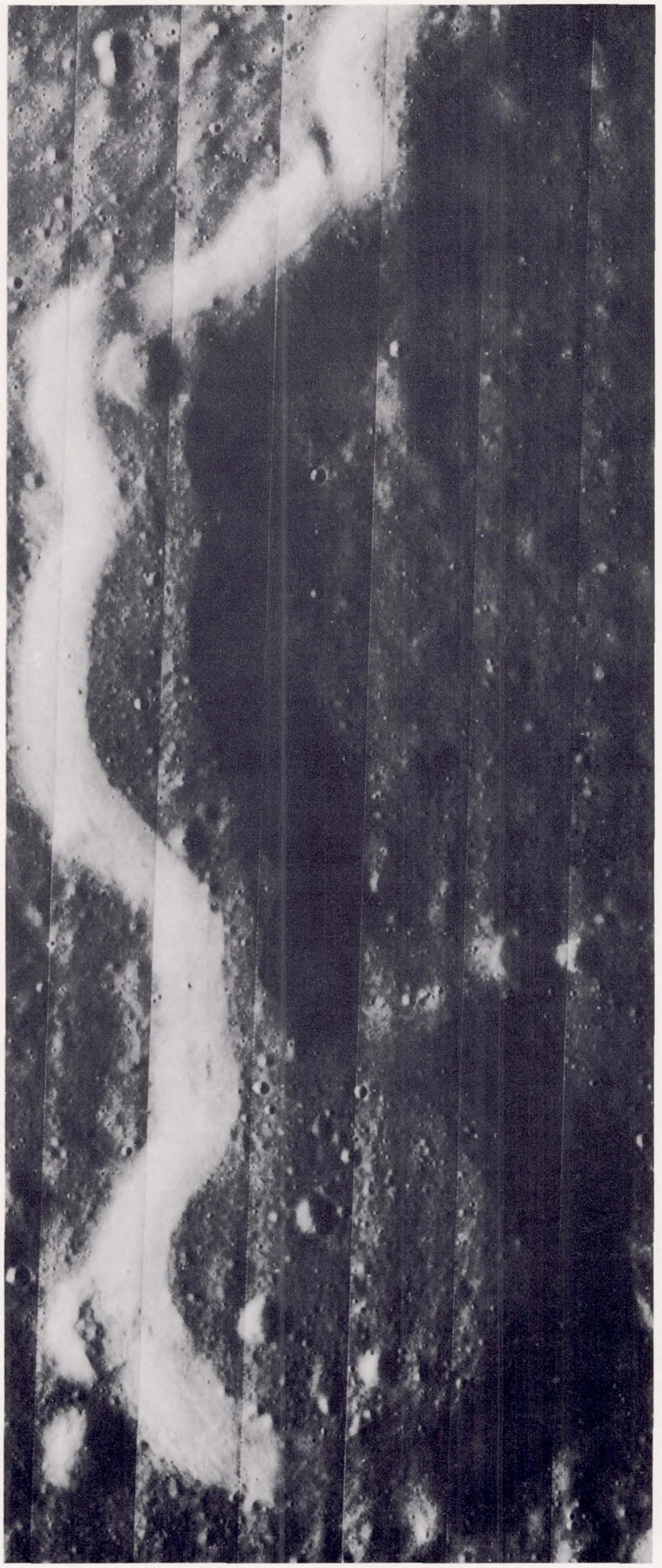

This photograph illustrates the southern end of a rille, just east of Rima Prinz II, that starts as a rimless, plains-filled depression and extends (without a break in the floor surface) toward topographically lower plains. Location: 27°N, 42°50′W. Framelet width: 580 meters.

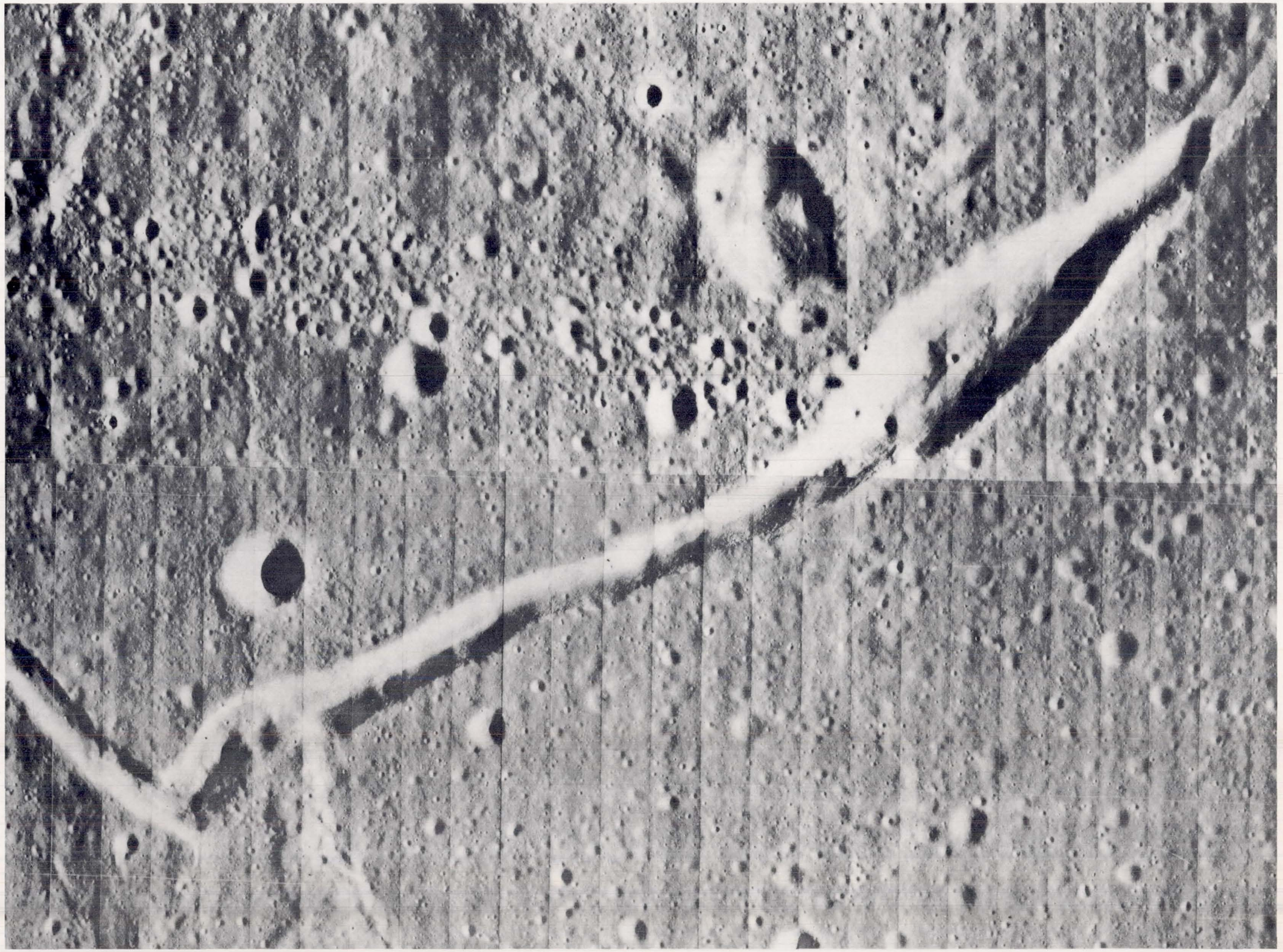

Telephoto mosaic of one end of a sinuous rille in the Marius Hills region (a 35,000-square-kilometer volcanic plateau described on subsequent pages). The rille originates in a pointed, spearhead depression with very sharp boundaries. The rille also exhibits sharp boundaries. It crosses a broad mare ridge at lower left. The rille's cross section is V-shaped east of the ridge and changes to U-shaped west of the ridge. Location: 14°10′ N, 56° W. Framelet width: 470 meters.

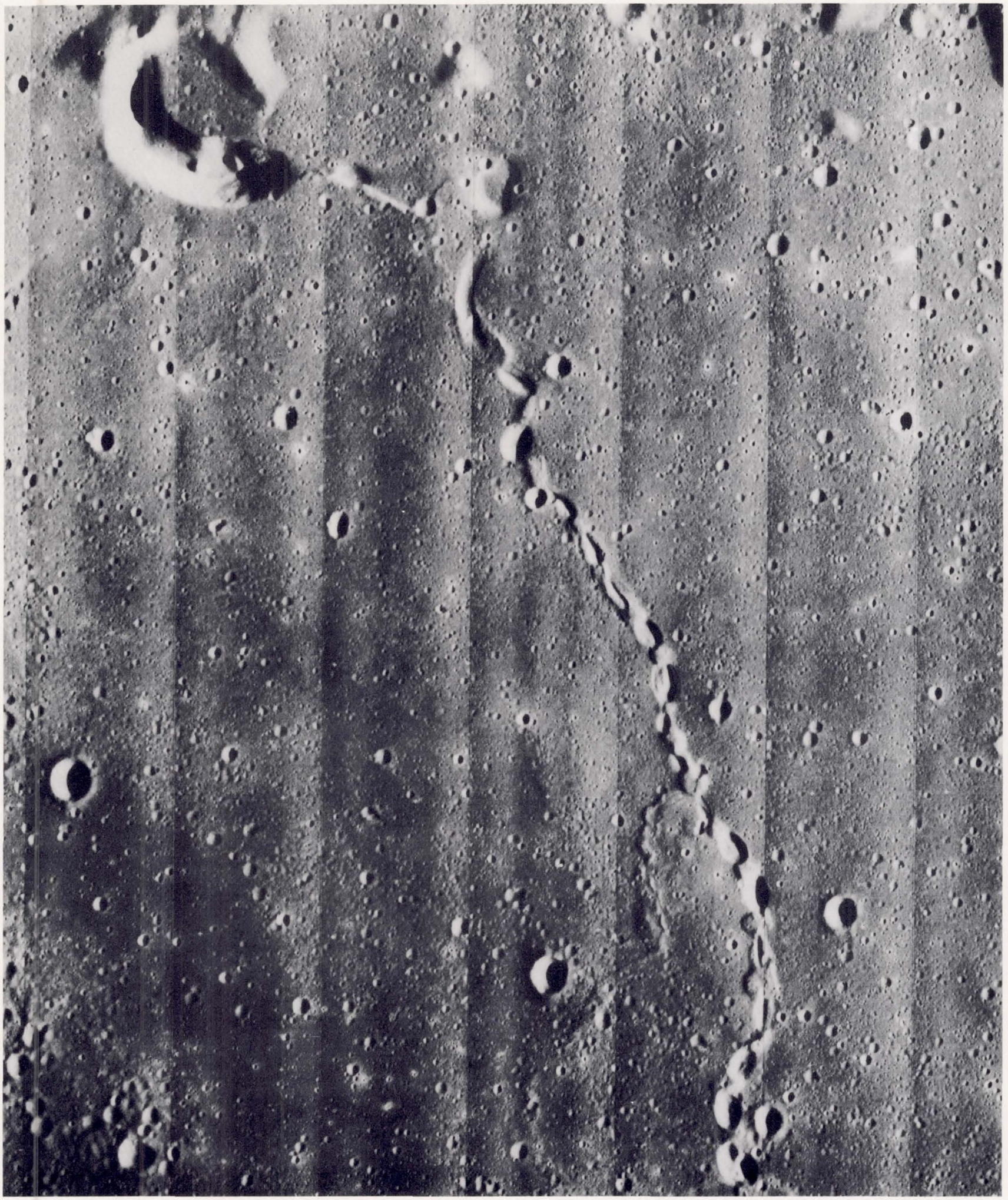

The chain of elongated craters alternating with low, nearly circular mounds shown here is in mare material near the north border of Oceanus Procellarum. The line extends south of this view as a mare ridge. A possible origin for this puzzling feature is the upwelling of mobile material along a line of weakness in the mare, with actual extrusion at a series of vents, and collapse to form elongated craters or troughs in between. Location: 34°30′N, 43°40′W. Framelet width: 5.4 kilometers.

A broad, low dome about 25 kilometers across, one of many in Oceanus Procellarum, southwest of the crater Tobias Mayer. This dome is bounded on the east by a highland ridge which is 35 kilometers long. The path of a sinuous rille in the mare just west of the dome appears to have been affected by the dome. Crater chains and clusters seen here are secondary to larger craters outside the field of view. Many of them trend northwestward, roughly parallel to the elongated, well-defined summit crater of the dome. Location: 13° N, 30°50′ W. Frame-let width: 3.5 kilometers.

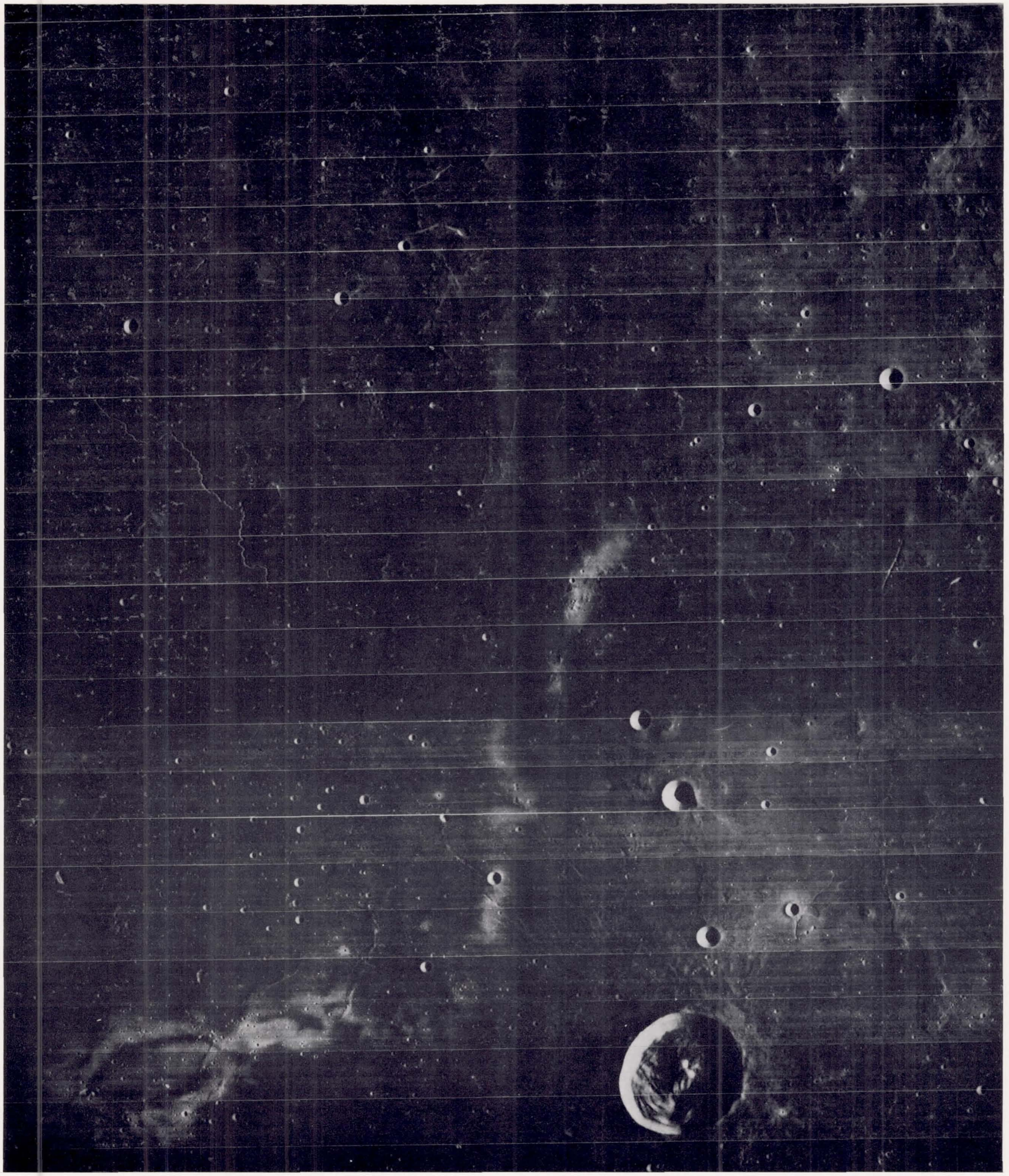

These are some of the numerous domes which occupy a part of Oceanus Procellarum. Morphologically, these domes (the Marius Hills) closely resemble terrestrial volcanic domes, laccolithic intrusions, and shield volcanos. For this reason, and because of other manifestations of volcanism in the area, geologists believe that they were formed by volcanic processes. The large crater (lower right) is Reiner, which is 30 kilometers in diameter. The peculiarly marked area of bright discoloration (lower left) is called Reiner γ. Location: 11°40′N, 58°10′W. Framelet width: 12 kilometers.

Lunar Orbiter II photographed this northward oblique view of the Marius Hills and the surrounding plateau in Oceanus Procellarum. These hills are believed to be the topographic expression of volcanic domes, plugs, and cones. The nearly continuous wrinkle ridges are part of a 1900-kilometer system of such structures in Oceanus Procellarum. The hills are named after the level-floored crater Marius (upper right), 41 kilometers across, which is located at 11°50′N, 50°50′W. This view covers a 230-kilometer stretch of the horizon, which was 400 kilometers north of the spacecraft.

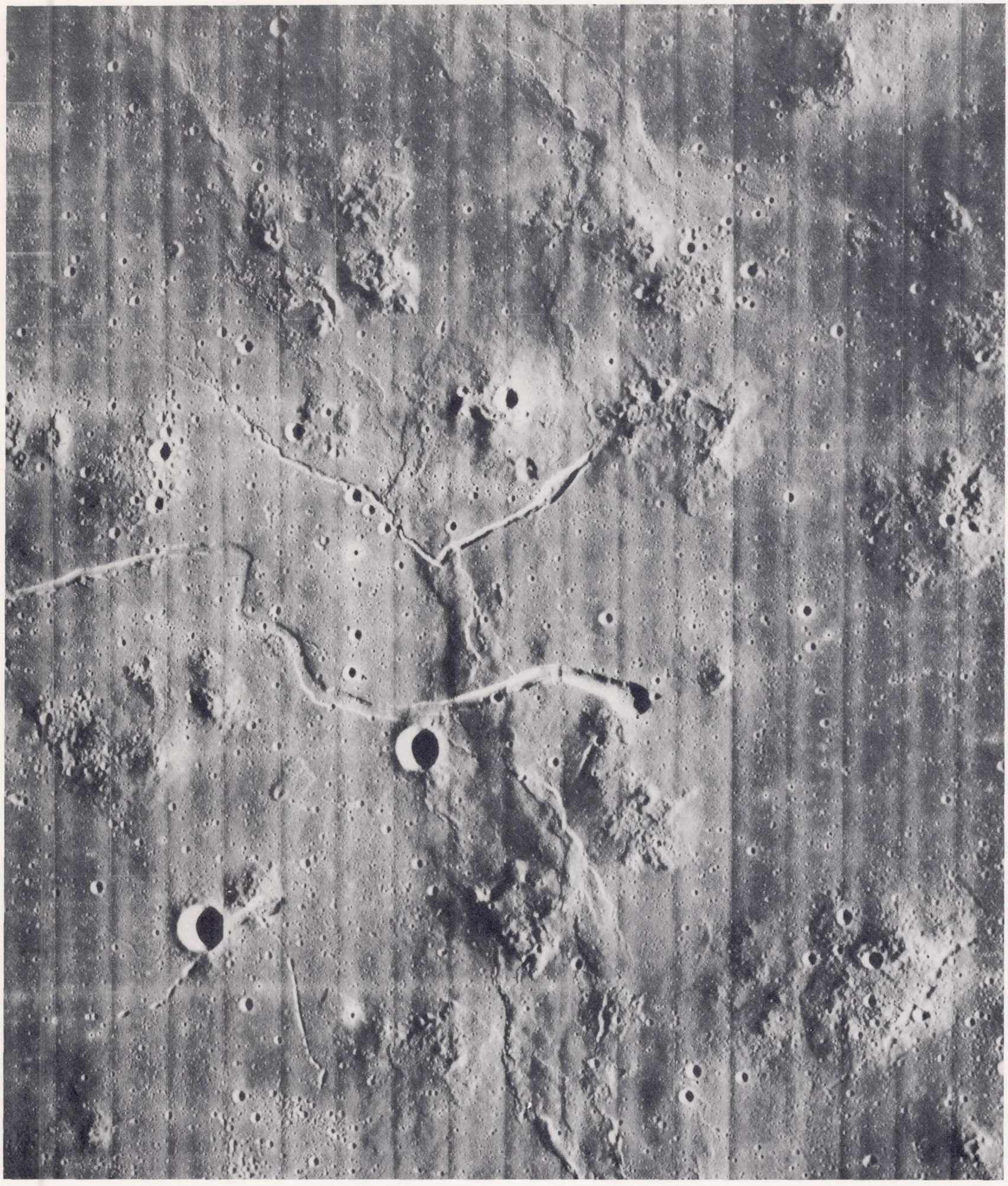

Part of the plateau west-northwest of the crater Marius, where a variety of volcanic domes, cones, and ridges typical of the Marius Hills region occur. Two sinuous rilles cut across the main broad ridge in the area. The larger rille has a nearly circular depression at its head, whereas the smaller rille (shown in detail on page 118) originates at an elongated spear head. Two distinct varieties of domes are discernible. These are the gently rising smooth low domes, and the rugged, heavily cratered, steep-sided domes. Location: 14° N, 56° W. Framelet width: 12 kilometers.

THE MOON'S FARSIDE

The lunar farside is markedly different from the frontside hemisphere in that it has fewer very large basins and virtually no maria comparable in the extent of fill to those on the frontside. Mare Orientale, the largest of all circular features on the farside, is only partially filled with mare material. Mare Moscoviense is comparable to Mare Nectaris, one of the smaller frontside circular maria. Although the floors of a few individual craters, most notably Tsiolkovsky, are substantially covered with smooth, dark mare material, the predominant impression is of the scarcity of such material. In this respect much of the farside could be compared in gross morphology to the frontside's southern highlands. The latter region's large basins with light-toned floors, exemplified by Bailly and Clavius, have about a score of farside counterparts, most of which are larger.

The sculpture which radiates from or is concentric with Mare Orientale dominates the eastern part of the lunar farside; ridges and furrows extend radially over 1000 kilometers from this multiringed circular basin, while secondary craters, believed to have originated from Orientale ejecta, overlie older features on much of the eastern farside.

As is the case in the southern highlands on the Moon's frontside, the structural and textural characteristics of the farside are complex. This is largely due to the existence of countless craters of various ages and sizes, each modified by younger ones. It should be remembered, too, that all of our information about farside features is the product of spacecraft photography accomplished within the last 10 years. Undoubtedly, it will take many years of study to decipher the nature and unravel the history of the surface of the lunar farside.

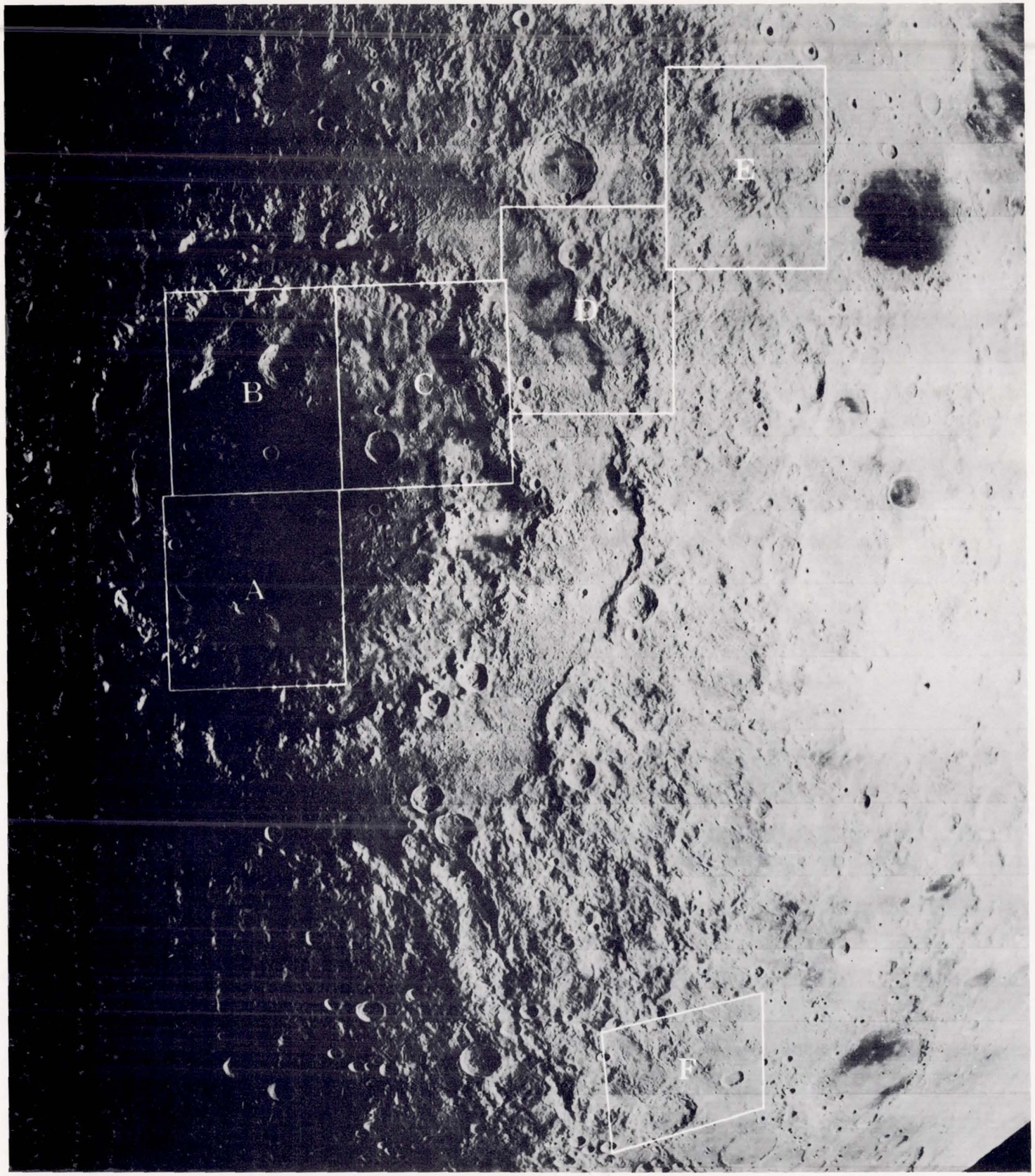

The central portion of the spectacular Mare Orientale photograph on page 19. The areas outlined in white are covered in greater detail on the following pages. They constitute a section across the complete triple-ringed basin and the deposits of ejected material beyond the outermost ring.

Mare Orientale ("eastern sea") was named at a time when the left side of the visible face was considered the eastern side. By the recently adopted convention followed throughout this book, Mare Orientale is located at the extreme western edge. A new name, Mare Annulatum, has been proposed for this basin.

Three concentric circular scarps ring the inner basin. The outermost and best developed, the Cordillera Mountains scarp, is almost 900 kilometers in diameter. The Cordillera and the Rook Mountains, which form the middle ring, are among the highest mountain chains on the Moon. Each rises to heights more than 3 kilometers above the adjacent terrain. The innermost ring is less continuous and not as high.

The inner basin is nearly (but not completely) filled with dark material such as is characteristic of mare areas. The unfilled portions, which retain the features of the original basin floor, provide important new data on the likely early configuration of other, older, large basins. Surrounding the basin center to distances up to 1000 kilometers is a coarsely braided blanket of material that clearly covers an older, cratered, terra surface. The beautifully preserved textures on this surface, and the sharpness of the mountain rings (both clearly shown on the following pages) lead to the conclusion that Mare Orientale is the youngest of the Moon's large circular basins.

The mare-filled crater Grimaldi, a dark, nearly circular patch near the upper right corner of the photograph, is beyond the blanket of material ejected from Mare Orientale. It is 220 kilometers across. The center of the photograph is located about 21° S, 85° W. Framelet width: 90 kilometers.

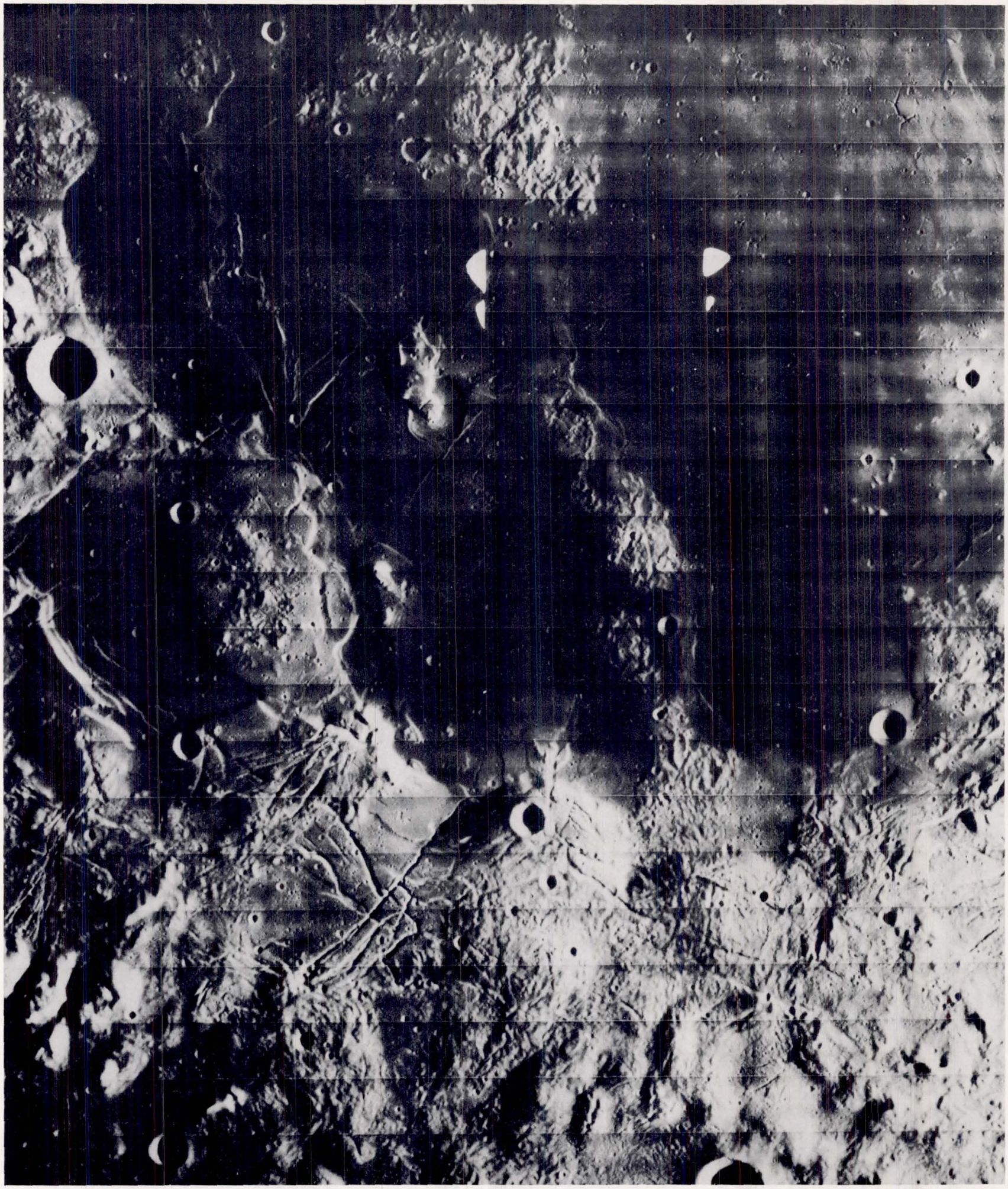

The mare filling of the inner Orientale basin (area A of the preceding photograph) may be quite shallow, as suggested by the numerous "islands" of older material that project through it. A number of steep-sided domes and ridges of complicated form are present. The circular, rectilinear, and irregular depressions (left) probably are collapse structures, formed under control of subsurface structures which also controlled the complex pattern of rilles and wrinkle ridges. All these structures formed some time after the flooding of the central depression. Location: 24°S, 96°W. Framelet width: 12 kilometers.

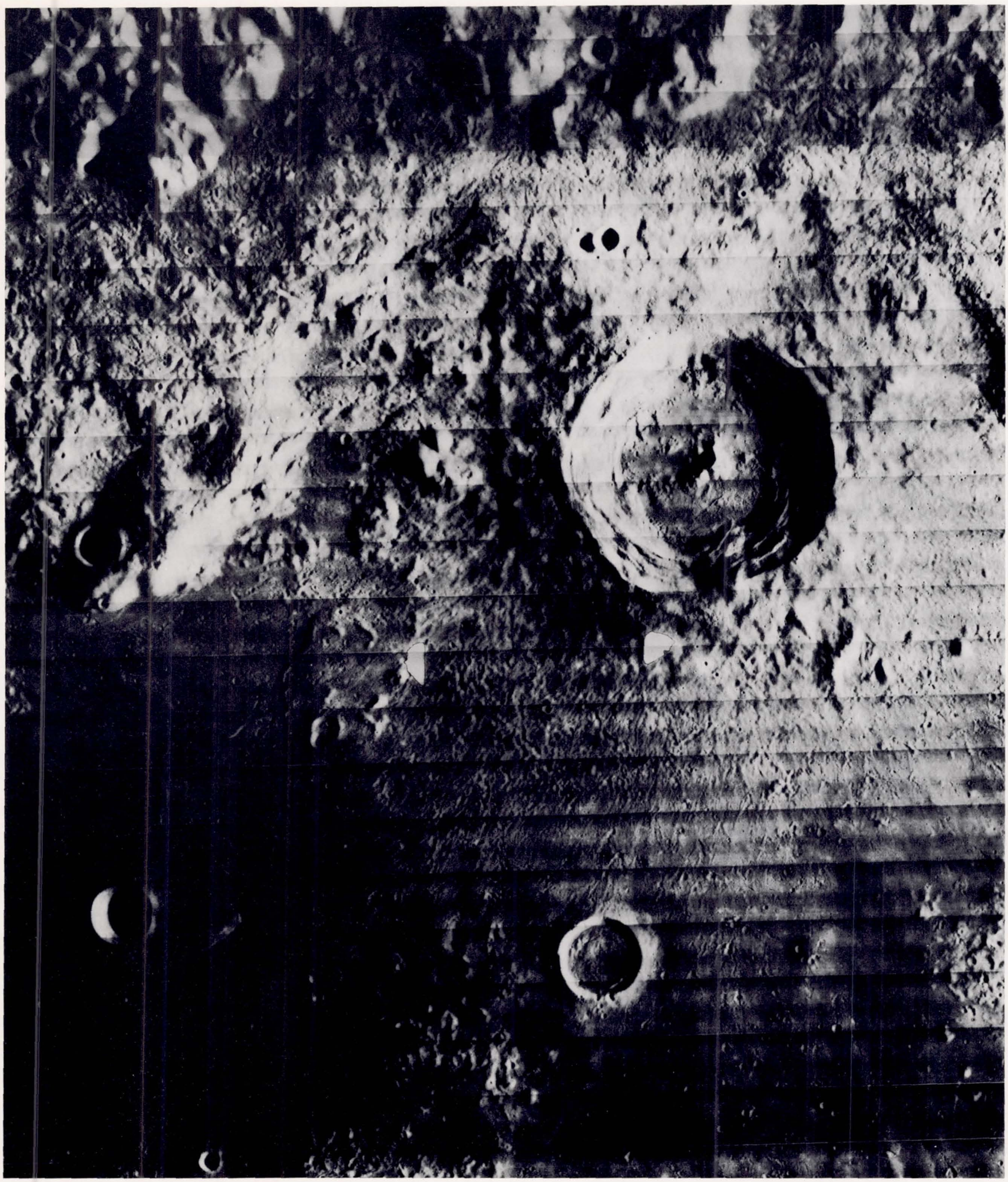

This large (55 kilometers in diameter), unnamed, young crater is at the northern edge of the inner Mare Orientale basin (area B). It shows well-developed interior terraces and a rough, high, inner rim which grades outward to radial braids. The abundant secondary craters and light-toned rays radiating from the crater are seen most clearly where they cover the dark mare floor material to the south. Smooth-textured blocks which form the innermost Mare Orientale basin scarp are visible along the upper edge of the photograph. Location: 16°S, 96°W. Framelet width: 12 kilometers.

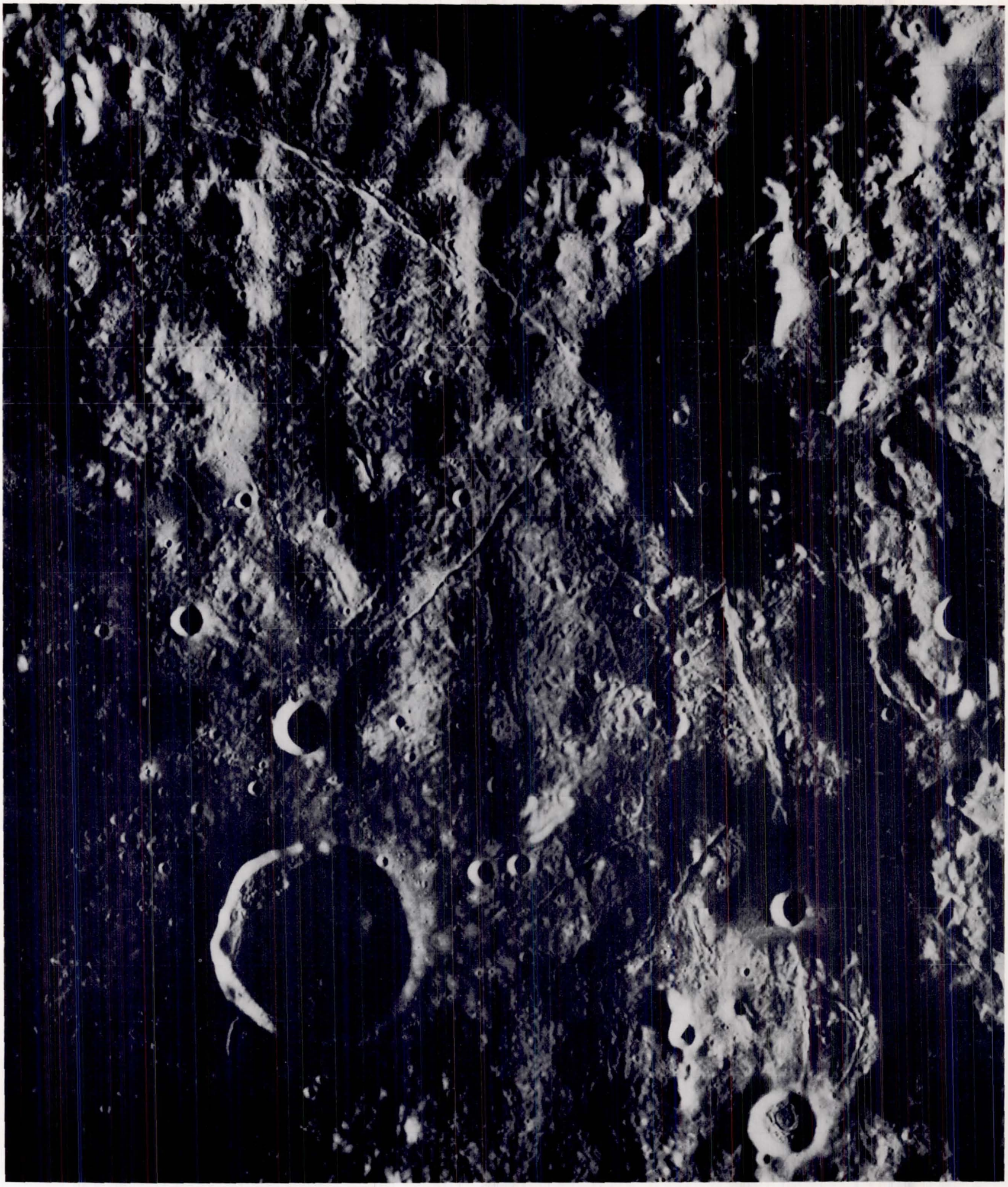

The band of smooth, dark material running across the right side of this view (area C) is part of Mare Veris, which occupies the low terrain at the foot of the Rook Mountain scarp. The rolling terrain to its left is part of the basin's innermost ring. The nearly continuous arcuate rille that runs diagonally across the photograph is concentric with the basin structure. The large, smooth-rimmed, largely flooded crater (lower left) is about 35 kilometers across. Its peculiar morphological characteristics (shown in more detail on page 72) suggest a volcanic origin. Location: 16° S, 90° W. Framelet width: 12 kilometers.

The Cordillera Mountain scarp, which is the outermost ring of the Orientale basin, crosses this view (area D) from the northwest to the southeast. It separates two distinct textural patterns: 1) an inner zone of small, closely spaced, low hills with isolated patches of mare material, and 2) an outer zone of coarsely braided material whose grooves and ridges are radial to the Mare Orientale basin. The large, smooth-textured, partly rectilinear blocks in the lower left corner are part of the Rook Mountains (the middle one of the basin's three rings). Location: 11°S, 84°W. Framelet width: 12 kilometers.

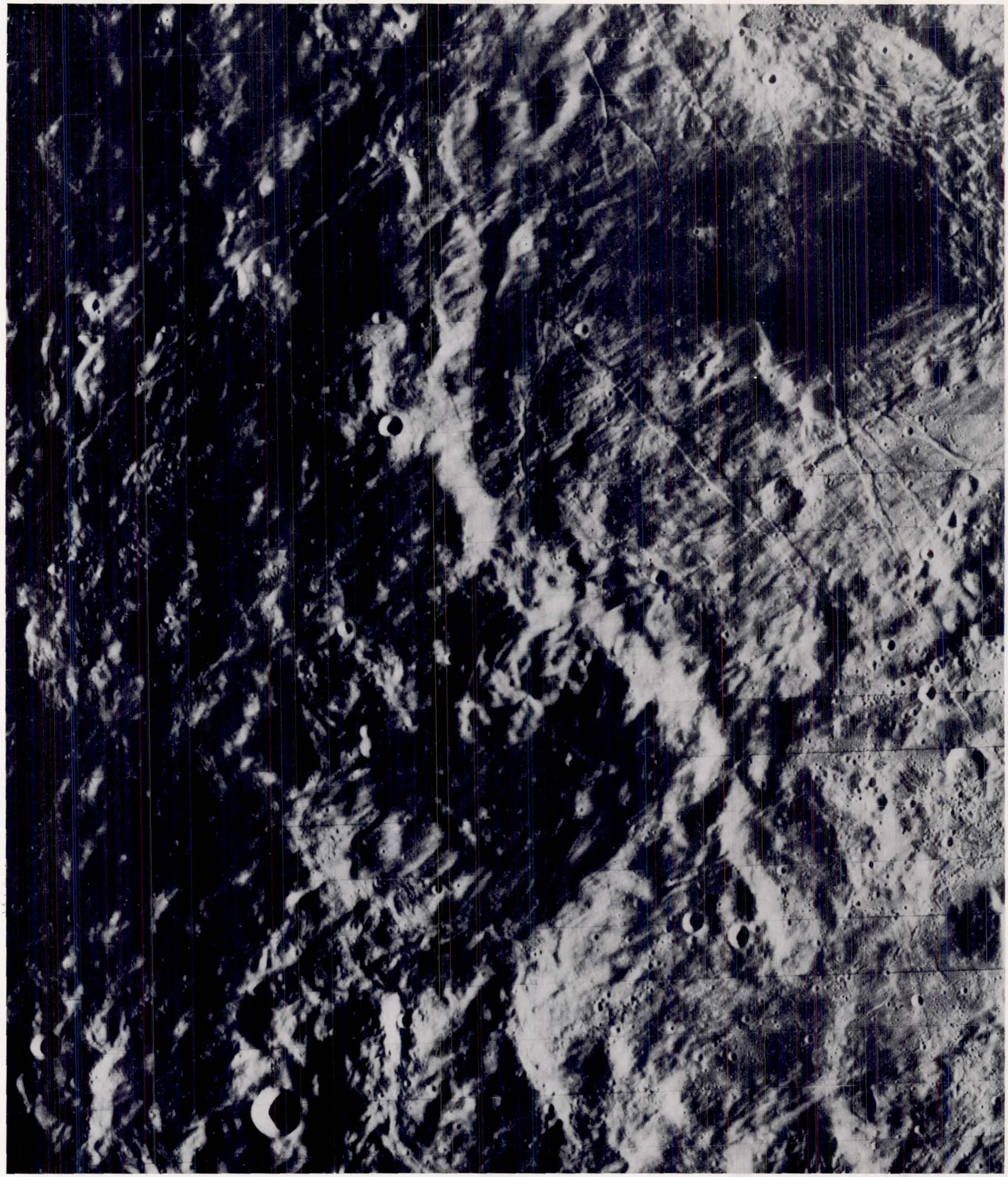

The 150-kilometer crater Riccioli, occupying the upper right quarter of this view (area E), is about 750 kilometers northeast of the center of Mare Orientale. It lies within the coarsely braided blanket which mantles older topographic features all around the Orientale basin. Textural characteristics of the blanket and the dunelike deposits at the base of Riccioli's far wall suggest that the material was probably transported outward from the basin's center by a base surge of a type observed in manmade nuclear and high-explosive cratering experiments. Location: 5°S, 76°W. Framelet width: 12 kilometers.

This view (area F) includes the edge of the base surge and ejecta blanket, about 1100 kilometers southeast of the center of Mare Orientale. Coarsely braided material thickly mantles earlier craters to the upper left, whereas the smoother area to the lower right is very thinly covered. Only part of the crater Inghirami (lower left, 90 kilometers across) is mantled with braided material; its southeast wall is not. The trough (upper left) shows evidence of differential surface flowage, as indicated by the shear or drag pattern along its western edge. Location: 45°S, 68°W. Framelet width: 13 kilometers.

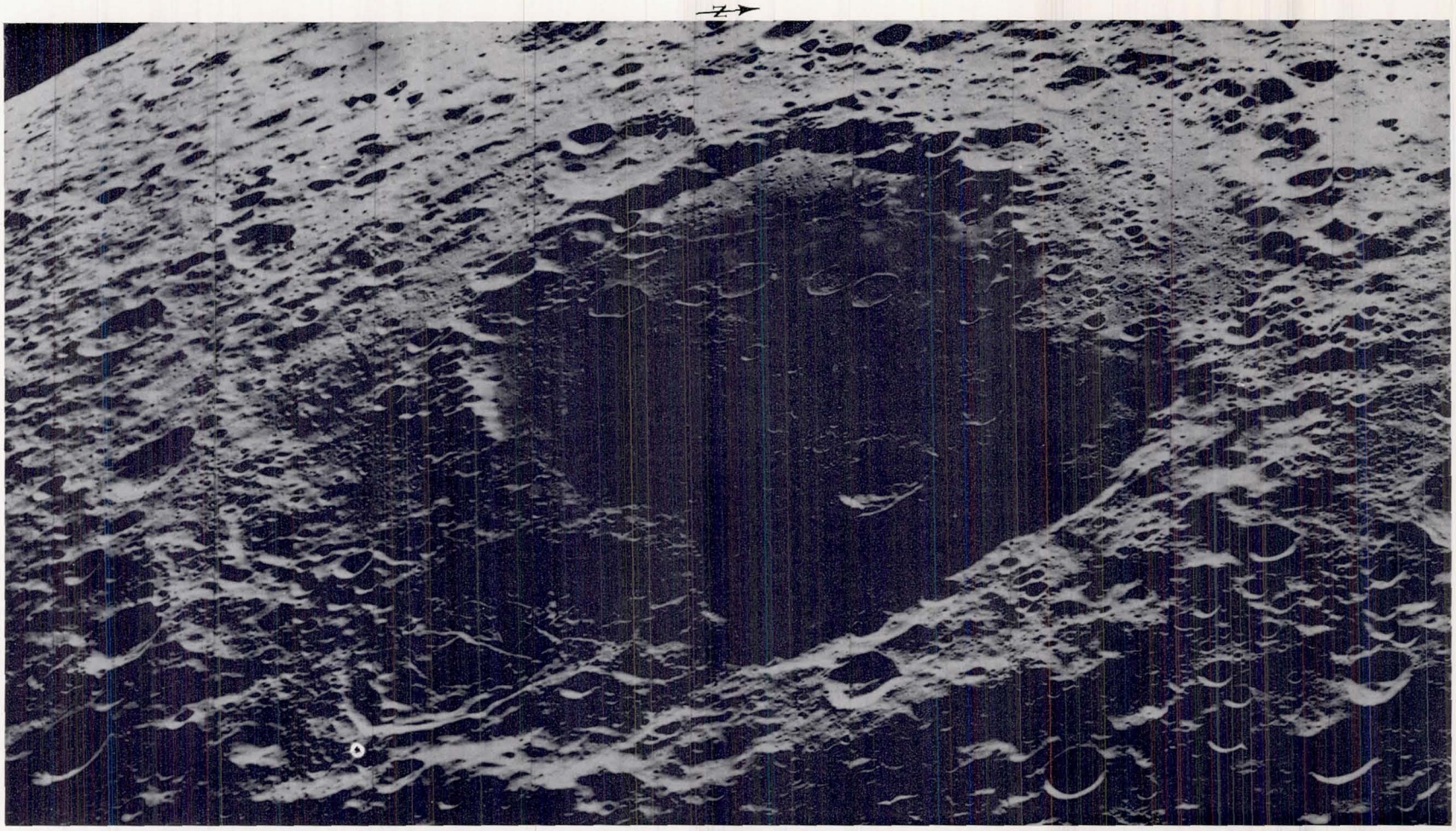

This Lunar Orbiter V photograph is an oblique view, looking westward, of Mare Moscoviense on the Moon's farside. Mare Moscoviense was named in honor of the city of Moscow by Soviet scientists when it was first photographed by Luna III. It is about 350 kilometers across and is similar in appearance to some frontside maria. Approximate location: 25°N, 145°E.

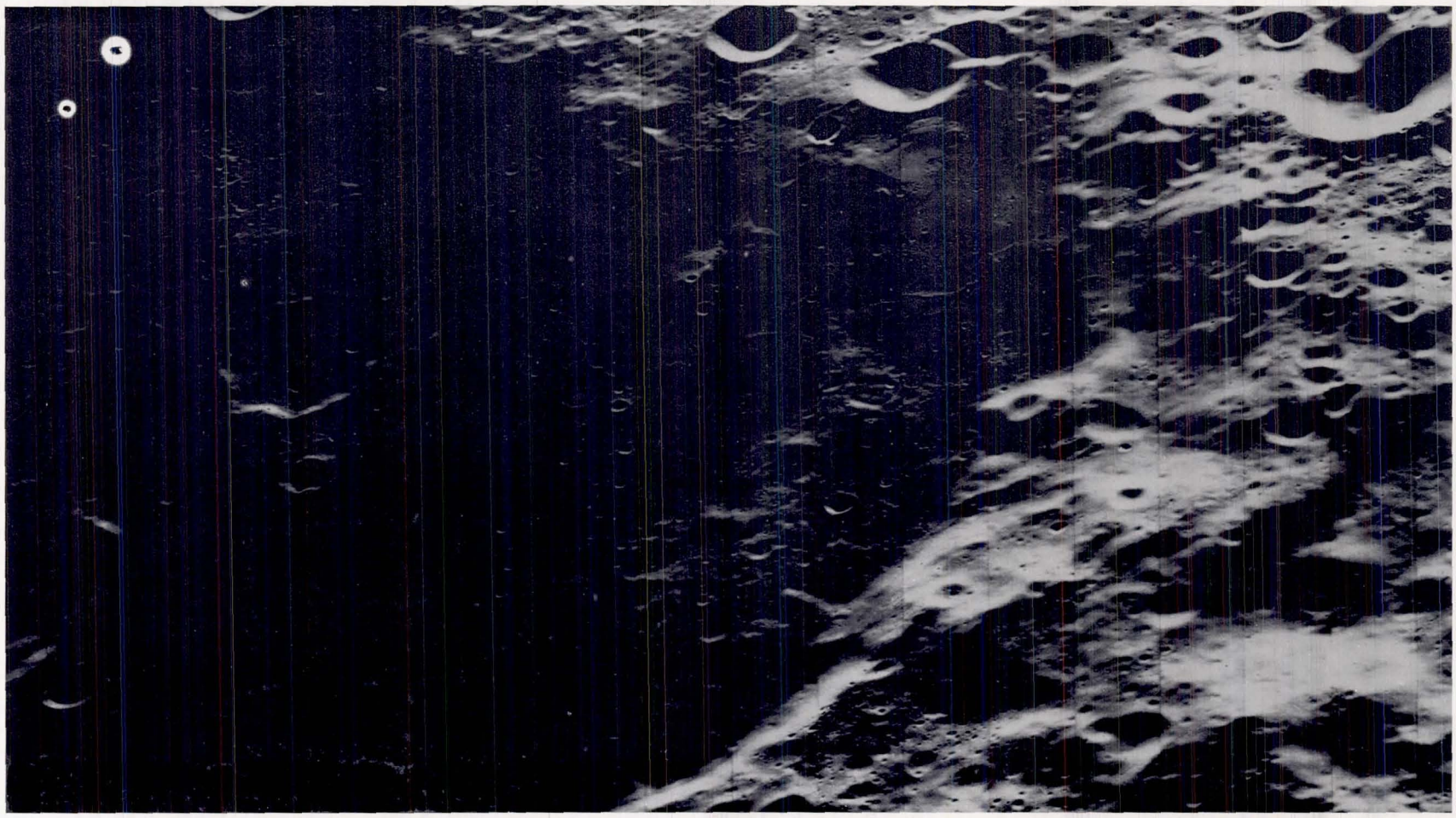

A telephoto view westward over the northern portion of Mare Moscoviense. In this area the dark mare material fills the floor to the basin's rim; to the west (top center) it does not. The floor is peppered with craters of various shapes and sizes, and with the "ghosts" of more or less completely filled craters. Located about 30°N, 148°E. Framelet width: about 6 kilometers.

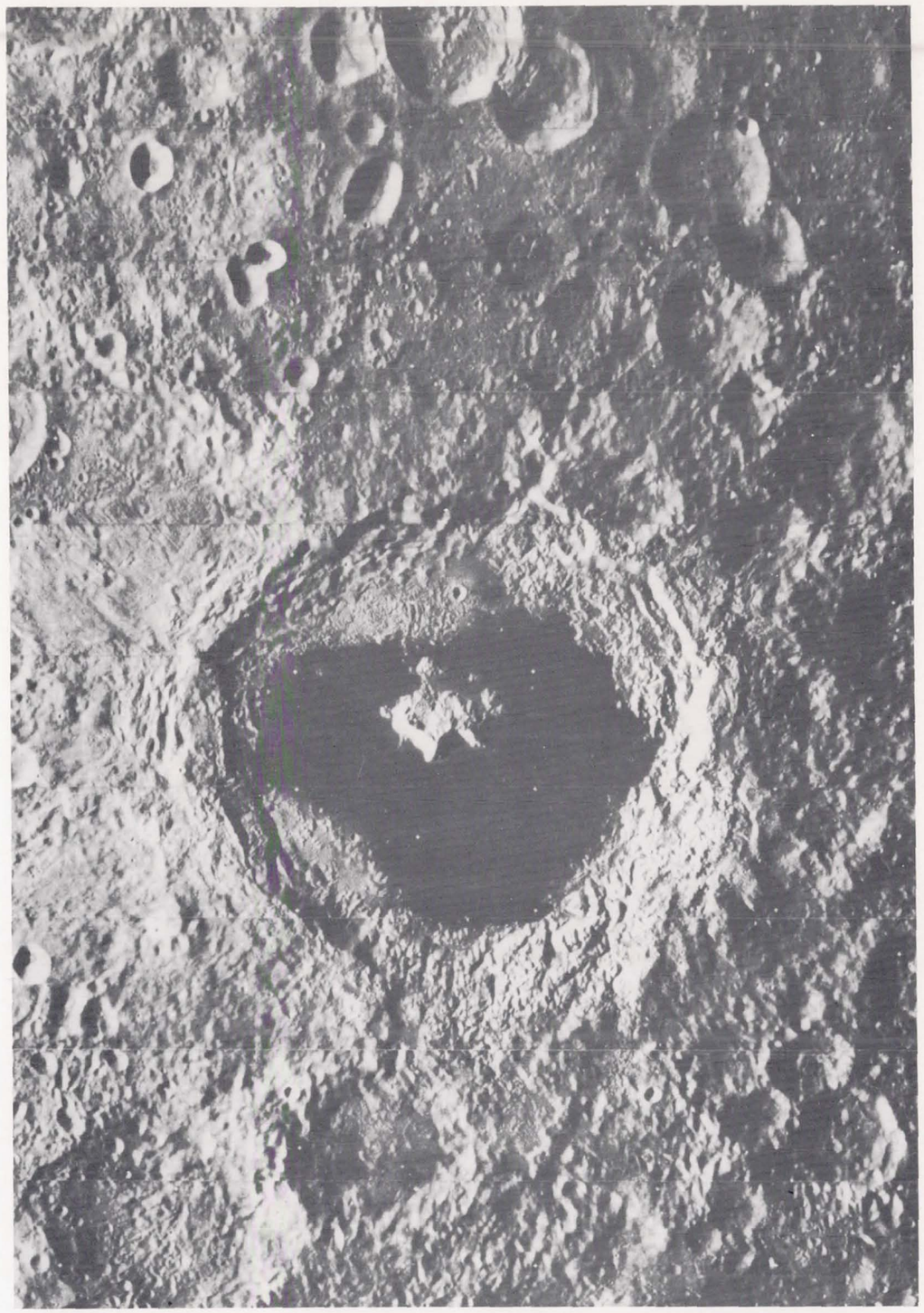

The large crater in the middle of this Lunar Orbiter III photograph of the Moon's farside is Tsiolkovsky, which measures about 200 kilometers in diameter. Its floor is partially filled with smooth, very dark mare material, through which protrudes a prominent central peak. The area of pronounced radial sculpture seen in detail in the photograph to the right lies just northwest of the crater's rim. Approximate location: 20°S, 129°E. Framelet width: 55 kilometers.

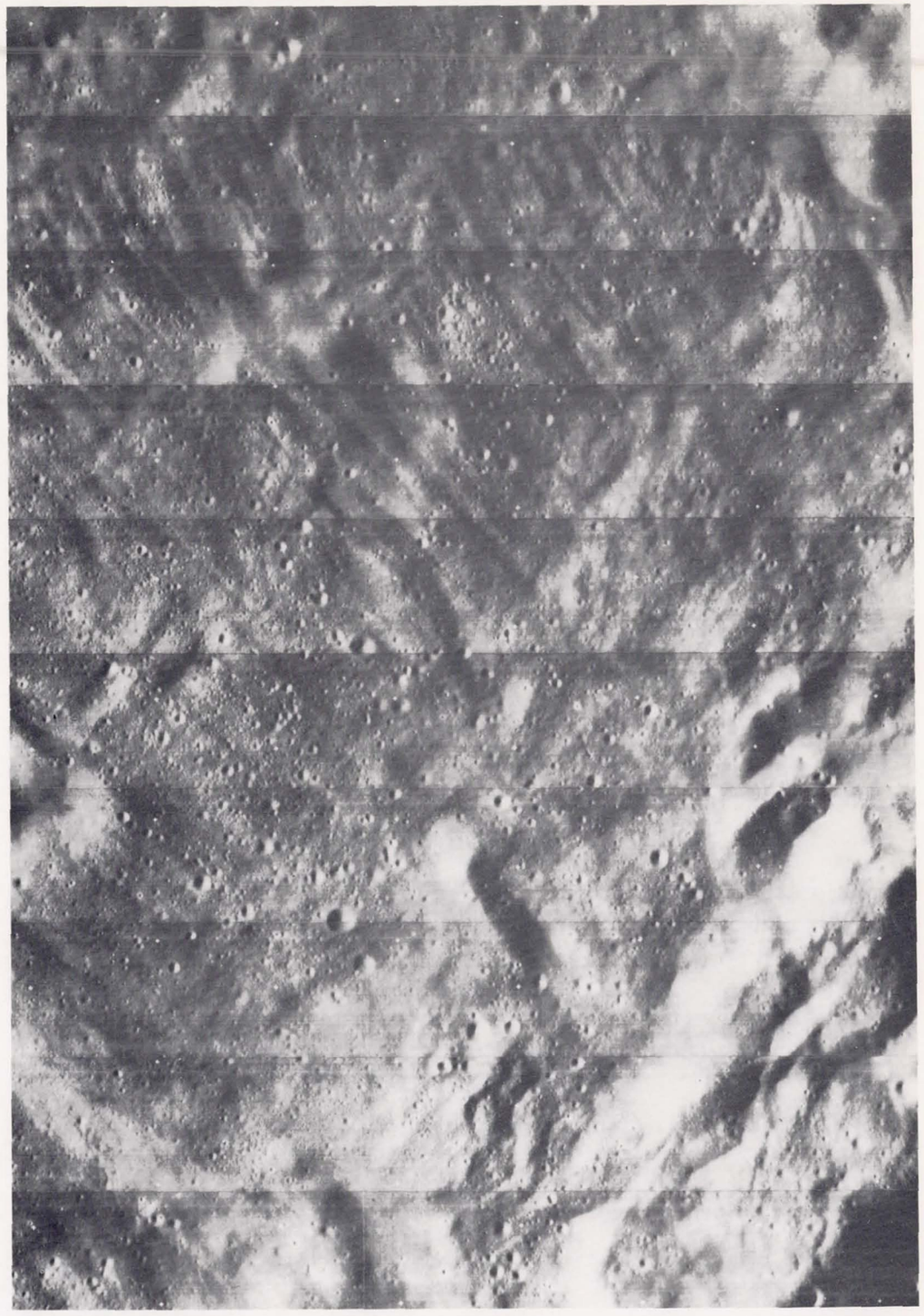

The rugged ridge in the lower right corner of this telephoto view is part of the northwestern rim crest of the crater Tsiolkovsky. The diagonal banding which gives the remainder of the photograph its characteristic swept appearance is the surface sculpture of a mass of material that may have been formed by an enormous downslope movement comparable in magnitude to a terrestrial avalanche. Framelet width: 7 kilometers.

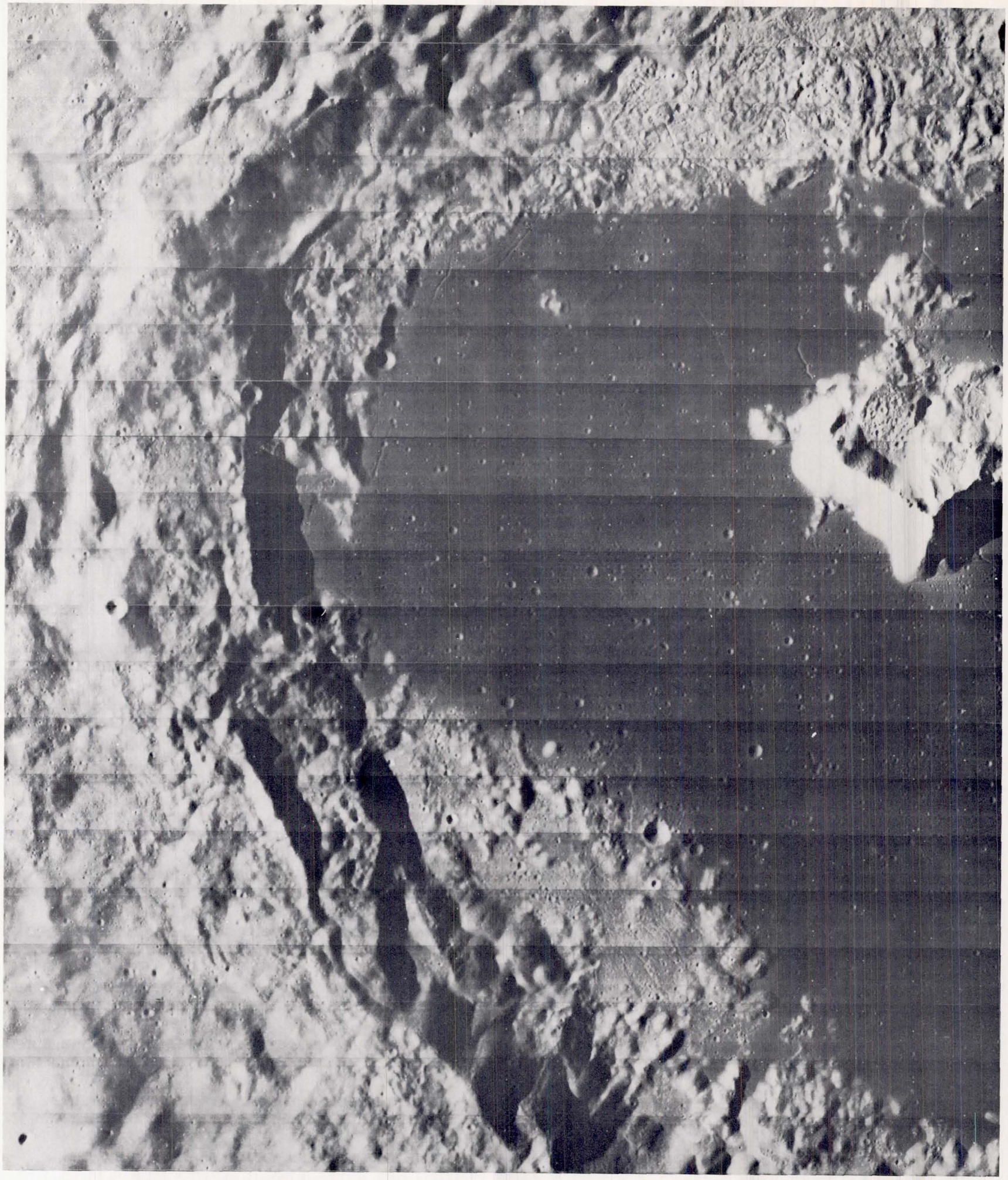

Telephoto view of the western half of the crater Tsiolkovsky, named in honor of the Russian pioneer student of space travel. The rim crest is conspicuously crenelated, and the inner rim slope is terraced. Much of the floor has been flooded by a dark material whose freshness is indicated by the absence of sizable craters and the sparse distribution of small ones. The unflooded areas of the crater floor are exceedingly rough on a fine scale. The bright mass of rock (center right) is a central peak on the crater floor, a feature common to many large lunar craters. Framelet width: 7 kilometers.

The events which produced the fresh-appearing crater (center left) deposited the ejected material in a radial pattern. The braided texture surrounding the crater (best seen extending to the southeast) resembles the "base surge" deposits observed around manmade nuclear craters. The chain of secondary craters extending to the northeast in a striking herringbone pattern was formed by material ejected in ballistic trajectories. Approximate location: 11°S, 163°W. Framelet width: 5.5 kilometers.

Telephoto view of a pair of farside craters having similar characteristics. Both are rather shallow and have fractured floors which appear to have been shaped by internal forces. The fracturing of the smaller crater is in a prominent polygonal pattern of rilles resembling an alligator hide. That of the larger crater is more subdued and roughly parallel to the margin of the floor. Approximate location: 5°S, 146°E. Framelet width: 6 kilometers.

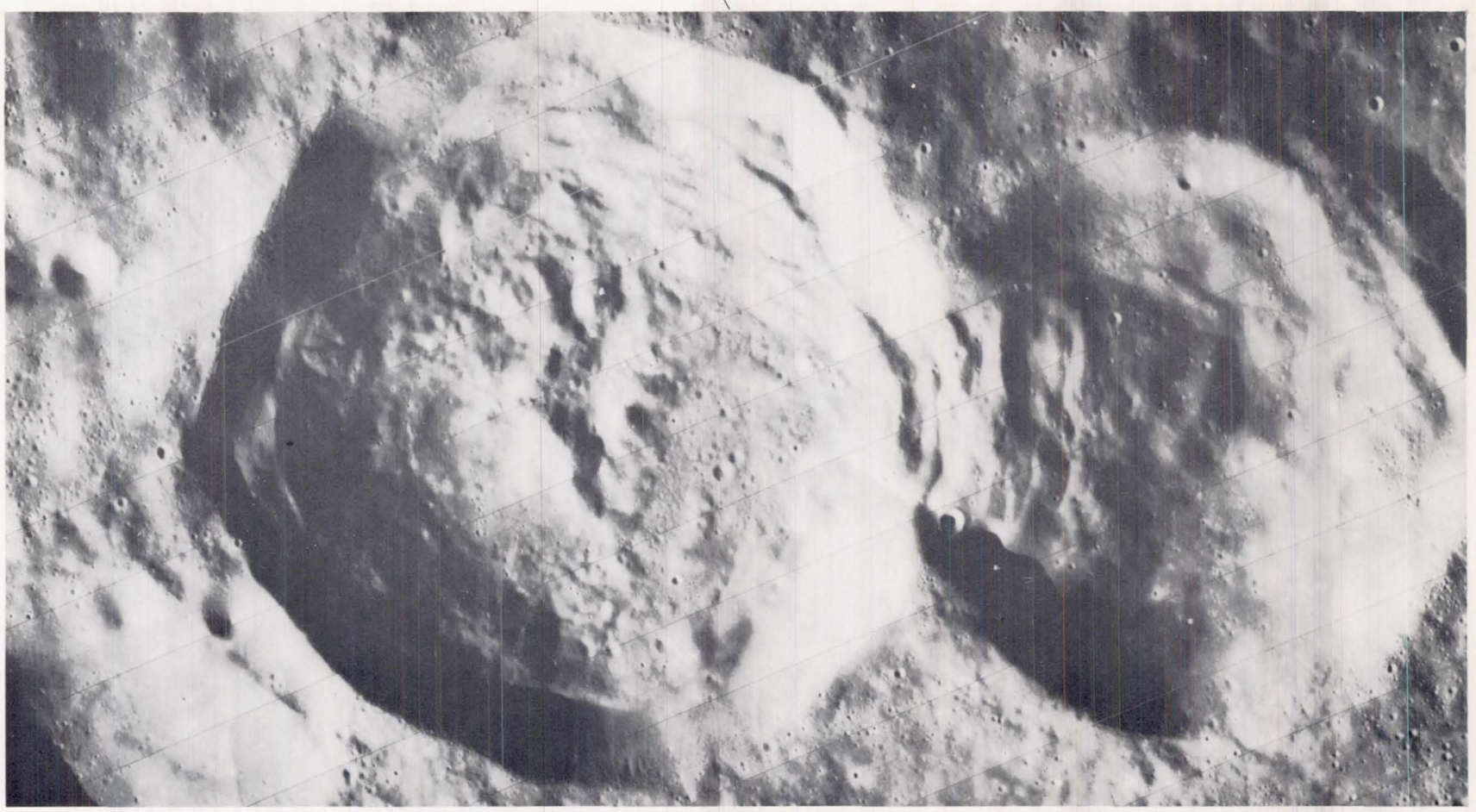

A pair of craters located about 270 kilometers due north of the farside crater Tsiolkovsky (page 133). It is evident that the two craters are of different ages, as formation of the larger crater forced a great mass of material to move into the smaller, older crater, partially filling it by what appear now to be a number of landslides. Framelet width: 6 kilometers.

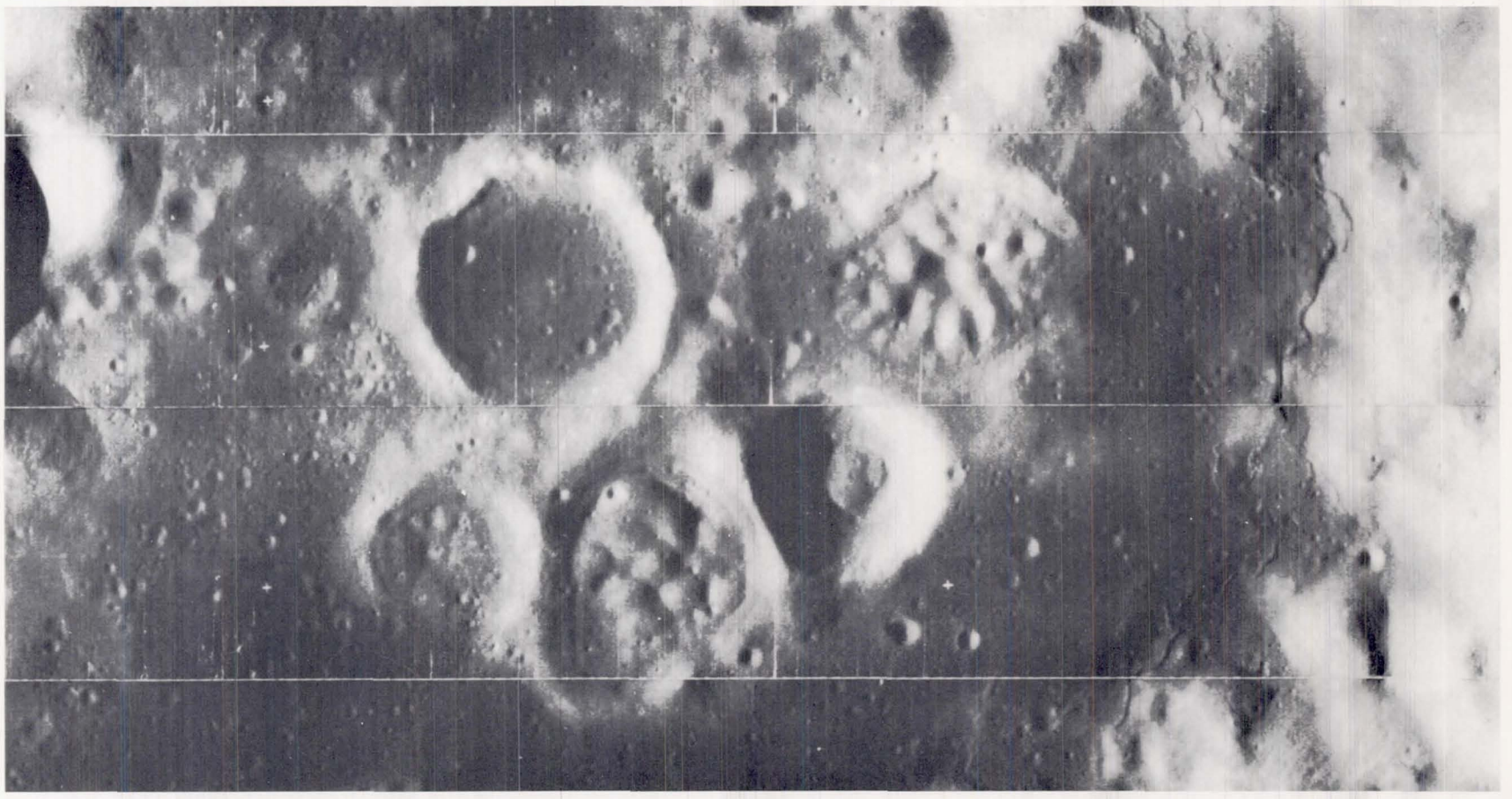

A crater cluster located within a large unnamed farside crater (seen on page 25). These craters are all of similar size, yet quite different depths, with two shallow ones displaying remarkable bulbous floors that appear to have formed as volcanic hills and domes. Lunar Orbiter photography has shown a number of similar craters on the frontside. The many small arcuate scarps (right) bounding the dark floor of the large crater face away from the floor. These may represent the fronts of successive flows on the crater floor. Approximate location: 17° S, 174° E. Framelet width: 6.3 kilometers.

APPENDIX

STEREOSCOPIC VIEWS

The photographs appearing on the next four pages are called anaglyphs. Each anaglyph comprises the duplicated portions of two overlapping medium-resolution frames. The two frames are printed in complementary colors, so that when the anaglyph is viewed through the colored spectacles (found in the envelope inside the book's back cover) each eye sees the image of a different frame. The spectacles should be held so that the red filter is over the left eye. This permits the reader to examine the photographs stereoscopically.

The areas covered by the four stereoscopic views are also shown monoscopically elsewhere in the book, as indicated in their captions. It will be noted that, whereas the monoscopic views are oriented so that north is at the top, all the anaglyphs are oriented with east at the top. The reason for this reorientation is that they are all Lunar Orbiter V photographs. Because the fifth mission was conducted in a nearly polar orbit, successive frames covering a site are separated in a north-south direction. Stereoscopic vision requires that the separation between successive camera locations be parallel to the imaginary line connecting the viewer's eyes. If the viewer keeps in mind that the solar illumination was coming from the east (i.e., the top of the anaglyph), the impression of depth created by the shadows will be in agreement with the stereoscopic impression.

The stereoscopic impression conveyed by these anaglyphs is an exaggerated one. The slopes appear to be steeper than they are in reality. The exaggeration is less extreme on these photographs than it is on the wide-angle photographs ordinarily used in aerial mapping, but it should not be ignored.

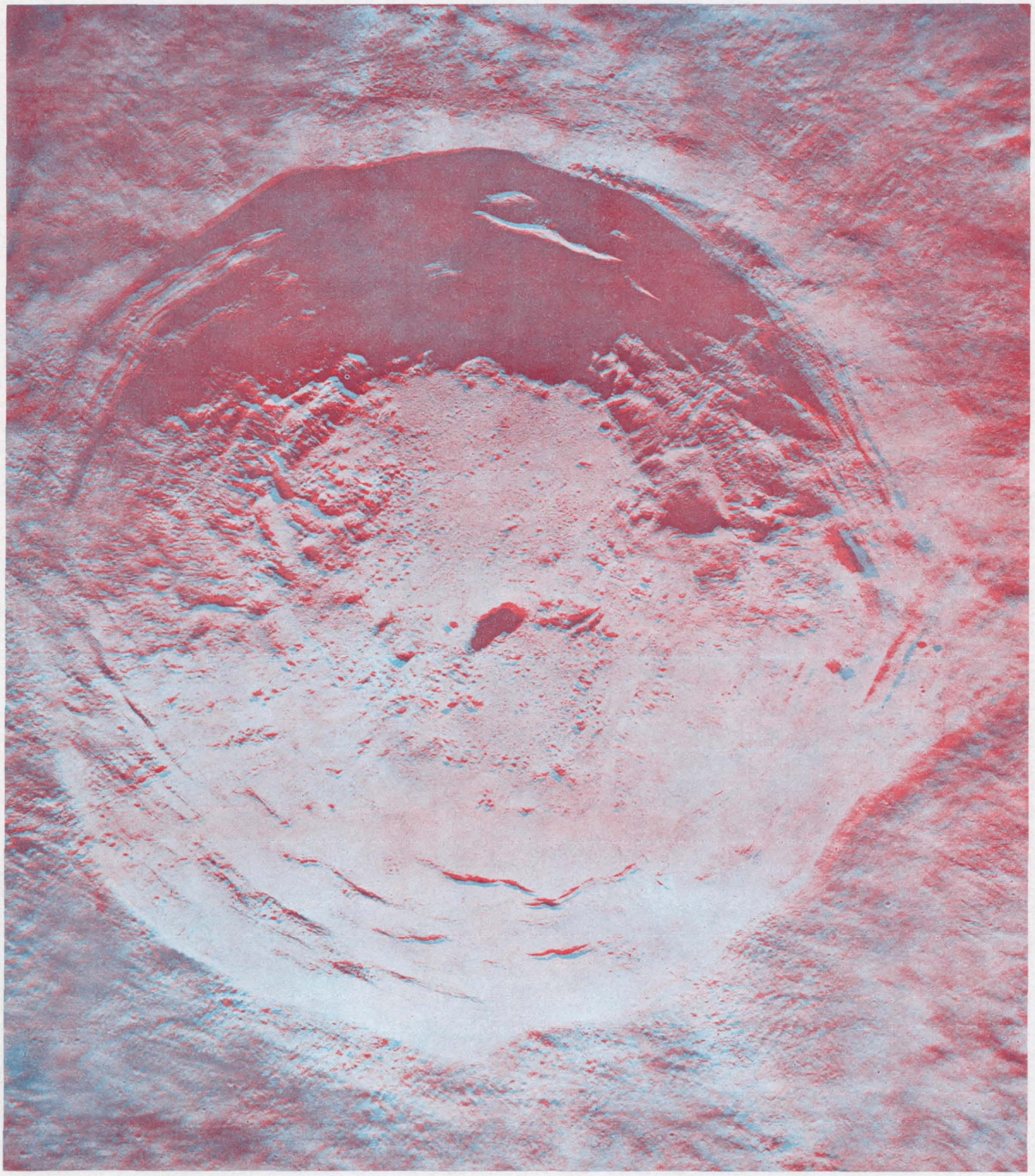

ARISTARCHUS ANAGLYPH

Stereoscopic view of the crater Aristarchus, 40 kilometers across and about 3.6 kilometers deep. The floor is partially covered with material that slumped down from the walls; its eastern portion (toward the top of the page), being least covered by this material, is the lowest and smoothest part. A long narrow central peak rises about 300 meters above the floor. Note the terracing of the inner crater walls and also the elevation of the rim crest above the outer ejecta blanket. See also page 75.

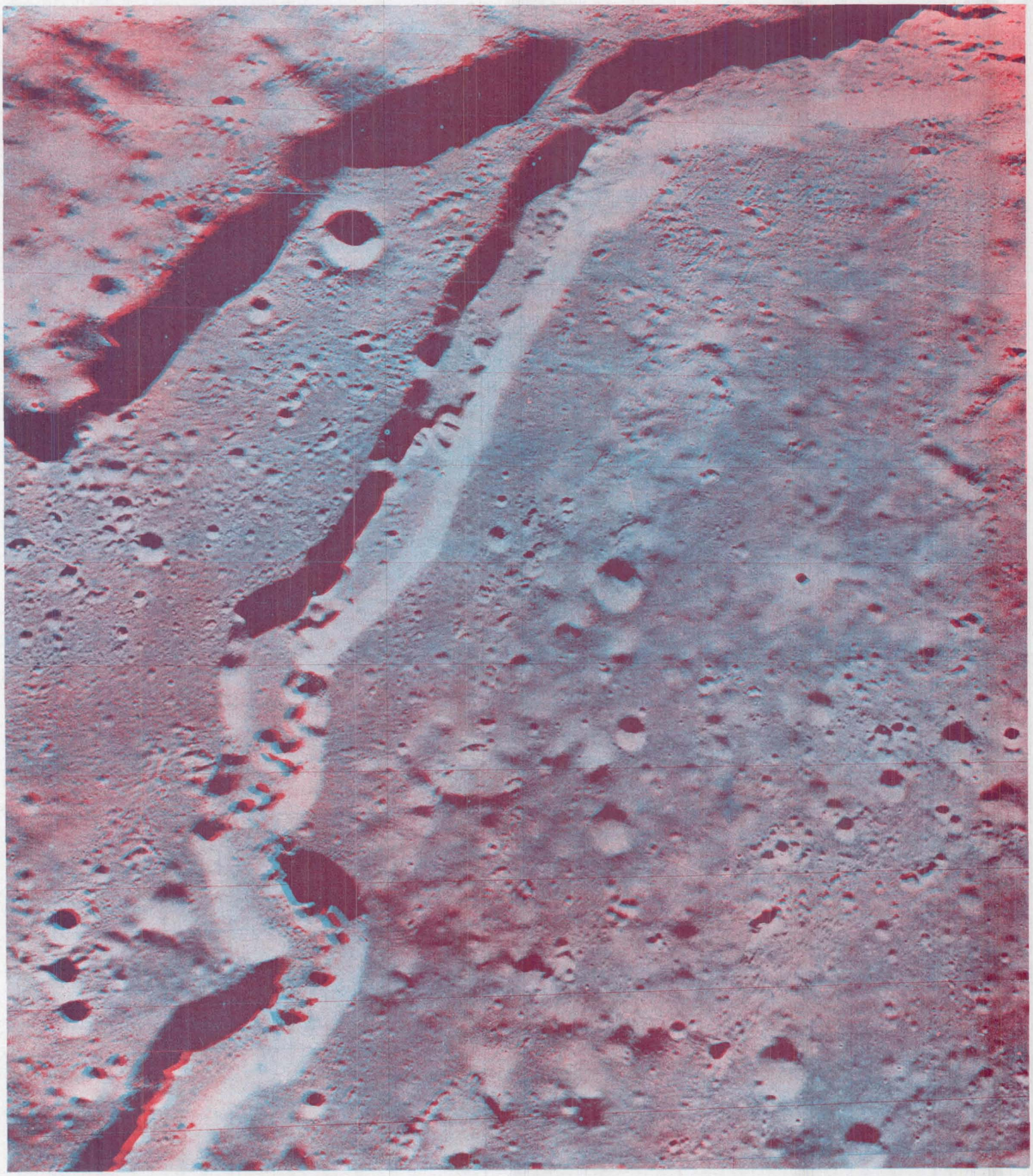

SCHRÖTERS VALLEY ANAGLYPH

Stereoscopic view of a part of Schröter's Valley, the meandering depression running from the upper right to the lower left corner of the anaglyph. This rille is about 7 kilometers wide and up to 1300 meters deep. Within its flat floor is a second, sinuous rille whose tightly packed meander loops are about 200 meters deeper. The ridge that is seen in the upper left portion of the photograph is about 1600 meters higher than the plateau surface into which the valley is cut. See also page 113.

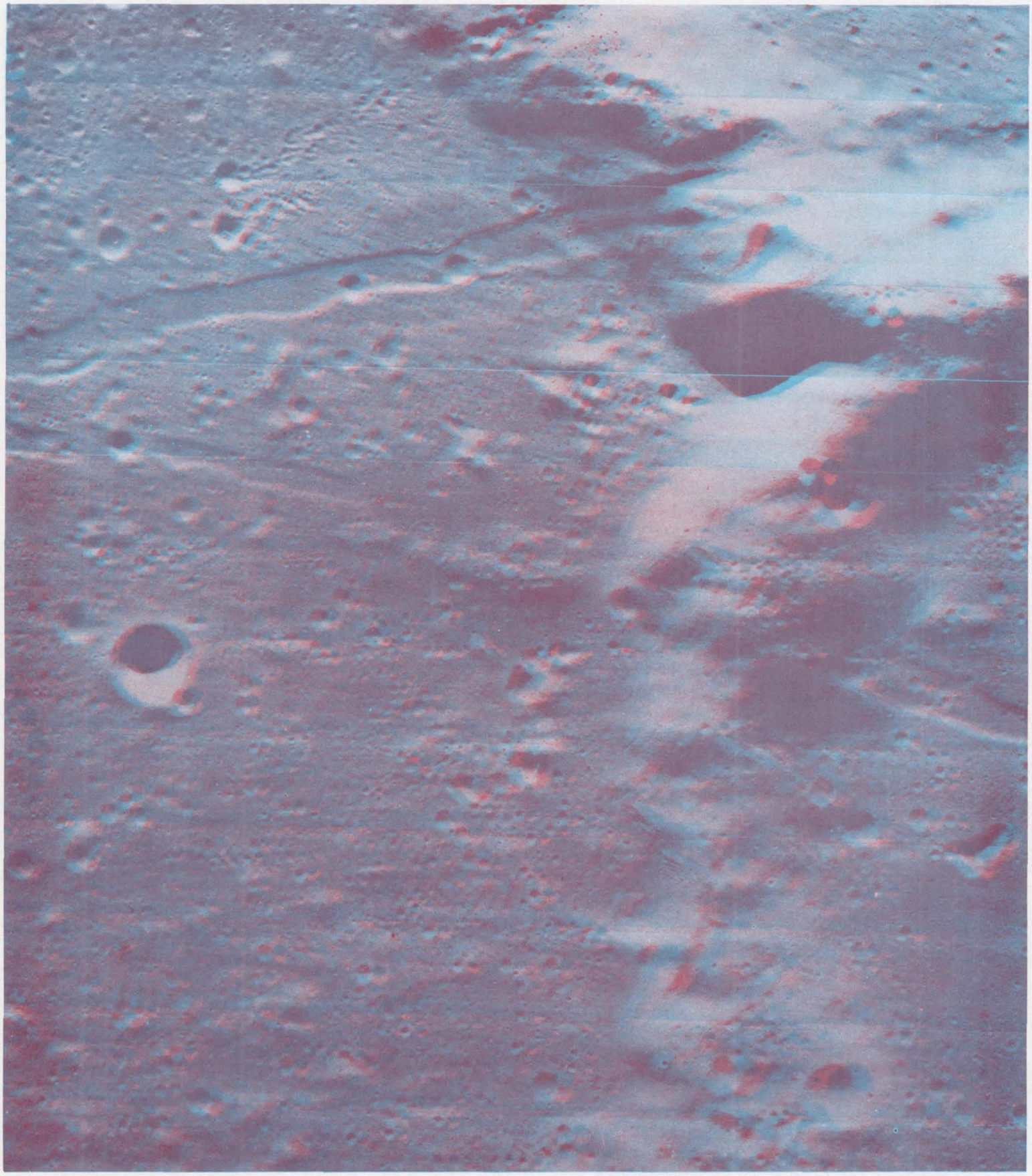

RIMAE PARRY ANAGLYPH

Stereoscopic view of three adjoining craters: Fra Mauro to the north (left), Parry (upper right), and Bonpland (lower right). The area where the three rims meet is about 1200 meters higher than the crater floors. The two linear rilles form a V whose apex is at the left edge of the photograph. They dissect the crater floors and rims alike. The more westerly rille is bordered on the west (near the center of the anaglyph) by a chain of low domes. The adjacent area of the rille is nearly filled with dark, smooth material that appears to have come from the domes. See also page 108.

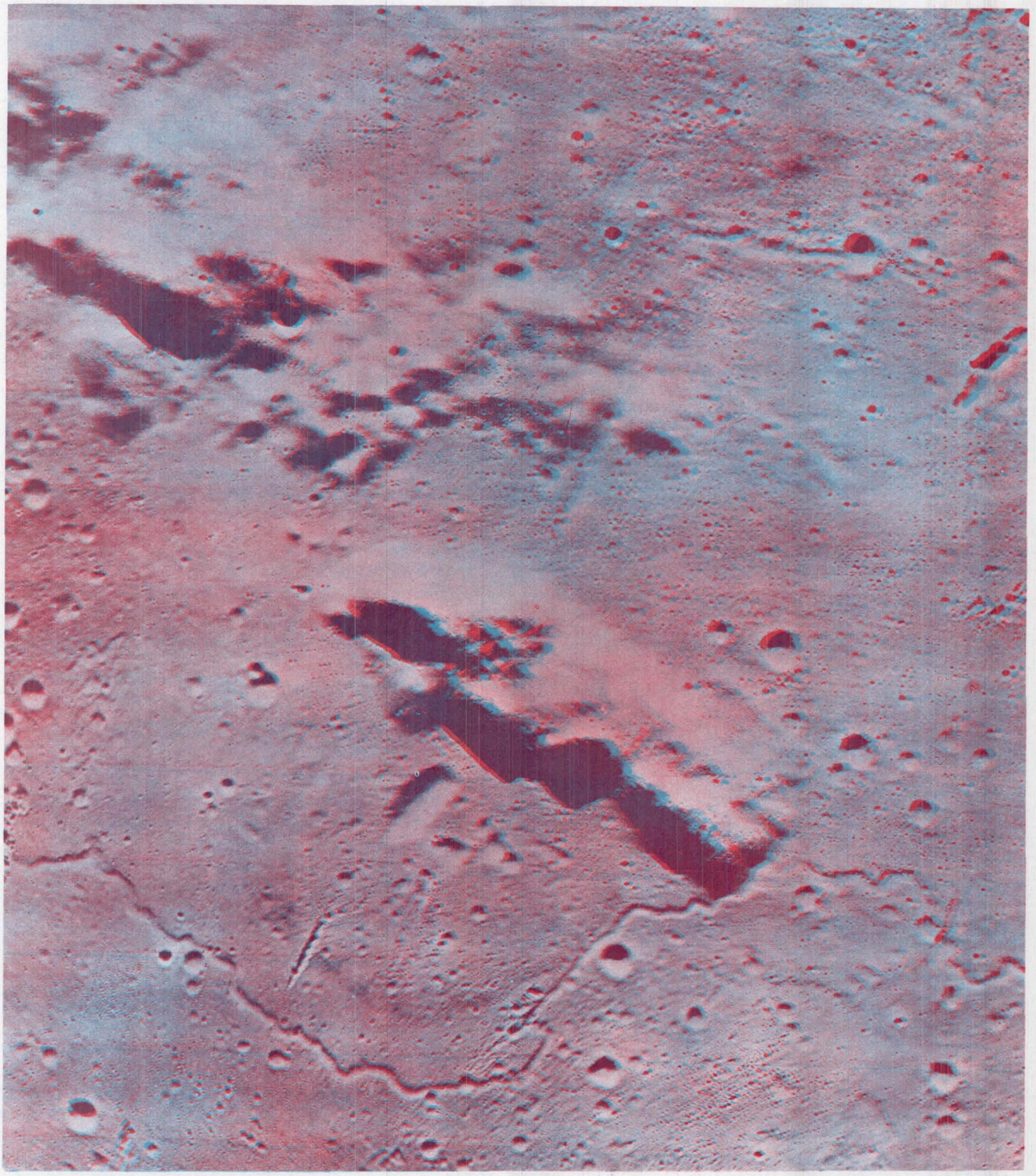

TOBIAS MAYER DOME ANAGLYPH

Stereoscopic view of an area southwest of the crater Tobias Mayer in Oceanus Procellarum. The highland ridge in the middle portion of the anaglyph is about 35 kilometers long and 2 kilometers high. A smooth mare dome abuts the western flank of the ridge. The dome is about 20 kilometers in diameter and exhibits an elongate summit crater, about 5 kilometers long. A sinuous rille meanders across the lower part of the photograph, detouring around the base of the dome. Note the presence of several crater chains in the lower half, and a large highland mass at upper left. See also page 120.

INDEX MAPS

Following the anaglyphs are six pages of index maps. They indicate the Lunar Orbiter photographic coverage for every portion of the Moon. Each mission's coverage has its own color, and the frame numbers are shown in the same colors. For example, the first map shows that the crater Tycho (located 43° S, 11° W) is covered by Mission IV Frame H119 and also by Mission V Frames M125 through M128. (Mission V Frames H125 through H128 fall inside the rectangle that shows the medium-resolution coverage.)

The first two index maps cover the latitude bands between 50° N and 50° S for the frontside and farside, respectively. The Apollo zone, indicated by the dashed outline on the first map, is covered by enlarged index maps on the last two pages. The polar zones are covered on the third and fourth pages.

For scientists interested in performing studies and analyses using the Lunar Orbiter photographs, the National Space Science Data Center (NSSDC) has prepared a *Data Users' Note,* "Lunar Orbiter Photographic Data" NSSDC 69-05, which presents detailed information about the availability and ordering procedures for photographic reproductions. In addition, as a further aid in ordering, the NSSDC has prepared a microfilmed catalog of all usable pictures available from the five Lunar Orbiter missions. Scientists in the United States who want to obtain Lunar Orbiter photographs for their investigations should direct their inquiries or requests to the National Space Science Data Center, Code 601.4, Goddard Space Flight Center, Greenbelt, Maryland 20771. Requests for Lunar Orbiter photographs from scientists located outside the United States should be directed to the World Data Center A for Rockets and Satellites, Code 601, Goddard Space Flight Center, Greenbelt, Maryland 20771, U.S.A. (Because of its location contiguous to the NSSDC, the World Data Center A for Rockets and Satellites can effectively assist scientists in obtaining data held in the NSSDC.)

NORTH

SOUTH

NEAR SIDE

PREPARED UNDER THE DIRECTION OF THE DEPARTMENT OF DEFENSE BY THE AERONAUTICAL CHART AND INFORMATION CENTER, UNITED STATES AIR FORCE FOR THE NATIONAL AERONAUTICS AND SPACE ADMINISTRATION.
Base Chart Compiled ACIC February 1968

AVAILABLE PHOTO COVERAGE FOR ALL ORBITER MISSIONS

Medium Resolution

High Resolution

Terminator Limit

Mission I

Mission II

Mission III

Mission V

Mission III

Mission IV

IV Oblique

Remaining area covered by Mission IV medium resolution.

Photo coverage within the Apollo Zone of Primary Interest (see dashed outline) is also shown on a separate photo index at a much larger scale.

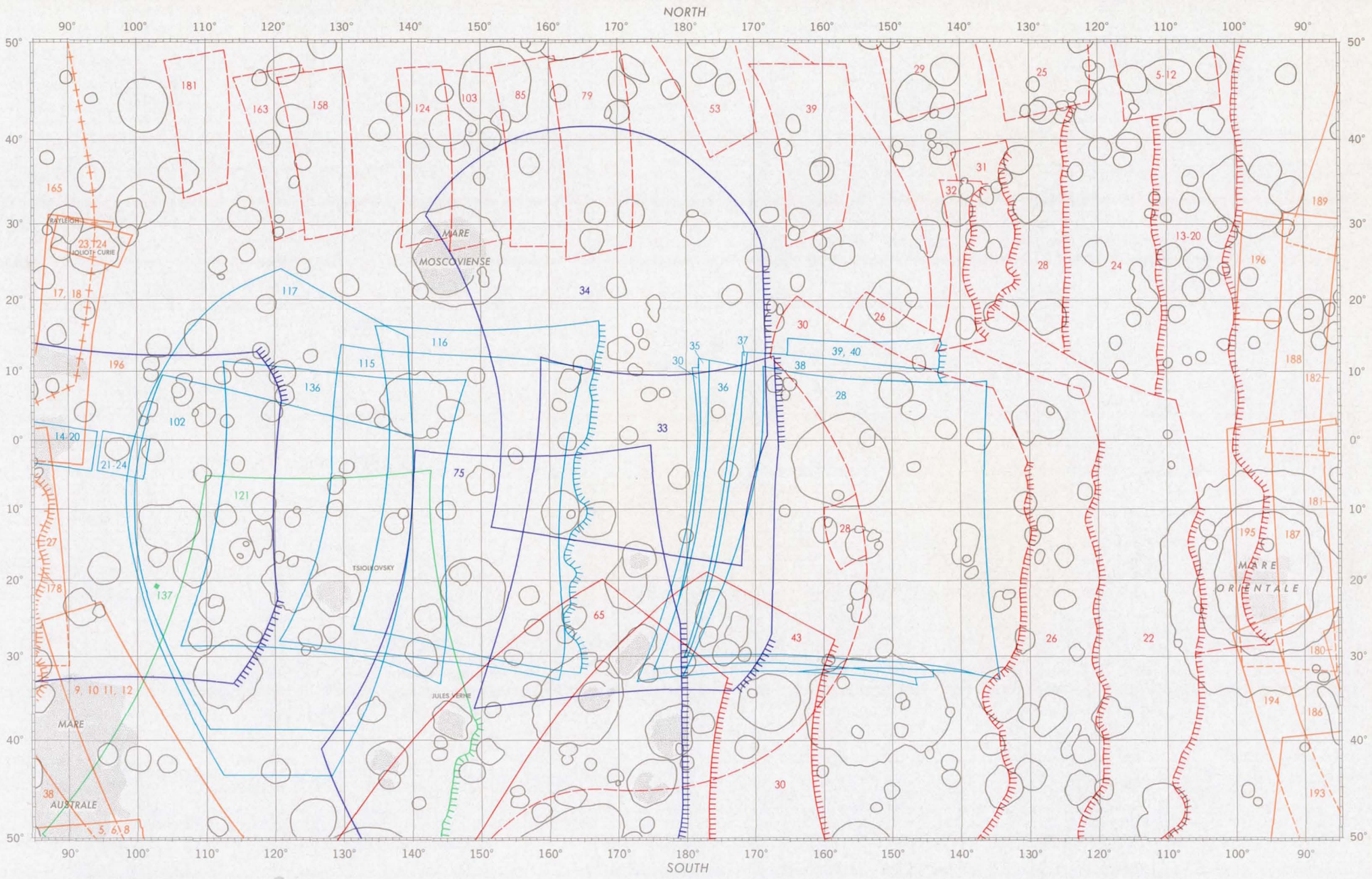

PREPARED UNDER THE DIRECTION OF THE DEPARTMENT OF DEFENSE BY THE AERONAUTICAL CHART AND INFORMATION CENTER, UNITED STATES AIR FORCE FOR THE NATIONAL AERONAUTICS AND SPACE ADMINISTRATION.
Base Chart Compiled ACIC February 1968

FAR SIDE

AVAILABLE PHOTO COVERAGE FOR ALL ORBITER MISSIONS

Medium Resolution

Mission I

Mission II

Mission III

Mission V

Mission III

Mission IV

High Resolution

Mission V

IV Oblique

Terminator Limit

Remaining area covered by Missions IV & V medium resolution.

APOLLO ZONE OF PRIMARY INTEREST

Available Photo Coverage For All Missions Except IV.

Medium Resolution

Mission I ☐ Mission III ☐

Mission II ☐ Mission V ☐

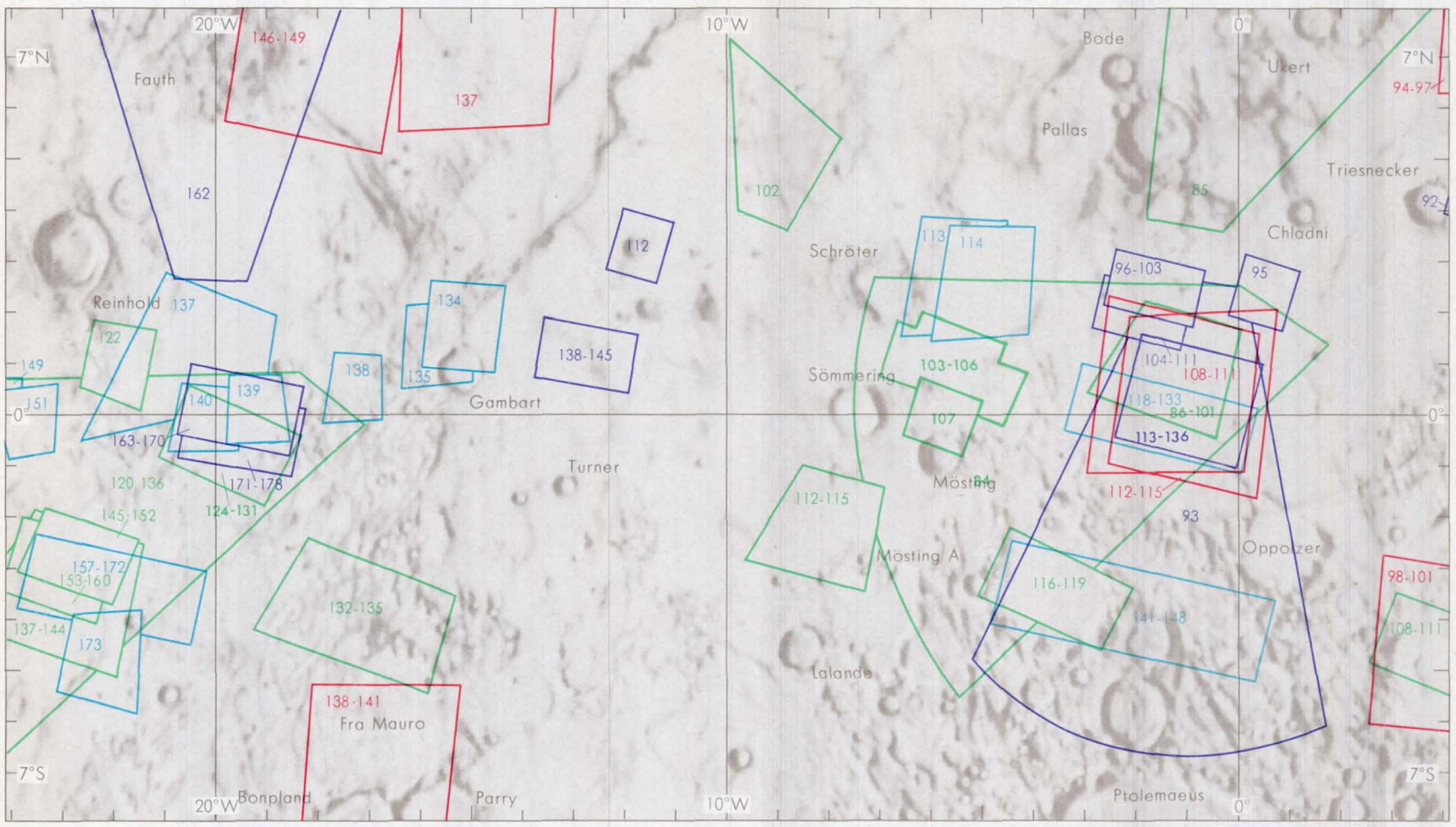

PREPARED UNDER THE DIRECTION OF THE DEPARTMENT OF DEFENSE BY THE AERONAUTICAL CHART AND INFORMATION CENTER, UNITED STATES AIR FORCE FOR THE NATIONAL AERONAUTICS AND SPACE ADMINISTRATION.
Base Chart Compiled ACIC February 1968

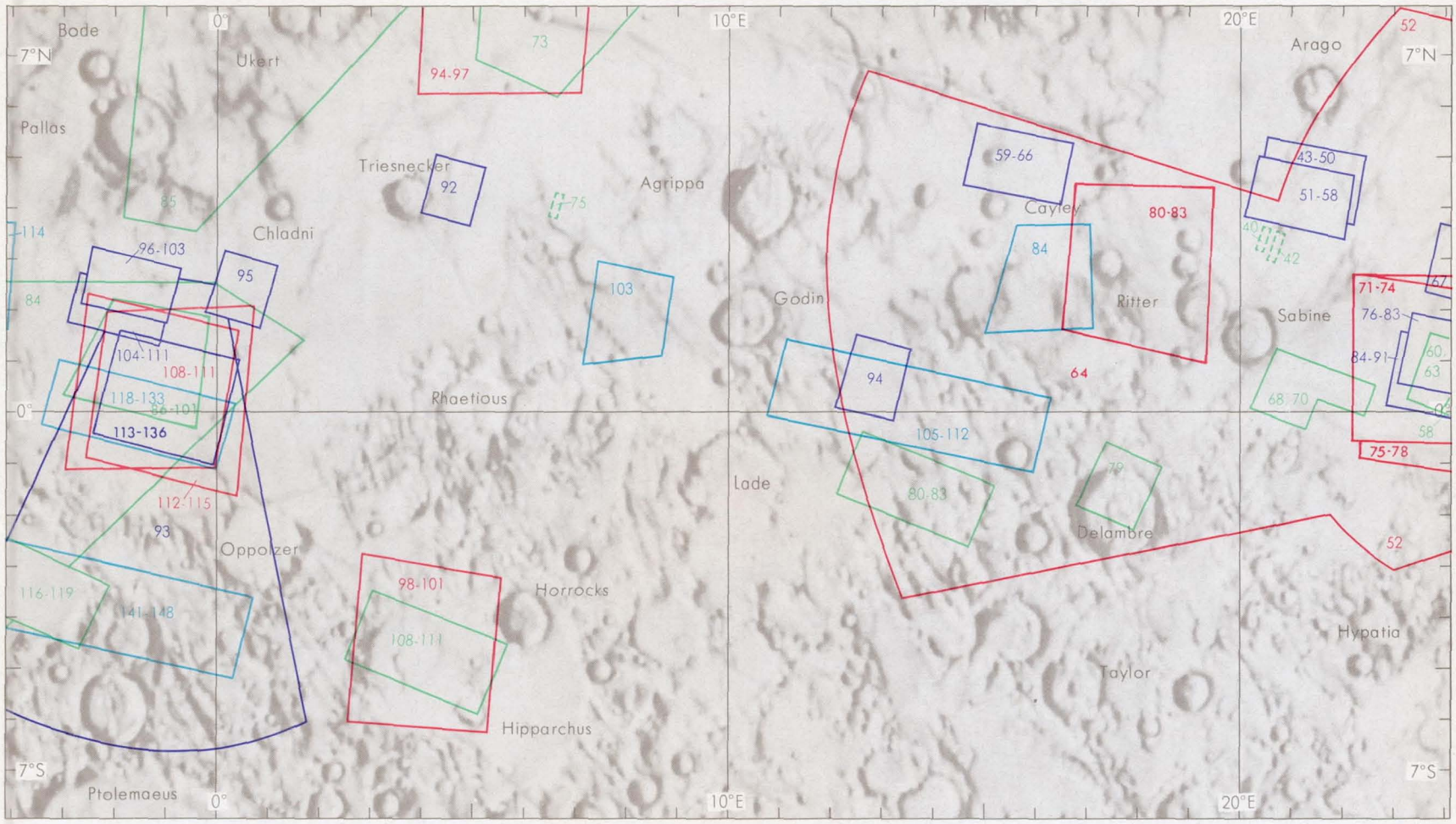

APOLLO ZONE OF PRIMARY INTEREST

Available Photo Coverage For All Missions Except IV.

Medium Resolution — Mission I, Mission III

High Resolution — Mission III

Mission II, Mission V

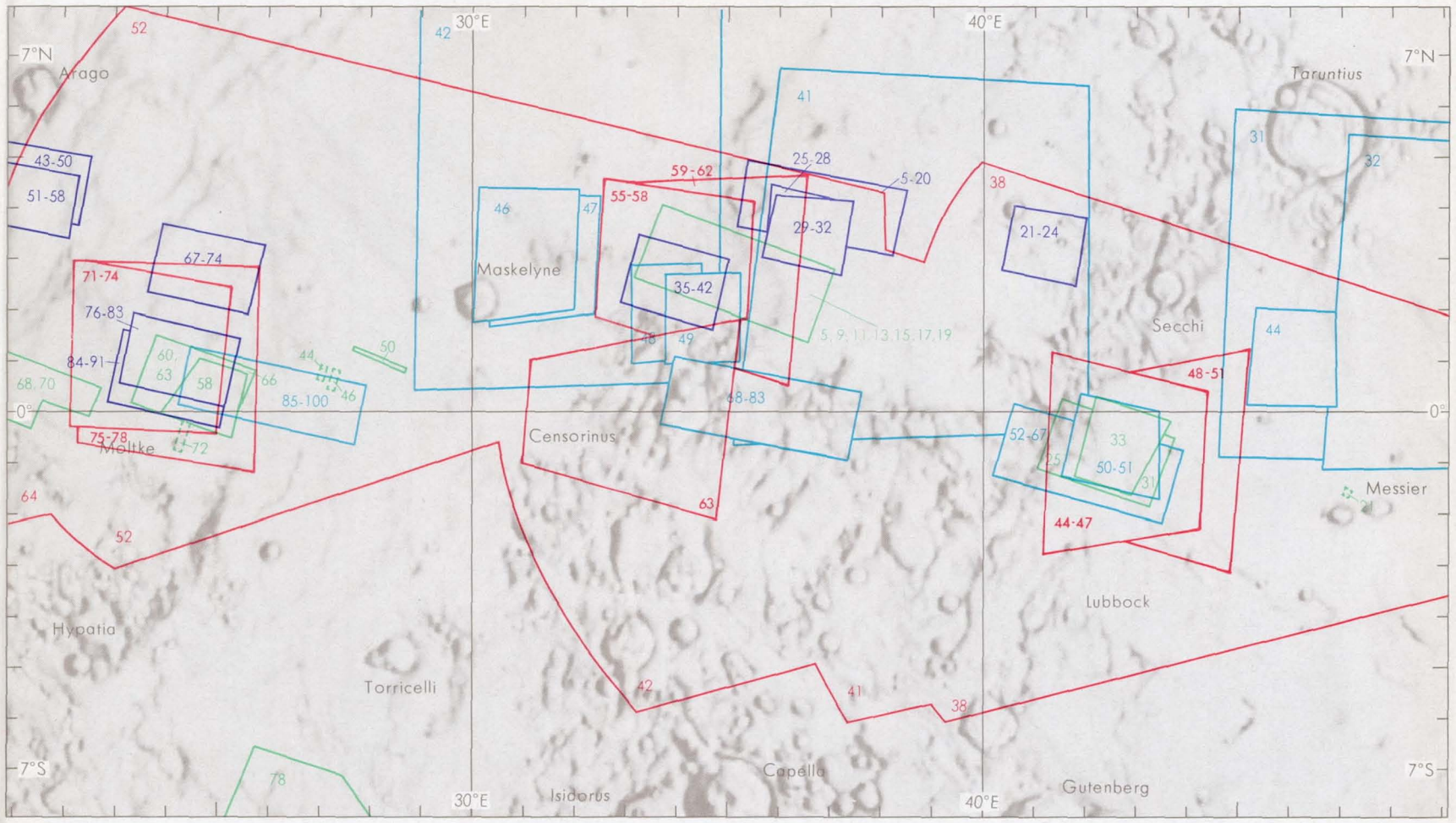

PREPARED UNDER THE DIRECTION OF THE DEPARTMENT OF DEFENSE BY THE AERONAUTICAL CHART AND INFORMATION CENTER, UNITED STATES AIR FORCE FOR THE NATIONAL AERONAUTICS AND SPACE ADMINISTRATION.
Base Chart Compiled ACIC February 1968

NORTH POLAR REGION

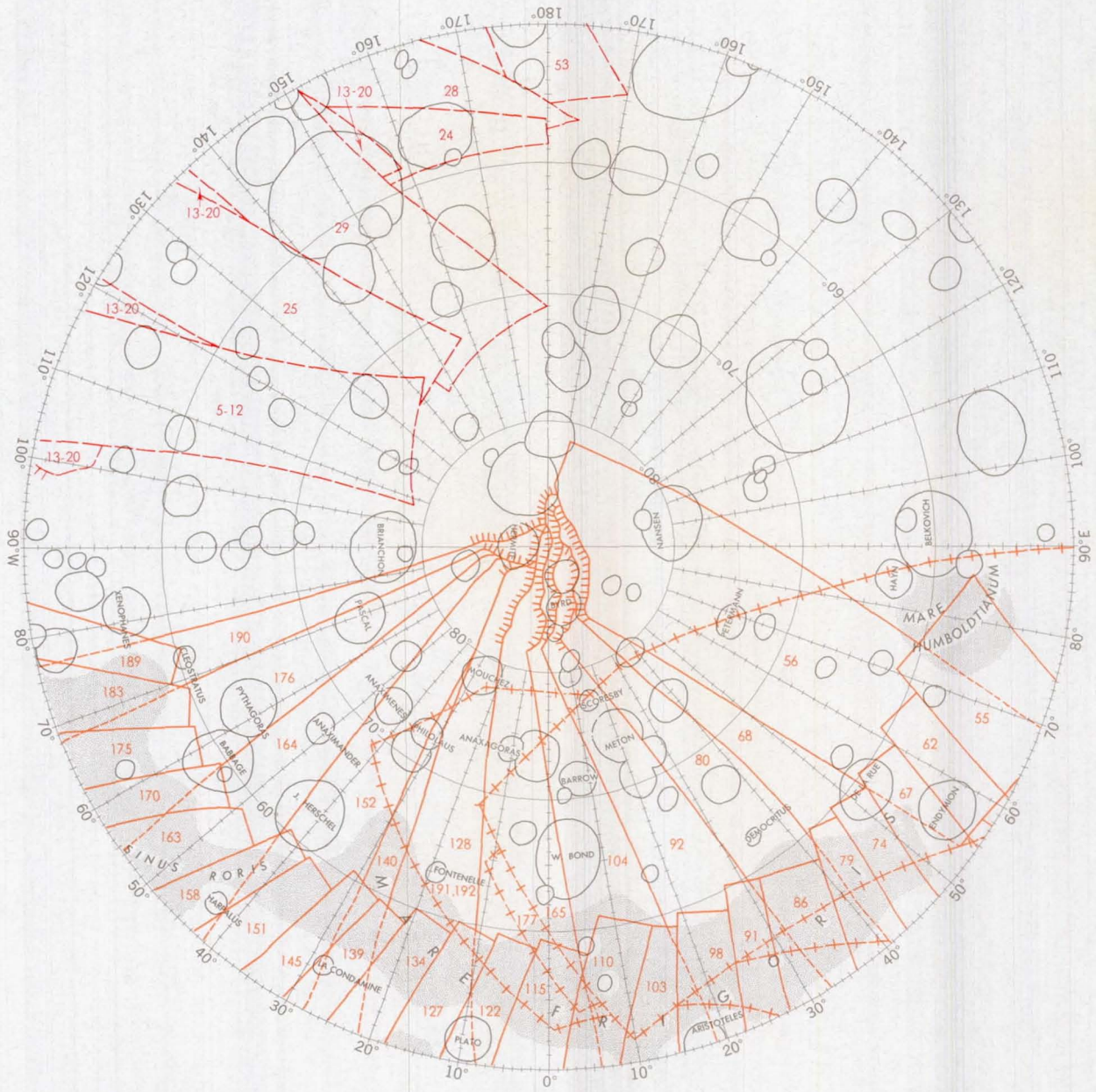

AVAILABLE PHOTO COVERAGE FOR ALL ORBITER MISSIONS

High Resolution

Mission Ⅳ ☐ Ⅳ Oblique ⊡ Terminator Limit ≡

Mission Ⅴ ⊡

Remaining area covered by Missions Ⅳ & Ⅴ medium resolution.

POLAR STEREOGRAPHIC PROJECTION

PREPARED UNDER THE DIRECTION OF THE DEPARTMENT OF DEFENSE BY THE AERONAUTICAL CHART AND INFORMATION CENTER, UNITED STATES AIR FORCE FOR THE NATIONAL AERONAUTICS AND SPACE ADMINISTRATION.

Base Chart Compiled ACIC February 1968

SOUTH POLAR REGION

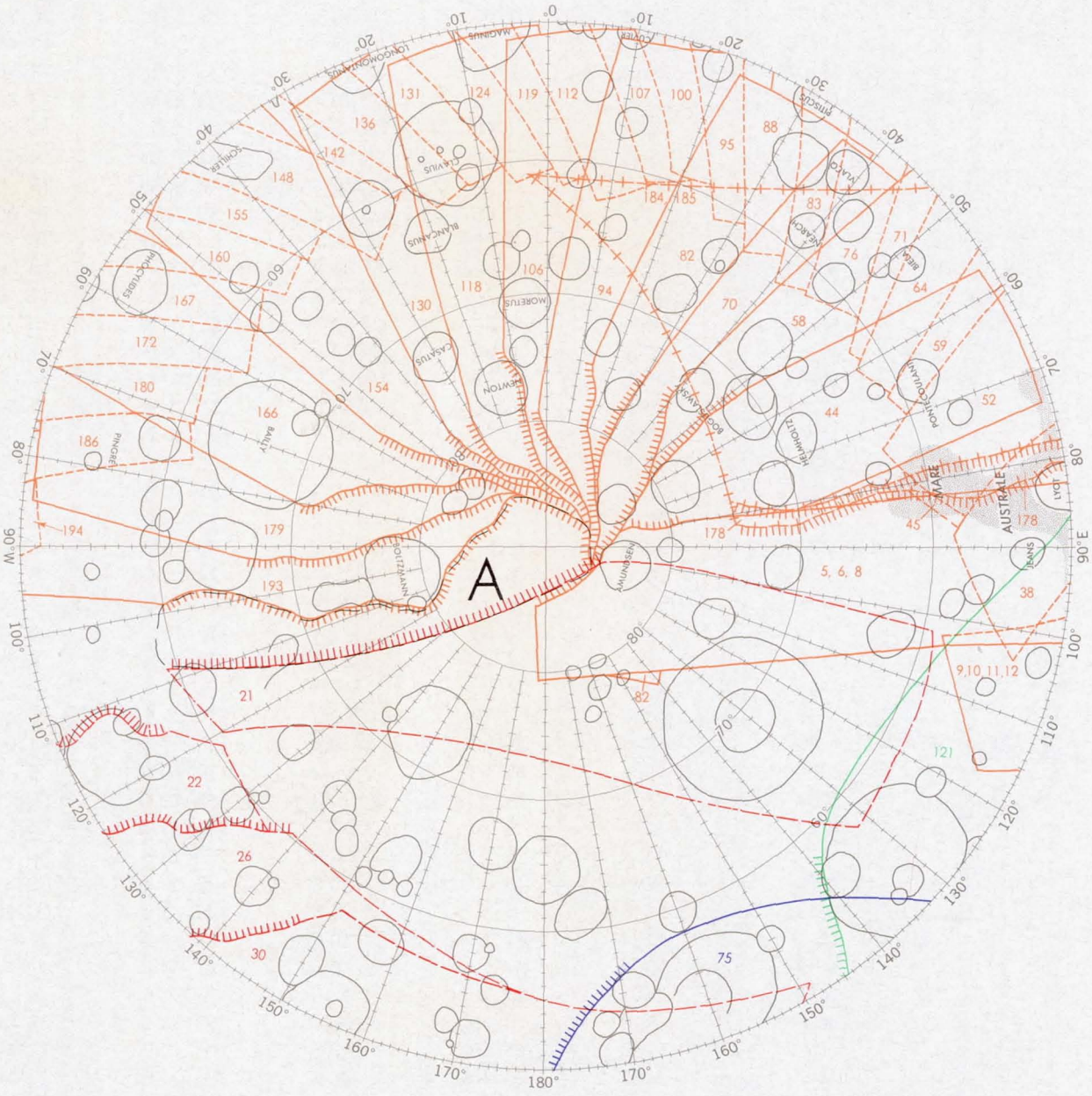

AVAILABLE PHOTO COVERAGE FOR ALL ORBITER MISSIONS

Medium Resolution

Mission II

Mission III

High Resolution

Mission IV

Mission V

IV Oblique

Terminator Limit

Remaining area covered by Missions IV & V medium resolution, except area A.

POLAR STEREOGRAPHIC PROJECTION

PREPARED UNDER THE DIRECTION OF THE DEPARTMENT OF DEFENSE BY THE AERONAUTICAL CHART AND INFORMATION CENTER, UNITED STATES AIR FORCE FOR THE NATIONAL AERONAUTICS AND SPACE ADMINISTRATION.

Base Chart Compiled ACIC February 1968

PHOTO REFERENCE TABLE

PAGE	PAGE POSITION	MISSION	FRAME	SPACECRAFT ALTITUDE (kilometers)	CAMERA TILT	FRAME CENTER DATA			
						LATITUDE	LONGITUDE	SUN ELEV.	FRAMELET BEARING
7	Right	IV	M23	2983	1°50′	43°40′N	99°00′E	26°50′	N69°30′W
8	Full	IV	M9	2989	4°20′	41°50′S	96°10′E	24°50′	N66°30′E
9	Full	IV	M86	2956	1°50′	41°00′N	31°10′E	23°40′	N71°20′W
10	Full	IV	M52	2976	4°30′	42°50′S	63°50′E	23°00′	N65°20′E
11	Full	IV	M109	2693	1°20′	13°50′N	3°30′W	20°30′	N85°00′W
12	Full	IV	M116	3397	0°40′	70°50′N	4°30′E	11°40′	N85°40′W
13	Full	IV	M107	2982	5°00′	42°20′S	6°30′E	21°40′	N64°10′E
14	Left	IV	H190	3373	1°50′	70°20′N	63°30′W	13°30′	N82°20′W
14	Right	IV	H94	3517	3°10′	72°10′S	20°10′E	8°50′	N83°10′E
15	Left	IV	M144	2669	0°30′	14°00′N	41°50′W	19°00′	N84°10′W
15	Right	IV	M121	2682	1°20′	13°50′N	16°50′W	19°30′	N84°50′W
16	Left	IV	M137	2718	0°40′	15°00′S	35°20′W	18°50′	N84°10′E
16	Right	IV	M113	2718	0°10′	14°40′S	9°30′W	20°10′	N84°10′E
17	Left	IV	M183	2875	2°50′	43°30′N	71°00′W	19°50′	N68°40′W
17	Right	IV	M162	2670	1°00′	13°10′N	62°10′W	17°10′	N84°10′W
18	Left	IV	M186	3006	4°40′	42°20′S	81°20′W	15°40′	N65°30′E
18	Right	IV	M167	3009	5°00′	42°00′S	60°40′W	17°30′	N65°00′E
19	Full	IV	M187	2723	0°30′	15°00′S	89°00′W	14°00′	N85°20′E
20	Left	V	M28	5015	8°40′	26°50′N	133°10′W	7°50′	N88°30′E
20	Center	V	M24	5009	8°50′	27°00′N	120°00′W	7°30′	N88°20′E
20	Right	V	M20	5758	7°30′	14°30′N	102°10′W	2°40′	N89°50′W
21	Left	V	M29	2548	11°00′	59°20′N	147°10′W	10°50′	N76°50′E
21	Right	V	M6	2648	9°40′	59°40′N	111°40′W	7°40′	N80°00′E
22	Left	V	M30	5069	9°30′	25°20′S	139°10′W	6°40′	N87°20′W
22	Center	V	M26	5069	9°20′	27°10′S	124°50′W	5°10′	N86°40′W
22	Right	V	M22	5106	9°40′	26°30′S	112°20′W	5°30′	N87°10′W
23	Left	I	M35	1339	0°30′	8°40′S	162°40′W	20°00′	N84°40′W
23	Right	I	M40	1454	7°30′	6°30′S	148°40′W	6°20′	N86°20′W
24	Full	II	M34	1453	16°10′	4°40′N	173°30′E	19°10′	N79°50′W
25	Full	II	M33	1455	0°40′	10°20′S	174°00′E	20°10′	N86°40′W
26	Left	V	M85	1239	25°50′	38°50′N	158°50′E	11°00′	N86°00′E
26	Right	V	M53	1191	25°40′	49°00′N	176°10′W	9°10′	N77°10′E
27	Left	V	M65	1192	19°50′	48°50′S	168°40′W	Dark	N89°00′W
27	Right	V	M43	1191	20°10′	47°30′S	151°30′W	Dark	N88°10′E
28	Full	I	M116	1456	*9°20′	1°10′S	153°20′E	10°50′	N83°00′W
29	Full	II	M75	1469	13°00′	21°10′S	158°00′E	19°20′	N89°00′E
30	Full	I	M136	1328	3°30′	*5°20′S	129°20′E	20°40′	N84°00′W
31	Left	V	M158	1233	24°10′	*38°00′N	126°50′E	11°00′	N85°10′E
31	Right	V	M124	1237	24°20′	38°40′N	143°50′E	10°10′	N85°40′E
32	Full	III	M121	1463	12°40′	24°10′S	126°50′E	19°20′	N88°50′E
33	Full	II	M196	1519	0°20′	9°00′S	100°30′E	19°50′	N87°20′W
34-35	Full	I	H102	1198	35°40′	14°40′S	104°20′E	78°40′	N73°50′W
36	Full	V	M181	1181	23°20′	42°00′N	109°20′E	11°20′	N84°20′E
37	Left	IV	M123	6151	0°30′	1°10′N	162°20′E	Dark	N70°50′E
38	Left	V	H27	——	——	——	——	——	——
40	Full	III	M213	59.0	66°30′	3°20′S	59°50′W	7°30′	N41°30′W
41	Full	IV	M137	2718	0°40′	15°00′S	35°20′W	18°50′	N84°10′E
42	Left	IV	H143	2719	*1°00′	14°20′S	41°20′W	18°50′	N84°10′E
42	Right	III	M200	54.6	12°50′	3°10′S	42°30′W	19°30′	N68°50′W
43	Left	III	H194	54.3	12°40′	2°50′S	43°20′W	18°30′	N68°40′W
43	Right	III	H194	54.3	12°40′	2°50′S	43°20′W	18°30′	N68°40′W
44	Top	V	M161	158.0	3°00′	32°40′N	22°00′W	17°10′	N 5°30′E
44*	Bottom	V	H161	158.0	3°00′	32°40′N	22°00′W	17°10′	N 5°40′E
44*	Bottom	V	H160	156.4	2°40′	32°20′N	22°10′W	17°10′	N 5°30′E
45	Left	V	M69	125.3	2°30′	22°30′N	29°20′E	21°10′	N 4°40′E
45	Right	V	M69	125.3	2°30′	22°30′N	29°20′E	21°10′	N 4°40′E
46	Top	V	M172	104.7	7°50′	3°00′S	36°10′W	14°50′	N 4°20′E
46	Bottom	V	H172	104.7	7°50′	3°00′S	36°10′W	14°50′	N 4°20′E
47	Left	III	M84	46.7	67°20′	0°50′N	1°00′W	9°50′	N35°40′W
47	Right	II	H85	51.4	1°10′	*0°50′N	23°40′E	29°50′	N77°50′W
48	Top	V	H114	97.4	19°50′	0°30′N	1°00′W	19°30′	N 4°00′E

*This photograph is a mosaic of 2 frames.

PHOTO REFERENCE TABLE

PAGE	PAGE POSITION	MISSION	FRAME	SPACECRAFT ALTITUDE (kilometers)	CAMERA TILT	FRAME CENTER DATA			
						LATITUDE	LONGITUDE	SUN ELEV.	FRAMELET BEARING
48	Bottom	V	H59	100.0	22°30′	2°10′N	34°20′E	22°30′	N 4°10′E
49	Left	II	H47	49.3	0°50′	4°30′N	21°20′E	13°20′	N78°30′W
49	Right	II	H42	48.8	1°20′	2°30′N	34°30′E	22°50′	N77°50′W
50	Left	II	H70	45.6	3°30′	2°40′N	24°40′E	22°00′	N77°50′W
50	Right	II	H21	50.1	3°50′	3°20′N	41°00′E	20°30′	N78°20′W
51	Left	III	H164	54.6	17°30′	1°40′N	42°20′W	10°50′	N67°10′W
51	Right	III	H209	56.7	29°50′	2°20′S	44°10′W	21°20′	N65°50′W
53	Left	IV	M114	2687	1°50′	13°30′N	11°00′W	19°20′	N85°30′W
53	Right	IV	M103	2927	1°40′	41°50′N	11°20′E	22°20′	N72°10′W
54	Full	V	M102	250.4	34°10′	48°10′N	1°00′E	12°10′	N26°40′W
55	Top	V	M54	132.8	57°50′	27°40′S	27°40′E	10°20′	N49°50′E
55	Bottom	V	M88	182.2	4°00′	39°00′N	13°30′E	18°30′	N 5°40′E
56	Full	III	M85	49.0	57°10′	5°00′N	0°20′W	12°10′	N50°20′W
57	Full	V	H84	114.8	2°30′	15°00′S	13°50′E	17°10′	N 4°40′E
58	Left	III	H199	54.5	12°50′	3°00′S	42°40′W	19°20′	N68°40′W
58*	Center	III	H199	54.5	12°50′	3°00′S	42°40′W	19°20′	N68°40′W
58*	Center	III	H200	54.6	12°50′	3°10′S	42°30′W	19°30′	N68°50′W
58	Right	III	H200	54.6	12°50′	3°10′S	42°30′W	19°30′	N68°50′W
59	Full	V	H177	130.8	6°50′	19°00′S	40°10′W	13°00′	N 4°00′E
60	Left	V	M182	167.5	5°40′	35°00′N	41°30′W	15°30′	N 5°00′E
60	Right	V	H118	114.0	14°20′	13°40′S	4°10′W	17°10′	N 3°10′E
61	Full	V	H130	236.0	7°20′	49°20′N	2°40′W	16°40′	N 8°50′E
63	Full	III	M113	44.0	35°20′	1°50′S	8°00′W	18°40′	N64°30′W
64	Top	III	H113	44.0	35°20′	1°50′S	8°00′W	18°40′	N64°30′W
64	Bottom	III	H113	44.0	35°20′	1°50′S	8°00′W	18°40′	N64°30′W
65	Full	V	H63	99.4	29°10′	0°20′S	32°50′E	22°30′	N 4°00′E
66	Full	V	M148	101.1	15°20′	7°00′N	18°10′W	18°30′	N 4°30′E
67	Full	V	H50	101.8	24°50′	0°40′S	43°00′E	23°00′	N 4°10′E
68	Full	V	H122	106.8	12°00′	13°00′N	4°00′W	19°40′	N 5°20′E
69*	Full	V	H183	169.1	5°40′	35°20′N	41°30′W	15°20′	N 5°10′E
69*	Full	V	H182	167.4	5°30′	35°00′N	41°30′W	15°30′	N 5°10′E
70	Top	V	H183	169.1	5°40′	35°20′N	41°30′W	15°20′	N 5°10′E
70	Bottom	V	M70	113.1	12°00′	17°20′N	26°20′E	20°30′	N 3°50′E
71	Top	V	H70	113.1	12°00′	17°20′N	26°20′E	20°30′	N 3°50′E
71	Bottom	V	H70	113.1	12°00′	17°20′N	26°20′E	20°30′	N 3°50′E
72	Full	IV	H187	2723	0°30′	15°00′S	89°00′W	14°00′	N85°20′E
73	Top	III	M162	54.7	69°30′	7°00′N	38°10′W	11°20′	N41°00′W
73	Bottom Left	V	M168	169.2	10°00′	30°30′S	37°40′W	9°30′	N 6°50′E
73	Bottom Right	V	H168	169.2	9°50′	30°30′S	37°40′W	9°30′	N 6°50′E
74	Full	IV	H150	2668	1°20′	12°40′N	49°20′W	17°50′	N84°30′W
75	Full	V	M197	129.8	2°10′	23°00′N	47°30′W	16°00′	N 5°30′E
76	Full	V	H199	131.4	2°40′	23°40′N	47°20′W	16°00′	N 5°30′E
77	Full	V	H200	132.3	3°00′	24°10′N	47°20′W	16°00′	N 5°40′E
78	Full	V	H197	129.8	2°10′	23°00′N	47°20′W	16°00′	N 5°30′E
79	Top Left	V	M198	130.6	2°30′	23°20′N	47°20′W	16°00′	N 5°30′E
79	Top Right	V	H197	129.8	2°10′	23°00′N	47°20′W	16°00′	N 5°30′E
79	Bottom Left	V	H197	129.8	2°10′	23°00′N	47°20′W	16°00′	N 5°30′E
79	Bottom Right	V	H201	133.2	3°20′	24°30′N	47°20′W	16°00′	N 5°40′E
80	Full	I	M31	242.5	11°00′	2°30′N	48°00′E	9°30′	N88°10′W
81	Full	V	M125	220.0	5°30′	42°50′S	11°40′W	8°50′	N 6°20′E
82	Full	V	H125	220.0	5°30′	42°50′S	11°40′W	8°50′	N 6°20′E
83	Full	V	H125	220.0	5°30′	42°50′S	11°40′W	8°50′	N 6°20′E
84	Full	V	H126	217.2	5°00′	42°20′S	11°40′W	9°00′	N 6°20′E
85*	Left	V	H128	211.6	3°50′	41°10′S	11°30′W	9°20′	N 6°10′E
85*	Left	V	H127	214.4	4°30′	41°40′S	11°30′W	9°10′	N 6°10′E
85	Right	V	H127	214.4	4°30′	41°40′S	11°30′W	9°10′	N 6°10′E
86	Full	IV	M121	2682	1°20′	13°50′N	16°50′W	19°30′	N84°50′W
87*	Full	V	M155	104.2	5°10′	10°40′N	20°20′W	18°00′	N 5°10′E
87*	Full	V	M150	102.9	5°00′	9°10′N	20°20′W	18°00′	N 5°00′E
88	Full	V	H154	103.9	5°10′	10°20′N	20°20′W	18°00′	N 5°10′E
89	Full	II	M162	45.9	69°30′	5°30′N	20°00′W	24°40′	N86°30′W

*This photograph is a mosaic of 2 frames.

PHOTO REFERENCE TABLE

PAGE	PAGE POSITION	MISSION	FRAME	SPACECRAFT ALTITUDE (kilometers)	CAMERA TILT	FRAME CENTER DATA			
						LATITUDE	LONGITUDE	SUN ELEV.	FRAMELET BEARING
90	Full	II	H162	45.9	69°20′	5°30′N	20°00′W	24°40′	N86°40′W
91	Full	V	M155	104.2	5°10′	10°40′N	20°20′W	18°00′	N 5°10′E
92*	Full	IV	H86	2956	1°50′	41°00′N	31°10′E	23°40′	N71°20′W
92*	Full	IV	H79	2964	2°10′	41°50′N	39°00′E	24°30′	N71°10′W
93	Full	IV	H127	2886	2°10′	41°10′N	14°20′W	21°50′	N71°20′W
94	Full	III	M78	56.8	68°50′	10°20′S	26°30′E	30°10′	N78°10′W
95*	Full	V	M178	127.4	6°00′	17°40′S	40°00′W	13°10′	N 4°00′E
95*	Full	V	M177	130.8	6°40′	19°00′S	40°10′W	13°00′	N 4°00′E
96	Full	IV	H27	2747	0°30′	15°10′S	82°40′E	26°20′	N85°00′E
97	Top	IV	H85	2717	0°50′	13°00′N	24°00′E	23°30′	N84°10′W
97	Bottom	IV	H108	2719	0°30′	14°20′S	2°20′W	21°10′	N84°20′E
98	Full	V	M41	103.3	53°40′	2°00′S	47°00′E	17°10′	N 3°20′E
99	Full	V	H41	103.3	53°30′	2°00′S	47°00′E	17°10′	N 3°20′E
100	Full	V	M97	100.3	19°20′	8°10′N	6°00′E	18°20′	N 3°40′E
101	Top	V	H95	99.9	19°10′	7°40′N	5°50′E	18°20′	N 4°00′E
101	Bottom	V	H95	99.9	19°10′	7°40′N	5°50′E	18°20′	N 4°00′E
102	Left	V	H121	106.4	12°00′	12°40′N	4°00′W	19°40′	N 5°20′E
102	Right	V	H19	5758	7°40′	14°00′N	102°20′W	2°40′	N89°30′W
104	Full	III	M73	62.8	*52°30′	7°40′N	6°40′E	6°40′	N53°20′W
105	Left	IV	H113	2718	0°20′	14°40′S	9°30′W	20°10′	N84°10′E
105	Right	IV	H161	2723	0°50′	15°10′S	62°00′W	16°30′	N84°50′E
106	Full	IV	M9	2989	4°20′	41°50′S	96°10′E	24°50′	N66°30′E
107	Full	V	H21	3342	16°50′	85°10′S	175°20′W	3°10′	N12°30′W
108	Full	V	M139	103.7	1°10′	7°10′S	16°50′W	16°20′	N 4°30′E
109	Full	V	M105	131.1	5°00′	25°00′N	3°00′E	19°00′	N 4°30′E
110	Top	V	H105	131.1	4°50′	25°00′N	3°00′E	19°00′	N 4°40′E
110	Bottom	V	H105	131.1	4°50′	25°00′N	3°00′E	19°00′	N 4°40′E
111	Top	IV	H137	2718	0°40′	15°00′S	35°20′W	18°50′	N84°10′E
111	Bottom	V	H130	236.0	7°20′	49°20′N	2°40′W	16°40′	N 8°50′E
112	Full	V	H130	236.0	7°20′	49°20′N	2°40′W	16°40′	N 8°50′E
113	Full	V	M202	134.4	6°10′	24°50′N	49°30′W	15°20′	N 5°00′E
114	Full	V	H204	136.4	6°20′	25°40′N	49°30′W	15°20′	N 5°00′E
115	Full	V	M191	142.0	2°50′	27°40′N	43°30′W	16°10′	N 5°20′E
116*	Full	V	H188	138.8	1°50′	26°30′N	43°40′W	16°10′	N 5°30′E
116*	Full	V	H187	137.8	1°30′	26°10′N	43°40′W	16°10′	N 5°20′E
117*	Left	V	H189	139.8	2°10′	26°50′N	43°40′W	16°10′	N 5°30′E
117*	Left	V	H188	138.8	1°50′	26°30′N	43°40′W	16°10′	N 5°30′E
117	Right	V	H189	139.8	2°10′	26°50′N	43°40′W	16°10′	N 5°30′E
118*	Full	V	H215	112.5	9°40′	14°10′N	56°00′W	14°40′	N 4°20′E
118*	Full	V	H214	112.1	9°40′	13°50′N	56°00′W	14°30′	N 4°30′E
119	Full	V	M183	169.2	5°50′	35°30′N	41°30′W	15°20′	N 5°00′E
120	Full	V	M164	109.2	0°40′	12°30′N	31°00′W	17°00′	N 4°40′E
121	Full	IV	H157	2669	1°20′	13°20′N	56°20′W	16°50′	N84°50′W
122	Full	II	M213	50.8	68°40′	8°00′N	52°50′W	21°10′	N52°50′W
123	Full	V	M214	112.1	9°50′	13°50′N	56°00′W	14°30′	N 4°20′E
125	Full	IV	M187	2723	0°30′	15°00′S	89°00′W	14°00′	N85°20′E
126	Full	IV	H195	2721	1°00′	14°50′S	94°40′W	14°30′	N84°50′E
127	Full	IV	H195	2721	1°00′	14°50′S	94°40′W	14°30′	N84°50′E
128	Full	IV	H187	2723	0°30′	15°00′S	89°00′W	14°00′	N85°20′E
129	Full	IV	H181	2724	1°00′	13°00′S	82°10′W	14°50′	N84°40′E
130	Full	IV	H173	2724	0°30′	14°50′S	75°20′W	15°20′	N85°00′E
131	Full	IV	H172	3011	4°50′	43°00′S	68°00′W	16°20′	N65°20′E
132	Top	V	M103	1237	25°20′	38°50′N	150°50′E	11°00′	N85°50′E
132	Bottom	V	H103	1236	25°20′	38°40′N	150°50′E	11°00′	N86°00′E
133	Left	III	M121	1463	12°40′	24°10′S	126°50′E	19°20′	N88°50′E
133	Right	III	H121	1463	12°40′	24°00′S	126°40′E	19°30′	N89°00′E
134	Full	III	H121	1463	12°40′	24°00′S	126°40′E	19°30′	N89°00′E
135	Left	I	H30	1299	2°20′	10°20′S	162°40′W	23°40′	N84°40′W
135	Right	I	H115	1381	6°50′	2°50′S	145°20′E	19°00′	N82°50′W
136	Top	I	H136	1328	3°30′	5°20′S	129°20′E	20°40′	N84°00′W
136	Bottom	II	H33	1455	0°30′	10°20′S	174°10′E	20°10′	N86°40′W

*This photograph is a mosaic of 2 frames.